CL/PACLIM-IATR/95-46

PROCEEDINGS OF THE TWELFTH ANNUAL PACIFIC CLIMATE (PACLIM) WORKSHOP

Asilomar, California — May 2-5, 1995

Edited by
Caroline M. Isaacs and Vera L. Tharp

Technical Report 46
of the
Interagency Ecological Program
for the
Sacramento-San Joaquin Estuary

April 1996

Sponsors

The Twelfth Annual Pacific Climate Workshop was sponsored by:

U.S. GEOLOGICAL SURVEY
Water Resources Division

U.S. GEOLOGICAL SURVEY
Geological Resource Division

NATIONAL OCEANIC AND ATMOSPHERIC ADMINISTRATION
Paleoclimatology Program

CALIFORNIA DEPARTMENT OF WATER RESOURCES
Environmental Services Office

SOUTHERN CALIFORNIA EDISON COMPANY

AMERICAN GEOPHYSICAL UNION

NAVAL POSTGRADUATE SCHOOL

Publication of this proceedings has been sponsored by the

INTERAGENCY ECOLOGICAL PROGRAM
for the
SACRAMENTO-SAN JOAQUIN ESTUARY

A Cooperative Program of:

California Department of Water Resources
State Water Resources Control Board
U.S. Bureau of Reclamation
U.S. Geological Survey
California Department of Fish and Game
U.S. Fish and Wildlife Service
U.S. Army Corps of Engineers
U.S. Environmental Protection Agency
National Marine Fisheries Service

These proceedings were published by the Interagency Ecological Program for the Sacramento-San Joaquin Estuary (Interagency Program)
in a cooperative effort with the
United States Department of the Interior, Geological Survey, Menlo Park, California.
Information generated by the PACLIM Workshop provides the Interagency Program with a climatological perspective that cannot be obtained from its own studies.
Views and conclusions contained in this publication do not necessarily reflect the opinions of the Interagency Program or its member agencies.

Contents

Sponsors . . . . . *iii*

Authors . . . . . *ix*

Acknowledgments . . . . . *xv*

Statement of Purpose . . . . . *xvii*

Introduction 1
Caroline M. Isaacs

Simulation of Recent Global Temperature Trends 17
Nicholas E. Graham

Mechanisms of Upper-Ocean Thermal Variability in a 1970-1988 Simulation and Observations 19
Arthur J. Miller, Daniel R. Cayan, Warren B. White

Climate Forcing by Changing Solar Radiation 33
Judith Lean

Effects of Interdecadal Climate Variability on the Oceanic Ecosystems of the Northeast Pacific Ocean 41
Robert C. Francis, S.R. Hare, A.B. Hollowed, Warren S. Wooster

Decadal Hydroclimatic Variability over Western North America 43
Dan Cayan, Mike Dettinger, Henry Diaz

Terrestrial Ecosystem Response to Interdecadal Climate Variability in the Western United States 45
Thomas W. Swetnam and Julio L. Betancourt

Paleorecords of Interdecadal Variability from Mid-Latitude Varved Sediments and Tropical Corals of the Eastern Pacific 47
Tim R. Baumgartner and Robert B. Dunbar

The Terrestrial Record of Interdecadal Climate Variability in Western North America 49
Malcolm K. Hughes

Decadal Climate Variability over the North Pacific and North America: Dynamics and Predictability 51
Mojib Latif and Tim P. Barnett

Interdecadal Variability in the Spatial Structure of Wind and SST in the California Current System 53
Franklin B. Schwing, Roy Mendelssohn, Richard Parrish

Interannual Variability in the PFEG Coastal Upwelling Indices 63
Heather A. Parker

Decadal Variability over the North Pacific Ocean 71
Dan Cayan, Warren White, Art Miller

Interdecadal Shifting of the North Pacific Jet Stream — El Niño Events 73
Stephen H. Holets

Long-Term Changes in the Equatorial Pacific Trade Winds 75
Allan J. Clarke and Anna Lebedeva

Recent Trends in the Climate of the Tropical Pacific Region 77
Nathan J. Mantua and Nicholas E. Graham

Analysis of Four Decades of High Elevation Climate Data 95
Mark Losleben

Relationships between Climate and Atmospheric Circulation in the Sonoran Desert Region 99
Connie A. Woodhouse

Geographic Patterns in the Lag of Temperature Response to Insolation for El Niño vs. La Niña Conditions. 105
R.C. Craig, J.L. Betancourt, D.E. Jones

Decadal Patterns in Atmospheric Carbon Dioxide as Indicators of Changing Growth and Decay of Terrestrial Vegetation. 107
Charles D. Keeling and Timothy Whorf

Offshore Coho Salmon Populations near the Pacific Northwest and Large-Scale Atmospheric Events 109
David Greenland

Decadal Variation in the Trans-Pacific Migration of Northern Bluefin Tuna (*Thunnus thynnus*) Coherent with Climate-Induced Change in Prey Abundance. 121
Jeffrey Polovina

Chronic and Catastrophic Influences of the Environment on the Population Dynamics of the Common Fishes 123
Paul E. Smith

A 10-Year Time Series of Zooplankton Anomalies off the British Columbia Coast. 125
David L. Mackas

Physical, Chemical, and Biological Characterization of Water Year Types in San Francisco Bay Estuary 127
Peggy W. Lehman

Climate-Related Long-Term Faunal Changes in a California Rocky Intertidal Community 129
James P. Barry, Charles H. Baxter, Sarah E. Gilman

California Water Conditions in 1995. 131
Maurice Roos

Recent Winters in the Western United States and Relationship to ENSO Patterns 141
Kelly T. Redmond

Changes in the Hydrometeorological Regime in the Pacific Southwest 143
John J. Vaccaro

River Salinity Variations in Response to Discharge: Examples from Western United States During the Early 1900s 145
David Peterson, Michael Dettinger, Daniel Cayan, Jeanne DiLeo, Caroline Isaacs, Larry Riddle, Richard Smith

Reconstructing 20th Century Flood Patterns in Havasu Creek, Arizona, Using Historical and Dendrochronologic Data 155
Theodore S. Melis and William M. Phillips

An 800-Year Paleoflood Record from the Sacramento Valley, California 157
Roger Byrne and Donald Sullivan

Can Lake Sediments Provide a Record of Tropical Storms? The Case of Laguna de Juanacatlan, Jalisco, Mexico 159
Roger Byrne, Douglas Allen, Eric Edlund, Clare Polansky

Influence of Climatography on Rainfall Thresholds for Initiation of Debris-Flows on the California Coast 161
Raymond C. Wilson

Disturbance Climate in the Columbia River Basin 163
Sue A. Ferguson and Miriam R. Peterson

Fire, Climate, and Vegetation: The Sedimentary Record of Fire in Montane Meadows, Sierra Nevada, California, USA. 165
R. Scott Anderson and Susan J. Smith

Changes in Mass Balance of South Cascade Glacier, North Cascades, 1959 to 1994 167
Steven M. Hodge, Robert M. Krimmel, Edward G. Josberger

Interannual to Decadal Time-Scale Variations in Glacier Mass Balance. 179
Roy A. Walters

The Little Ice Age: Glacier Variations and Climate Since AD 1250 181
Stephen C. Porter

The Terrestrial Paleorecord of Climate Change over the Past Thousand Years in the Canadian Rockies 183
Brian H. Luckman

Variability in a Radiolarian Time Series and Its Relationship to Climate 185
Amy L. Weinheimer and Daniel R. Cayan

Evidence for Changes in Large-Scale Upwelling in the California Current over the Past 700 Years. 197
Tim R. Baumgartner and John Southon

On the Strength of the California Current: A Record from the Southern Baja California Margin 199
Juan Carlos Herguera, Tim Herbert, Vicente Ferreira Bartrina

Oceanographic Variability at Clipperton Atoll Since the 1880s: Stable Isotopic Evidence from Massive Corals. 201
Braddock K. Linsley and Robert B. Dunbar

Oxygen Isotope Analysis of Corals from the Gulf of California and the Gulf of Panama: Application and Implications for Coral-Based Paleoclimate Reconstructions 203
William A. Jones, Robert B. Dunbar, Gerard M. Wellington

Integrating Varve and Tree-Ring Time Series for Southern California Climate Reconstruction: A 20th Century Outlook 205
Franco Biondi, Carina B. Lange, Kimberly Cobb, Wolfgang Berger

Synoptic Dendroclimatology: A Process-Based Approach for Linking Tree-Ring Information to Atmospheric Circulation over the Pacific and Western North America 207
Katherine K. Hirschboeck, Fenbiao Ni, Michelle L. Wood, Connie A. Woodhouse

Atmospheric Circulation Patterns Associated with Tree Growth Anomalies in the Central and Southern Sierra Nevada Mountains 209
Gregg M. Garfin

Climate-Driven Hydrologic Transients in Holocene Lake Records 211
Alison J. Smith, Joseph J. Donovan, Daniel R. Engstrom, Emi Ito, Valerie Panek, Eric Gong

High-Resolution Record of Climate Change in the Owens Lake Basin, California, for the Period 52,500 to 12,500 YBP 217
Larry Benson, James Burdett, Michaele Kashgarian, Steve Lund, Robert Rye

A Late Pleistocene Paleohydrologic Record of Sierra Nevada Runoff from Owens Lake, California 231
J. Platt Bradbury

A Detailed 2,000-Year Late-Holocene Pollen Record from Lower Pahranagat Lake, Southern Nevada, USA 233
Peter E. Wigand and Martha L. Hemphill

Response of Pacific Northwest Vegetation to Large-Scale Changes in Climate During the Last 100,000 Years 235
Cathy Whitlock and Patrick J. Bartlein

Multiple-Proxy Lacustrine Record of Moisture Transport over Western North America from 24,000 to 12,000 YBP, Lake Estancia, New Mexico 237
Bruce D. Allen, Roger Y. Anderson, Crayton J. Yapp

A Rock-Magnetic and Geomagnetic Secular Variation Record from Late-Pleistocene Lake Estancia, New Mexico 239
H.D. Rowe, J.W. Geissman, Bruce D. Allen, Roger Y. Anderson

The QBO, El Niño, and Tidal Resonance Model 241
Thor Karlstrom

Chronological Records of Climate-Related Events and Societal Consequences 255
Gary D. Sharp

Appendixes

A Agenda 257

B Poster Presentations 263

C Attendees 267

Authors

Bruce D. Allen
Department of Earth and Planetary Sciences
University of New Mexico
Albuquerque, NM 87131

Douglas Allen
Department of Geography
501 McCone Hall
University of California, Berkeley
Berkeley, CA 94720
510/643 9170; Fax 510/642-3370

R. Scott Anderson
Environmental Sciences Program
Northern Arizona University
Flagstaff, AZ 86011

Roger Y. Anderson
Department of Earth and Planetary Sciences
University of New Mexico
Albuquerque, NM 87131

Tim P. Barnett
Scripps Institution of Oceanography, 0224
La Jolla, CA 92093

James P. Barry
Monterey Bay Aquarium Resist Institute
160 Central Avenue
Pacific Grove, CA 93950

Patrick J. Bartlein
Geology Department
University of Oregon
Eugene, OR 97403

Vicente Ferreira Bartrina
Centro de Investigacion Cientifica y de
Ensenanza Superior
Carretera Transpeninsular KM 107
Ensenada, Baja California 22830
Mexico

Tim R. Baumgartner
Scripps Institution of Oceanography
University of California, San Diego
Marine Life Research Group
9500 Gilman Drive, Dept. 0227
La Jolla, CA 92093-0227
619/534-2171; Fax 619/534-7641
trbaumgartner@ucsd.edu
tbaumgar@cicese.mx

Charles H. Baxter
Hopkins Marine Station of Stanford University
Pacific Grove, CA 93950

Larry V. Benson
U.S. Geological Survey
3215 Marine St.
Boulder, CO 80303-1066
303/541-3005

Wolfgang Berger
Scripps Institution of Oceanography
Geological Resources Division
9500 Gilman Drive
La Jolla, CA 92093-0215

Julio L. Betancourt
U.S. Geological Survey
Desert Laboratory
1675 W. Anklam Road
Tucson, AZ 85745

Franco Biondi
Scripps Institution of Oceanography
Geological Resources Division
9500 Gilman Drive
La Jolla, CA 92093-0215

J. Platt Bradbury
U.S. Geological Survey
P.O. Box 25046, MS 919
Federal Center
Denver, CO 80225

James W. Burdett
U.S. Geological Survey
MS 963, Denver Federal Center
Lakewood, CO 80225
303/236-5916

Roger Byrne
Department of Geography
University of California, Berkeley
Berkeley, CA 94720
510/643-9170; Fax 510/642-3370

Daniel R. Cayan
Scripps Institution of Oceanography
La Jolla, CA 92093-0220
619/534-4507; Fax 619/534-8561
dcayan@ucsd.edu

Allan J. Clarke
Oceanography Department
Florida State University
Tallahassee, FL 32306-3048
904/644-2240
clarke@ocean.fsu.edu

Kimberly Cobb
P.O. Box 20416
New Haven, CT 06520

R.C. Craig
Department of Geology
Kent State University
Kent, OH 44240
216/672-7987; Fax 216/672-7949
rcraig@gilbert.kent.edu

Michael Dettinger
U.S. Geological Survey
5735 Kearny Villa Road, Suite O
San Diego, CA 92123-1135
619/637-6856; Fax 619/637-9201
mddettin@s101pcasnd.wr.usgs.gov

Henry Diaz
NOAA-ERL-CDC
325 Broadway
Boulder, CO 80303
303/497-6649; Fax 303/497-7013
hfd@ncdc.noaa.gov

Jeanne DiLeo
U.S. Geological Survey
345 Middlefield Road
Menlo Park, CA 94025

Joseph J. Donovan
Dept. Of Geology & Geography
West Virginia University
Morgantown, WV 26506
304/293-5603
donovan@wvugeo.wvnet.edu

Robert B. Dunbar
Department of Geology
Rice University
P.O. Box 1892F
Houston, TX 77251
713/527-4883

Eric Edlund
Department of Geography
501 McCone Hall
University of California, Berkeley
Berkeley, CA 94720
510/643 9170; Fax 510/642-3370

Daniel R. Engstrom
St. Croix Watershed Research Station
Science Museum of Minnesota
Marine on St. Croix, MN 55047
612/433-5953
dre@maroon.tc.umn.edu

Sue A. Ferguson
USDA Forest Service
Pacific Northwest Research Station
4043 Roosevelt Way NE
Seattle, WA 98105-6497

Robert C. Francis
School of Fisheries WH-10
University of Washington
Seattle, WA 98195

Gregg M. Garfin
Laboratory of Tree-Ring Research
University of Arizona
Tucson, AZ 85721

J.W. Geissman
Dept. of Earth and Planetary Sciences
University of New Mexico
Albuquerque, NM 87131
505/277-6529

Sarah E. Gilman
Hopkins Marine Station of Stanford University
Pacific Grove, CA 93950

Eric Gong
Limnological Research Center
Dept. of Geology & Geophysics
University of Minnesota
Minneapolis, MN 55455
612/624-1333

Nicholas E. Graham
Scripps Institution of Oceanography
Climate Research Division, Mail Code A024
La Jolla, CA 92093-0224
graham@grace.ucsd.edu

David Greenland
Department of Geography
University of Oregon
Eugene, OR 97403-1251
503/346-4555 (Fax 503/346-2067)

S.R. Hare
International Pacific Halibut Commission
P.O. Box 95009
University of Washington
Seattle,WA 98145-2009

Martha L. Hemphill
Quaternary Sciences Center
Desert Research Institute
University and Community College System of Nevada
P.O. Box 60220
Reno, NV 89506
702/673-7387

Timothy Herbert
Department of Geological Sciences
Brown University
Providence, RI 02912
401/863-1207
timothy_herbert@brown.edu

Juan Carlos Herguera
Centro de Investigacion Cientifica y de Ensenanza Superior
Carretera Transpeninsular KM. 107
Ensenada, Baja California 22830
Mexico

Katherine K. Hirschboeck
Laboratory of Tree Ring Research
University of Arizona
Tucson, AZ 85721

Steven M. Hodge
Ice and Climate Project
U.S. Geological Survey
University of Puget Sound
Tacoma, WA 98416
206/593-6516

Stephen H. Holets
Pacific Gas & Electric Co.
77 Beale St., Room 1651
San Francisco. CA 94177

A.B. Hollowed
Alaska Fisheries Science Center
National Marine Fisheries Service
7600 Sand Point Way NE
Seattle, WA 98115

Malcolm K. Hughes
Laboratory of Tree-Ring Research
University of Arizona
Tucson, AZ 85721

Caroline M. Isaacs
U.S. Geological Survey
345 Middlefield Road - MS 999
Menlo Park, CA 94025

Emi Ito
Limnological Research Center
Dept. Of Geology & Geophysics
University of Minnesota
Minneapolis, MN 55455
612/624-7881
eito@maroon.tc.umn.edu

David E. Jones
Kent State University
Kent, OH 44242
216/672-7987
djones@gilbert.kent.edu

William A. Jones
Department of Geology and Geophysics
Rice University
Houston, TX 77251

Edward G. Josberger
Ice and Climate Project
U.S. Geological Survey
University of Puget Sound
Tacoma, WA 98416
206/593-6516

Thor Karlstrom
4811 SW Brace Point Drive
Seattle, WA 98136
206/935-7087

Michelle Kashgarian
Lawrence Livermore National Laboratory
P.O. Box 808, L-397
Livermore, CA 94550
510/422-3703

Charles D. Keeling
Scripps Institution of Oceanography
La Jolla, CA 92093-0224

Robert M. Krimmel
Ice and Climate Project
U.S. Geological Survey
University of Puget Sound
Tacoma, WA 98416
206/593-6516

Carina B. Lange
Scripps Institution of Oceanography
Geological Resources Division
9500 Gilman Drive
La Jolla, CA 92093-0215

Mojib Latif
Scripps Institution of Oceanography, 0224
La Jolla, CA 92093

Judith Lean
E.O. Hulburt Center for Space Research
Code 7673L, Naval Research Laboratory
Washington, DC 20375
202/767-5116
lean@demeter.nrl.navy.mil

Anna Lebedev
Oceanography Department
Florida State University
Tallahassee, FL 32306-3048
904/644-2240

Peggy W. Lehman
Environmental Services Office
Department of Water Resources
3251 S Street
Sacramento, CA 95816-7017
916/227-7551; Fax 916/227-7554

Braddock K. Linsley
Department of Geology and Geophysics, MS-126
Rice University
6100 South Main Street
Houston, TX 77005-1892

Mark Losleben
Mountain Research Station
University of Colorado
Nederland, CO 80466
303/492-8841
markl@culter.colorado.edu

Brian H. Luckman
Department of Geography
University of Western Ontario
London, Canada N6A 5C3

Steve Lund
Department of Geological Sciences
University of Southern California
Los Angeles, CA
213/740-5835

David L. Mackas
Institute of Ocean Sciences
Fisheries and Oceans Canada
Sidney, BC V8L 4B2

Nathan. J. Mantua
University of Washington
JISAO, Box 354235
Seattle, WA, 98195-4235
mantua@atmos.washington.edu

Theodore S. Melis
U.S. Geological Survey
Tucson, AZ 85745

Roy Mendelssohn
Pacific Fisheries Environmental Group
1352 Lighthouse Avenue
Pacific Grove, CA 93950
408/648-9034

Arthur J. Miller
Scripps Institution of Oceanography
La Jolla, California 92093-0224
619/534-8033; Fax 619/534-8561
ajmiller@ucsd.edu

Fenbiao Ni
Laboratory of Tree Ring Research
University of Arizona
Tucson, AZ 85721

Heather A. Parker
Pacific Fisheries Environmental Group
1352 Lighthouse Avenue
Pacific Grove, CA 93950
408/648-9032

Valerie Panek
Department of Geology & Geography
West Virginia University
Morgantown, WV 26506
304/293-5603

Richard Parrish
Pacific Fisheries Environmental Group
1352 Lighthouse Avenue
Pacific Grove, CA 93950
408/648-9034

David Peterson
U.S. Geological Survey
345 Middlefield Road
Menlo Park, CA 94025
415/354-3366; Fax 415/254-3363
dhpete@rcamnl.wr.usgs.gov

Miriam R. Peterson
USDA Forest Service
Pacific Northwest Research Station
4043 Roosevelt Way NE
Seattle, WA 98105-6497

William M. Phillips
Department of Geosciences
University of Arizona
Tucson, AZ 85721

Clare Polansky
Department of Geography
501 McCone Hall
University of California, Berkeley
Berkeley, CA 94720
510/643 9170; Fax 510/642-3370

Jeffrey Polovina
Honolulu Laboratory
Southwest Fisheries Science Center
National Marine Fisheries Service
2570 Dole Street
Honolulu, HI 96822-2396

Stephen C. Porter
Quaternary Research Center
University of Washington
Seattle, WA 98195

Roger Pulwarty
National Oceanic and Atmospheric Administration
Boulder, CO

Kelly T. Redmond
Regional Climatologist
Western Regional Climate Center
Desert Research Institute
Reno, NV 89506-0220
702/677-3139; Fax 702/677-3157
krwrcc@nimbus.sage.unr.edu

Larry Riddle
Scripps Institution of Oceanography
Climate Research, UCSD, 0224
La Jolla, CA 92093-0224
lriddle@ucsd.edu

Maurice Roos
California Department of Water Resources
P.O. Box 942836
Sacramento, CA 94236-0001
916/574-2625

H.D. Rowe
Dept. of Earth and Planetary Sciences
University of New Mexico
Albuquerque, NM 87131
505/277-6529
hrowe@unm.edu

Robert Rye
U.S. Geological Survey
MS 963, Denver Federal Center
Lakewood, CO 80225

Franklin B. Schwing
Pacific Fisheries Environmental Group
1352 Lighthouse Avenue
Pacific Grove, CA 93950
408/648-9034
franklin_schwing@ccgate.ssp.nmfs.gov

Gary D. Sharp
Scientific Director
Cooperative Institute for Research in the
Integrated Ocean Sciences, and
Center for Climate/Ocean Resources Study
P.O. Box 2223
Monterey, CA 93940

Alison J. Smith
Department of Geology
Kent State University
Kent, OH 44242
216/672-3709
asmith@kentvm.kent.edu

Paul E. Smith
NOAA/NMFS Southwest Fisheries Science Center
8604 La Jolla Shores Drive
La Jolla, CA 92038

Richard Smith
345 Middlefield Road - MS 496
Menlo Park, CA 94025
415/354-3317; Fax 415/354-3363

Susan J. Smith
Bilby Research Center
Northern Arizona University
Flagstaff, AZ 86011

John Southon
Lawrence Livermore National Laboratory
Livermore, CA 94550

Donald Sullivan
Department of Geography
University of Denver
Denver, CO 80208-0183
303/871-22513; Fax 303/871-4000

Thomas W. Swetnam
Laboratory of Tree-Ring Research
University of Arizona
Tucson, AZ 85721

John J. Vaccaro
U.S. Geological Survey
1201 Pacific Avenue, Suite 600
Tacoma, WA 98402
206/593-6510; Fax 206/593-6514
jvaccaro@fs01dwatcm.wr.usgs.gov

Roy A. Walters
U.S. Geological Survey
1201 Pacific Avenue
Tacoma, WA 98402

Amy L. Weinheimer
Scripps Institution of Oceanography
La Jolla, CA 92093-0220
619/534-7549; Fax 619/534-0784
aweinheimer@ucsd.edu

Gerard M. Wellington
Deptartment of Biology
University of Houston
Houston, Texas 77204-5513

Warren B. White
Scripps Institution of Oceanography
La Jolla, CA 92093-0224
619/534-4826
wbwhite@ucsd.edu

Cathy Whitlock
Geology Department
University of Oregon
Eugene, OR 97403

Timothy Whorf
Scripps Institution of Oceanography
La Jolla, CA 92093-0224

Peter E. Wigand
Quaternary Sciences Center
Desert Research Institute
University and Community College System of Nevada
P.O. Box 60220
Reno, NV 89506
702/673-7387
pwigand@maxey.dri.edu

Raymond C. Wilson
U.S. Geological Survey
345 Middlefield Road, MS998
Menlo Park, CA 94025

Michelle L. Wood
Laboratory of Tree Ring Research
University of Arizona
Tucson, AZ 85721

Connie A. Woodhouse
818 County Road 116
Nederland, CO 80466
303/492-8841
woodhous@culter.colorado.edu

Warren S. Wooster
School of Marine Affairs HF-05
University of Washington
Seattle, WA 98195

Crayton J. Yapp
Department of Earth and Planetary Sciences
University of New Mexico
Albuquerque, NM 87131

PROCEEDINGS OF THE TWELFTH ANNUAL PACIFIC CLIMATE (PACLIM) WORKSHOP

Asilomar, California — May 2-5, 1995

Edited by
Caroline M. Isaacs and Vera L. Tharp

Technical Report 46
of the
Interagency Ecological Program
for the
Sacramento-San Joaquin Estuary

PACLIM

Climate Variability
of the
Eastern North Pacific
and
Western North America

Sponsors

The Twelfth Annual Pacific Climate Workshop was sponsored by:

U.S. GEOLOGICAL SURVEY
Water Resources Division

U.S. GEOLOGICAL SURVEY
Geological Resource Division

NATIONAL OCEANIC AND ATMOSPHERIC ADMINISTRATION
Paleoclimatology Program

CALIFORNIA DEPARTMENT OF WATER RESOURCES
Environmental Services Office

SOUTHERN CALIFORNIA EDISON COMPANY

AMERICAN GEOPHYSICAL UNION

NAVAL POSTGRADUATE SCHOOL

Publication of this proceedings has been sponsored by the

INTERAGENCY ECOLOGICAL PROGRAM
for the
SACRAMENTO-SAN JOAQUIN ESTUARY

A Cooperative Program of:

California Department of Water Resources
State Water Resources Control Board
U.S. Bureau of Reclamation
U.S. Geological Survey
California Department of Fish and Game
U.S. Fish and Wildlife Service
U.S. Army Corps of Engineers
U.S. Environmental Protection Agency
National Marine Fisheries Service

These proceedings were published by the Interagency Ecological Program for the Sacramento-San Joaquin Estuary (Interagency Program)
in a cooperative effort with the
United States Department of the Interior, Geological Survey, Menlo Park, California.
Information generated by the PACLIM Workshop provides the Interagency Program with a climatological perspective that cannot be obtained from its own studies.
Views and conclusions contained in this publication do not necessarily reflect the opinions of the Interagency Program or its member agencies.

Contents

Sponsors iii

Authors ix

Acknowledgments xv

Statement of Purpose xvii

Introduction 1
Caroline M. Isaacs

Simulation of Recent Global Temperature Trends 17
Nicholas E. Graham

Mechanisms of Upper-Ocean Thermal Variability in a 1970-1988 Simulation and Observations 19
Arthur J. Miller, Daniel R. Cayan, Warren B. White

Climate Forcing by Changing Solar Radiation 33
Judith Lean

Effects of Interdecadal Climate Variability on the Oceanic Ecosystems of the Northeast Pacific Ocean 41
Robert C. Francis, S.R. Hare, A.B. Hollowed, Warren S. Wooster

Decadal Hydroclimatic Variability over Western North America 43
Dan Cayan, Mike Dettinger, Henry Diaz

Terrestrial Ecosystem Response to Interdecadal Climate Variability in the Western United States 45
Thomas W. Swetnam and Julio L. Betancourt

Paleorecords of Interdecadal Variability from Mid-Latitude Varved Sediments and Tropical Corals of the Eastern Pacific 47
Tim R. Baumgartner and Robert B. Dunbar

The Terrestrial Record of Interdecadal Climate Variability in Western North America 49
Malcolm K. Hughes

Decadal Climate Variability over the North Pacific and North America: Dynamics and Predictability 51
Mojib Latif and Tim P. Barnett

Interdecadal Variability in the Spatial Structure of Wind and SST in the California Current System 53
Franklin B. Schwing, Roy Mendelssohn, Richard Parrish

Interannual Variability in the PFEG Coastal Upwelling Indices 63
Heather A. Parker

Decadal Variability over the North Pacific Ocean 71
Dan Cayan, Warren White, Art Miller

Interdecadal Shifting of the North Pacific Jet Stream — El Niño Events 73
Stephen H. Holets

Long-Term Changes in the Equatorial Pacific Trade Winds 75
Allan J. Clarke and Anna Lebedeva

Recent Trends in the Climate of the Tropical Pacific Region 77
Nathan J. Mantua and Nicholas E. Graham

Analysis of Four Decades of High Elevation Climate Data 95
Mark Losleben

Relationships between Climate and Atmospheric Circulation in the Sonoran Desert Region 99
Connie A. Woodhouse

Geographic Patterns in the Lag of Temperature Response to Insolation for El Niño vs. La Niña Conditions 105
R.C. Craig, J.L. Betancourt, D.E. Jones

Decadal Patterns in Atmospheric Carbon Dioxide as Indicators of Changing Growth and Decay of Terrestrial Vegetation 107
Charles D. Keeling and Timothy Whorf

Offshore Coho Salmon Populations near the Pacific Northwest and Large-Scale Atmospheric Events 109
David Greenland

Decadal Variation in the Trans-Pacific Migration of Northern Bluefin Tuna (*Thunnus thynnus*) Coherent with Climate-Induced Change in Prey Abundance 121
Jeffrey Polovina

Chronic and Catastrophic Influences of the Environment on the Population Dynamics of the Common Fishes 123
Paul E. Smith

A 10-Year Time Series of Zooplankton Anomalies off the British Columbia Coast 125
David L. Mackas

Physical, Chemical, and Biological Characterization of Water Year Types in San Francisco Bay Estuary 127
Peggy W. Lehman

Climate-Related Long-Term Faunal Changes in a California Rocky Intertidal Community 129
James P. Barry, Charles H. Baxter, Sarah E. Gilman

California Water Conditions in 1995 131
Maurice Roos

Recent Winters in the Western United States and Relationship to ENSO Patterns 141
Kelly T. Redmond

Changes in the Hydrometeorological Regime in the Pacific Southwest 143
John J. Vaccaro

River Salinity Variations in Response to Discharge: Examples from Western United States During the Early 1900s 145
David Peterson, Michael Dettinger, Daniel Cayan, Jeanne DiLeo, Caroline Isaacs, Larry Riddle, Richard Smith

Reconstructing 20th Century Flood Patterns in Havasu Creek, Arizona, Using Historical and Dendrochronologic Data 155
Theodore S. Melis and William M. Phillips

An 800-Year Paleoflood Record from the Sacramento Valley, California 157
Roger Byrne and Donald Sullivan

Can Lake Sediments Provide a Record of Tropical Storms? The Case of Laguna de Juanacatlan, Jalisco, Mexico 159
Roger Byrne, Douglas Allen, Eric Edlund, Clare Polansky

Influence of Climatography on Rainfall Thresholds for Initiation of Debris-Flows on the California Coast 161
Raymond C. Wilson

Disturbance Climate in the Columbia River Basin 163
Sue A. Ferguson and Miriam R. Peterson

Fire, Climate, and Vegetation: The Sedimentary Record of Fire in Montane Meadows, Sierra Nevada, California, USA. 165
R. Scott Anderson and Susan J. Smith

Changes in Mass Balance of South Cascade Glacier, North Cascades, 1959 to 1994 167
Steven M. Hodge, Robert M. Krimmel, Edward G. Josberger

Interannual to Decadal Time-Scale Variations in Glacier Mass Balance. 179
Roy A. Walters

The Little Ice Age: Glacier Variations and Climate Since AD 1250 181
Stephen C. Porter

The Terrestrial Paleorecord of Climate Change over the Past Thousand Years in the Canadian Rockies 183
Brian H. Luckman

Variability in a Radiolarian Time Series and Its Relationship to Climate 185
Amy L. Weinheimer and Daniel R. Cayan

Evidence for Changes in Large-Scale Upwelling in the California Current over the Past 700 Years. 197
Tim R. Baumgartner and John Southon

On the Strength of the California Current: A Record from the Southern Baja California Margin 199
Juan Carlos Herguera, Tim Herbert, Vicente Ferreira Bartrina

Oceanographic Variability at Clipperton Atoll Since the 1880s: Stable Isotopic Evidence from Massive Corals. 201
Braddock K. Linsley and Robert B. Dunbar

Oxygen Isotope Analysis of Corals from the Gulf of California and the Gulf of Panama: Application and Implications for Coral-Based Paleoclimate Reconstructions 203
William A. Jones, Robert B. Dunbar, Gerard M. Wellington

Integrating Varve and Tree-Ring Time Series for Southern California Climate Reconstruction: A 20th Century Outlook 205
Franco Biondi, Carina B. Lange, Kimberly Cobb, Wolfgang Berger

Synoptic Dendroclimatology: A Process-Based Approach for Linking Tree-Ring Information to Atmospheric Circulation over the Pacific and Western North America 207
Katherine K. Hirschboeck, Fenbiao Ni, Michelle L. Wood, Connie A. Woodhouse

Atmospheric Circulation Patterns Associated with Tree Growth Anomalies in the Central and Southern Sierra Nevada Mountains 209
Gregg M. Garfin

Climate-Driven Hydrologic Transients in Holocene Lake Records 211
Alison J. Smith, Joseph J. Donovan, Daniel R. Engstrom, Emi Ito, Valerie Panek, Eric Gong

High-Resolution Record of Climate Change in the Owens Lake Basin, California, for the Period 52,500 to 12,500 YBP 217
Larry Benson, James Burdett, Michaele Kashgarian, Steve Lund, Robert Rye

A Late Pleistocene Paleohydrologic Record of Sierra Nevada Runoff from Owens Lake, California 231
J. Platt Bradbury

A Detailed 2,000-Year Late-Holocene Pollen Record from Lower Pahranagat Lake, Southern Nevada, USA 233
Peter E. Wigand and Martha L. Hemphill

Response of Pacific Northwest Vegetation to Large-Scale Changes in Climate During the Last 100,000 Years 235
Cathy Whitlock and Patrick J. Bartlein

Multiple-Proxy Lacustrine Record of Moisture Transport over Western North America from 24,000 to 12,000 YBP, Lake Estancia, New Mexico 237
Bruce D. Allen, Roger Y. Anderson, Crayton J. Yapp

A Rock-Magnetic and Geomagnetic Secular Variation Record from Late-Pleistocene Lake Estancia, New Mexico 239
H.D. Rowe, J.W. Geissman, Bruce D. Allen, Roger Y. Anderson

The QBO, El Niño, and Tidal Resonance Model 241
Thor Karlstrom

Chronological Records of Climate-Related Events and Societal Consequences 255
Gary D. Sharp

Appendixes

A Agenda 257

B Poster Presentations 263

C Attendees 267

Authors

Bruce D. Allen
Department of Earth and Planetary Sciences
University of New Mexico
Albuquerque, NM 87131

Douglas Allen
Department of Geography
501 McCone Hall
University of California, Berkeley
Berkeley, CA 94720
510/643 9170; Fax 510/642-3370

R. Scott Anderson
Environmental Sciences Program
Northern Arizona University
Flagstaff, AZ 86011

Roger Y. Anderson
Department of Earth and Planetary Sciences
University of New Mexico
Albuquerque, NM 87131

Tim P. Barnett
Scripps Institution of Oceanography, 0224
La Jolla, CA 92093

James P. Barry
Monterey Bay Aquarium Resist Institute
160 Central Avenue
Pacific Grove, CA 93950

Patrick J. Bartlein
Geology Department
University of Oregon
Eugene, OR 97403

Vicente Ferreira Bartrina
Centro de Investigacion Cientifica y de
Ensenanza Superior
Carretera Transpeninsular KM 107
Ensenada, Baja California 22830
Mexico

Tim R. Baumgartner
Scripps Institution of Oceanography
University of California, San Diego
Marine Life Research Group
9500 Gilman Drive, Dept. 0227
La Jolla, CA 92093-0227
619/534-2171; Fax 619/534-7641
trbaumgartner@ucsd.edu
tbaumgar@cicese.mx

Charles H. Baxter
Hopkins Marine Station of Stanford University
Pacific Grove, CA 93950

Larry V. Benson
U.S. Geological Survey
3215 Marine St.
Boulder, CO 80303-1066
303/541-3005

Wolfgang Berger
Scripps Institution of Oceanography
Geological Resources Division
9500 Gilman Drive
La Jolla, CA 92093-0215

Julio L. Betancourt
U.S. Geological Survey
Desert Laboratory
1675 W. Anklam Road
Tucson, AZ 85745

Franco Biondi
Scripps Institution of Oceanography
Geological Resources Division
9500 Gilman Drive
La Jolla, CA 92093-0215

J. Platt Bradbury
U.S. Geological Survey
P.O. Box 25046, MS 919
Federal Center
Denver, CO 80225

James W. Burdett
U.S. Geological Survey
MS 963, Denver Federal Center
Lakewood, CO 80225
303/236-5916

Roger Byrne
Department of Geography
University of California, Berkeley
Berkeley, CA 94720
510/643-9170; Fax 510/642-3370

Daniel R. Cayan
Scripps Institution of Oceanography
La Jolla, CA 92093-0220
619/534-4507; Fax 619/534-8561
dcayan@ucsd.edu

Allan J. Clarke
Oceanography Department
Florida State University
Tallahassee, FL 32306-3048
904/644-2240
clarke@ocean.fsu.edu

Kimberly Cobb
P.O. Box 20416
New Haven, CT 06520

R.C. Craig
Department of Geology
Kent State University
Kent, OH 44240
216/672-7987; Fax 216/672-7949
rcraig@gilbert.kent.edu

Michael Dettinger
U.S. Geological Survey
5735 Kearny Villa Road, Suite O
San Diego, CA 92123-1135
619/637-6856; Fax 619/637-9201
mddettin@s101pcasnd.wr.usgs.gov

Henry Diaz
NOAA-ERL-CDC
325 Broadway
Boulder, CO 80303
303/497-6649; Fax 303/497-7013
hfd@ncdc.noaa.gov

Jeanne DiLeo
U.S. Geological Survey
345 Middlefield Road
Menlo Park, CA 94025

Joseph J. Donovan
Dept. Of Geology & Geography
West Virginia University
Morgantown, WV 26506
304/293-5603
donovan@wvugeo.wvnet.edu

Robert B. Dunbar
Department of Geology
Rice University
P.O. Box 1892F
Houston, TX 77251
713/527-4883

Eric Edlund
Department of Geography
501 McCone Hall
University of California, Berkeley
Berkeley, CA 94720
510/643 9170; Fax 510/642-3370

Daniel R. Engstrom
St. Croix Watershed Research Station
Science Museum of Minnesota
Marine on St. Croix, MN 55047
612/433-5953
dre@maroon.tc.umn.edu

Sue A. Ferguson
USDA Forest Service
Pacific Northwest Research Station
4043 Roosevelt Way NE
Seattle, WA 98105-6497

Robert C. Francis
School of Fisheries WH-10
University of Washington
Seattle, WA 98195

Gregg M. Garfin
Laboratory of Tree-Ring Research
University of Arizona
Tucson, AZ 85721

J.W. Geissman
Dept. of Earth and Planetary Sciences
University of New Mexico
Albuquerque, NM 87131
505/277-6529

Sarah E. Gilman
Hopkins Marine Station of Stanford University
Pacific Grove, CA 93950

Eric Gong
Limnological Research Center
Dept. of Geology & Geophysics
University of Minnesota
Minneapolis, MN 55455
612/624-1333

Nicholas E. Graham
Scripps Institution of Oceanography
Climate Research Division, Mail Code A024
La Jolla, CA 92093-0224
graham@grace.ucsd.edu

David Greenland
Department of Geography
University of Oregon
Eugene, OR 97403-1251
503/346-4555 (Fax 503/346-2067)

S.R. Hare
International Pacific Halibut Commission
P.O. Box 95009
University of Washington
Seattle,WA 98145-2009

Martha L. Hemphill
Quaternary Sciences Center
Desert Research Institute
University and Community College System of Nevada
P.O. Box 60220
Reno, NV 89506
702/673-7387

Timothy Herbert
Department of Geological Sciences
Brown University
Providence, RI 02912
401/863-1207
timothy_herbert@brown.edu

Juan Carlos Herguera
Centro de Investigacion Cientifica y de Ensenanza Superior
Carretera Transpeninsular KM. 107
Ensenada, Baja California 22830
Mexico

Katherine K. Hirschboeck
Laboratory of Tree Ring Research
University of Arizona
Tucson, AZ 85721

Steven M. Hodge
Ice and Climate Project
U.S. Geological Survey
University of Puget Sound
Tacoma, WA 98416
206/593-6516

Stephen H. Holets
Pacific Gas & Electric Co.
77 Beale St., Room 1651
San Francisco. CA 94177

A.B. Hollowed
Alaska Fisheries Science Center
National Marine Fisheries Service
7600 Sand Point Way NE
Seattle, WA 98115

Malcolm K. Hughes
Laboratory of Tree-Ring Research
University of Arizona
Tucson, AZ 85721

Caroline M. Isaacs
U.S. Geological Survey
345 Middlefield Road - MS 999
Menlo Park, CA 94025

Emi Ito
Limnological Research Center
Dept. Of Geology & Geophysics
University of Minnesota
Minneapolis, MN 55455
612/624-7881
eito@maroon.tc.umn.edu

David E. Jones
Kent State University
Kent, OH 44242
216/672-7987
djones@gilbert.kent.edu

William A. Jones
Department of Geology and Geophysics
Rice University
Houston, TX 77251

Edward G. Josberger
Ice and Climate Project
U.S. Geological Survey
University of Puget Sound
Tacoma, WA 98416
206/593-6516

Thor Karlstrom
4811 SW Brace Point Drive
Seattle, WA 98136
206/935-7087

Michelle Kashgarian
Lawrence Livermore National Laboratory
P.O. Box 808, L-397
Livermore, CA 94550
510/422-3703

Charles D. Keeling
Scripps Institution of Oceanography
La Jolla, CA 92093-0224

Robert M. Krimmel
Ice and Climate Project
U.S. Geological Survey
University of Puget Sound
Tacoma, WA 98416
206/593-6516

Carina B. Lange
Scripps Institution of Oceanography
Geological Resources Division
9500 Gilman Drive
La Jolla, CA 92093-0215

Mojib Latif
Scripps Institution of Oceanography, 0224
La Jolla, CA 92093

Judith Lean
E.O. Hulburt Center for Space Research
Code 7673L, Naval Research Laboratory
Washington, DC 20375
202/767-5116
lean@demeter.nrl.navy.mil

Anna Lebedev
Oceanography Department
Florida State University
Tallahassee, FL 32306-3048
904/644-2240

Peggy W. Lehman
Environmental Services Office
Department of Water Resources
3251 S Street
Sacramento, CA 95816-7017
916/227-7551; Fax 916/227-7554

Braddock K. Linsley
Department of Geology and Geophysics, MS-126
Rice University
6100 South Main Street
Houston, TX 77005-1892

Mark Losleben
Mountain Research Station
University of Colorado
Nederland, CO 80466
303/492-8841
markl@culter.colorado.edu

Brian H. Luckman
Department of Geography
University of Western Ontario
London, Canada N6A 5C3

Steve Lund
Department of Geological Sciences
University of Southern California
Los Angeles, CA
213/740-5835

David L. Mackas
Institute of Ocean Sciences
Fisheries and Oceans Canada
Sidney, BC V8L 4B2

Nathan. J. Mantua
University of Washington
JISAO, Box 354235
Seattle, WA, 98195-4235
mantua@atmos.washington.edu

Theodore S. Melis
U.S. Geological Survey
Tucson, AZ 85745

Roy Mendelssohn
Pacific Fisheries Environmental Group
1352 Lighthouse Avenue
Pacific Grove, CA 93950
408/648-9034

Arthur J. Miller
Scripps Institution of Oceanography
La Jolla, California 92093-0224
619/534-8033; Fax 619/534-8561
ajmiller@ucsd.edu

Fenbiao Ni
Laboratory of Tree Ring Research
University of Arizona
Tucson, AZ 85721

Heather A. Parker
Pacific Fisheries Environmental Group
1352 Lighthouse Avenue
Pacific Grove, CA 93950
408/648-9032

Valerie Panek
Department of Geology & Geography
West Virginia University
Morgantown, WV 26506
304/293-5603

Richard Parrish
Pacific Fisheries Environmental Group
1352 Lighthouse Avenue
Pacific Grove, CA 93950
408/648-9034

David Peterson
U.S. Geological Survey
345 Middlefield Road
Menlo Park, CA 94025
415/354-3366; Fax 415/254-3363
dhpete@rcamnl.wr.usgs.gov

Miriam R. Peterson
USDA Forest Service
Pacific Northwest Research Station
4043 Roosevelt Way NE
Seattle, WA 98105-6497

William M. Phillips
Department of Geosciences
University of Arizona
Tucson, AZ 85721

Clare Polansky
Department of Geography
501 McCone Hall
University of California, Berkeley
Berkeley, CA 94720
510/643 9170; Fax 510/642-3370

Jeffrey Polovina
Honolulu Laboratory
Southwest Fisheries Science Center
National Marine Fisheries Service
2570 Dole Street
Honolulu, HI 96822-2396

Stephen C. Porter
Quaternary Research Center
University of Washington
Seattle, WA 98195

Roger Pulwarty
National Oceanic and Atmospheric Administration
Boulder, CO

Kelly T. Redmond
Regional Climatologist
Western Regional Climate Center
Desert Research Institute
Reno, NV 89506-0220
702/677-3139; Fax 702/677-3157
krwrcc@nimbus.sage.unr.edu

Larry Riddle
Scripps Institution of Oceanography
Climate Research, UCSD, 0224
La Jolla, CA 92093-0224
lriddle@ucsd.edu

Maurice Roos
California Department of Water Resources
P.O. Box 942836
Sacramento, CA 94236-0001
916/574-2625

H.D. Rowe
Dept. of Earth and Planetary Sciences
University of New Mexico
Albuquerque, NM 87131
505/277-6529
hrowe@unm.edu

Robert Rye
U.S. Geological Survey
MS 963, Denver Federal Center
Lakewood, CO 80225

Franklin B. Schwing
Pacific Fisheries Environmental Group
1352 Lighthouse Avenue
Pacific Grove, CA 93950
408/648-9034
franklin_schwing@ccgate.ssp.nmfs.gov

Gary D. Sharp
Scientific Director
Cooperative Institute for Research in the
Integrated Ocean Sciences, and
Center for Climate/Ocean Resources Study
P.O. Box 2223
Monterey, CA 93940

Alison J. Smith
Department of Geology
Kent State University
Kent, OH 44242
216/672-3709
asmith@kentvm.kent.edu

Paul E. Smith
NOAA/NMFS Southwest Fisheries Science Center
8604 La Jolla Shores Drive
La Jolla, CA 92038

Richard Smith
345 Middlefield Road - MS 496
Menlo Park, CA 94025
415/354-3317; Fax 415/354-3363

Susan J. Smith
Bilby Research Center
Northern Arizona University
Flagstaff, AZ 86011

John Southon
Lawrence Livermore National Laboratory
Livermore, CA 94550

Donald Sullivan
Department of Geography
University of Denver
Denver, CO 80208-0183
303/871-22513; Fax 303/871-4000

Thomas W. Swetnam
Laboratory of Tree-Ring Research
University of Arizona
Tucson, AZ 85721

John J. Vaccaro
U.S. Geological Survey
1201 Pacific Avenue, Suite 600
Tacoma, WA 98402
206/593-6510; Fax 206/593-6514
jvaccaro@fs01dwatcm.wr.usgs.gov

Roy A. Walters
U.S. Geological Survey
1201 Pacific Avenue
Tacoma, WA 98402

Amy L. Weinheimer
Scripps Institution of Oceanography
La Jolla, CA 92093-0220
619/534-7549; Fax 619/534-0784
aweinheimer@ucsd.edu

Gerard M. Wellington
Deptartment of Biology
University of Houston
Houston, Texas 77204-5513

Warren B. White
Scripps Institution of Oceanography
La Jolla, CA 92093-0224
619/534-4826
wbwhite@ucsd.edu

Cathy Whitlock
Geology Department
University of Oregon
Eugene, OR 97403

Timothy Whorf
Scripps Institution of Oceanography
La Jolla, CA 92093-0224

Peter E. Wigand
Quaternary Sciences Center
Desert Research Institute
University and Community College System of Nevada
P.O. Box 60220
Reno, NV 89506
702/673-7387
pwigand@maxey.dri.edu

Raymond C. Wilson
U.S. Geological Survey
345 Middlefield Road, MS998
Menlo Park, CA 94025

Michelle L. Wood
Laboratory of Tree Ring Research
University of Arizona
Tucson, AZ 85721

Connie A. Woodhouse
818 County Road 116
Nederland, CO 80466
303/492-8841
woodhous@culter.colorado.edu

Warren S. Wooster
School of Marine Affairs HF-05
University of Washington
Seattle, WA 98195

Crayton J. Yapp
Department of Earth and Planetary Sciences
University of New Mexico
Albuquerque, NM 87131

Acknowledgments

The PACLIM workshops are produced by an array of enthusiastic volunteers. For 1995, enormous thanks go to Don Gautier, the new general workshop chairman, and his able assistant Tim Klett for their multitudinous behind-the-scenes activities. Special thanks also go to Bonnie Claus and Shirley Person for registration at the meeting (and much other assistance), Tom Murphree for providing the audiovisual equipment, and Jeanne DiLeo for designing the PACLIM 1995 mugs.

Sponsorship and funding for the workshops comes from a wide variety of sources. In addition to the agencies and programs responsible (listed separately), we also thank all those who helped in the funding process, including Walt Dean, Harry Lins, Dick Poore, Mark Eakin, Jim Young, Fred Spilhaus, and Randy Brown.

For the scientific agenda of the workshop, we thank the indomitable Dan Cayan, with secretarial assistance from Nicki Pyles and logistic support from Larry Riddle. We also salute Tim Baumgartner who, together with Dan, co-organized and co-chaired the workshop theme session on "Interdecadal Climate Variability over the Pacific and Western Americas", raised the funds to provide travel for invited speakers, and enlisted the *Journal of Climate* in publishing the session as a special issue. The other meeting chairs and moderators are also gratefully acknowledged — Paul Smith, Larry Benson, and Mike Dettinger. Finally, we thank all our speakers and poster presenters for their contributions and enthusiasm — Nathan Mantua, Kelly Redmond, Ray Wilson, Maurice Roos, Nick Graham, Art Miller, Judith Lean, Dan Cayan, Tom Swetnam, Bob Francis, Malcolm Hughes, Tim Baumgartner, Roger Pulwarty, Stephen Porter, David Greenland, Anna Lebedeva, Dave Peterson, Franklin Schwing, David Mackas, James Barry, Charles Keeling, Paul Smith, Roger Byrne, Jeffrey Polovina, Tim Barnett, Brian Luckman, Katherine Hirschboeck, Franco Biondi, Larry Benson, William Jones, Scott Anderson, Bruce Allen, Roger Anderson, Platt Bradbury, Eric Edlund, Julio Betancourt, David Jones, Sue Ferguson, Gregg Garfin, Juan Herguera, Steve Hodge, Stephen Holets, Thor Karlstrom, Peggy Lehman, Brad Linsley, Rob Dunbar, Mark Losleben, Theodore Melis, Heather Parker, Harry Rowe, Bruce Allen, Gary Sharp, Alison Smith, John Vaccaro, Roy Walters, Amy Weinheimer, Cathy Whitlock, Peter Wigand, and Connie Woodhouse.

For the Proceedings volume, enormous thanks go to Vera Tharp for her patience with diverse format types and her incredible expertise with technical editing, graphics, tables, and highly skilled pasting. Invaluable precedents for the 1995 volume were established by the previous editors of the PACLIM Proceedings — Dave Peterson (1984-1988) with the able assistance of Lucenia Thomas, Julio Betancourt and Ana MacKay (1989-1990), and Kelly Redmond and Vera Tharp (1991-1993). Special thanks also go to all the authors who contributed.

Caroline Isaacs
U.S. Geological Survey
Menlo Park, California

STATEMENT OF PURPOSE
Pacific Climate (PACLIM) Workshops

In 1984, a workshop was held on "Climatic Variability of the Eastern North Pacific and Western North America". From it has emerged an annual series of workshops held at the Asilomar Conference Center, Monterey Peninsula, California. These annual meetings, which involve 80-100 participants, have come to be known as PACLIM (Pacific Climate) Workshops, reflecting broad interests in the climatologies associated with the Pacific Ocean and western Americas in both the northern and southern hemispheres. Participants have included atmospheric scientists, hydrologists, glaciologists, oceanographers, limnologists, and both marine and terrestrial biologists. A major goal of PACLIM is to provide a forum for exploring the insights and perspectives of each of these many disciplines and for understanding the critical linkages between them.

PACLIM arose from growing concern about climate variability and its societal and ecological impacts. Storm frequency, snowpack, droughts and floods, agricultural production, water supply, glacial advances, stream chemistry, sea surface temperature, salmon catch, lake ecosystems, and wildlife habitat are among the many aspects of climate and climatic impacts addressed by PACLIM Workshops. Workshops also address broad concerns about the impact of possible climate change over the next century. From observed changes in the historical record, the conclusion is evident that climate change would have large societal impacts through effects on global ecology, hydrology, geology, and oceanography.

Our ability to predict climate, climate variability, and climate change critically depends on an understanding of global processes. Human impacts are primarily terrestrial in nature, but the major forcing processes are atmospheric and oceanic in origin and transferred through geologic and biologic systems. Our understanding of the global climate system and its relationship to ecosystems in the Eastern Pacific area arises from regional study of its components in the Pacific Ocean and western Americas, where ocean/atmosphere coupling is strongly expressed. Empirical evidence suggests that large-scale climatic fluctuations force large-scale ecosystem response in the California Current and in a very different system, the North Pacific central gyre. With such diverse meteorologic phenomena as the El Niño-Southern Oscillation and shifts in the Aleutian Low and North Pacific High, the Eastern Pacific has tremendous global influences and particularly strong effects on North America. In the western United States, where rainfall is primarily a cool-season phenomenon, year-to-year changes in the activity and tracking of North Pacific winter storms have substantial influence on the hydrological balance. This region is rich in climatic records, both instrumental and proxy. Recent research efforts are beginning to focus on better paleoclimatic reconstructions that will put present-day climatic variability in context and allow better anticipation of future variations and changes.

The PACLIM Workshops address the problem of defining regional coupling of multifold elements, as organized by global phenomena. Because climate expresses itself throughout the natural system, our activity has been, from the beginning, multidisciplinary in scope. The specialized knowledge from different disciplines has brought together climatic records and process measurements to synthesize an understanding of the complete system. Our interdisciplinary group uses diverse time series, measured both directly and through proxy indicators, to study past climatic conditions and current processes in this region. Characterizing and linking the geosphere, biosphere, and hydrosphere in this region provides a scientific analogue and, hence, a basis for understanding similar linkages in other regions, as well as for anticipating the response to future climate variations. Our emphasis in PACLIM is to study the interrelationships among diverse data. To understand these interactive phenomena, we incorporate studies that consider a broad range of topics both physical and biological, time scales from months to millennia, and space scales from single sites to the entire globe.

An overview of the PACLIM Workshops was published in the December 30, 1986, issue of *EOS*.
Proceedings of PACLIM Workshops are published annually by the
California Department of Water Resources as Technical Reports of the
Interagency Ecological Program for the Sacramento-San Joaquin Estuary.
A multi-disciplinary collection of research papers, spawned at least partially by interactions in the initial PACLIM Workshops, was published as *AGU Geophysical Monograph 55* (Peterson, ed., 1989).

Introduction

Caroline M. Isaacs

The Twelfth Annual PACLIM Workshop was held at the Asilomar Conference Center on May 2-5, 1995. The workshop included 32 talks and 26 posters presentations. The talks consisted of a 1-day theme session of nine 45-minute talks and two featured evening talks (Appendix A). Throughout the remainder of the meeting were over 20 shorter 20-minute presentations. Poster presenters gave a 1-2 minute introduction to their posters, which were displayed during the entire meeting (Appendix B). About 100 participants were registered at the workshop (Appendix C).

In this Proceedings volume, talks and posters have been combined and grouped by broad categories of subject matter — Theme Session on Interdecadal Climate Variability, Ocean/Atmosphere System, Fisheries, Hydrology, Hazards, Glaciers, Proxy Calibration, Pollen and Lake Records, and Time-Series Compilations. All presenters were invited to expand their abstracts into a manuscript for inclusion in the Proceedings volume, and all presentations (except Pulwarty's) are included in manuscript or abstract form. In addition to this year's Proceedings volume, the theme session is being prepared separately for journal publication.

Interdecadal Climate Variability

As previous PACLIM workshops have detailed for some years, climate variability is expressed at many time scales — from daily variations to millennial and longer changes. One scale especially important to societal and scientific concerns is decadal-scale variability. Regimes lasting several years to decades are widely observed in the climate record — and, because of their persistence, may have broad impact on natural systems (Swetnam and Betancourt, this volume). Famine-producing droughts, persistent "abnormal" flooding, high or low snowpacks, major changes in fish and other ecosystems all occur at a decadal scale. The Dust Bowl of the 1930s and the California drought of the 1980s are two examples from the recent historical record. Increasing resolution and spatial coverage of paleoclimate by proxy records shows that decadal-scale variability has been a persistent feature of the climate system for millennia (*eg*, Thompson and Mosley-Thompson 1989; Thompson 1991). For the scientist, interdecadal variability also introduces a "wild card" in trend analysis. Because most instrumental records cover no more than 100 years, and many records just a decade or so, interdecadal variability makes deciphering long-term trends often problematic. The 1976 step-like change in Pacific climate (Ebbesmeyer *et al* 1991) and similar "regime shifts" (*eg*,

Schimmelmann and Tegner 1992; Schwing 1994) are examples of interdecadal climate variability that can confound simple trend analysis.

What are the characteristics and causes of decadal-scale climate variability? At the 1995 PACLIM workshop, simulations of interdecadal changes in the ocean/atmosphere system explore a variety of important mechanisms and feedback scenarios. **Graham** (this volume) addresses the apparent rise in global average tropospheric temperatures over the last century and the apparent sharp rise since the mid-1970s. Using model simulation, Graham attributes the rise to enhancement of the tropical hydrologic cycle — principally an increase in the flux of moisture through the cycle — driven by increasing tropical ocean temperatures.

Miller *et al* (this volume) focus on upper-ocean temperature in the North Pacific, modeling the thermal and velocity fields over a two-decade period as forced by monthly "observed" total surface heat flux anomalies and wind stress anomalies. This simulation reproduces prominent North Pacific thermal anomalies at monthly to decadal time scales, providing some justification that such models can be used to explain the underlying physics and to "fill in" characteristics of the ocean variability that are not adequately observed. Miller *et al* also discuss maintenance of climate regimes through ocean dynamics, such as re-emerging wintertime SST anomalies surviving beneath the shallow summer mixed layer.

One of the most obvious candidates for climate forcing at an interdecadal scale is solar irradiance, which has a well known 11-year cycle superimposed on many other scales of variability. **Lean** (this volume) reviews current knowledge of the amplitudes and time scales of variability in solar radiative output available from contemporary monitoring and historical reconstructions. From the high correlation (0.86) between decadal mean reconstructed solar irradiance and decadal mean Northern Hemisphere surface temperature anomalies, Lean concludes that solar influences were predominant on decadal-scale climate variations during the pre-industrial period, 1610-1800.

Hydrologic and ecosystem responses to interdecadal ocean/atmosphere variability may be rather complex. **Francis *et al*** (this volume) point out that linkages between physical conditions and biological responses in the ocean often differ across time and space scales, and present knowledge contains only hints of the mechanisms of interaction. Although hydrologic responses also vary temporally and spatially, **Cayan *et al*** (this volume) show that precipitation, snowpack, and streamflow records reveal mutually consistent decadal-scale fluctuations over regional spatial scales (about 1000 kilometers). This decadal-scale hydrological variability has its roots in low-frequency fluctuations in atmospheric circulation. Some evidence suggests, however, that both hydrological and atmospheric circulation fluctuations may be associated with Pacific

Basin scale (and larger) anomaly patterns in sea surface temperature. Interestingly, the decadal SST anomaly patterns are spatially very similar to patterns that occur on ENSO time scales.

In terrestrial ecosystems, decadal scale climatic shifts have broadscale impacts. Examples include the drought of the 1930s in the Great Plains — the well-known Dust Bowl — and the drought of the 1950s in the southwestern United States, which culminated in widespread vegetation dieoff (**Swetnam and Betancourt**, this volume). Such episodes raise questions about the scale and amplitude of natural variability in comparison to anthropogenic influences, emphasizing the increasing importance of high-resolution proxies to determine natural ranges of variability for ecosystem management (Swetnam and Betancourt, this volume).

Two presentations discuss proxy time series at an interdecadal scale. **Baumgartner and Dunbar** (this volume) compare paleorecords of oxygen isotopes in coral bands at subannual resolution from the Galapagos Islands and fish scale abundance in varved sediment at 5-year resolution from the Santa Barbara Basin. Both records show spectral peaks at 17 years, 30 years, and 50 years, but each cycle length occurs in a distinct epoch — the 50-year cycle in the period 1670-1750 AD, the 33-year cycle in the period 1750-1850, and the 17-year cycle in the period 1860-1925. **Hughes** (this volume) reviews the wealth of natural records in western North America for studying interdecadal climate variability. Emphasis is on sub-continental tree-ring networks yielding spatial distribution of summer temperatures and winter half-year precipitation over the past 300-400 years.

In a synthesis of the dynamics and predictability of decadal climate variability, **Latif and Barnett** (this volume) describe a state-of-the-art coupled ocean/atmosphere general circulation model supporting the thesis that decadal variability over the North Pacific and North America is based on a cycle involving an organized pattern of ocean/atmosphere interactions over the North Pacific. The cycle, with a period of a few decades, involves the subtropical ocean gyre and the Aleutian low, the two major circulation fixtures in the North Pacific ocean/atmosphere system. Knowledge of such a cycle would provide a powerful tool for climate forecasting several years ahead over North America.

Ocean/Atmosphere System

A series of contributions discuss important aspects of variability in the ocean/atmosphere system at interdecadal and shorter scales. The first two papers examine spatial variability in long-term trends. Applying state-space statistical models to time series of wind stress and sea

surface temperature from the California Current (22°-48°N) for 1946-1990, **Schwing *et al*** (this volume) show that trends are not coherent between different regions along this coastal domain. The distinct latitudinal regionalization and cross-shelf variability has important implications for ecosystems studies as well as fisheries management and illustrates the value of evaluating the entire spectrum of temporal and spatial variability in climate research.

In the same area, **Parker** (this volume) examines 49-year time series of monthly mean upwelling indices along the North American coast during 1946-1994. Significant changes in the seasonal cycle of upwelling are apparent at interannual to decadal scales, but these changes are manifested quite differently at the three locations examined (57°N, 39°N, and 21°N). The most notable change is a sharp increase in spring upwelling at 21°N since the summer of 1976, apparently the result of relatively small shifts in atmospheric pressure gradients.

Cayan *et al* (this volume) examine instrumental records of the ocean/atmosphere system in the North Pacific for decadal-scale variability. The primary mode identified resembles a low frequency PNA pattern, involving strengthening and weakening of the Aleutian Low with cool anomalies in the central/western North Pacific mid-latitudes and warm anomalies in tropics/subtropics and along the eastern boundary — alternating to opposite phase after about 12 years. Decadal variations beyond the North Pacific are also discussed, and possible mechanisms — including ocean/atmosphere feedback — are considered.

Also in the North Pacific, **Holets** (this volume) compares wintertime polar-front jet stream positions during El Niño events before and after the 1975-1976 step-like change in SST. Although the wintertime jet stream patterns were similar across the North Pacific during El Niños within the two time periods, composites of the two jet stream patterns show a change in position, suggesting an interdecadal shift with implications for California rainfall.

Interdecadal changes in equatorial Pacific trade winds are analyzed by **Clarke and Lebedeva** (this volume). Using surface pressure difference as a proxy for zonally integrated wind stress, they suggest that equatorial trade winds have varied on decadal scales throughout the century — strengthening during the 1920s and 1930s, weakening from the mid-1940s to late 1950s, strengthening during the 1960s, and weakening rapidly since. Comparison with eastern Pacific sea surface temperature proxy records from corals suggests that similar oscillations extend back at least to 1600 AD.

According to **Mantua and Graham** (this volume), upper ocean temperature records from the tropical Pacific show broad-scale warming in the two periods 1976-1983 and 1990-1994. Numerous other climatic

indices — including upper ocean temperature records, the Southern Oscillation Index, central Pacific precipitation, and surface windstress across the equatorial Pacific — exhibit multi-year variability that is physically coherent with the upper ocean records, showing the system-wide scale of the warmings.

Analyzing more than 40 years of instrumental climate records on Niwot Ridge in the Colorado Rockies, **Losleben** (this volume) concludes that long-term trends show no significant changes in annual temperature averages but a long-term trend of decreasing fall temperatures and, at high elevation, increased precipitation. A notable feature of the record is the 1981-1985 "cold event", with annual temperature averages 3°C colder than in the rest of the record.

Turning to the influence of large-scale atmospheric circulation on regional climate, **Woodhouse** (this volume) focuses on winters of the Sonoran Desert. Based on principal component analysis of wintertime climate (the number of rainy days and average maximum temperatures) at 50 stations with six circulation indices (Southern Oscillation, equatorial Pacific sea surface temperature, modified Pacific North American, cyclone frequency, southwestern trough, and Pacific high/southwestern low), two components are identified that explain a significant amount of the climate variation. The two patterns can be described as a "typical" ENSO/positive PNA-type pattern, and a reverse PNA-type pattern characterized by a trough over the southwestern United States.

Also looking at climate characterization, **Craig *et al*** (this volume) explore moisture-driven modulations of the annual temperature cycle by examining the lag between insolation and maximum daily temperature at 252 stations in the western United States for 1961-1990. Results show that largest lags are in maritime settings and smallest lags are in semiarid regions. Interannual variations related to El Niño/La Niña also show the influence of moisture entrained by the jet stream.

Keeling and Whorf (this volume) discuss decadal patterns in atmospheric CO_2 as indicators of changing growth and decay of terrestrial vegetation. After adjustment for combustion of fossil fuels, residual trends of atmospheric CO_2 show a relationship to decadal-scale variations in surface air temperature, and new evaluation suggests that residual trends may also reflect seasonal variations. Because the amplitude of the seasonal cycle in atmospheric CO_2 measures the large-scale metabolic activity of land plants, changes in these relationships allow estimate of the fraction of CO_2 sequestered in the terrestrial biosphere during especially warm periods.

Fisheries and Biological Communities

Fisheries, and the character and complexity of linkages between climate and marine ecosystems, are addressed by a series of workshop presentations. **Greenland** (this volume) discusses the interrelationship between Coho salmon population offshore the Pacific Northwest and large-scale atmospheric events. Greenland identifies relationships at two time scales: (1) a 3-7 year variation related to the El Niño/Southern Oscillation, associated with warmwater anomalies and depressed salmon catches; and (2) a postulated 20-year variation related to Subarctic Current modes, with depressed salmon catches associated with strong water movement into the Alaskan gyre and enhanced salmon catches associated with strong water movement into the California Current. At lower latitudes, decadal-scale variations are also noted in the trans-Pacific migration of northern bluefin tuna (**Polovina**, this volume). Because the bluefin spawns only in the western Pacific, the proportion of juveniles migrating to the eastern Pacific determines the stock in that area. Decadal-scale variations in eastern Pacific abundance are apparently related to the distribution of the Japanese sardine, a key bluefin prey.

Paul Smith (this volume) overviews modeling environmental influences on the population dynamics of the common fishes. For chronic influences — seasonal, interannual, decadal, and centennial influences — fisheries models can now fairly successfully describe and predict population dynamics, requiring input of precise information at low time resolution. By contrast, fisheries models have difficulty predicting the effect of catastrophic influences — such as massive expatriation due to rapid transport of large surface volumes — and successful monitoring and predictive modeling would require information that, although cruder, was available at higher time resolution.

Spatial and temporal variability in zooplankton is detailed by **Mackas** (this volume) who examines 10-year time series of both zooplankton biomass and species composition at multiple sample locations off the British Columbia coast. An interesting feature of his results is the marked interannual anomalies in species composition lasting 0.3-5 years. Though not notably stronger in El Niño years, the anomalies are apparently coupled to longer-term changes in North Pacific ocean/atmosphere conditions since 1988. Reviewing a 23-year time series of physical and environmental variables in the San Francisco Bay estuary, **Lehman** (this volume) characterizes conditions associated with wet, normal, dry, and critical water year types. Results show that the biological community (phytoplankton chlorophyll *a* concentration and community composition) varied significantly more than did environmental conditions.

In the intertidal zone, a resurvey of invertebrate species — in a transect originally surveyed in 1931 — assesses shifts in community structure over the last 60 years (**Barry *et al*,** this volume). Of 45 species in the transect, the abundance of eight (out of nine) southern species increased and the abundance of five (out of eight) northern species decreased, a pattern consistent with poleward migration due to warming over the period. Measurements at the site also show that annual mean shoreline ocean temperatures increased 0.75°C, and mean summer maximum temperatures increased 2.2°C between 1921-1931 and 1983-1993.

Hydrology

The next series of contributions address hydrologic issues. At the 1994 PACLIM workshop, Maurice Roos of the California Department of Water Resources, in surveying recent years of precipitation, queried "Has the California Drought Returned?" (Roos, 1995). After 6 years of drought during 1987-1992, the 1993 water year ended the California drought with about 150% of average precipitation and good carryover reservoir capacity (Roos, 1994), but the low 1994 water year again placed California in a "drought watch" mode. The "drought watch" ended with two large rain months (January and March 1995), which made 1995 one of the wettest years of the century. **Roos** (this volume) describes the season in detail, the major storms, and the performance of reservoirs and flood control systems at near capacity.

Addressing the relationship between recent winters in the western United States and ENSO patterns, **Redmond** (this volume) points out the impact of recent droughts on water allocation throughout the west and salmon population in the Pacific Northwest. He describes a new tool — the Standardized Precipitation Index — to replace the Palmer Drought Index for evaluating climate elements on different time scales. His analysis suggests that the last four winters represent more or less constant El Niño conditions, and that resulting snowpack conditions have been consistent with patterns of the last 60 years.

In a longer view of Pacific Northwest precipitation and hydrologic response, **Vaccaro** (this volume) examines precipitation records for 50 sites and streamflow records for 112 sites throughout the period of instrumental data. Three different periods of persistent conditions were identified — pre-1947, 1947-1976, and post-1976. The base period (1947-1976) had consistently higher water-year precipitation and stream discharge than earlier or later periods, but the highest runoff-season precipitation was in the post-1976 period. Together, the data suggest a change in the hydrometeorological regime post-1976 with increased runoff-season precipitation over part of the Pacific Northwest and decreased water-year precipitation and streamflow over most of the region.

Because river salinity and soil salinization are major issues affecting water use throughout the western United States, the impact of climate on salinity is explored by **Peterson *et al*** (this volume). Overall, the effect of wetter climate is to increase river discharge and decrease soil and river salinity; the effect of dryer climate is the reverse. Applying statistical-dynamical methods to water quality surveys from the early 1900s to minimize the effects of human impact, the study shows that much variability in river salinity in the western United States can be characterized as a response to storm and annual discharge.

Hazards — Floods, Fires, and Ecosystem Disturbances

One of the most prominent hazards of short-term climate variability is flooding. Because of the episodic nature of floods, however, flood histories are rarely known well enough to predict the full range of likely magnitudes and frequencies. An excellent example of resulting unexpected havoc was the 1990 flood of Havasu Creek, an inhabited tributary of the Colorado River in the Grand Canyon (**Melis and Phillips,** this volume). Although perennial streamflow averages about 2 m^3/s, the 1990 flood peaked at about 575 m^3/s, scouring local trees, reshaping pools and waterfalls, and causing severe damage to a nearby town. Using historical accounts and photographs, Melis and Phillips reconstructed flood histories for the creek, finding that similar large floods occurred frequently in the late 19th and early 20th centuries. While floods in 1940-1990 were unusually small, the recent flood pattern more closely resembles the dynamic flood regime of the early 20th century.

Turning to flood histories in the more distant geologic past, **Byrne and Sullivan** (this volume) present preliminary results on paleoflood records for the past 800 years in the Sacramento Valley. The records derive from sediment cored in an oxbow lake, and identification of the flood deposits is based on x-radiograph density and magnetic susceptibility. Judged from chronologies derived from Pb210 and radiocarbon dates, calibration with the historical record over the past 150 years looks promising, and three major flood events are apparently recorded for the period 1440-1525 AD.

In a similar approach, **Byrne *et al*** (this volume) are studying varved lake sediments as a possible paleorecord of large tropical storms in the State of Jalisco, Mexico. Dense laminae 2-4 times thicker than typical layers are hypothesized to represent above-average erosion in the watershed during tropical storm events, and preliminary calibration with the historical record in the period 1921-1990 tentatively confirms the interpretation. If so, reconstruction suggests a total of about 10 large tropical storms in the area over the past 7,000 years.

Another major climate-related hazard — especially notable in urban areas of California — is debris flows, which can be triggered by severe rainstorms and result in sudden destruction of life and property. **Wilson** (this volume) describes the debris flow warning system operated jointly since 1986 by the U.S. Geological Survey and National Weather Service in the San Francisco Bay region. Based on a network of radiotelemetered rain gauges, the system is used to issue public advisories when local rainfall reaches critical levels. The value of the system was well demonstrated during the severe flooding of the winter of 1994-95.

Swetnam and Betancourt (this volume) argue that the most important climatically driven terrestrial ecosystem changes are annual- to decadal-scale episodic events manifested as regionally synchronized disturbance events, such as floods, fires, and insect outbreaks. In the Columbia River Basin, management planning for disturbance events focuses on blown-down trees, cold damage to infant plants, rain-on-snow floods, lightning fire ignition, drought stress, and frontal winds during fire season (**Ferguson and Peterson,** this volume). Analytic tools for management include pattern identification and simple algorithms using common indices, such as the Palmer Drought Severity Index and McKee's Precipitation Deficit Index.

On a longer time scale, **Anderson and Smith** (this volume) address fire history, natural biomass burning, and their relationship to climate over the past 9,000 years. Based on the integration of paleo-fire histories from tree-ring studies with paleo-vegetation sequences from sediments of montane meadows at several locations in the Sierra Nevada, preliminary results suggest that natural burning was high during the period about 9200-8700 YBP, low 8700-4500 YBP, and high again for the past 4500 years. This pattern is hypothesized to result from greater conifer forest development (and associated burning) due to Holocene climate changes.

Glaciers

Like river discharge, glaciers show complex responses to climate variability. **Hodge *et al*** (this volume) elegantly illustrate the impact of interdecadal variability on glacial conditions in a study of the South Cascades Glacier in Washington. Based on a 36-year time series, the study shows that the winter (and net) glacier balance underwent an abrupt step-like decrease in one year, between 1976 and 1977. The summer glacier balance shows no long-term trend, and changes in the winter balance are not associated with decreased total winter precipitation or with increased regional winter temperature, but with changes in conditions allowing snow to accumulate.

Extending Walters and Meier's (1989) evaluation to the longer time-series now available, **Walters** (this volume) employs empirical orthogonal function analysis to mass balance time series of seven western North America glaciers. Comparison of the results with climatological variables shows strong correlation with large-scale variations in seasonal 700-millibar height and sea level pressure and weaker correlations with the Southern Oscillation Index and the Pacific North American Index. The study concludes that the response of individual glaciers is more closely related to large-scale atmospheric conditions than to local-scale meteorological differences.

Putting the present century's climate variations in perspective, **Porter** (this volume) details glacial variations and climate during the Little Ice Age. Using a combination of historical data (paintings, maps, photographs, *etc*), dendrochronology, and studies of crustose lichens, Porter dates the onset of the Little Ice Age to the middle of the 13th century (AD 1250). For the next several centuries, glacial advances, expanding sea ice, crop failures, and famine resulted in much of Europe and the North Atlantic, with peak glacial advance in the early 1600s and glacial retreat beginning about the middle of the 19th century. Porter concludes that glacial fluctuations of the Little Ice Age were unrelated to orbital forcing and not obviously related to solar variations, but they closely resemble the succession of major sulfur-emitting volcanic eruptions.

Even at century scales, however, spatial variability is indicated by **Luckman's** (this volume) review of evidence from the terrestrial paleorecord of climate change over the last thousand years in the Canadian Rockies. Combining data from glaciers, glaciolacustrine sediments, dendrochronology, and tree-line fluctuations, Luckman suggests that most of the classic features of the European climate over the last millennium — the Medieval Warming and Little Ice Age — are not apparent in the Canadian Rockies. There, the broad pattern over the last millennium was progressively more extensive glacial advances, culminating in the 18th and 19th centuries.

Proxy Calibration

One of the major challenges in understanding the scale of natural variability in the climate system is extending instrumental time series by the construction of high-resolution proxy indicators. Tree-ring width, oxygen isotopes in corals, ice accumulation in glaciers, sediment varve thickness, and many other parameters have been discussed, compared, and integrated at previous PACLIM workshops (*eg*, Baumgartner *et al* 1989). As new techniques evolve and new time-series are developed in new locations, the calibration of proxy indicators must be continuously re-examined and re-evaluated.

The next series of contributions address proxy calibration using a variety of indicators in a number of different settings. **Weinheimer and Cayan** (this volume) report recent results on radiolarian assemblages in 20th century varved sediment from Santa Barbara Basin cores. Fluxes of total radiolarians, percent specimens with warm affinities, and percent specimens with cool affinities all reflect SST fairly well for 1950-1991 as previously reported (Weinheimer *et al* 1995), suggesting a promising proxy for paleo-SST in the California Current. However, although new data show that the same relationships apply to sediment deposited in the period 1914-1930, opposite relationships are observed in the period 1930-1950. Neither the varve chronology nor statistical analysis of the radiolarian assemblages points to a simple explanation of this mismatch, so future research will focus on further investigation of the relationships.

Also in the Santa Barbara Basin, **Baumgartner and Southon** (this volume) are developing a detailed series of ^{14}C ages of oceanic materials from samples of the pelagic pteropod *Limacina helicina*, which lives in the upper 100 meters of the water column. Preliminary calibration of terrestrial and marine ^{14}C ages over the period AD 1260-1900 exhibit differences at centennial scales interpreted as the result of variations in large-scale upwelling associated with changes in the intensity of the California Current. Other proxy indicators discussed from varved sediment records are planktic foraminifera fluxes and paleotemperature determinations based on the alkenone biomarker index U^{K}_{37} in Soledad Basin along the southern California Baja margin (**Herguera *et al***, this volume).

Coral records from Clipperton Atoll in the eastern Pacific, on the periphery of the influence of ENSO warm events, were developed by subsampling at 10-20 intervals per year (**Linsley and Dunbar**, this volume). Calibration of oxygen isotope ratios with existing instrumental and satellite-derived datasets show that the corals represent an apparently accurate record of SST in the region. Evaluation of a 120-year time series shows that SST has been stable for the past 120 years, except for a 0.5°C warming over the past 10 years consistent with SST data. **Jones *et al*** (this volume) evaluate oxygen isotope records from corals near the tip of Baja California and from the Gulf of Panama. Calibration of the Baja coral with temperature records shows that the coral data exhibit a strong annual temperature cycle but correlate poorly with temperature records at an annually averaged scale. The Panama coral data correlate strongly with salinity at a bimonthly scale and moderately at an annual scale but are not significantly related to temperature. Coherence between three records in the Panama region, however, show that the corals record regional signals.

The goal a study by **Biondi *et al*** (this volume) is the integration of terrestrial and oceanic records in southern California for reconstructing west coast climate. Using tree rings and marine laminated sediments,

large-scale ocean/atmosphere parameters (including precipitation, temperature, sea level pressure, and primary productivity) can be reconstructed in high-resolution time series. Comparing indicators of precipitation in a varve chronology from Santa Barbara Basin sediment cores with a newly developed tree-ring chronology for the Torrey pine, the study concludes that dark varve layer thickness relates mostly to local rainfall, while tree-ring indices reflect more regional precipitation.

Synoptic dendroclimatology is the subject of the contribution by **Hirschboeck *et al*** (this volume). Using connections between large-scale circulation and tree-ring-width variation at local sites, the authors compared tree-ring chronologies from central Oregon and northern New Mexico. Results show that high and low tree growth at the two sites is associated with totally different large-scale circulation patterns for the prior winter. In Oregon, growth is enhanced by lower-than-normal 500-millibar pressure heights over the Gulf of Alaska; in New Mexico, high growth years are correlated with a belt of lower-than-normal 500-millibar pressure heights extending across the North Pacific into the Southwest. For the Sierra Nevada, **Garfin** (this volume) also examines the relationship between tree growth and large-scale circulation patterns.

Pollen and Lake Records

The next set of contributions looks at longer, lower-resolution time-series illuminating ecosystem and lake histories extending as far back as 800,000 years.

The first paper reports a multidisciplinary approach to quantitatively linking climate changes with the hydrologic cycle, with the goal of providing tools for future forecasting of regional hydrologic responses to climate change (**Smith *et al***, this volume). The study is focused on Elk Lake in Minnesota, a lake with a well-documented record of mid-Holocene climate change characterized by lower precipitation, higher summer insolation, and lower lake levels. The region also has a known history of drought during the 1930s, which can be used to calibrate the mid-Holocene record to reconstruct climate-driven hydrologic transients and thereby obtain estimates of past hydrologic conditions. The paper discusses modeling of present lake/ground water interaction, and analysis of mid-Holocene cores for ostracode assemblages, trace metals, and oxygen isotopes.

Benson *et al* (this volume) examine oxygen isotopic ratios in sediment cores from Owens Lake in eastern California to evaluate their linkage with North Atlantic climate events such as the Younger Dryas and Heinrich events (circa 50, 33, 27, 20.6, 14.6, and 11-10 ka). Detailed reconstruction of the Owens Lake chronology shows that the lake was hydrologically open (overflowing) most of the time between 52.5 and

12.5 ka, but desiccated between about 15.5 and 13.7 ka. Evaluation of the oxygen isotope record suggests that most oscillations in the hydrologic balance of Owens Lake do not strongly correspond to climate oscillations recorded in the North Atlantic.

Also from Owens Lake but covering a longer period, the diatom record suggests a shallow open-water environment from 800-440 ka and a deeper basin environment thereafter, with short intervals of shallow saline conditions (**Bradbury**, this volume). Calibration of the lake chronology with oxygen isotope stages recorded in marine deposits indicates a good correlation, with glacial conditions represented by diatom assemblages dominated by freshwater planktic species, indicating abundant Sierra Nevada precipitation.

Pollen records in the western United States are discussed in two contributions. **Wigand and Hemphill** (this volume) present preliminary analyses of a 5-meter core from Lower Pahranagat Lake in southern Nevada. Spanning the past 2,000 years, long-term trends in the pollen record illustrate the increasing dominance of steppe and desert scrub species compared to grasses in southern Nevada. Further work is planned, including analysis of ostracods and pollen analysis of additional core recently recovered with a basal data of 5.6 ka. On a longer timescale, **Whitlock and Bartlein** (this volume) examine pollen records extending back to 75 ka from Carp Lake and Little Lake in Oregon.

Proxy records from Lake Estancia in New Mexico (32-12 ka) are discussed in another pair of contributions. **Allen *et al*** (this volume) report preliminary results from a number of sedimentologic and proxy indicators (including stable isotopes and trace-metal ratios of ostracods) suggesting that climatic conditions in the area shifted episodically (and rapidly) toward drier and then wetter conditions. The fluctuations in climate indicate that dramatic changes in the transport of Pacific moisture occurred during the last Ice Age. To correlate the climate record from Lake Estancia with records from the Pacific and west coast of North America, **Rowe *et al*** (this volume) are conducting a study of rock-magnetic and geomagnetic secular variation in the same sequence.

Time-Series Compilations

The last two contributions compile and compare numerous datasets from a wide variety of sources. **Karlstrom** (this volume) refines his earlier analysis of time series based on the forcing function of the 556-year maximum tidal force (Karlstrom 1995) to focus on the 2-2.5 year quasi-biennial oscillation (QBO). The paper focuses on the QBO in stratospheric winds and correlations with the El Niño/Southern Oscillation, suggesting that one or both of these oscillations is modulated or amplified by the same tidal-resonance system.

Finally, **Sharp** (this volume) focuses on understanding societal and ecosystem responses to climate regime shifts. Collating regional and global warm and cold events with records of documented ecosystem response and health threat for the historical period, the presentation associates climate shifts with stimulation of disease vectors and considerable human health impacts.

References

Baumgartner, T.R., J. Michaelsen, L.G. Thompson, G.T. Shen, A. Soutar, and R.E. Casey. 1989. The recording of interannual climatic change by high-resolution natural systems: Tree-rings, coral bands, glacial ice layers, and marine varves. Pages 1-14 in *Aspects of Climate Variability in the Pacific and the Western Americas*. D.H. Peterson, editor. Geophysical Monograph 55, American Geophysical Union, Washington, D.C.

Ebbesmeyer, C.C., D.R. Cayan, D.R. McLain, F.H. Nichols, D.H. Peterson, and K.T. Redmond. 1991. 1976 step in the Pacific climate: Forty environmental changes between 1968-1975 and 1977-1984. Pages 115-126 in *Proceedings of the Seventh Annual Pacific Climate (PACLIM) Workshop, April 1990.* J.L. Betancourt and V.L. Tharp, editors. California Department of Water Resources, Interagency Ecological Studies Program Technical Report 26.

Karlstrom, T. 1995. A 139-year dendroclimatic cycle, cultural/environmental history, sunspots, and longer-term cycles. Pages 137-159 in *Proceedings of the Eleventh Annual Pacific Climate (PACLIM) Workshop, April 19-22, 1994.* C.M. Isaacs and V.L. Tharp, editors. California Department of Water Resources, Interagency Ecological Studies Program Technical Report 40.

Roos, M. 1994. Is the California drought over? Pages 123-128 in *Proceedings of the Tenth Annual Pacific Climate (PACLIM) Workshop, April 4-7, 1993.* K.T. Redmond and V.L. Tharp, editors. California Department of Water Resources, Interagency Ecological Studies Program Technical Report 36.

Roos, M. 1995. Has the California drought returned? Pages 181-183 in *Proceedings of the Eleventh Annual Pacific Climate (PACLIM) Workshop, April 19-22, 1994.* C.M. Isaacs and V.L. Tharp, editors. California Department of Water Resources, Interagency Ecological Studies Program Technical Report 40.

Schimmelmann, A., and M.J. Tegner. 1992. Historical evidence of abrupt coastal climatic change in Southern California, 1790-1880. Pages 47-56 in *Proceedings of the Eighth Annual Pacific Climate (PACLIM) Workshop, March 10-13, 1991.* K.T. Redmond, editor. California Department of Water Resources, Interagency Ecological Studies Program Technical Report 31.

Schwing, F.B. 1994. Long-term and seasonal patterns in coastal temperature and salinity along the North American west coast. Pages 129-143 in *Proceedings of the Tenth Annual Pacific Climate (PACLIM) Workshop, April 4-7, 1993.* K.T. Redmond and V.L. Tharp, editors. California Department of Water Resources, Interagency Ecological Studies Program Technical Report 36.

Thompson, L.G. 1991. Initial global perspective of climate for the last thousand years: The ice core record. Pages 147-151 in *Proceedings of the Seventh Annual Pacific Climate (PACLIM) Workshop, April 1990.* J.L. Betancourt and V.L. Tharp, editors. California Department of Water Resources, Interagency Ecological Studies Program Technical Report 26.

Thompson, L.G., and E. Mosley-Thompson. 1989. One-half millennia of tropical climate variability as recorded in the stratigraphy of the Quelccaya ice cap, Peru. Pages 15-31 in *Aspects of Climate Variability in the Pacific and the Western Americas*. D.H. Peterson, editor. Geophysical Monograph 55, American Geophysical Union, Washington, D.C.

Walters, R.A., and M.F. Meier. 1989. Variability of glacier mass balances in western North America. Pages 365-374 in *Aspects of Climate Variability in the Pacific and the Western Americas*. D.H. Peterson, editor. Geophysical Monograph 55, American Geophysical Union, Washington, D.C.

Weinheimer, A.L., and D.R. Cayan. 1995. Radiolarian flux in the Santa Barbara Basin as an index of climate variability. Pages 107-118 in *Proceedings of the Eleventh Annual Pacific Climate (PACLIM) Workshop, April 19-22, 1994.* C.M. Isaacs and V.L. Tharp, editors. California Department of Water Resources, Interagency Ecological Studies Program Technical Report 40.

Simulation of Recent Global Temperature Trends

Nicholas E. Graham

Abstract

Observations show that global average tropospheric temperatures have been rising during the past century, with the most recent portion of record showing a sharp rise since the mid-1970s. Whether these changes are real and, if so, what processes are responsible are subjects of much discussion. A suite of observational evidence collected during the past 40 years suggests that the temperature changes may be a manifestation of an enhancement in the tropical hydrologic cycle driven by increasing tropical ocean temperatures. New results show that the most recent portion of the global temperature record (1970-1988) can be reproduced by atmospheric models forced with observed ocean surface temperatures. Analysis of the model atmospheric heat budget shows that the upward trend in simulated global air temperature is due principally to an increase in the flux of moisture through the tropical hydrologic cycle, a response to increasing tropical ocean temperatures. This behavior has been especially evident in the tropical Pacific. Other recently completed model experiments using decadally-composited SST data show that major features of the global surface air temperature record during the 20th century can also be reproduced by a GCM and that these changes also arise in large part as a response to fluctuations in the tropical hydrologic cycle.

In: C.M. Isaacs and V.L. Tharp, Editors. 1996. *Proceedings of the Twelfth Annual Pacific Climate (PACLIM) Workshop, May 2-5, 1995.* Interagency Ecological Program, Technical Report 46. California Department of Water Resources.

Mechanisms of Upper-Ocean Thermal Variability in a 1970-1988 Simulation and Observations

Arthur J. Miller, Daniel R. Cayan, Warren B. White

Abstract: Variations in temperature that occurred in the North Pacific thermocline (250 to 400 meters) during the 1970s and 1980s are described in both a numerical simulation and XBT observations. We identify, in both model and observations, two distinct midlatitude variations: a decadal change in the thermocline, which is western intensified; and westward propagating thermocline anomalies with ENSO time scales. The decadal change is associated with a deepened thermocline off the coast of California after 1976-77. The ENSO scale variations are associated with shorter-lived thermocline changes off the coast of California. The decadal change is driven by a basin-scale change in wind stress curl, and the ENSO scale thermocline anomalies appear to be at least partly forced by large-scale midlatitude wind stress curl variations as well. The observed and modeled ENSO-scale anomalies are distinct from the baroclinic Rossby waves radiated from coastally trapped Kelvin-like waves previously identified in high-resolution numerical models because they have larger wavelengths and appear to be wind forced.

Introduction

Decadal scale changes have been observed in numerous physical, chemical and biological variables in the North Pacific (*eg*, Douglas *et al* 1982; Ebbesmeyer *et al* 1991; Roemmich and McGowan 1995). One especially interesting change occurred in the mid-1970s (*eg*, Trenberth 1990; Graham 1994; Trenberth and Hurrell 1994) for which, in previous work (Miller *et al* 1994a,b), we have attempted to explain the oceanic physics involved in switching the ocean from a warm central (cool eastern) North Pacific state to an oppositely signed regime after the winter of 1976-77.

In this study, we take a look underneath the mixed layer to identify:

- What changes were observed in the oceanic thermocline, and
- What controls these changes.

Toward that end, we analyze a dataset of upper-ocean (to 400-meter depth) XBT (expandable bathythermograph) observations from the period 1970-1988 [*see* White and Cayan 1996 (submitted) for details] and compare it with the response of an ocean general circulation model forced by observed fluxes and winds over the same period. By identifying which signals are common to both the model and the observations, we are able to have more faith in the data (which is sparsely sampled in space and time) and to interpret the variations using the model output, which is dynamically consistent with the input forcing.

In: C.M. Isaacs and V.L. Tharp, Editors. 1996. *Proceedings of the Twelfth Annual Pacific Climate (PACLIM) Workshop, May 2-5, 1995.* Interagency Ecological Program, Technical Report 46. California Department of Water Resources.

Figure 1 shows differences from the early 1970s to the early 1980s of the upper ocean temperature field of the North Pacific in both the observations and the model. (The time differencing interval is motivated by results to be presented in subsequent sections.) In the surface mixed layer, one sees the well known structure of the cooling in the central Pacific and the warming of the eastern Pacific. This structure is commensurate with the large-scale structure of the atmospheric variables (heat fluxes and wind stresses) that drive the variability (Cayan 1992; Miller et al 1994a,b). The time series of SST variability in a rectangular region in the central North Pacific (180°W-150°W, 30°N-40°N) reveals a good correspondence between model (dotted) and observations (dashed) and shows the steplike character of the SST change during the winter of 1976-77.

Looking beneath the mixed layer at 200 meters and 400 meters (Figure 1), where little or no direct contact with the atmosphere occurs, one sees a progression into a region where ocean dynamics are expected to dominate the response. Indeed the thermal structures at 400 meters bear a western intensified structure reminiscent of gyre-scale circulation theory. The variability at 400 meters depth is much weaker and, though the model does not capture the higher-frequency variability in the time series, both model and data reveal a more gradual change in temperature from the 1970s to the 1980s in contrast to the steplike change in the surface layer (*cf*, Deser *et al* 1996, submitted).

Statistical Analysis

Difference maps like Figure 1 are useful to understand gross features of the response, but the figure fails to give a clear picture of the coherency of variations over large scales. Empirical orthogonal function (EOF) analysis is useful for just such a purpose. To better isolate stationary features from propagating ones, we use an extended EOF (EEOF) analysis of 400-meter temperature, whereby time-lagged maps of the variables are included in the input vector. Also, we use combined EEOF analysis (two input variables) to identify relationships between variables. Seasonal anomalies (with monthly mean climatological values removed) defined as DJF, *etc*, are analyzed with lags out to 12 seasons (3 years) in constructing the covariance matrix. We consider only the region of the North Pacific east of 155°E and north of 20°N to avoid including the poorly resolved (in both the model and XBT dataset) Kuroshio region and the ENSO-dominated low latitudes.

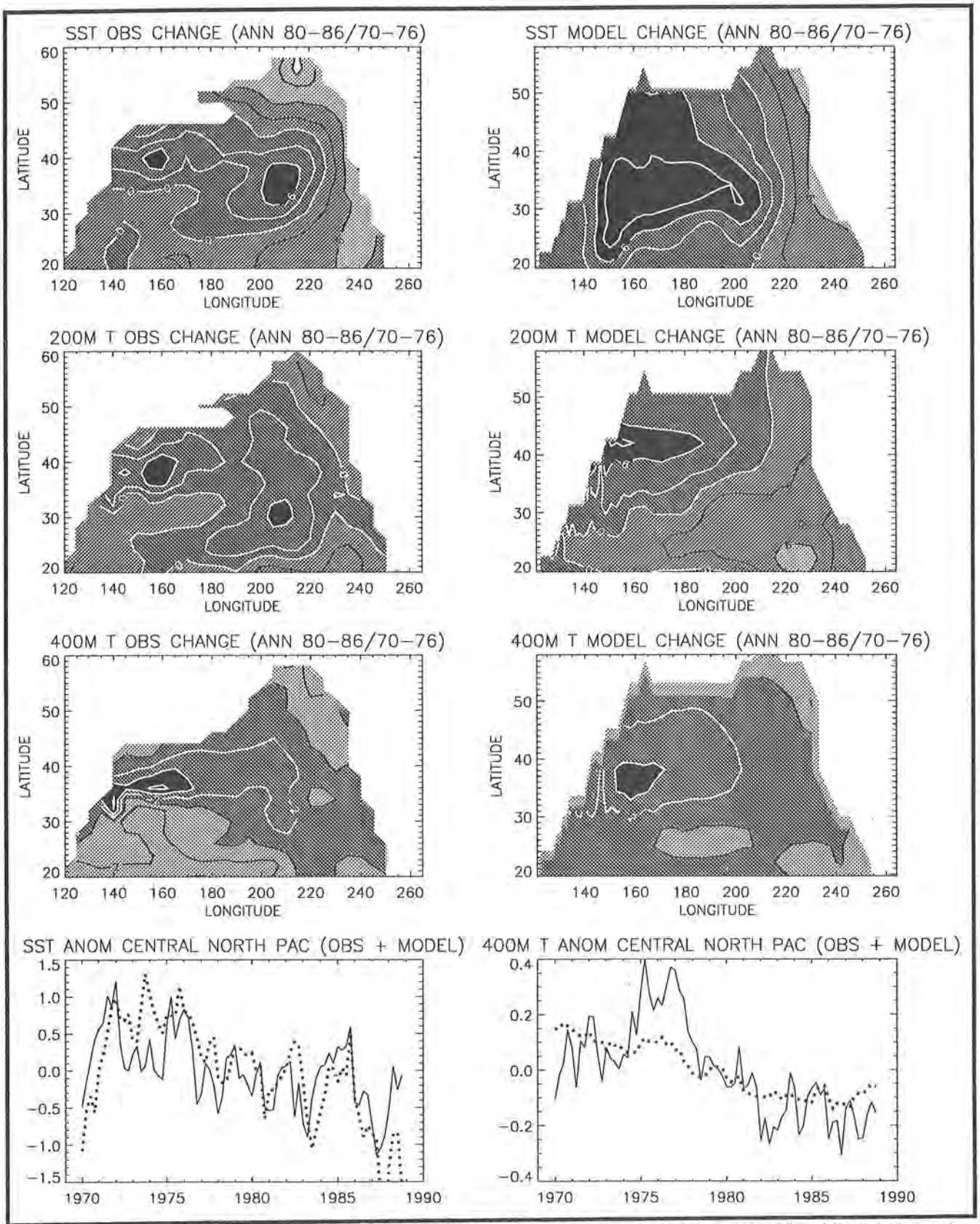

Figure 1. Difference maps of the 7-year periods 1980-1986 relative to 1970-1976 for *(top)* sea-surface *(middle)* 200-meter and *(lower)* 400-meter temperature for *(left)* observations and *(right)* model. Contour intervals are 0.3°C for SST and 200 meters and 0.2°C for 400 meters with dark *(light)* shading negative *(positive)*. Time series *(bottom)* of observed *(solid)* and modeled *(dotted)* temperature at surface *(left)* and 400 meters *(right)* averaged over the region 180°W-150°W, 30°N-40°N.

Results

In all of our results, two dominant time scales emerge from the EEOF analyses. The first is a decadal change as depicted in Figure 1. The second is a pair of propagating EEOF modes that bear ENSO time scales. Typically the decadal mode explains 25% of the field variance and the two ENSO modes together explain 10% of the total variance. Both signals are equivalent barotropic in the sense that similar changes at 250-300 meters are coherent with the 400-meter response but with larger amplitudes.

Decadal Thermocline Change

Figure 2 shows a synopsis of the decadal temperature change in observations and in the model. Since this mode is nearly stationary, we plot the average of the 13 lags together, rather than showing the individual lags. The top two maps show the first combined EEOF of observations and model 400-meter temperature with the time series (scaled amplitude) shown as the thin line in the bottom plot. (The two temperature fields are normalized by 0.25°C and 0.13°C, respectively, because model variability is weaker than observed). The observed pattern is essentially the same as that of the first EEOF of observations alone (not shown), and the combined EEOF time series has very similar time variation to that of the EEOF of observations alone (bottom, thick line).

Both the model and the observations reveal a cooling of the basin-scale thermocline from the early 1970s to the early 1980s (as seen in the time coefficient), which is western intensified as expected from inspection of Figure 1. Since this signal explains 29% of the combined variance, it represents a significant deviation of the basin-scale thermocline structure and can be expected to be associated with gyre-scale changes in upper-ocean circulation. Indeed, the combined EEOF of model 400-meter temperature and model 400-meter velocity (second panel of Figure 2 and dotted time series at bottom) reveals that the decadal signal is nearly geostrophically balanced over this 10-year transitional time scale. The flow field reveals a 10% increase in the strength of the Kuroshio extension and the subpolar gyre return flow (*cf*, Sekine 1991; Trenberth and Hurrell 1994). A stronger than normal northward flow into the central Gulf of Alaska (*cf*, Tabata 1991; Lagerloef 1995) is also seen during the early 1980s in the model diagnosis. It is interesting to note that little change in the California Current System is associated with this decadal signal, even though the thermocline (Figures 1, 2) did deepen off the West Coast of America.

Since wind stress curl is the dominant forcing function for the gyre-scale circulation, we anticipate that it is associated with the observed and modeled changes seen in Figures 1 and 2. Indeed combined extended

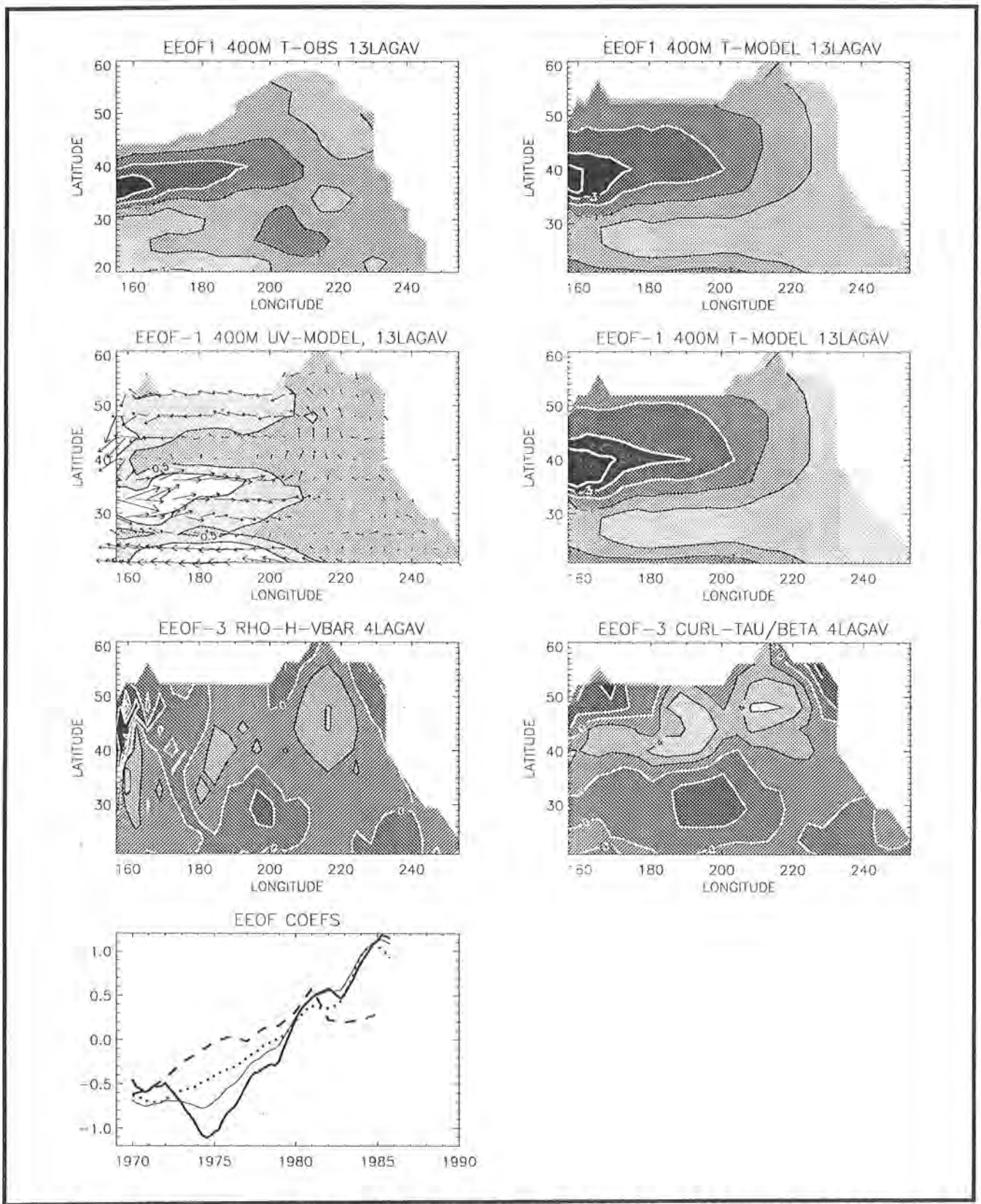

Figure 2. A synopsis of three separate combined extended EOF analyses. *(Top)* Combined EEOF-1 of observed *(left)* and modeled *(right)* 400-meter temperature, plotted as an average over all 13 lags. *(Middle)* Same as top but for combined EEOF-1 of *(left)* model 400-meter velocity and *(right)* model 400-meter temperature. *(Lower)* Combined EEOF-3 of north-south 0-1500 meter transport (scaled by density and depth) and wind stress curl over b, plotted as an average over all 4 lags (0 to 3 years). *(Bottom)* Corresponding principal components of top *(thin)*, middle *(dotted)* and lower *(dashed)* EEOFs, along with that of EEOF-1 of the observations alone *(thick)*; each scaled arbitrarily to fit on same plot.

EEOFs of wind stress curl and north-south transport (integrated from 0 to 1500 meters) yields an EEOF mode (third panel of Figure 2 and dashed time series at bottom) that corresponds to the decadal change in temperature and velocity (panels 1 and 2). The pattern of basin-scale wind stress curl seen in Figure 2 is the same pattern one obtains when differencing the early 1980s and early 1970s, as done in Figure 1. Figure 2 indicates that in the eastern basin the flow field is nearly in Sverdrup balance (to within a factor or two) and supports the notion that the wind stress is the forcing function of the decadal thermocline change.

ENSO-Scale Thermocline Variations

The second most important signal in the EEOF analysis of the 400-meter temperature observations alone is a pair of modes (third and fourth EEOFs), which together explain 10% of the variance. (This is greater than the 8% variance explained by the second EEOF, which explains a midbasin nearly stationary feature.) Figure 3 shows maps of EEOFs 3 and 4 for three of the 13 lags included in the analysis of observations alone, along with the time series (bottom). Westward propagating 400-meter temperature anomalies are clearly evident from 20°N up to 45°N, which is a previously unidentified feature of basin-scale thermocline observations. They appear to reach as far west as the dateline, at which point they are either arrested or obscured by the ambient noise of the Kuroshio extension. Anomalies farther south in the analysis domain near 20°N propagate faster and farther westward as expected.

EEOF-3 leads EEOF-4 by about 1 year, as can be seen in the time series and in the map patterns, which are nearly identical when accounting for the 1-year lag. The largest signals in the time series correspond to the mid-1980s and the mid-1970s and have a stochastic periodicity of 3-4 years. Clearly, the signals are indicators of ENSO time scale activity and are suggestive of radiated baroclinic Rossby waves, which have been identified in high-resolution numerical models in association with coastally trapped Kelvin-like waves of tropical origin (Pares-Sierra and O'Brien 1989; Shriver *et al* 1991; Jacobs *et al* 1995). However, the thermocline waves identified here differ from those identified in those model studies in several respects. They have longer east-west wavelengths (roughly 3000 kilometers compared to 800-1200 kilometers) at 30-45°N and, therefore, larger phase speeds than those thermocline anomalies associated with coastal variability of equatorial origin; *nb*, our observational grid (5° longitude by 2° latitude) is likely insufficient to resolve the shorter waves. Also, their amplitude appears to increase away from the eastern boundary. They also occur in our low-resolution model which, although it admits a poleward propagating Kelvin-like wave (*eg*, O'Brien and Parham 1992), the numerical analogue Kelvin wave is seriously damped as it propagates northward and is trapped to one grid point in the offshore direction.

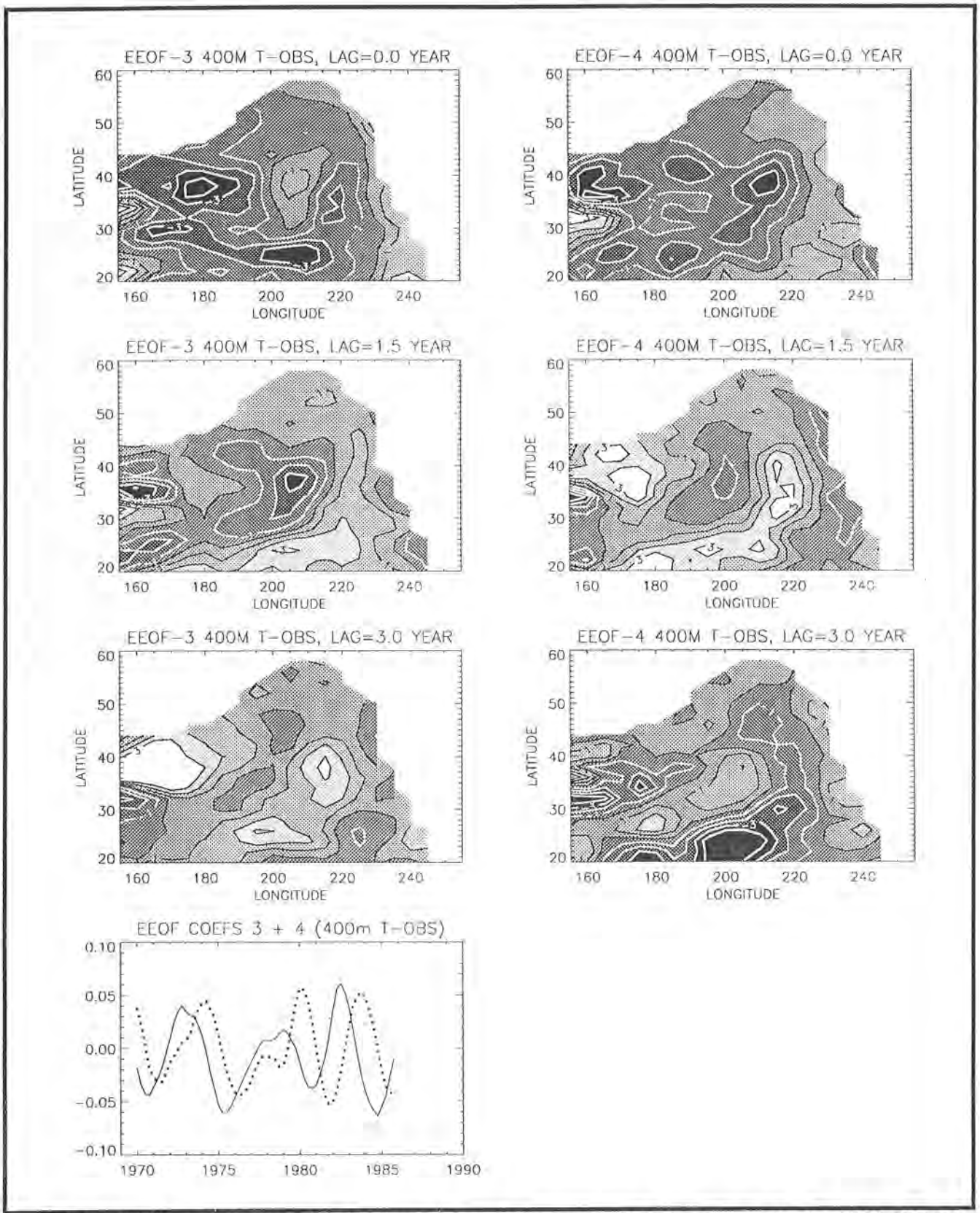

Figure 3. Third *(left)* and fourth *(right)* extended EOFs of the observed 400-meter temperature alone for 3 of the 13 lags. (Top) lag-0, *(middle)* lag-1.5 yr and *(lower)* lag-3 yr. *(Bottom)* Corresponding principal components of third *(solid)* and fourth *(dotted)* EEOFs.

To explore the dynamics of the ENSO-scale thermocline anomalies, we study the model's version of the phenomenon. Figure 4 shows maps of three cases of the combined EEOFs (only one lag of the analogue to EEOF-4 of Figure 3 is shown for brevity; refer to Figure 3 for phase propagation information). In the top panel of Figure 4 are maps of one phase (*cf*, Figure 3, top right) of the combined EEOF of the observed and modeled thermocline anomalies, which show that the model captures the large-scale westward propagating behavior and the time series (bottom; thin line) is coherent with that of the observations alone (bottom; thick line is from EEOF-4 of Figure 3). Figure 4 (middle panel, with time series at bottom; dotted line) also shows the combined EEOF of model 400-meter temperature and velocity and reveals that the large-scale circulation anomalies associated with the thermocline perturbations are nearly geostrophically balanced.

The bottom panel of Figure 4 shows the combined EEOF of north-south integrated (0-1500 meters) velocity and curl t scaled to allow for potential Sverdrup balance (time series at bottom; dashed line). Instead of nearly Sverdrup-balanced velocities as seen in the decadal mode, we find that the model thermocline anomalies occur in phase with large-scale deepening and weakening of the Aleutian Low. This result suggests that the midlatitude thermocline anomalies seen in the model (which mimic those observed, though the model anomalies are weaker) are at least partly driven by midlatitude forcing. It is unclear to what degree the midlatitude waves are forced by signals propagating along the eastern boundary, but this model does not properly resolve this process and models that do resolve the process yield shorter-wavelength thermocline anomalies. Ramp *et al* (1996, submitted) also found evidence for wind-stress curl forcing of thermocline anomalies in the North Pacific during the 1992 El Niño.

Basinwide plots (*eg*, Figure 5) of the full, unfiltered seasonal thermocline anomalies for both model and observations reveal that the strongest signal is associated with the 1982-1983 ENSO. One can follow the warm thermocline anomaly from the western North American coast across the basin until it encounters the western boundary (at low latitudes) and the Kuroshio region (in middle latitudes). The observed and modeled thermocline anomalies encounter the Kuroshio region in late 1987/early 1988, at which point they are no longer discernible due to the high variability there. It is interesting to note that these waves travel twice as fast as those identified by Jacobs *et al* (1995) in satellite-derived sea level observations and high-resolution model thermocline anomalies, which showed trans-Pacific transit times of nearly 10 years of model thermocline anomalies and observed sea-level height anomalies. Chelton and Schlax (1996, submitted) also identified sea level variations that travel twice as fast as their theoretical Rossby wave analogues. Apparently two types of ENSO-scale responses occur in the midlatitude thermocline.

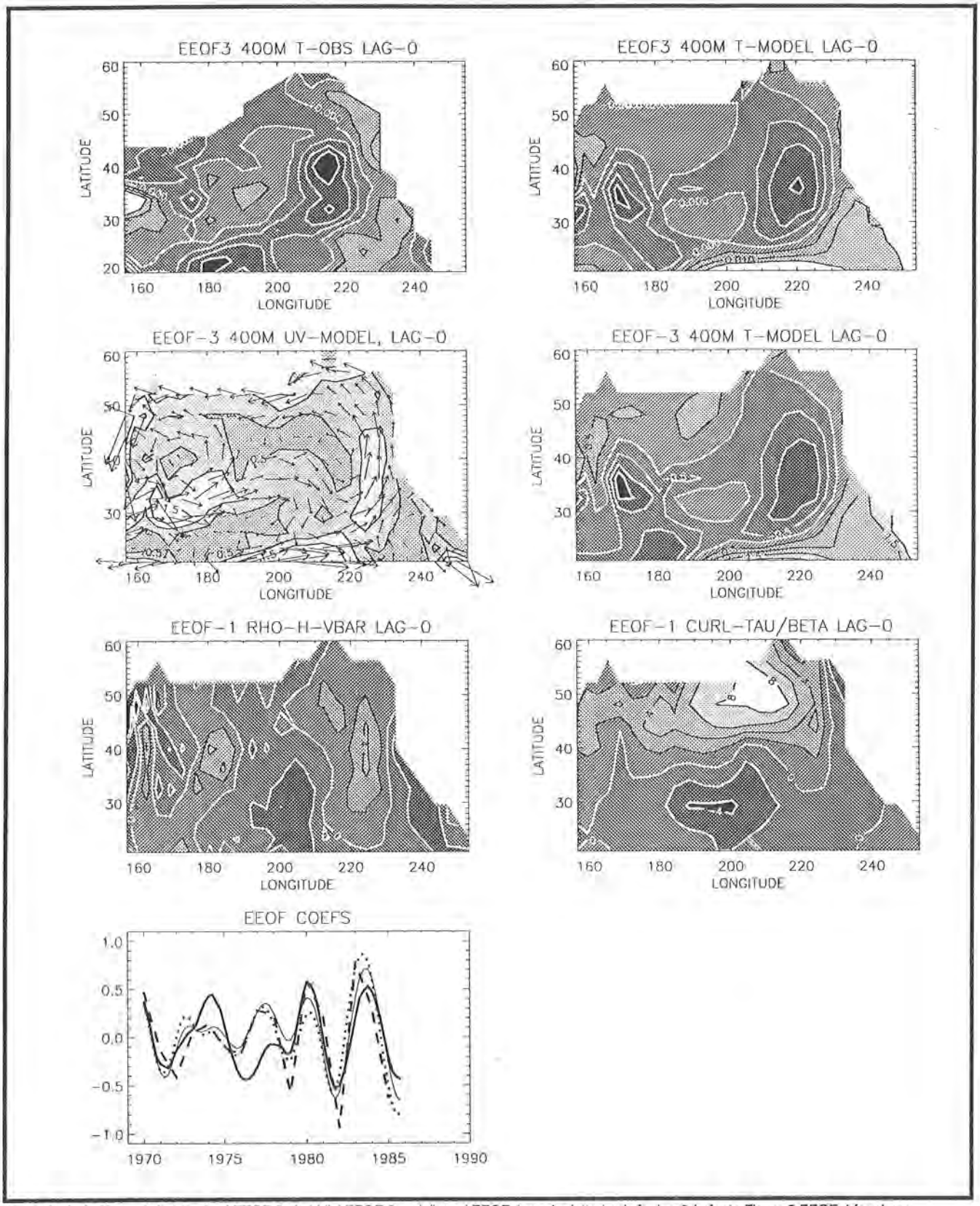

Figure 4. As in Figure 2, but for *(top)* EEOF-3, *(middle)* EEOF-3 and *(lower)* EEOF-1, each plotted only for lag-0 (refer to Figure 3 EEOF-4 for phase propagation). *(Bottom)* Corresponding principal components, along with that of EEOF-4 of the observations alone.

Discussion

We have identified two dominant signals in observations of 400-meter temperature (thermocline) variations in the North Pacific. The strongest feature is a decadal scale change in the gyre-scale thermocline, and the other signal represents ENSO-time scale waves propagating westward in the eastern North Pacific. Very similar features exist in a numerical simulation forced by surface heat flux and wind stress anomalies. The model suggests that the thermocline variations are both predominantly forced by wind stress curl. Further details of these results are described by Miller *et al* 1996a,b (submitted).

Figure 6 shows how these signals influence the thermocline off the California Coast (*cf*, Roemmich and McGowan 1995). The top panel shows the observations averaged over a region off western North America (130°W-120°W, 25°N-45°N) as a function of depth and time, with the

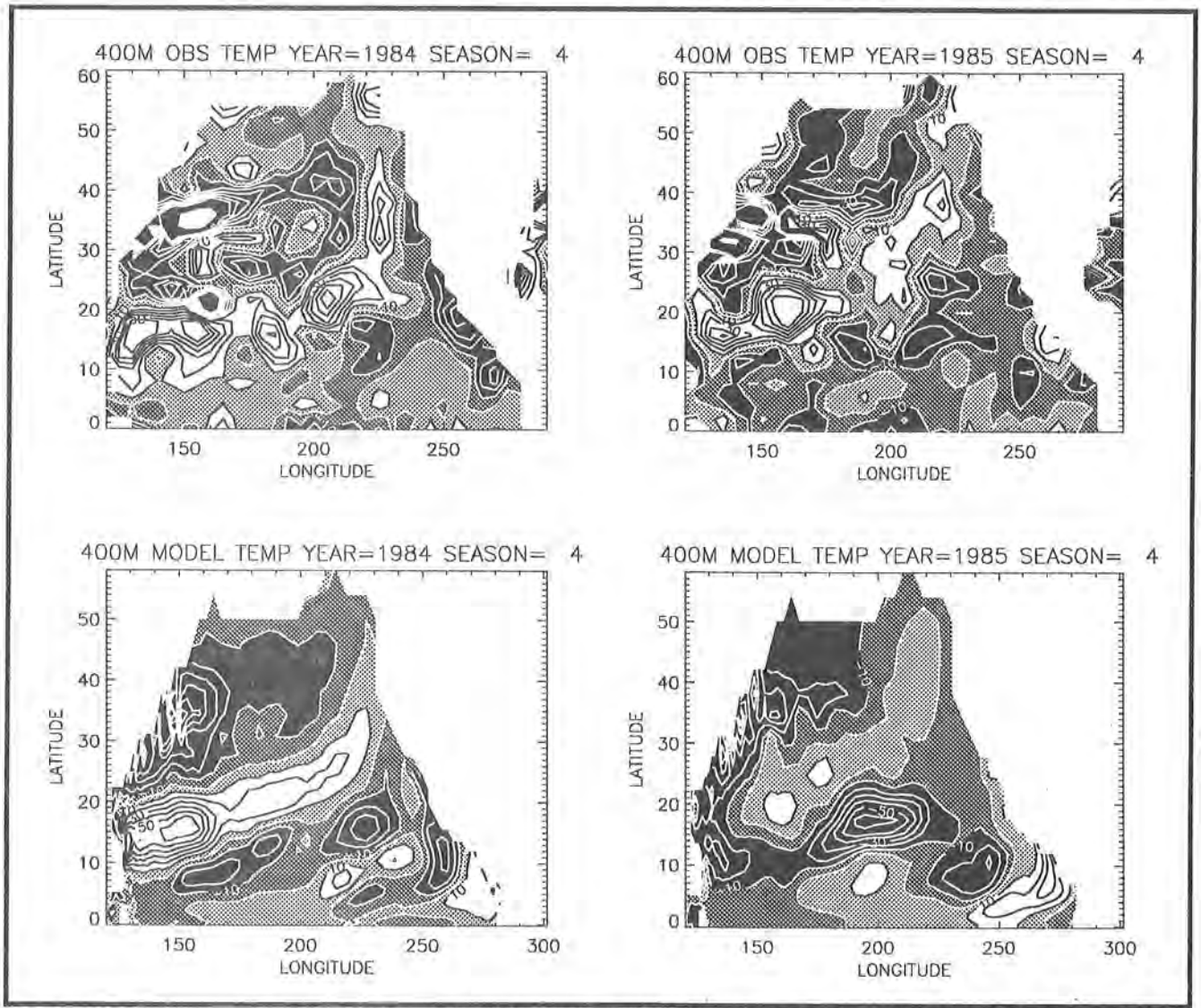

Figure 5. 400-meter temperature anomalies for fall season (SON) 1984 *(left)* and 1985 *(right)* for observations *(top)* and model *(bottom)* after the 1982-83 ENSO event. Contour interval is 0.1°C.

bottom showing the model version of reality. Although the decadal thermocline change has its strongest component in the western part of the North Pacific, it is still associated with a deepening of thermocline (warmer upper ocean) along the eastern boundary as well.

Figure 7 shows the depth anomalies of a model isopycnal layer (24.7 s layer), which has a mean depth of roughly 180 meters. Figure 7 shows that the model thermocline deepens by 5-10 meters, although in the observations the change is probably larger and at a shallower depth. Also shown is the local wind stress curl, which reveals no obvious local correlation to the thermocline anomalies; the basin-scale effect of the wind stress curl instead is the key factor. Besides the decadal change, the ENSO time-scale thermocline oscillations are evident in Figures 6 and 7 as well. These events are dynamically distinct from the decadal change, last for roughly one year, and are associated with temperature anomalies with local maximum at 50-100

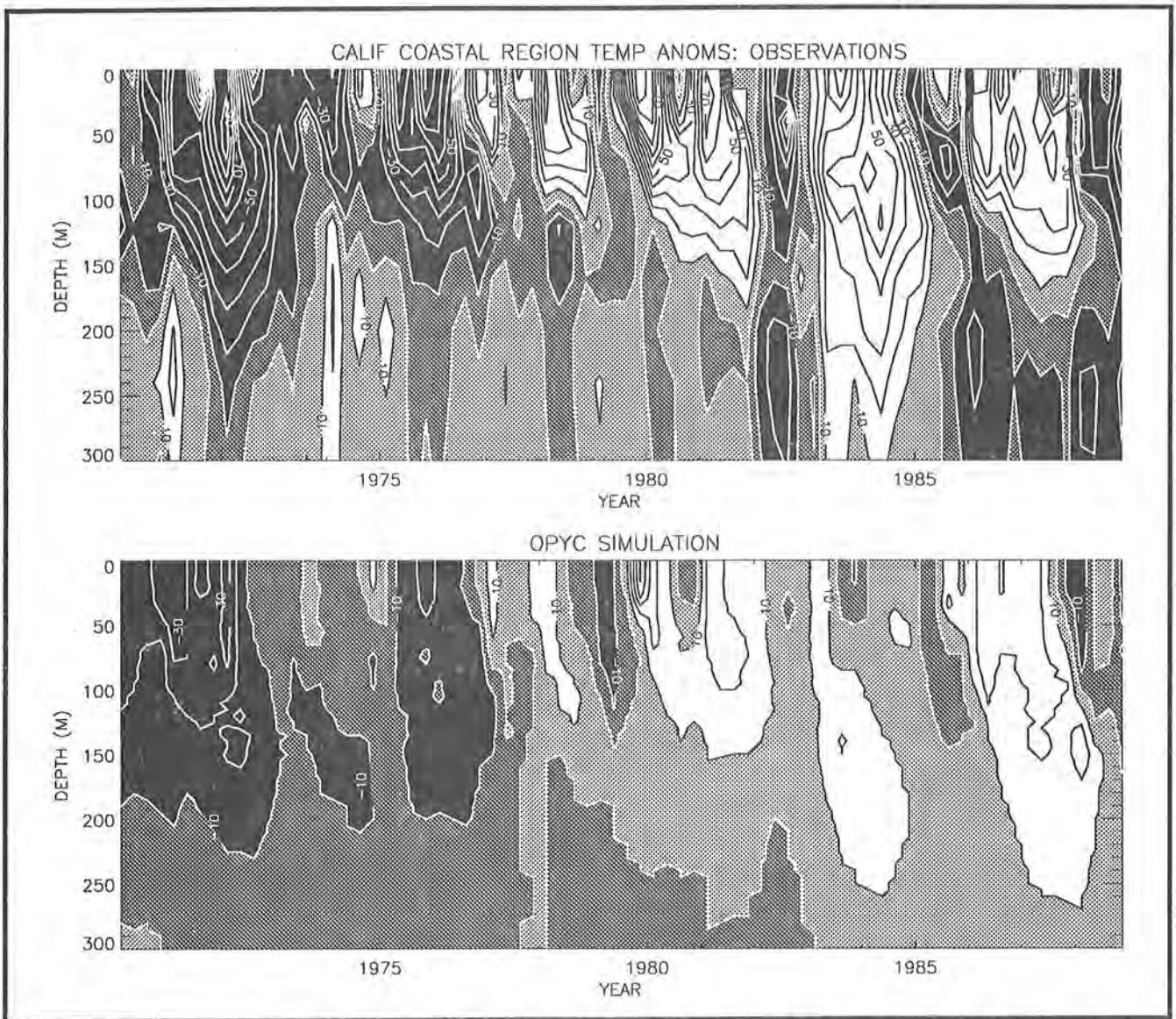

Figure 6. Temperature anomalies averaged over the region 130°W-120°W, 25°N-45°N from the surface to 300-meter depth from 1970-1988 in the observations *(top)* and in the model *(bottom)*. Contour interval is 0.1°C.

meters depth in the observations (*cf*, Norton and McLain 1994) and somewhat deeper in the model (50-150 meters depth).

In the central North Pacific (Figure 8) the thermal anomalies tend to be generated near the surface and tend to occur with opposite sign to those near the eastern boundary (Figure 6). As Deser *et al* (1996, submitted) noted, in their independent analysis of this same dataset, the surface-generated anomalies tend to migrate downward with time to depths of 400 meters in the observations. The model only admits downward propagation to roughly 250 meters, suggesting that it is not properly subducting the surface-generated anomalies. Indeed, Deser *et al* show that a large cold anomaly generated at the surface in the interior North Pacific during 1977-1981 eventually subducted and migrated along isopycnal levels through the mid-to-late 1980s. Although the model was unable to capture this subductive aspect of the thermodynamics, the fact that the model simulated the wind-stress curl driven decadal thermocline change suggests that the two signals (western-intensified decadal change and subducted decadal change) differ dynamically.

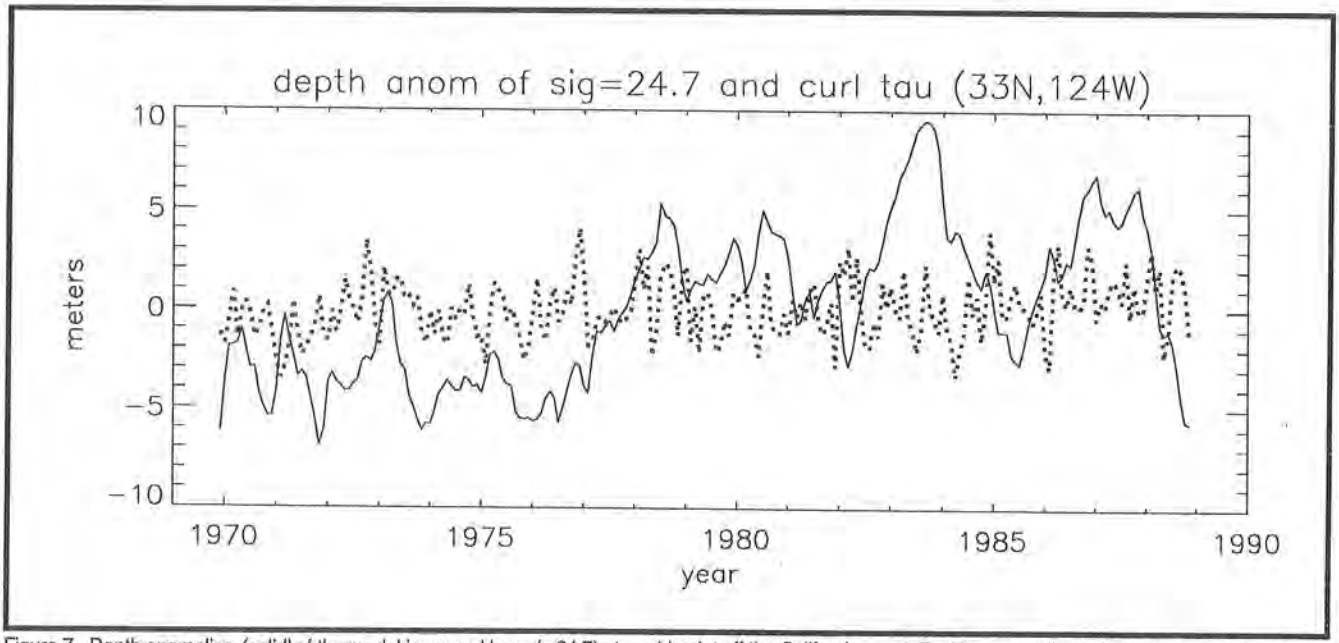

Figure 7. Depth anomalies *(solid)* of the model isopycnal layer (s 24.7) at a grid point off the California coast. Positive anomalies indicate a deeper thermocline at mean level of roughly 180 meters. Local wind stress curl anomalies *(dotted)* at the same point.

Acknowledgments

Funding was provided by NOAA under the Scripps Experimental Climate Prediction Centre (NA36GPO372) and the Lamont/Scripps Consortium for Climate Research (NA47GPO188) and (to AJM) by the G. Unger Vetlesen Foundation. AJM thanks Weimin Xu, Tim Baumgartner, Mike Alexander, Clara Deser, Steve Meyers, Jim O'Brien, Dave Battisti, Jeff Polovina, Gregg Jacobs, Dudley Chelton, and Julie McClean for discussions and/or preprints of their work.

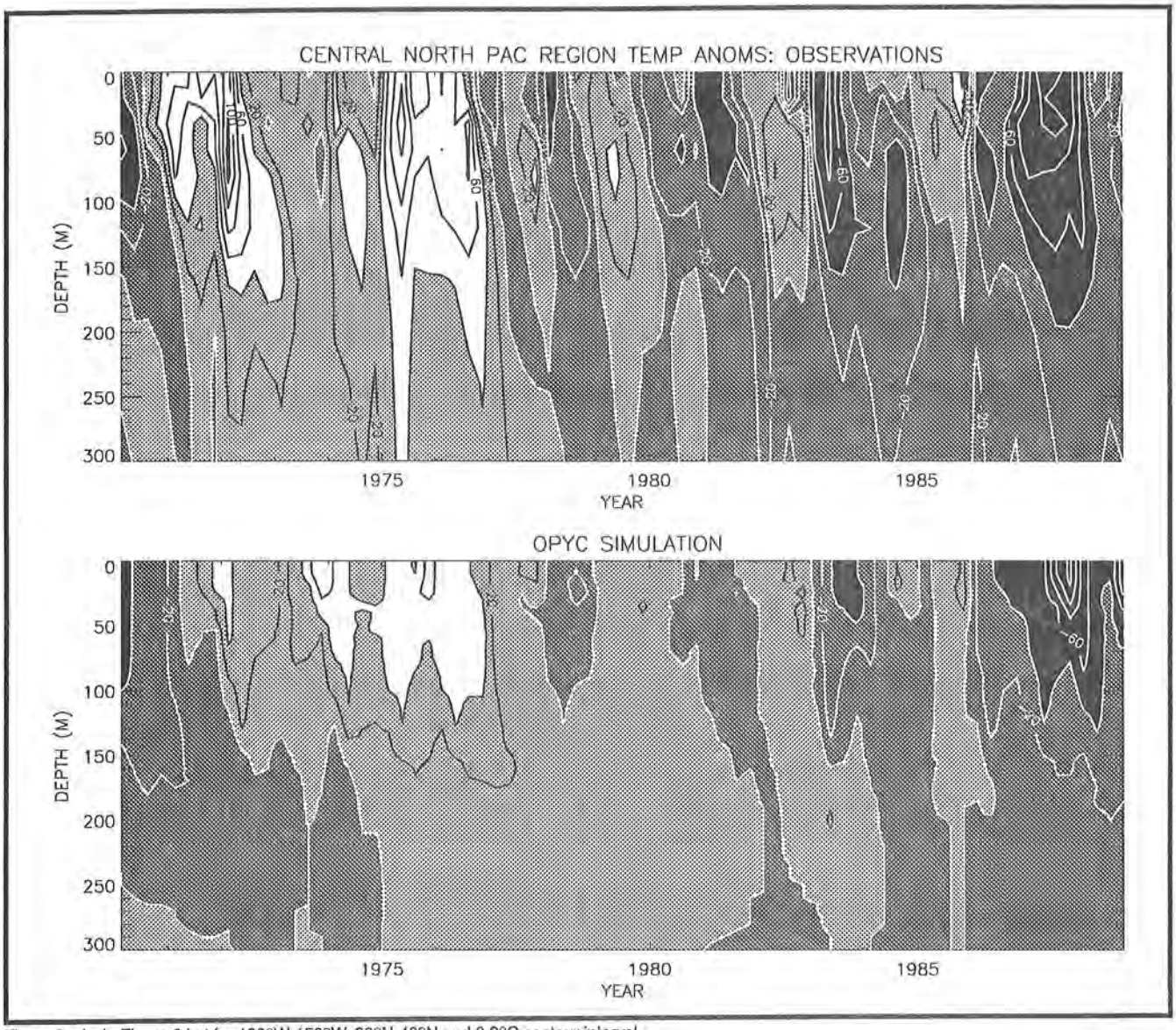

Figure 8. As in Figure 6 but for 180°W-150°W, 30°N-40°N and 0.2°C contour interval.

References

Cayan, D.R. 1992. Latent and sensible heat flux anomalies over the northern oceans: Driving the sea surface temperature. *J. Phys. Oceanogr.* 22:859-881.

Chelton, D.B., and M.G. Schlax. 1996. Global observations of oceanic Rossby waves. *Science, sub judice.*

Deser, C., M.A. Alexander, M.S. Timlin. 1996. Upper ocean thermal variations in the North Pacific during 1970-1991. *J. Climate, sub judice.*

Douglas, A.V., D.R. Cayan, J. Namias. 1982. Large-scale changes in North Pacific and North American weather patterns in recent decades. *Mon. Wea. Rev.* 110:1851-1862.

Ebbesmeyer, C.C., D.R. Cayan, D.R. McLain, F.H. Nichols, D.H. Peterson, K.T. Redmond, 1991. 1976 step in the Pacific climate: Forty environmental changes between 1968-75 and 1977-1984. In: *Proc. 7th Ann. Pacific Climate Workshop,* Calif. Dept. of Water Resources, Interagency Ecol. Stud. Prog. Report 26.

Graham, N.E. 1994. Decadal scale variability in the 1970's and 1980's: Observations and model results. *Clim. Dyn.* 10:135-162.

Jacobs, G.A., H.E. Hurlburt, J.C. Kindle, E.J. Metzger, J.L. Mitchell, W.J. Teague, A.J. Wallcraft. 1995. Decade-scale trans-Pacific propagation and warming effects of an El Niño anomaly. *Nature*, 370:360-363.

Lagerloef, G.S.E. 1995. Interdecadal variations in the Alaska Gyre. *J. Phys. Oceanography*, 25:2242-2258.

Miller, A.J., D.R. Cayan, T.P. Barnett, N.E. Graham, J.M. Oberhuber. 1994a. Interdecadal variability of the Pacific Ocean: Model response to observed heat flux and wind stress anomalies. *Clim. Dyn.* 9:287-302.

Miller, A.J., D.R. Cayan, T.P. Barnett, N.E. Graham, J.M. Oberhuber. 1994b. The 1976-77 climate shift of the Pacific Ocean. *Oceanography* 7:21-26.

Miller, A.J., D.R. Cayan, W.B. White. 1996a. A decadal change in the North Pacific thermocline and gyre-scale circulation. *J. Climate, sub judice.*

Miller, A.J., W.B. White, D.R. Cayan. 1996b. Thermocline fluctuations in the North Pacific ocean with ENSO time scales. *J. Phys. Oceanogr., sub judice.*

O'Brien, J.J., and F. Parham. 1992. Equatorial Kelvin waves do not vanish. *Mon. Wea. Rev.* 120:1764-1767.

Pares-Sierra, A., and J.J. O'Brien. 1989. The seasonal and interannual variability of the California Current System. *J. Geophys. Res.*, 94:3159-3180.

Norton, J.G., and D.R. McLain. 1994. Diagnostic patterns of seasonal and interannual temperature variation off the west coast of the United States: Local and remote large-scale atmospheric forcing. *J. Geophys. Res.*, 99:16,019-16,030.

Ramp, S.R., J.L. McClean, C. A. Collins, A. J. Semtner, K.A.S. Hays. 1996. Observations and modeling of the 1991-1992 El Niño signal off Central California. *J. Geophys. Res., sub judice.*

Roemmich, D., and J. McGowan. 1995. Climatic warming and the decline of zooplankton in the California Current. *Science*, 267:1324-1326.

Sekine, Y. 1991. Anomalous southward intrusion of the Oyashio east of Japan. I. Influence of the interannual and seasonal variations in the wind stress over the North Pacific. *J. Geophys. Res.* 93:2247-2255.

Shriver, J.F., M.A. Johnson, J.J. O'Brien, 1991. Analysis of remotely forced oceanic Rossby waves off California. *J. Geophys. Res.*, 96:749-757.

Tabata, S. 1991. Annual and interannual variability of baroclinic transports across Line P in the northeast Pacific Ocean. *Deep-Sea Res.* 38(S1):S221-S245.

Trenberth, K.E. 1990. Recent observed interdecadal climate changes in the Northern Hemisphere. *Bull. Am. Met. Soc.*, 71:988-993.

Trenberth, K.E., and J.W. Hurrell. 1994. Decadal atmosphere-ocean variations in the Pacific. *Clim. Dyn.* 9:303-319.

White, W.B., and D.R. Cayan. 1996. ENSO signals in the North Pacific Basin: Part 1 — Coupled Rossby waves. *J. Climate, sub judice.*

Climate Forcing by Changing Solar Radiation

Judith Lean

By how much does changing radiation from the Sun influence Earth's climate compared with other natural and anthropogenic processes? Answering this question is necessary for making policy regarding anthropogenic global change, which must be detected against natural climate variability. Current knowledge of the amplitudes and time scales of solar radiative output variability available from contemporary solar monitoring and historical reconstructions (Lean 1991) (Figure 1) can help specify climate forcing by changing radiation over multiple time scales.

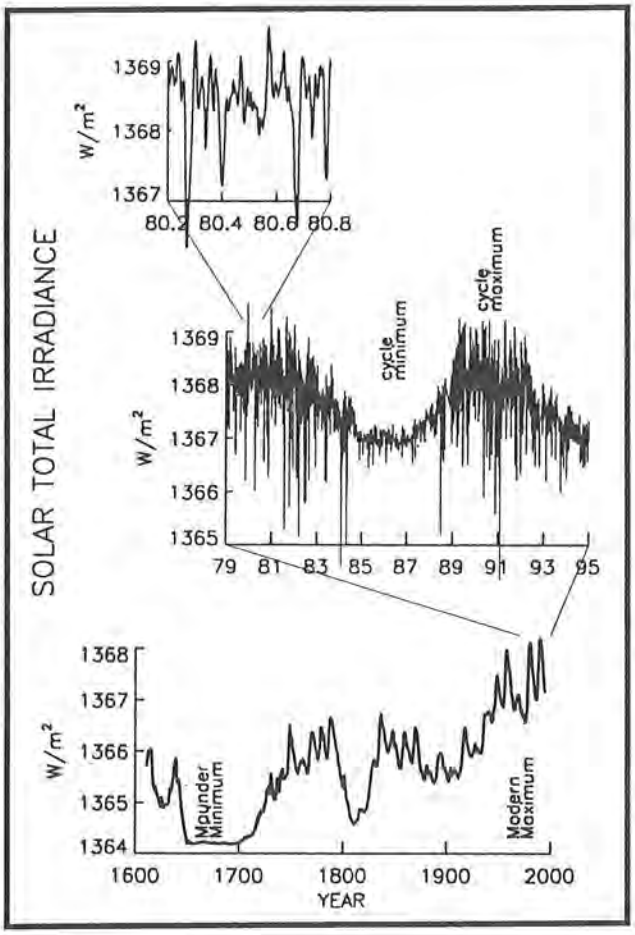

Figure 1 Time scales of observed solar total irradiance variability include the Sun's 27-day rotation (upper panel) and 11-year cycle (middle panel). The extant database is too short to verify longer term changes, such as the larger amplitude variability speculated to have occurred from the Maunder Minimum to the present (bottom panel).

Changes of a few tenths percent (2-3W/m^2) occur regularly in the Sun's total radiative output as the Sun rotates on its axis every 27 days. This rotational modulation is superimposed on an 11-year irradiance cycle with an amplitude of about 0.1%. Enhanced solar activity (such as during

In: C.M. Isaacs and V.L. Tharp, Editors. 1996. *Proceedings of the Twelfth Annual Pacific Climate (PACLIM) Workshop, May 2-5, 1995.* Interagency Ecological Program, Technical Report 46. California Department of Water Resources.

maxima of the 11-year activity cycle in 1980 and 1990) increases both the overall irradiance level and the range of the rotational modulation. Of course previous and subsequent total irradiance cycles may have quite different amplitudes, depending on the strength of solar activity and other activity-related properties. Solar total radiative output variations with larger amplitude than the 11-year cycle — 0.24% relative to the mean of present levels — are estimated to have occurred during the seventeenth century Maunder Minimum (1645-1715), based on parameterizations of the variability mechanisms identified for the 11-year cycle using proxies of solar and stellar variability (Lean *et al* 1992).

Irradiance variations associated with solar activity potentially cause natural climate fluctuations such as those evident in paleoclimate records obtained from ice-cores, tree-rings, pollen, corals, and glacial events. Other potential causes of natural climate change are volcanic eruptions and internal oscillations and couplings between the ocean and the atmosphere (Rind and Overpeck 1993; Mehta and Delworth 1995). Global mean annual surface temperature increased 0.55°C from 1860 to 1990 (Parker *et al* 1994). It is uncertain whether this warming is a response of the climate system to increasing concentrations of industrially produced CO_2 gas in the Earth's atmosphere (which increased from 280 to 353 ppmv over this period) or to combinations of the various natural influences which have also varied during this epoch (Figure 2). That the cause of the warming is indeed more complex than the influence of increasing greenhouse gases alone is suggested by statistical analyses of the climate record since 1860, which reveal significant interannual and

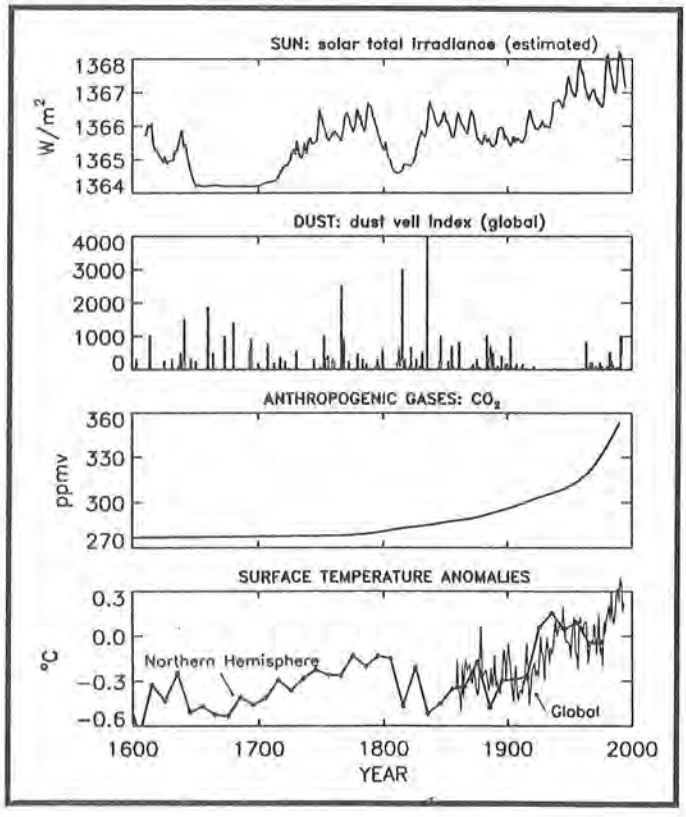

Figure 2 Compared are annual averages of:
(a) estimated solar total irradiance (Lean *et al* 1995);
(b) the volcanic aerosol loading according to the global dust veil index (Lamb 1977; Robuck and Free 1995); and
(c) the concentration of CO_2 (Keeling and Whorf 1994).
The Bradley and Jones (1993) record of decadal Northern Hemisphere surface temperature, shown in (d), suggests that the warming recorded by the IPCC (1992) data over the past 150 years is part of a longer-term trend that commenced prior to the industrial revolution.

interdecadal variability (Allen and Smith 1994; Mann and Park 1994). Furthermore, the surface temperature increase of the past 130 years appears to be part of a longer term warming that commenced in the seventeenth century (Bradley and Jones 1993), prior to the industrial epoch.

Dominant climate forcing in the past century (of the order of 2.4 W/m^2) is ascribed with some confidence to increasing concentrations of greenhouse gases (CO_2, CH_4, N_2O and halocarbons). But like greenhouse gas concentrations, the overall activity level of the Sun has risen steadily in the past few hundred years (NRC 1994) (Figure 1). Although direct solar irradiance monitoring exists only for 16 years, increasing irradiance is inferred to accompany solar activity increases over the past few centuries, based on cosmogenic isotope records of solar variability (Beer *et al* 1994; Stuiver and Braziunas 1995) and long-term monitoring of ionized Ca emission in the Sun and Sunlike stars (Baliunas and Jastrow 1990; White *et al* 1992). As well, tropospheric anthropogenic sulfate aerosol increases have accompanied the greenhouse gas increase of the industrial era (Penner *et al* 1994) while the amount of aerosols ejected into the atmosphere by volcanic eruptions decreased markedly in most of the twentieth century relative to the nineteenth century (Lamb 1977; Robuck and Free 1995). Global ozone concentrations have decreased in the stratosphere and increased in the troposphere (de Gruijl 1995). Surface albedo is changing too (Hannah *et al* 1994).

In a globally averaged sense, increasing solar radiative output and greenhouse gases both provide positive climate forcings and warmer surface temperatures because of the net increased energy input to the climate system. In contrast, increased industrial and volcanic aerosols inhibit the penetration of the Sun's radiation to the Earth's surface and lead to surface cooling. Decreasing ozone in the lower stratosphere is also thought to have a net cooling effect on surface temperature, as well as enabling increased penetration of biologically harmful solar UV radiation to the biosphere. Tropospheric ozone changes may mitigate these effects to some extent.

Amplitudes of climate forcings other than greenhouse gas concentrations, including solar radiative output variations, are thought to be smaller, but are also uncertain (Figure 3). Poorly known is the magnitude of the potentially large negative forcing (of the order of -1 W/m^2 or more) by tropospheric aerosols. Cancellation by aerosol cooling of a portion of the greenhouse gas warming increases the fraction of the net forcing potentially attributable to solar variability.

In fact, surface temperatures correlate well with solar activity over the past 140 years (Reid 1991; Friis-Christensen and Lassen 1991), with correlation coefficients as high (0.7) as the correlation between surface

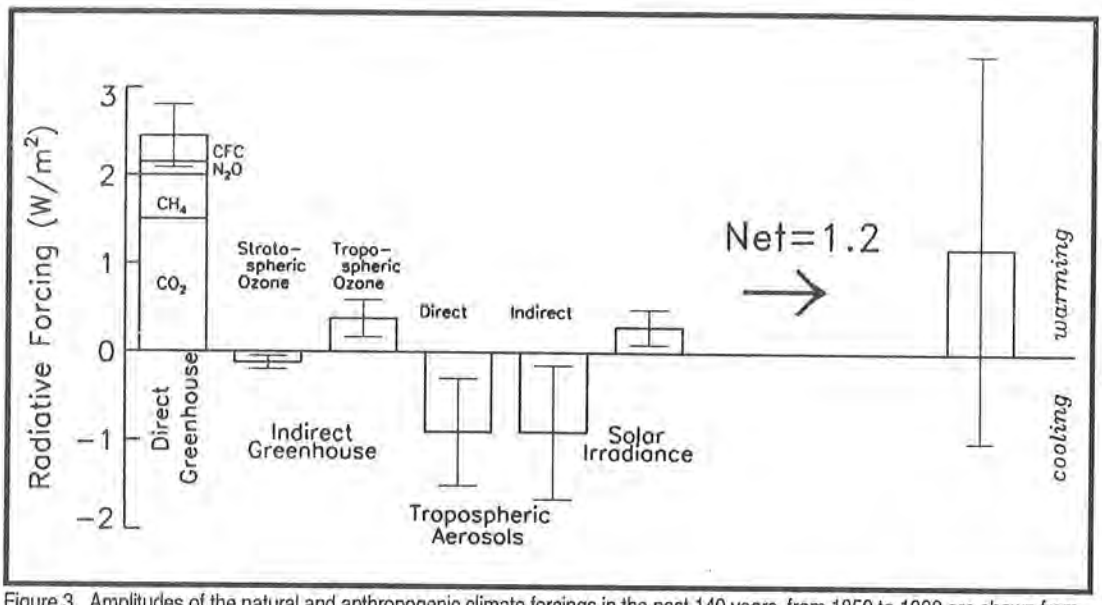

Figure 3 Amplitudes of the natural and anthropogenic climate forcings in the past 140 years, from 1850 to 1990 are shown from IPCC (1995). Each individual forcing is expected to impact the climate system in different ways depending on its latitude, altitude and history. However, climate change assessments lack the complexity to account for the myriad pathways of the climate system response, and global scale studies often assume a common climate sensitivity to the different forcings (see also, Hansen *et al* 1993).

temperatures and greenhouse gas concentrations. Eleven and 22-year periods evident in solar activity proxies also appear in many climate and paleoclimate records (Mitchell *et al* 1979; Newell *et al* 1989; Dunbar *et al* 1994), and some solar and climate time series correlate strongly over multi-decadal and centennial time scales (Wigley and Kelly 1990; Burroughs 1992). These statistical relationships suggest a response of the climate system to the changing Sun.

Examination of the pre-industrial period from 1610 to 1800 can provide insight to climate forcing by changing solar radiation in an epoch prior to the influence of anthropogenic greenhouse gases. The correlation of decadal means of reconstructed solar irradiance S and Northern Hemisphere surface temperature anomalies ΔT from 1610 to 1800 (using data such as those shown in Figure 2) is 0.86, implying a predominant solar influence on climate during this period and allowing an empirical quantification of the effect ($\Delta T = -200.44 + 0.1466 \times S$). Extending the pre-industrial correlation to the present suggests that solar forcing may have contributed about half of the observed 0.55°C surface warming since 1860 but only one-third of the warming since 1970 (Figure 4) (Lean *et al* 1995). An equilibrium simulation by the GISS GCM predicts a Northern Hemisphere surface temperature change of 0.51°C for a 0.25% solar irradiance reduction (Rind and Overpeck 1993), in general agreement with the estimate from the pre-industrial parameterization of the warming from the Maunder Minimum to the present.

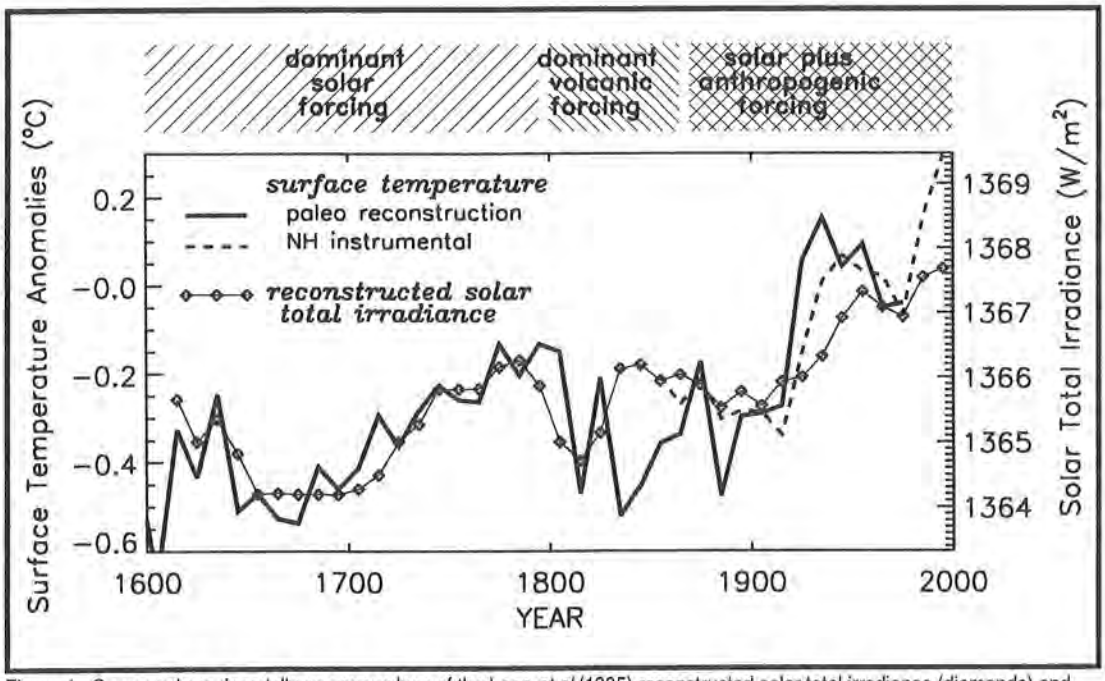

Figure 4 Compared are decadally average values of the Lean *et al* (1995) reconstructed solar total irradiance (diamonds) and Northern Hemisphere summer temperature anomalies from 1610 to the present (similar annually averaged data are shown in Figures 1 and 2). The solid line is the Bradley and Jones (1993) Northern Hemisphere summer surface temperature reconstruction from paleoclimate data (primarily tree rings), scaled to match the Northern Hemisphere instrumental data (IPCC 1992) (dashed line) during the overlap period.

However, attributing a significant fraction of recent climate warming to solar forcing presents serious ambiguities about the impact of increasing greenhouse gas concentrations whose radiative forcing has been significantly larger than solar forcing over this period. Attempts to attribute the entire surface warming of the industrial epoch by solar radiative forcing alone have been refuted, because simulations of this scenario with simple climate-ocean energy balance models require climate sensitivities beyond the expected conservative range of 0.3 to 1.0°C/Wm^{-2}, or solar irradiance variability larger than the 0.1% change observed over a recent Schwabe (11-year) cycle (Schlesinger and Ramankutty 1992; Kelly and Wigley 1992). More generally, however, presently specified climate sensitivity overpredicts the magnitude — and cannot replicate the shape — of the observed surface warming expected from radiative forcing by greenhouse gases alone, of amplitude shown in Figure 3. This underscores the need to better quantify all other natural and anthropogenic influences, including those of lesser magnitude than greenhouse gases, since the assumption of similar climate response to forcings of similar magnitude may not be valid.

Given the apparent climate system response to solar irradiance variability implied by a variety of Sun/climate statistical relationships over the past few centuries, continued space-based solar irradiance monitoring is important to quantify natural solar forcing of future climate. Additional

work is needed to improve understanding of the physical pathways by which the climate system responds to direct as well as indirect solar radiative forcing, such as potentially associated with UV irradiance variability impacts on the Earth's atmosphere, and coupling of this influence to the biosphere and climate system (Rind and Balachandran 1995). Ultimately, the impact of changing solar radiation on the climate system must be understood over decadal and centennial time scales, and regional and global spatial scales, in different epochs. This will likely require time-dependent simulations over past centuries, in the present, and into the future, with GCMs appropriately coupled to middle atmosphere models, utilizing realistic, spectrally-dependent solar irradiance variations with properly parameterized wavelength-dependent impact on the climate system. Importantly, analysis of paleoclimate data from over the globe must be integrated into the assessment of results of the simulations. Such studies are only just beginning. Sun/climate studies in the future require cross-disciplinary endeavors such as promoted and conceived by the Pacific Climate Workshop and Analysis of Rapid and Recent Climatic Change.

Acknowledgments

This work was supported in part by the Strategic Environmental Research and Development Program. Portions of the text are from *Climate Forcing by Changing Solar Radiation*, by J. Lean and D. Rind, submitted to the special PACLIM95 publication of the *Journal of Climate*.

References

Allen, M.R., and L.A. Smith. 1994. Investigating the origins and significance of low-frequency modes of climate variability. *Geophys. Res. Lett.* 21:883-886.

Baliunas, S., and R. Jastrow. 1990. Evidence for long-term brightness changes of solar-type stars. *Nature* 348:520-523.

Beer, J., S.T. Baumgartner, B. Dittrich-Hannen, J. Hauenstein, P. Kubik, C. Lukasczyk, W. Mende, R. Stellmacher, M. Suter. 1994. Solar variability traced by cosmogenic isotopes. Pages 291-300 in *The Sun as a Variable Star.* J.M. Pap, C. Fröhlich, H.S. Hudson, and S.K. Solanki (eds.), Cambridge University Press.

Bradley, R.S., and P.D. Jones. 1993. "Little Ice Age" summer temperature variations: Their nature and relevance to recent global warming trends. *The Holocene* 3(4):367-376.

Burroughs, W.J. 1992. *Weather Cycles Real or Imaginary?* Cambridge University Press, Cambridge.

de Gruijl, F.R. 1995. Impacts of a projected depletion of the ozone layer. *Consequences* 1:13-21.

Dunbar, R.B., G.M. Wellington, M.W. Colgan, P.W. Glynn, 1994. Eastern Pacific sea surface temperature since 1600 AD. The Δ18O record of climate variability in Galápagos corals. *Paleoceanography* 9:291-315.

Friis-Christensen, E., and K. Lassen. 1991. Length of the solar cycle: An indicator of solar activity closely associated with climate. *Science* 254:698-700.

Hannah L., D. Lohse, C. Hutchinson, J.L. Carr, A. Lankerani, 1994. A preliminary inventory of human disturbances of world ecosystems. *Ambio* XXIII:246-250.

Hansen, J., A. Lacis, R. Ruedy, M. Sato, H. Wilson. 1993. How sensitive is the world's climate? *Natl. Geogr. Res. Explor.* 9:142.

Intergovernmental Panel on Climate Change. 1992. Climate Change 1992: *The Supplementary Report to the IPCC Scientific Assessment.* J.T. Houghton, B.A. Callander, and S.K. Varney (eds.). Cambridge University Press.

Intergovernmental Panel on Climate Change. 1995. *Climate Change 1994: Radiative Forcing of Climate Change and An Evaluation of the IPCC IS92 Emission Scenarios.* J.T. Houghton, L.G. Meira Filho, J. Bruce, HoeSun Lee, B.A. Callander, E. Haites, N. Harris, K. Maskell (eds.). Cambridge University Press.

Keeling, C.D., and T.P. Whorf. 1994. Atmospheric CO2 records from sites in the SIO air sampling network. Pages 16-26 in *Trends '93: A Compendium of Data on Global Change.* T.A. Boden, D.P. Kaiser, R.J. Sepanski, F.W. Stoss (eds.), ORNL/CDIAC-65, Carbon Dioxide Information Analysis Center, Oak Ridge National Laboratory, Oak Ridge, Tenn.

Kelly, P.M., and T.M.L. Wigley. 1992. Solar cycle length, greenhouse forcing and global climate. *Nature* 360:328-330.

Lamb, H.H. 1977. Supplementary volcanic dust veil assessments. *Climate Monitor* 6:57-67.

Lean, J. 1991. Variations in the Sun's radiative output. *Reviews of Geophys.* 29:505-535.

Lean, J., A. Skumanich, O. White. 1992. Estimating the Sun's radiative output during the Maunder Minimum. *Geophys. Res. Lett.* 19:1591-1594.

Lean, J., J. Beer, R. Bradley. 1995. Reconstruction of solar irradiance since 1610: Implications for climate change. *Geophys. Res. Lett.* 22:3195-3198.

Mann, M.E., and J. Park. 1994. Global-scale modes of surface temperature variability on interannual to century timescales. *J. Geophys. Res.* 99:25,819-25,833.

Mehta, V.M., and T. Delworth. 1995. Decadal variability of the tropical Atlantic ocean surface temperature in shipboard measurements and in a global ocean-atmosphere model. *J. Climate* 8:172-190.

Mitchell, J.M., C.W. Stockton, D.M. Meko. 1979. Evidence of a 22-year rhythm of drought in the western United States related to the Hale solar cycle since the 17th century. Pages 124-144 in *Solar Terrestrial Influences on Weather and Climate.* B.M. McCormac, and T.A. Seliga (eds), D. Reidel, Hingham, Mass.

National Research Council. 1994. *Solar Influences on Global Change.* National Academy Press, Washington, D.C.

Newell, N.E., R.E. Newell, J. Hsuing, W. Zhongxiang. 1989. Global marine temperature variation and the solar magnetic cycle. *Geophys. Res. Lett.* 16:311-314.

Parker, D.E., P.D. Jones, C.K. Folland, A. Bevan. 1994. Interdecadal changes of surface temperature since the late nineteenth century. *J. Geophys. Res.* 99:14,373-14,399.

Penner, J.E., R.J. Charlson, J.M. Hales, N.S. Laulainen, R. Leifer, T. Novakov, J. Ogren, L.F. Radke, S.E. Schwartz, T. Travis. 1994. Quantifying and minimizing uncertainty of climate forcing by anthropogenic aerosols. *Bulletin Amer. Meteor. Soc.* 75:375-400.

Reid, G. 1991. Solar total irradiance variations and the global sea surface temperature record. *J. Geophys. Res.* 96:2835-2844.

Rind, D., and J. Overpeck. 1993. Hypothesized causes of decade-to-century climate variability: Climate model results. *Quat. Sci. Rev.* 12:357-374.

Rind, D., and N.K. Balachandran. 1995. Modeling the effects of UV variability and the QBO on the troposphere-stratosphere system. Part II: The troposphere. *J. of Climate* 8:2080-2095.

Robuck, A., and M.P. Free. 1995. Ice-cores as an index of global volcanism from 1850 to the present. *J. Geophys. Res.* 100:11,549-11,567.

Schlesinger, M.E., and N. Ramankutty. 1992. Implications for global warming of intercycle solar irradiance variations. *Nature* 360:330-333.

Stuiver, M., and T.F. Braziunas. 1995. Solar variability over the last 2000 years. In *Climate Variations and Forcing Mechanims of the Last 200 Years.* P. Jones, J. Jouzel and R. Bradley (eds.), NATO ASI Series I: Global Environmental Change, in press.

White, O.R., A. Skumanich, J. Lean, W.C. Livingston, S. Keil. 1992. The Sun in a non-cycling state. *Public. Astron. Soc. Pacif.* 104:1139-1143.

Wigley, T.M.L., and P.M. Kelly. 1990. Holocene climatic change, 14C wiggles and variations in solar irradiance. Pages 547-560 in *The Earth's Climate and Variability of the Sun over Recent Millennia: Geophysical, Astronomical and Archaeological Aspects.* Phil. Trans. R. Soc. Lond. A 330.

Effects of Interdecadal Climate Variability on the Oceanic Ecosystems of the Northeast Pacific Ocean

Robert C. Francis, S.R. Hare, A.B. Hollowed, Warren S. Wooster

Abstract

It is increasingly apparent that a major reorganization of the Northeast Pacific biota transpired following a climatic "regime shift" in the mid-1970s. In this paper, we characterize the effects of interdecadal climate forcing on the oceanic ecosystems of the northeastern Pacific Ocean. Our approach is to first discuss the concept of scale in three dimensions: time, space, and oceanic ecosystem. In so doing, we develop a conceptual model to illustrate how climate variability is linked to ecosystem change. Next we describe a number of recent studies relating climate to marine ecosystem dynamics in the northeastern Pacific Ocean. These studies have focused on the major components of marine ecosystems — primary and secondary producers; primary, secondary, and top level predators. They have been undertaken at different time and space scales. Taken together, however, they reveal a more coherent picture of how decadal-scale climate forcing may affect the large oceanic ecosystems of the northeastern Pacific. Finally, we conclude by synthesizing the insight gained from interpreting these studies. Several general conclusions can be drawn:

- There are large-scale, low frequency, and sometimes very rapid changes in the distribution of atmospheric pressure over the North Pacific, which are, in turn, reflected in ocean properties and circulation.
- Oceanic ecosystems respond on similar time and space scales to variations in physical conditions.
- Linkages between the atmosphere/ocean physics and biological responses are often different across time and space scales.
- While the cases presented here demonstrate oceanic ecosystem response to climate forcing, they provide only hints of the mechanisms of interaction.
- A model whereby ecosystem response to specified climate variation can be successfully predicted will be difficult to achieve because of scale mismatches and nonlinearities in the atmosphere-ocean-biosphere system.

In: C.M. Isaacs and V.L. Tharp, Editors. 1996. *Proceedings of the Twelfth Annual Pacific Climate (PACLIM) Workshop, May 2-5, 1995.* Interagency Ecological Program, Technical Report 46. California Department of Water Resources.

Decadal Hydroclimatic Variability over Western North America

Dan Cayan, Mike Dettinger, Henry Diaz, Nicholas Graham

Abstract

Variability of precipitation over North America on ENSO and decadal time scales is examined from several decades of precipitation and snow course records. Band pass (periods of 3-7 years) and decadal (periods of 7 years and greater) filtering was performed on gridded precipitation data (obtained from Eischeid and Diaz, NOAA) to isolate ENSO and decadal period fluctuations. For both time scales, three prominent patterns that emerge, via a rotated principal components (RPC) analysis, have anomaly centers over (1) the Pacific Northwest and (2) the Southwest, and (3) California-Nevada. Components of these same patterns are also present in the high elevation springtime snow accumulation fields as measured at a set of snow courses over the western United States. In the time domain, similar decadal filtered historical time series of snow accumulation and streamflow confirm the decadal RPC fluctuations _ there is a close comparison between the RPC time-varying amplitudes, regional snow course records, and a representative stream gage record in the three respective regions.

To begin to understand the causes of these low-frequency variations in precipitation, the RPC series were correlated with gridded historical sea level pressure (SLP) and sea surface temperature (SST), which were also filtered at the ENSO or decadal bands.

The fields of correlation that emerged indicate that anomalous precipitation is driven by low-frequency changes in the atmospheric circulation. In general, anomalously low pressure over a particular region or just upstream to the northwest is associated with heavier-than-normal precipitation. There are also associated anomalous regional and larger scale patterns in SST, but the question remains whether SST is a *causal factor* or just another *symptom* of altered circulation?

There is some evidence that western North America precipitation modes associate with *global* SLP and SST anomalies. In these cases, the SLP anomalies cross the hemisphere and cross the equator, while SST patterns show significant correlation over the global ocean basins. The Southwest decadal precipitation pattern (mode 1) relates to an El Niño-like SST anomaly pattern and an inter-hemispheric pressure mode. This mode, which has seen increased precipitation and snowpack since the 1970s, projects quite strongly upon a global decadal precipitation pattern with primary center in the Sahel. Thus, there is some evidence of a global component in western North America precipitation.

In: C.M. Isaacs and V.L. Tharp, Editors. 1996. *Proceedings of the Twelfth Annual Pacific Climate (PACLIM) Workshop, May 2-5, 1995.* Interagency Ecological Program, Technical Report 46. California Department of Water Resources.

Terrestrial Ecosystem Response to Interdecadal Climate Variability in the Western United States

Thomas W. Swetnam and Julio L. Betancourt

Abstract

We argue that the most important climatically-driven terrestrial ecosystem changes are concentrated in annual- to decadal-scale episodic events. These rapid ecosystem responses to climate change are manifested as regionally synchronized disturbance events (*eg*, floods, fires, and insect outbreaks) and increased drought-caused plant mortality rates. Ecological experiments and simulation models of climate change impacts, however, most commonly focus on relatively constant, slower, and smaller-scale processes (*eg*, plant growth and competition), while regional-scale disturbance and mortality events are treated only anecdotally. Regional-scale, climate-driven vegetation changes are partly a function of interdecadal climate shifts caused by changes in persistent features of the atmosphere, such as the SO, PNA, and the breakdown in monsoonal circulation. In the United States, decadal-scale climatic shifts with broad-scale impacts on terrestrial ecosystems include the change in Pacific climate since 1976 and the multi-year subcontinental-scale droughts of the 1930s (Dust Bowl) in the Great Plains and the 1950s in the North American subtropics. The 1950s drought culminated in widespread vegetation die-off in the southwestern United States. Recent improvement in rangeland conditions and increased wildfire number and area burned in the western United States may be more closely related to the post-1976 climate shift than to management activities. The value of high-resolution proxies several times longer than the instrumental record is highlighted by the need to determine if these changes are unique to the 20th century or if they fall within the envelope of long-term, natural variability. We will describe several examples of multi-century, regional to subcontinental-scale patterns of disturbance and tree demographic responses to climate change in the western United States. These perspectives suggest a new framework for observing and interpreting past and current ecosystem response to climate change patterns across multiple spatial and temporal scales.

In: C.M. Isaacs and V.L. Tharp, Editors. 1996. *Proceedings of the Twelfth Annual Pacific Climate (PACLIM) Workshop, May 2-5, 1995*. Interagency Ecological Program, Technical Report 46. California Department of Water Resources.

Paleorecords of Interdecadal Variability from Mid-Latitude Varved Sediments and Tropical Corals of the Eastern Pacific

Tim R. Baumgartner and Robert B. Dunbar

Abstract

Reconstruction of proxy variables from massive corals and varved sediments of the eastern Pacific allow us to compare variability in the ocean climate from equatorial and mid-latitude sites for a significantly longer period than is available from the instrumental record. The coral proxy consists of the yearly oxygen isotope ratios from *Pavona clavus* and *P. gigantea* of the Galapagos Islands and extends from AD 1600 to 1980. The varve records extends from AD 500 to 1970 and consists of 5-year averages of fish-scale deposition rates in the Santa Barbara Basin, reflecting the population sizes of the Pacific sardine and northern anchovy off southern California. Although the recording mechanisms are very different, each record provides an index of regional ocean surface temperature. Both the coral isotope record and the varve record of scale-deposition show important spectral peaks at periods of about 50 years, 30 years, and 17 years. Construction of the evolutionary spectra of the coral data for the interval 1670-1925 shows that these periods are not contemporaneous in that series. Rather, there are three distinct epochs with progressively shorter periods characterizing the interdecadal variability. The 50-year period dominated during the earliest epoch from about AD 1670 to 1750; the 33-year period dominated from 1750 to about 1850; and the 17-year period dominated from roughly 1860 through the end of the analysis to 1925. Transitions between the dominant periods of these epochs appear to be quite abrupt.

Comparison of the Santa Barbara sardine record to the isotope record of the Galapagos corals (after converting the coral series to comparable 5-year averages) shows that the character of the relationship between the Santa Barbara and Galapagos records changes markedly across the transition at about 1750 and again at about 1850. The early epoch (1610-1750) is characterized by a clear inverse relationship between the sardine record and the coral record, indicating an inverse relationship in regional ocean surface temperatures during that interval. The succeeding epoch is characterized by a strong dampening of the variability in the sardine record and weakening of the inverse relationship. During the final epoch (about 1850-1930), the interdecadal variability of the two records is in phase, although the lower frequency (centennial scale) variability still appears to be inversely correlated. These observations suggest that the significant changes in the nature of variability over multi-decadal time scales in the tropics have also occurred at mid-latitudes along the eastern boundary. They also indicate that the large-scale spatial coherence in the variability of ocean climate along the eastern boundary at the interannual (ENSO) time scale is not maintained over the interdecadal time scale.

In: C.M. Isaacs and V.L. Tharp, Editors. 1996. *Proceedings of the Twelfth Annual Pacific Climate (PACLIM) Workshop, May 2-5, 1995.* Interagency Ecological Program, Technical Report 46. California Department of Water Resources.

The Terrestrial Record of Interdecadal Climate Variability in Western North America

Malcolm K. Hughes

Abstract

Western North America is particularly rich in natural records of climate that have potential to reveal features of interdecadal climate variability. The records reviewed in this paper will be either annual continuous, such as tree rings or laminated sediments, or episodic, such as traces of events associated with pluvial lakes. Particular emphasis will be given to (1) the use of subcontinental-scale tree-ring networks to study interdecadal variability over the past 300-400 years, and (2) to exploration of changes in interdecadal variability on centennial and millennial time scales using long tree-ring chronologies.

In: C.M. Isaacs and V.L. Tharp, Editors. 1996. *Proceedings of the Twelfth Annual Pacific Climate (PACLIM) Workshop, May 2-5, 1995.* Interagency Ecological Program, Technical Report 46. California Department of Water Resources.

Decadal Climate Variability over the North Pacific and North America: Dynamics and Predictability

Mojib Latif and Tim P. Barnett

Abstract

The dynamics and predictability of decadal climate variability over the North Pacific and North America are investigated by analyzing various observational datasets and the output of a state-of-the-art coupled ocean-atmosphere general circulation model, which was integrated for 120 years. The observations and the model results both support the picture that the decadal variability in the region of interest is based on a cycle involving unstable ocean-atmosphere interactions over the North Pacific. The period of this cycle is on the order of a few decades.

The cycle involves the two major circulation regimes in the North Pacific climate system, the subtropical ocean gyre and the Aleutian low. When, for instance, the subtropical ocean gyre is anomalously strong, more warm tropical waters are transported poleward by the Kuroshio and it extension, leading to a positive SST anomaly in the North Pacific. The atmospheric response to this SST anomaly involves a weakened Aleutian low, and the associated fluxes at the air/sea interface reinforce the initial SST anomaly, so that the ocean and atmosphere act as a positive feedback system. Both the anomalous heat flux and reduced ocean mixing in response to a weakened storm track contribute to this positive feedback. The atmospheric response, however, consists also of a wind stress curl anomaly that spins down the subtropical ocean gyre, thereby reducing the poleward heat transport and the initial SST anomaly. The ocean adjusts with some time lag to the change in the wind stress curl, and it is this transient ocean response that allows continuous oscillations. The transient response can be expressed in terms of baroclinic planetary waves, and the decadal time scale of the oscillation is, therefore, determined to first order by wave time scales.

In: C.M. Isaacs and V.L. Tharp, Editors. 1996. *Proceedings of the Twelfth Annual Pacific Climate (PACLIM) Workshop, May 2-5, 1995.* Interagency Ecological Program, Technical Report 46. California Department of Water Resources.

Interdecadal Variability in the Spatial Structure of Wind and SST in the California Current System

Franklin B. Schwing, Roy Mendelssohn, Richard Parrish

Introduction

The physical environment of eastern boundary current systems is rarely uniform in time. ENSO and other perturbations produce profound anomalies in the atmosphere and ocean on interannual to decadal and century time scales. Analogously, eastern boundary currents can be separated into discrete spatial regions, dominated by different physical processes, and presumably analogously different biological structure. These regions may be separated by sharp gradients in physical forcing and characteristics or by broad transition zones that extend over several degrees of latitude. The timing and intensity of large-scale climate events may not be coherent between regions.

To better understand how eastern boundary current ecosystems might respond to climate variability, it is crucial to describe their primary scales of spatial and temporal variability and discern the dynamics responsible for this variance, rather than treat eastern boundary currents as spatially homogeneous systems or use seasonally-averaged data to describe their climatology. The objective of this paper is to describe the temporal variability in the spatial texture of the California Current system, a major eastern boundary current system off the west coast of North America, to provide a base from which to evaluate the effect of climate change — in the recent past, at present, and for the future.

State-space statistical models are applied to long environmental time series of wind stress and sea surface temperature (SST) from the California Current (22-48°N) for the period 1946-1990. These data are expressed as monthly averages of the Comprehensive Ocean-Atmosphere Data Set (COADS) for 2° latitude boxes, which extend laterally from the coast to nominally 4° offshore. The models estimate a non-parametric and non-linear trend, a non-stationary and non-deterministic seasonal signal, and an autoregressive term (Schwing and Mendelssohn 1995). The models are applied to long time series of SST from selected coastal sites as well, for comparison to the COADS series.

In: C.M. Isaacs and V.L. Tharp, Editors. 1996. *Proceedings of the Twelfth Annual Pacific Climate (PACLIM) Workshop, May 2-5, 1995.* Interagency Ecological Program, Technical Report 46. California Department of Water Resources.

Results

From the state-space model trend series, the California Current can be divided into three distinct geographical regions. The northern region (north of 40°N) features a rapid transition from strongly equatorward to poleward wind stress with distance north (Figure 1). The mean stress north of 44°N is poleward and has become increasingly poleward over time. The transition zone in wind stress has expanded southward over time, strengthening the zonal gradient in poleward stress. The California Current north of 40°N features spatially uniform mean SST (Figure 2). These SST trends show a series-length cooling tendency. This region of uniform SST has expanded southward over time as well.

Winds south of 40°N are equatorward and can be described in terms of central and southern regions (Figure 1). The central region (32-40°N) exhibits the greatest wind stress magnitudes in the California Current.

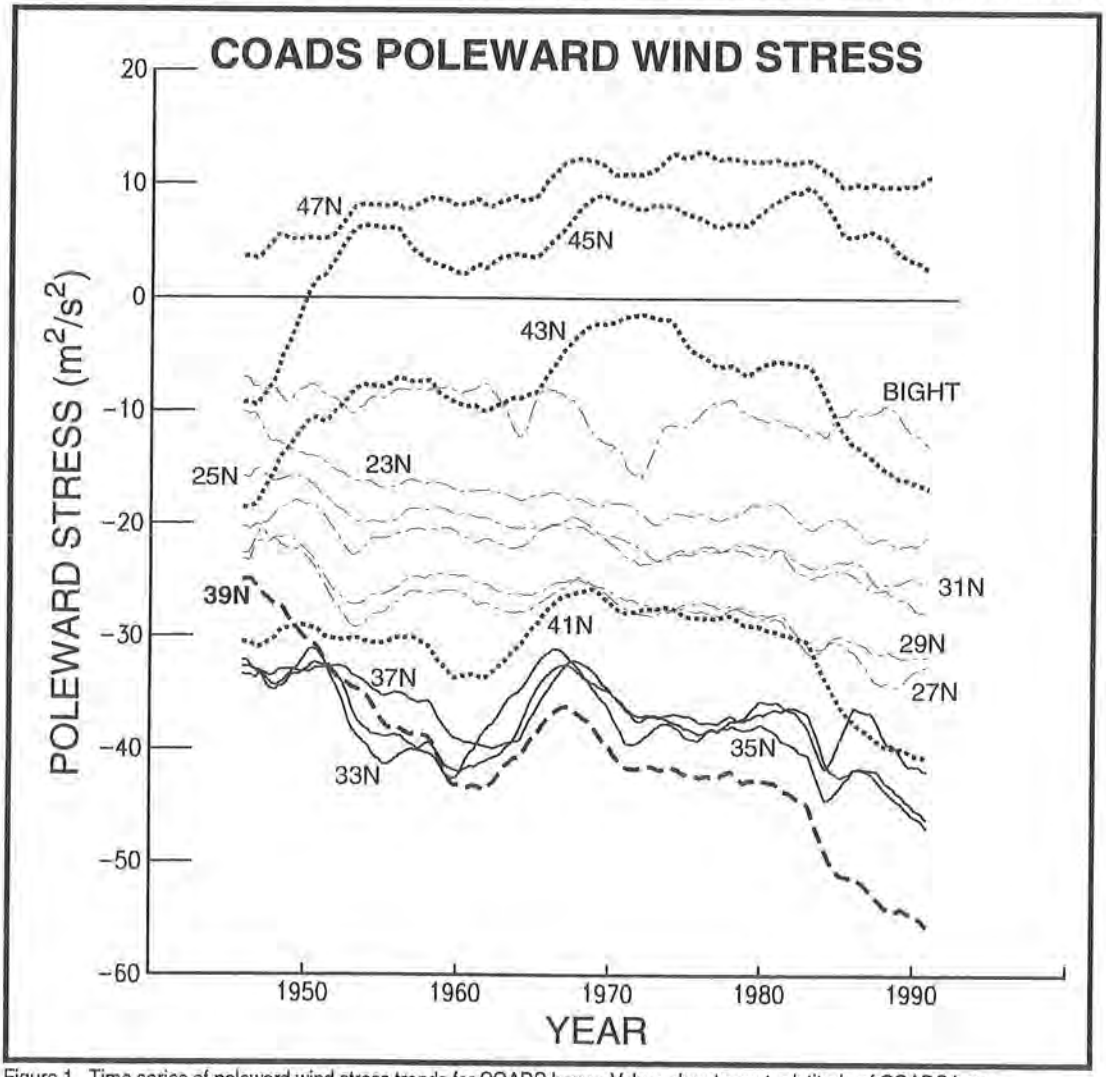

Figure 1 Time series of poleward wind stress trends for COADS boxes. Values denote center latitude of COADS boxes. Dashed-dotted lines represent time series from southern region (22-32°N). Solid lines represent time series from central region (32-40°N). Bold dotted lines represent time series from northern region (40-48°N). Bold dashed line represents 38-40°N time series.

Equatorward stress has intensified over time more here than in the northern and southern regions. This region features the greatest scales of interannual-to-decadal variation in stress (Figure 1) and SST (Figure 2) as well. Stress in the southern region (22-32°N) has become increasingly equatorward over time in a monotonic pattern, with relatively little interannual variation. Mean SST decreases consistently with increasing latitude in the central and southern regions. SST over about 30-38°N appears to warm rapidly in response to the 1957 and 1983 ENSO events as well as the well-documented 1976 regime shift (cf. Trenberth 1990). SSTs off Washington and Oregon (40-48°N) and most of Baja California (south of 30°N), on the other hand, take several months to years following the 1976 shift to warm by similar amounts.

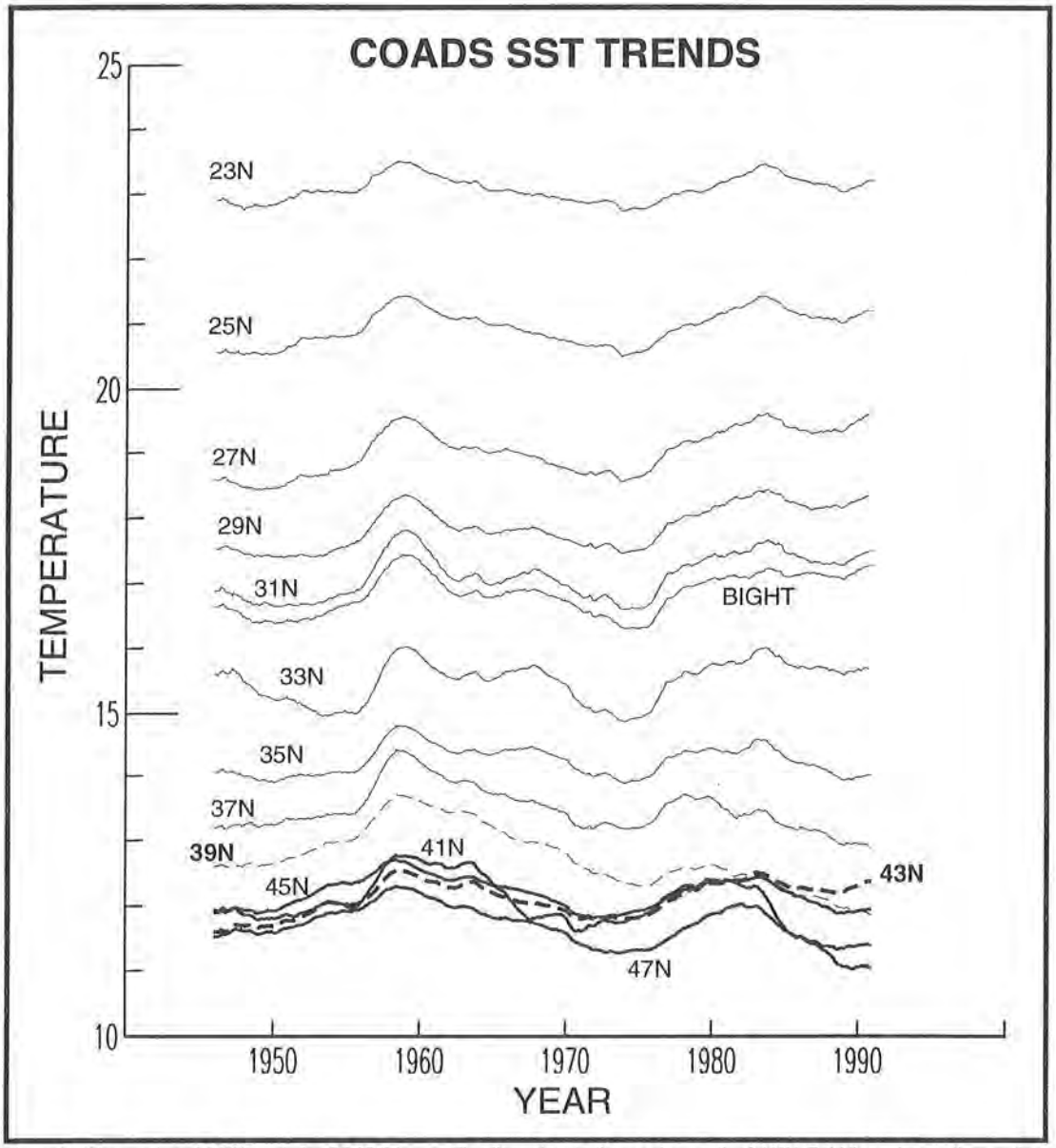

Figure 2 Time series of SST trends for COADS boxes. Fine lines denote time series south of 40°N. Bold lines denote time series north of 40°N. Fine and bold broken lines denote time series for 38-40°N and 42-44°N COADS boxes, respectively.

Although shore-based SST trends along the entire United States west coast display a significant warming tendency over the past several decades (Figure 3), the COADS (*ie*, California Current) SSTs show a cooling tendency north of 36°N (Figures 2 and 3). On shorter time scales, SST has decreased significantly since the 1983 ENSO north of about 34°N, but SSTs south of about 32°N have returned to near 1983 levels after a brief period of cooling following this event. The entire California

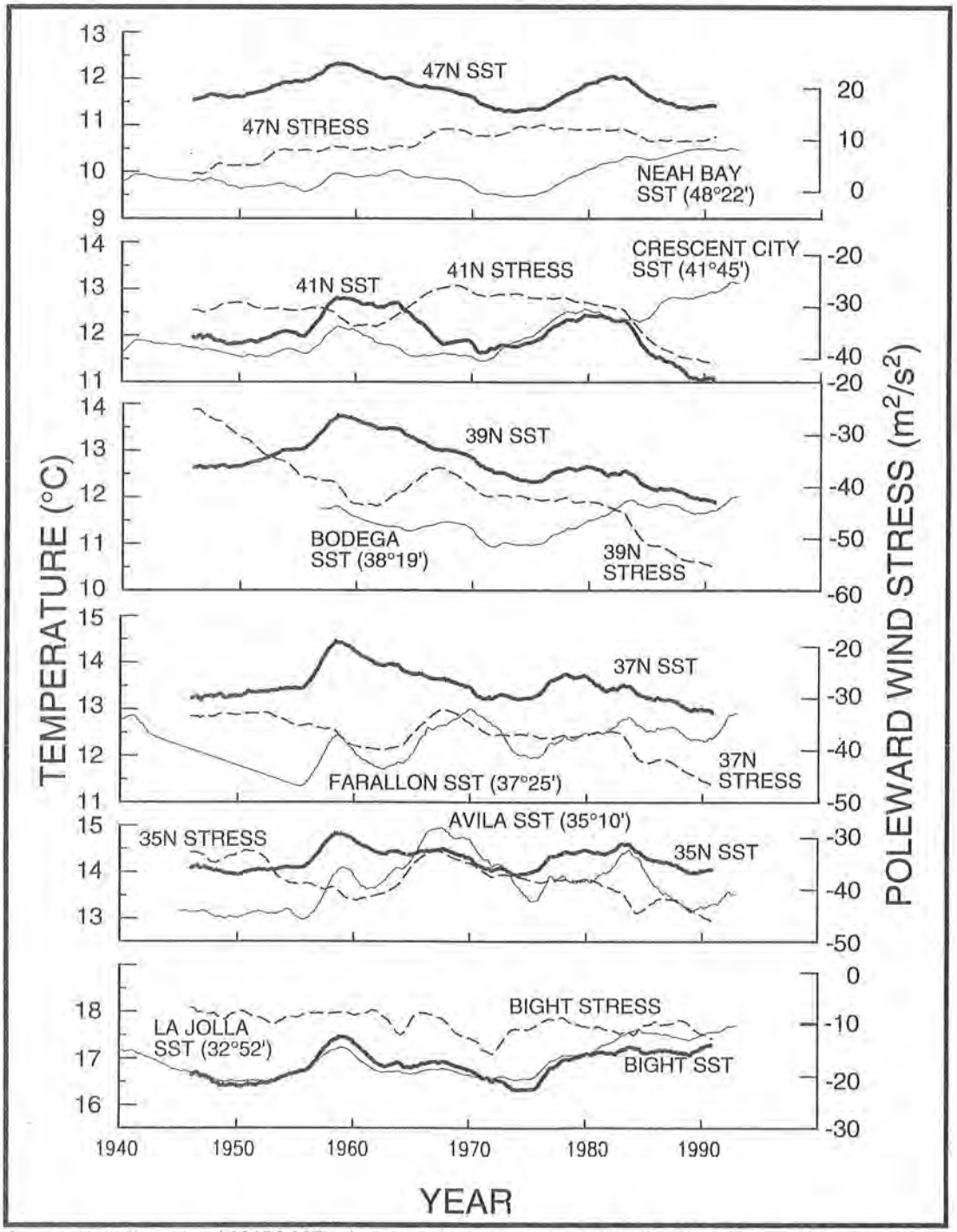

Figure 3 Trend time series of COADS SST and poleward wind stress, compared with selected nearby coastal SST series. Bold solid lines represent COADS SST series. Fine solid lines represent coastal SST series. Broken lines represent wind stress series. Location of time series shown in each plot.

Current warmed and cooled system-wide on decadal time scales prior to 1983, but displays a more heterogeneous pattern since 1983. A lack of correspondence between the 2° COADS and coastal SST time series north of about 34°N (Figure 3) suggests there is considerable cross-shelf as well as latitudinal variability in the California Current. This is confirmed by examination of the COADS data on 1° space scales (Schwing *et al* 1995).

SST trends are visually more correlated on interannual scales than wind stress trends. Major ENSOs and the 1976 regime shift dominate the SST trends series, particularly south of 38°N, but are not apparent in the wind trends. Instead ENSO wind variance is seen more clearly in the model autoregressive and error components of the state-space model, presumably because of the rapid atmospheric response to ENSO events. Multi-year perturbations in the wind trend series do occur (cf, 32-40°N, Figure 1) but are not coincident with ENSO or other documented large-scale atmospheric events. SST also shows decadal-scale periods of warm and cool anomalies that extend through the entire California Current. Wind stress anomalies are less extensive latitudinally and uncorrelated with local SST (Figure 3), suggesting that decadal-scale SST variability in the California Current is controlled by the basin- to global-scale pressure and wind fields, rather than local wind forcing.

Discussion

The different regions of the California Current, as described above, and the likely relationship between wind forcing and SST on long time scales are illustrated in Figure 4. The figure shows the slopes (±99% C.I.) of linear fits to the time series of poleward stress and SST in each COADS box (*ie*, the linear tendency of each trend series). The correlation between poleward stress and SST is positive in much of the central region. A statistically significant tendency for increasing equatorward stress coincides with a cooling trend in SST. A reasonable explanation for this is that the increasing equatorward stress leads to greater offshore Ekman transport and more coastal upwelling that cools the surface waters of the California Current at these latitudes. This region coincides roughly with the geographic range of the upwelling maxima along the west coast. Increasing equatorward stress also would contribute to cooler SST through greater turbulent mixing of the upper ocean and could be associated with increased south- ward transport of cool water by the California Current. Changes in Ekman divergence and wind curl may be occurring as well. The influence of mixing and wind gradients on SST is the focus of ongoing analysis.

Outside of the central region, however, the trends in stress and SST are negatively correlated. Increasing equatorward stress coincides with warming SST south of 34°N, while greater poleward stress accompanies a cooling trend north of 44°N. The cooler SSTs off Oregon and Washington (north

of 42°N) may be due to greater wind mixing (Schwing *et al* 1995). Greater poleward stress could be linked to a larger (gyre) scale pattern in atmospheric circulation, such as the documented intensification of the Aleutian Low in 1976, which could lead to fundamental changes in the region's ocean circulation. Long-term changes in wind curl could impact

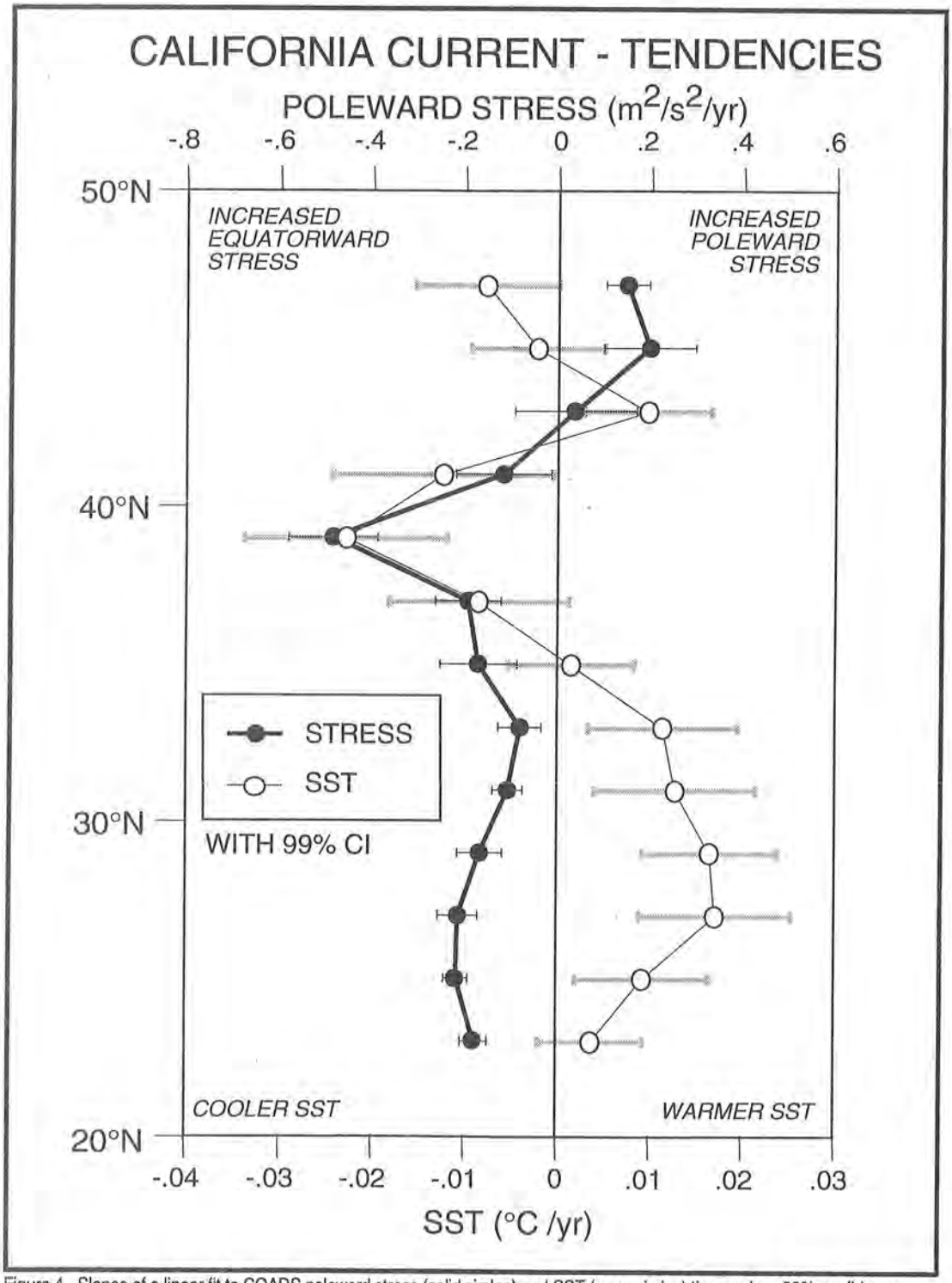

Figure 4 Slopes of a linear fit to COADS poleward stress (solid circles) and SST (open circles) time series. 99% confidence intervals shown by vertical bars (gray for stress, black for SST).

SST as well. We suspect that the transitional region between the Subarctic and California Currents could be extending southward, based on the expanding region of high northward wind stress divergence (Figure 1) and spatially uniform SST (Figure 2). This would be consistent with cooler SSTs.

The relationship between wind stress and SST in the southern region is less straightforward. Roemmich and McGowan (1995) present results consistent with ours for southern California, and speculate that increasing stratification over the last 45 years (due to an increasing heat flux from the atmosphere into the upper ocean) has led to shallower upwelling and a smaller "cooling" effect from increasing upwelling- favorable stress. The extension of this idea to the region farther north implies a different dynamical balance, such that increased stratification of surface water, a consequence of atmospheric warming, is overwhelmed by the contribution of wind in driving more cool water from ocean depths into, and/or vertical mixing of, the surface layer of the California Current.

It is apparent that over the last several decades, surface waters in the California Current south of 34°N have experienced a different set of forcing conditions from those farther north. Not only are the tendencies of wind and SST different in these regions of the California Current, but the changing linear relationship between stress and SST implies that the primary mechanisms that drive variability in SST, and probably the general ocean circulation, on decadal time scales is fundamentally different in these regions. It is not possible to develop a more firm conclusion about the mechanisms leading to these tendencies without a more thorough three-dimensional analysis of the temporal variability of wind vector fields over the north Pacific Ocean. A complex interaction of spatially as well as temporally varying Ekman transport, wind mixing, and direct heating appears to be responsible for the long-term fluctuations in SST in the California Current.

The temporal and spatial variability of the physical environment of the California Current must be considered when analyzing changes in the biological structure of this and other eastern boundary current ecosystems. Roemmich and McGowan (1995) have found that zooplankton biomass off southern California has decreased by 80% since 1951, while the surface layer has warmed by more than 1.5°C over the same time. They suggest this decrease is due to an increase in stratification of the surface layer, which has led to a shallower, hence lower nutrient, source of upwelling. However, their observations, which are in accord with our analysis of COADS data in the southern region, are restricted to south of 35°N. The results reported here show that regional differences in environmental variability have existed in the California Current over the last five decades; therefore it is conceivable that analogous differences in biological productivity have occurred as well. Specifically, Roemmich and

McGowan note a correlation between declining zooplankton biomass and increasing near-surface temperature and stratification. This model implies that biomass could be increasing in the northern California Current in association with the cooling tendencies of the COADS SST series.

Some of the observed substantial anomalies (*eg*, 1965-75, Figure 3) in the California Current are unrelated to well-defined climate events such as ENSO. Nevertheless, these periods of unusual environmental conditions are likely to have significant ecosystem consequences. "Warm" years, when conditions off California are similar to those during ENSO events despite the absence of an equatorial ENSO signal, are linked to poor recruitment of central California rockfish, while "cool" years feature enhanced recruitment (S.V. Ralston, Tiburon, NMFS, pers. comm.). Extreme year classes of several species of fish over large geographical areas tend to occur in association with unusual environmental conditions (Hollowed and Wooster 1992).

The results presented here clearly demonstrate the highly variable nature of the California Current environment in time and space, and argue against oversimplifying eastern boundary current climate change as a constant linear trend, or in terms of a record from a single location. The distinct latitudinal regionalization and cross-shelf variability of the California Current wind and SST fields has key implications for ecosystems studies as well as fisheries management. For example, which time series or regions are more important to study in terms of defining a stock's environment? Regional differences also mean that widespread stocks, or stocks that are highly migratory over their life history, face a spatially heterogeneous changing climate. Fisheries scientists must evaluate the relative environmental differences in each region, as they pertain to the climate signal and its variability, and compare them to a species' distribution and behavior as a function of life stage, to fully understand the consequences of climate change on populations. Widespread stocks also may display a very different long-term variability from species whose domain is limited to one of the homogeneous regions of the California Current described here.

In closing, the long-term trends described here cannot be considered without considering changes in seasonal patterns. Mendelssohn and Durand (1995) provide an eloquent discussion of how climate change can be interpreted in a number of ways. Schwing and Mendelssohn (1995) highlight an example of how seasonal changes over long time scales can have a clear signal that is independent of patterns in the model trend series described here. State-space models are a powerful tool for separating interannual-to-interdecadal fluctuations in environmental time series from seasonal patterns of variability. The results presented here demonstrate the importance of evaluating the entire spectrum of temporal and spatial variability, rather than simply at global climate scales, when

examining long-term environmental fluctuations. This will improve our understanding of the linkages between long-term variations in atmospheric forcing and the coastal ocean's response to this variability on regional scales, and ultimately an improved assessment of the impact of climate variability on living marine resources.

References

Hollowed, A.B., and W.S. Wooster. 1992. Variability of winter ocean conditions and strong year classes of Northeast Pacific fish stocks. *ICES Marine Science Symposium* 195:433-444.

Mendelssohn, R., and M.-H. Durand. 1995. Changes in oceanographic time series: how to detect and model it on both local and global scales. Submitted to *CEOS Workshop Proceedings.*

Roemmich, D., and J. McGowan. 1995. Climatic warming and the decline of zooplankton in the California Current. *Science* 267:1324-1326.

Schwing, F.B., and R. Mendelssohn. 1995. Increased coastal upwelling in the California Current System. Submitted to *Journal of Geophysical Research.*

Schwing, F.B., R. Mendelssohn, and R.H. Parrish. 1995. Recent trends in the spatial variability of the SST and wind fields of the California Current System. Submitted to *CEOS Workshop Proceedings.*

Trenberth, K.E. 1990. Recent observed interdecadal climate changes in the Northern Hemisphere. *Bulletin of the American Meteorological Society* 71:988-993.

Interannual Variability in the PFEG Coastal Upwelling Indices

Heather A. Parker

Introduction

Numerous studies (Miller *et al* 1994a,b) examine decadal-scale variability in basin-scale parameters in the Northern Pacific. Characterizing such interannual-to-interdecadal variability is essential to identifying long-term climate changes. The Pacific Fisheries Environmental Group (PFEG) coastal upwelling indices display variability on these time scales and may help explain the mechanisms responsible for such climate variability.

Coastal upwelling is a wind-stress induced phenomenon. In the Northern Hemisphere, alongshore equatorward winds at the eastern boundary of an ocean cause offshore Ekman transport of surface water. Divergence at the coastline results, producing an upward advection of water and an upward slope in isopycnals toward the coast. Alternatively, poleward wind stress leads to onshore transport, convergence, and downwelling. At the coastal region along the eastern boundary of the North Pacific, upwelling is frequently observed. PFEG maintains a lengthy record of modeled upwelling indices.

On a monthly basis, PFEG generates 6-hourly and monthly indices of the intensity of large-scale, wind-induced coastal upwelling at 15 standard locations along the west coast of North America, as described in Bakun (1973). The indices, often referred to as the Bakun indices, are based on estimates of cross-shore Ekman surface transport from geostrophic wind, calculated from surface atmospheric pressure data. Upwelling indices are expressed in cubic meters per second per hundred meters of coastline. Positive indices denote offshore transport and upwelling. The atmospheric pressure fields are provided by the U.S. Navy Fleet Numerical Meteorology and Oceanography Center (FNMOC), Monterey, California.

In this study, examination of 49-year time series of monthly mean upwelling indices at the 15 PFEG-standard positions along the west coast of North America revealed variability on large spatial scales as well as temporal scales. Upwelling time series at three of these locations are described here to characterize patterns of variability for the surrounding geographical regions.

In: C.M. Isaacs and V.L. Tharp, Editors, 1996. *Proceedings of the Twelfth Annual Pacific Climate (PACLIM) Workshop, May 2-5, 1995.* Interagency Ecological Program, Technical Report 46. California Department of Water Resources.

Observations

Upwelling index time series at 57°N 137°W, 39°N 125°W, and 21°N 107°W were examined in this study. Within each of these time series (Figure 1), there are notable periods of anomalously high and low coastal upwelling present for several years. Figures 2 through 4 highlight these temporal shifts for selected periods. Comparison of distinct periods for each region examined reflects the fact that interannual-to-decadal changes do not occur systemwide.

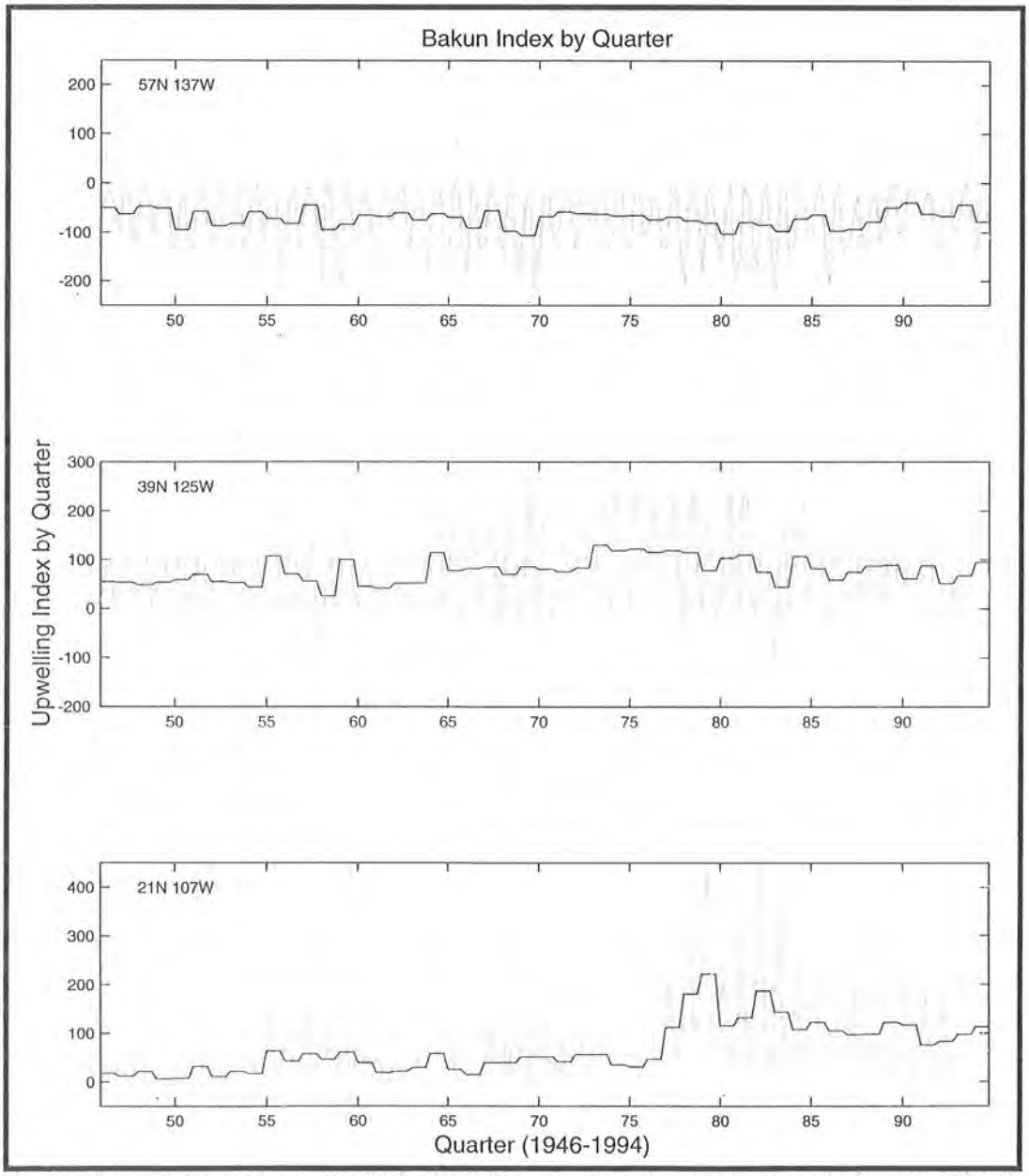

Figure 1 Time series of quarterly-mean Coastal Upwelling Indices and each yearly-mean value at three locations: 57°N 137°W, 39°N 125°W, and 21°N 107°W.
Upwelling indices are expressed in $m^3/s/100m$ coastline.

The coastal upwelling series at 57°N 137°W represents the upwelling history in the region north of 50°N. Variations in wind stress in this region are dominated by variability in the intensity and position of the Aleutian Low pressure system in winter (Trenberth and Hurrell 1994), the season when variability in coastal upwelling is greatest (Figure 1). Between 1977 and 1983, the coastal upwelling signal in this region had an unusually large annual amplitude (Figure 2), corresponding to a strengthening of the low in 1976. During this time, the series shows larger negative values in winter, implying increased local convergence, and more downwelling at the coast. The cross-shore atmospheric pressure gradients at this location are decreased during this period, based on surface pressure analysis. The magnitude of winter upwelling indices became less negative in the mid-1980s, returning to the range of values seen prior to 1977. The small positive upwelling indices in summer have remained similar in magnitude throughout the 49-year series (Figure 1), and do not show any significant variance during 1977 to 1983 (Figure 2).

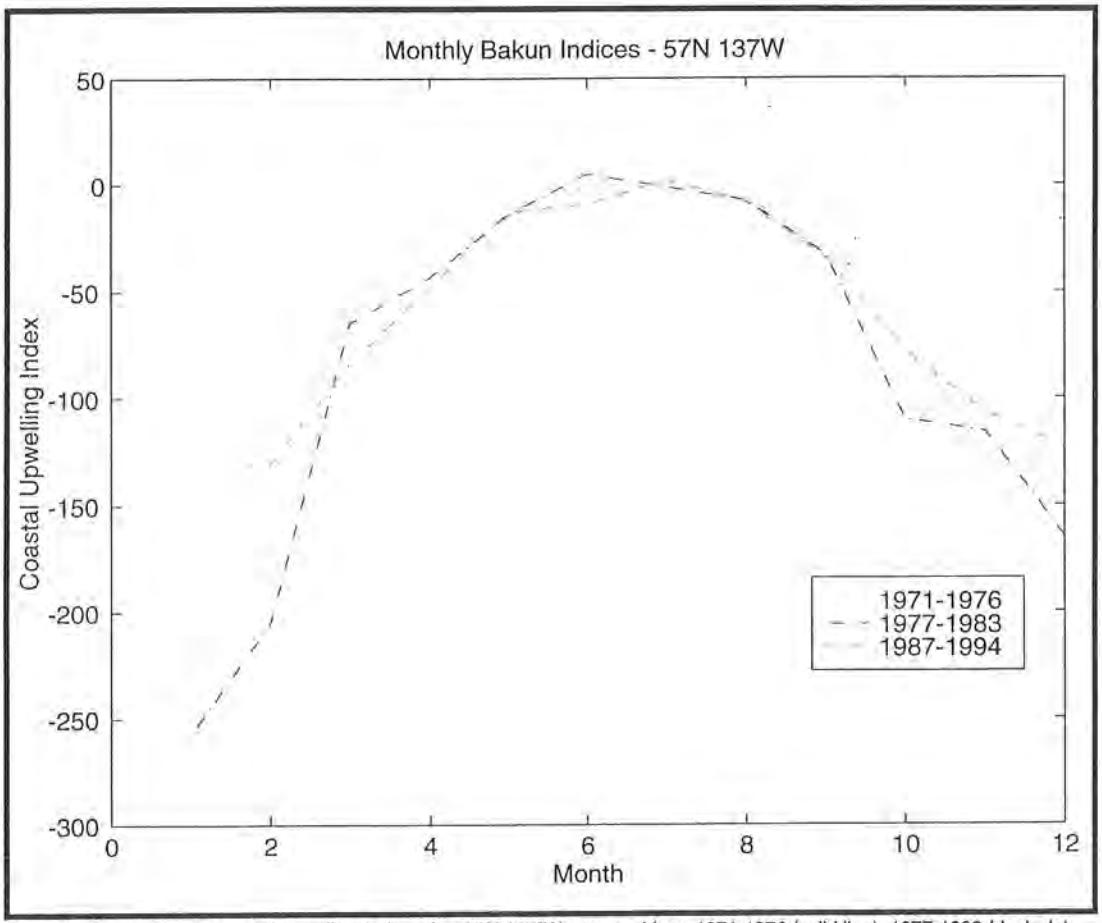

Figure 2 Monthly mean coastal upwelling indices for 57°N 137°W averaged from 1971-1976 (solid line), 1977-1983 (dash-dot line), and 1987-1994 (dashed line) illustrating notable changes in the seasonal cycle on interannual time scales. Upwelling indices are expressed in $m^3/s/100m$ coastline.

The coastal upwelling index series at 39°N 125°W represents interannual variability in Ekman transport for the northern California region. At these latitudes (36°N to 42°N), the seasonal cycle is characterized by maximum upwelling during late spring and summer (Figure 3). This is in contrast with the annual cycle of upwelling indices in the area north of 50°N, where the negative upwelling indices (*ie*, downwelling) in winter exhibit the greatest interannual variance (Figure 1). The most significant decadal-scale variability along northern California is during spring and summer. Wind stress patterns are influenced most strongly in this region by variations in the Subtropical High pressure system that intensifies offshore during summer and a low that develops in summer over the continental United States. The pressure gradient that develops between these systems leads to intense equatorward geostrophic wind and strong seasonal upwelling.

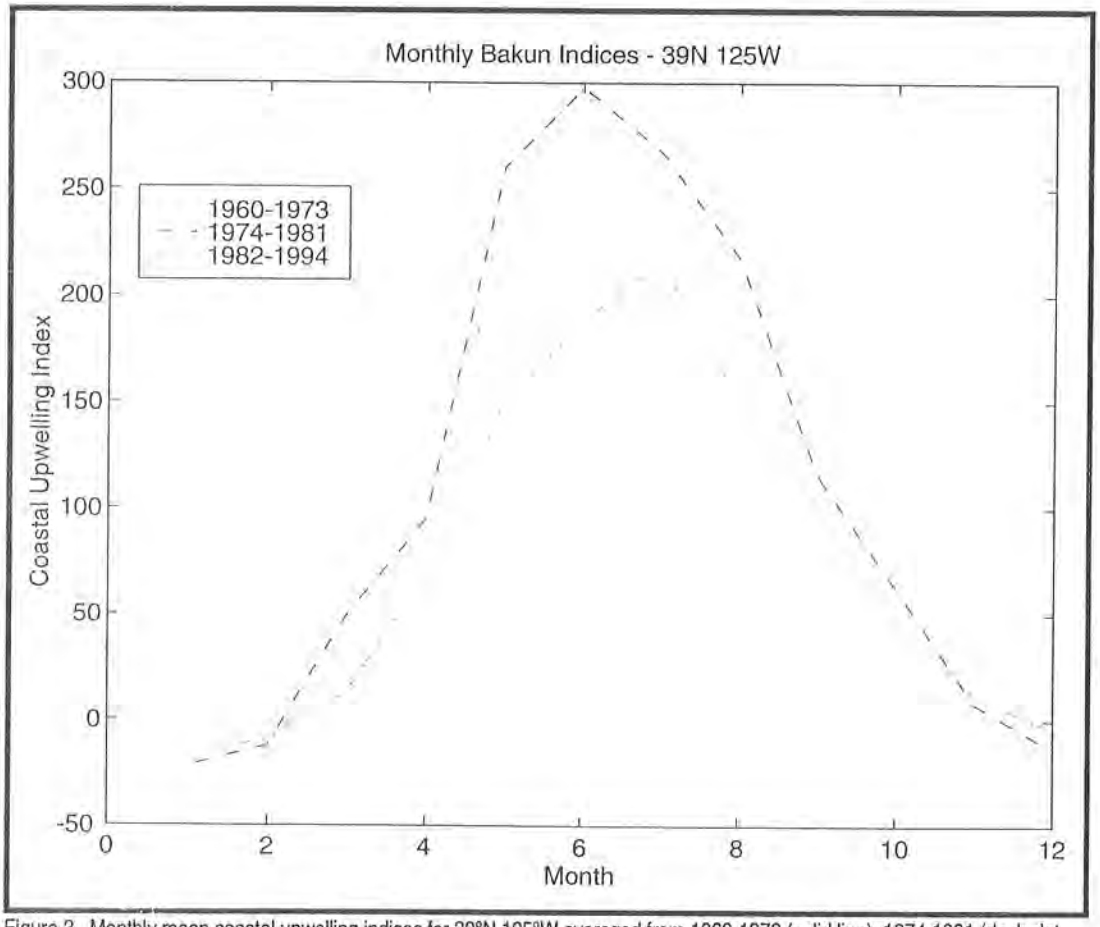

Figure 3 Monthly mean coastal upwelling indices for 39°N 125°W averaged from 1960-1973 (solid line), 1974-1981 (dash-dot line), and 1982-1994 (dashed line) illustrating notable changes in the seasonal cycle on interannual time scales. Upwelling indices are expressed in $m^3/s/100m$ coastline.

During 1974 to 1981, a large increase in coastal upwelling occurred along northern California during summer. Analyses of FNMOC monthly mean surface pressure maps from this period revealed steeper pressure gradients between the Subtropical High and continental low along northern California. Equatorward wind stress increased along the California coast as a result, producing greater offshore Ekman transport and coastal upwelling. Changes in the intensity of the pressure system were subtle, but they translated into significant changes in coastal upwelling.

The coastal upwelling signal at 21°N 107°W represents the variability in upwelling for the extreme southern portion of the California Current. Maximum upwelling in the proximity of the Gulf of California occurs during spring (Figure 4). Two significant pressure cells in this region are the Subtropical High and a continental low that develops over the southwestern United States. The cross-shore pressure gradient between the two systems dominates spring wind stress at nearby latitudes. This region exhibits the greatest range of interannual variability in coastal upwelling along the North American west coast (Figure 1).

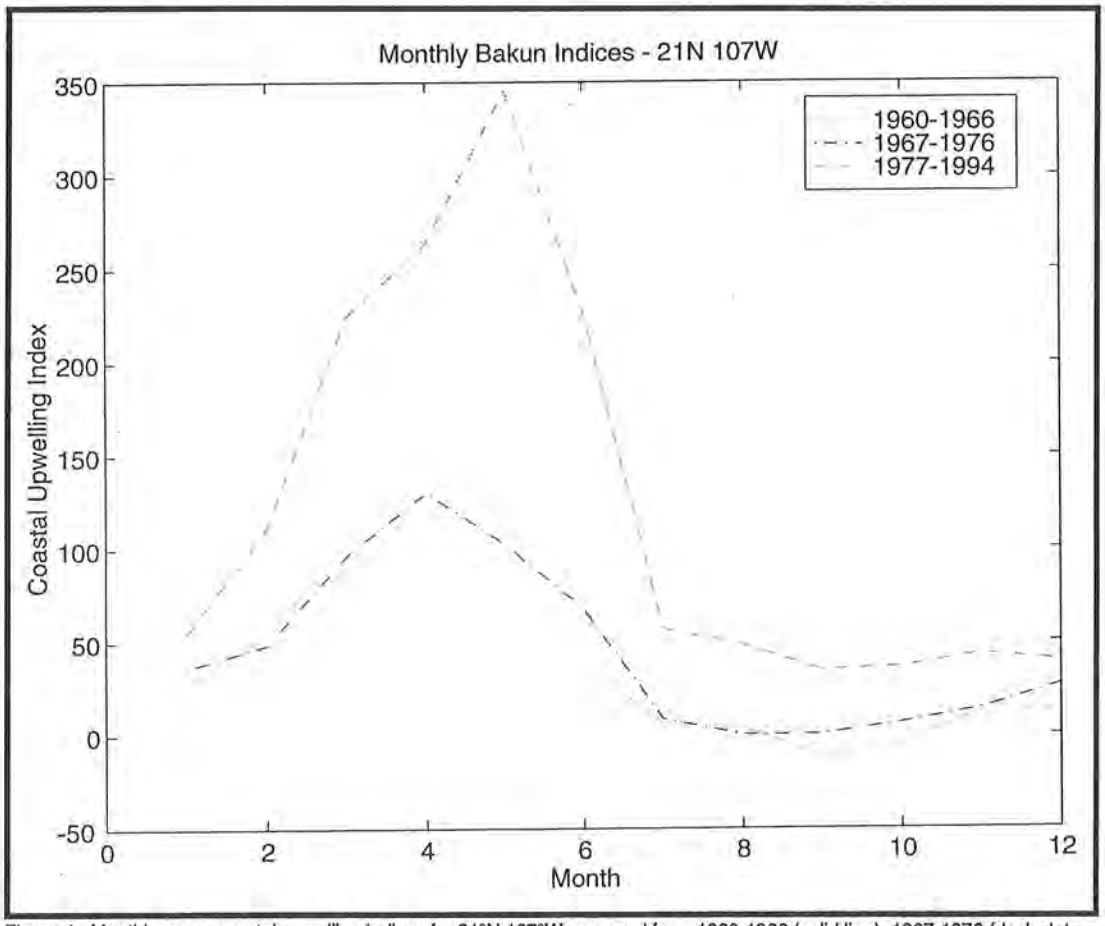

Figure 4 Monthly mean coastal upwelling indices for 21°N 107°W averaged from 1960-1966 (solid line), 1967-1976 (dash-dot line), and 1977-1994 (dashed line) illustrating notable changes in the seasonal cycle on interannual time scales. Upwelling indices are in $m^3/s/100m$ coastline.

A dramatic increase in spring upwelling indices occurred at 21°N 107°W after 1976. Surface pressure analyses provided clues to the cause of this marked increase. The continental low over the southwestern United States appears to have intensified in the mid-1970s. The Subtropical High was also strong in this period, resulting in a strengthening of the cross-shore surface pressure gradient over the Gulf of California. Equatorward wind stress intensified and led to substantially greater coastal upwelling.

Summary

Regions north of 50°N in the North Pacific are dominated by the Aleutian Low and its fluctuations and, therefore, exhibit the greatest variability in winter (Seckel 1993). South of Vancouver Island (south of 48°N), the dominant forcing mechanism controlling local upwelling-favorable winds over the California Current is the pressure gradient associated with the Subtropical High pressure system and the continental low. Under the influence of these systems, variance in wind stress and coastal upwelling are most evident in summer. This variability increases progressively to the south. In a transition zone from about 42°N to 45°N, variance of the Aleutian Low is still evident during winter months, while variability caused by changes in the Subtropical High is reflected in upwelling magnitude in the summer.

Variations in coastal upwelling intensity on interannual and longer scales are common features in an eastern boundary region, yet do not occur systemwide. The interannual variability in the coastal upwelling series is visually consistent within about 10 degrees of latitude. Since the seasonal cycle of upwelling is not coherent for the entire west coast, or even within the California Current system, seasonal differences in decadal-scale variability must be considered to better define what mechanisms may be responsible for climate change in each region.

Examination of monthly mean pressure field maps provided snapshots of the intensity and position of dominant atmospheric features and gradients between them. During periods of substantial anomalies in coastal upwelling, only subtle variations were seen in these atmospheric features. The significant increase in upwelling at 21°N since the summer of 1976 was most likely the result of an intensification of the thermal low over the southwestern United States, coupled with a steepening of gradients on the eastern side of the Subtropical High. This subtle increase in the cross-shore pressure gradient caused stronger equatorward wind stress and greatly increased coastal upwelling. Thus, it appears that even small shifts in the surface pressure fields, which may be attributed to climate change, may lead to significant changes in the magnitude of coastal upwelling on interannual-to-decadal time scales.

Conclusions

Coastal upwelling in eastern boundary current systems is influenced on regional scales by larger-scale climate changes. The 49-year PFEG coastal upwelling index time series provide a good environmental indicator of climate variations. Analyses of these series at each location indicate that the interannual-to-decadal time scale variance present in coastal upwelling is not homogeneous along the length of the North American west coast. Discrete regions of these eastern boundary current systems differ in the particular atmospheric pressure systems that influence local wind stress and coastal convergence or divergence. It is clear from these series that small variations in atmospheric pressure gradients can cause large fluctuations in coastal upwelling. The most significant changes in the annual cycle of coastal upwelling occur on interannual-to-decadal time scales.

Sources of interannual climate variations evident in these indices include El Niño events, *eg*, 1957, 1983 (Norton *et al* 1985), and the 1976-1977 regime shift (Trenberth and Hurrell 1994). Global warming may also contribute to changes in coastal upwelling, through intensification of cross-shore pressure gradients due to preferentially increased radiative heating over continental masses and the resultant deepening of the continental low (Bakun 1990). Regardless of the mechanism driving climate variation, slight shifts in surface pressure systems can have a dramatic impact upon coastal upwelling and the ecosystems influenced by this process.

References

Bakun, A. 1973. *Coastal Upwelling Indices, West Coast of North America, 1946-71.* U. S. Dept. of Comm., NOAA Tech. Report, NMFS SSRF-671, 103 pp.

Bakun, A. 1990. Global Climate Change and Intensification of Coastal Ocean Upwelling. *Science* 247:198-201.

Miller, A.J., D.R. Cayan, T.P. Barnett, N.E. Graham, and J.M. Oberhuber. 1994a. Interdecadal variability of the Pacific Ocean: Model response to observed heat flux and wind stress anomalies. *Climate Diagnostics* 9:287-302.

Miller A.J., D.R. Cayan, T.P. Barnett, N.E. Graham, and J.M. Oberhuber. 1994b. The 1976-77 climate shift of the Pacific Ocean. *Oceanography* 7:21-26.

Norton, J.N., D. McLain, R. Brainard, D. Husby. 1985. The 1982-83 El Niño event off Baja and Alta California and its ocean climate context. Pages 44-72 in *El Niño North.* W.S. Wooster and D.L. Fluharty, editors. University of Washington, Seattle, WA.

Seckel, G.R. 1993. Zonal gradient of the winter sea level atmospheric pressure at 50°N: An indicator of atmospheric forcing of north Pacific surface conditions. *J. Geophysical Research.* 98:22615-22628.

Trenberth, K.E., and J.W. Hurrell. 1994. Decadal atmosphere-ocean variations in the Pacific. *Climate Dynamics* 9:303-319.

Decadal Variability over the North Pacific Ocean

Dan Cayan, Warren White, Art Miller

Abstract

In this study we use ocean and atmosphere datasets from observations and from an ocean general circulation model integration to examine decadal time scale variability that is centered in the Pacific basin. We know that decadal variability is likely to have a strong expression in the Pacific basin; for example, a marked "shift" of cool season climate in the mid-1970s introduced major changes in Pacific SST and atmospheric circulation, along with many other physical and biological properties (see Miller *et al* 1994(a,b); Graham 1994; and other references).

Variables considered include upper ocean temperature, sea surface temperature, surface air temperature (land only), sea level pressure, and related atmospheric fields over the Pacific basin from almost 4 decades of instrumental observations. Modeled aspects of the interannual-decadal variability are taken from the OPYC Pacific basin model simulation (Miller *et al* 1994a,b), which was driven by observed winds and heat fluxes over 1970-1988. The subsurface temperature variability contains a rather strong component within the decadal time scale, so it is emphasized in several of the illustrations herein. To accentuate the decadal variability, a low-passed filter (periods of 7 years and greater) was employed in many of the analyses. Shown here are differences before and after the mid-1970s shift, empirical orthogonal function (EOF) analyses, and extended EOF (EEOF) analyses. Key questions about the North Pacific decadal variability concern:

- Whether it is adequately represented by the observations,
- A description of its spatial and temporal priorities,
- The expression of this variability within and beyond the Pacific basin, and
- Its causes and effects.

As viewed from a relatively short period (20-40 years), decadal (>7-year) variability has a strong expression over the North Pacific. EOF analyses reveal a first mode (or pair of modes) with periods about 20-25 years. This mode is expressed by several climate variables, including upper ocean temperature (both SST and subsurface temperature) and atmospheric circulation (SLP). The primary atmospheric decadal mode is a kind of low frequency PNA pattern, involving strengthening and weakening of the Aleutian Low. The primary ocean temperature pattern has cool anomalies in the central/western North Pacific mid-latitudes and warm anomalies in tropics/subtropics and along the eastern boundary; this pattern alternates to the opposite phase after about 12 years. Interestingly, this pattern is similar to those found for ENSO time-scale variations and even higher frequency oscillations (Tanimoto *et al* 1993). However, while the ENSO variations tend to propagate around the Pacific basin over a roughly 4-year "cycle", the decadal anomalies more nearly resemble a standing wave.

The decadal variability simulated by the OPYC model Pacific Ocean is quite realistic over the 1970-1988 wind/heat flux forced integration. The model reproduces key aspects of the mid-1970s "shift", and from its upper ocean temperature and sea level, the OPYC model showed an increase in the gradients between the subtropics and mid-latitudes, which suggests that the North Pacific gyre strengthened in the mid-1970s.

In: C.M. Isaacs and V.L. Tharp, Editors. 1996. *Proceedings of the Twelfth Annual Pacific Climate (PACLIM) Workshop, May 2-5, 1995.* Interagency Ecological Program, Technical Report 46. California Department of Water Resources.

The analyses employed have smoothed the data; this treatment, along with EOF techniques, suggests that a nearly sinusoidal primary mode of decadal variability exists. However, with only a short record available, whether decadal changes typically occur as rapid regime shifts, such as some of the aspects of the mid-1970s transition, or whether they are evolving more regularly, is an open question.

The decadal variations are not confined to the North Pacific. Heat storage anomalies have important extensions to the tropical and South Pacific and at times to the Atlantic and Indian oceans. The extension beyond the Pacific basin is particularly evident from the analysis of global SST/Tair, where patterns often take on dimensions of a full hemisphere. There are several examples where coherent decadal temperature anomalies envelope large ocean/land regions.

Causes and effects are not completely understood. The North Pacific decadal temperature anomaly pattern can be partly explained by local air/sea interactions associated with fluctuations in the Aleutian Low atmospheric circulation. However, there are complications. First, if the ocean was purely a slave to the atmosphere, the ocean temperature variations should lag the atmospheric variations by one-quarter cycle; instead, the two are more closely in sync (phase lag near zero). Second, what allows the Aleutian Low anomalies to persist for several years? Recent observational and modeling studies suggest this persistence is tied to feedback from the low-frequency ocean temperature anomalies, but this feedback could operate from the tropics (*eg*, Graham 1994) or the extratropics (Latif and Barnett 1995). Finally, some evidence from the observational data suggests that advection by the mean ocean circulation may play a role in distributing the upper layer (0-400 meter) temperature anomalies.

The dataset employed is very short, considering the time scales of interest. There is clearly a need for longer datasets (instrumental and proxies) and more modeling experiments (coupled as well as uncoupled OGCMs) to describe and explain this variability.

Interdecadal Shifting of the North Pacific Jet Stream — El Niño Events

Stephen H. Holets

Abstract

Researchers have shown a step-like increase in worldwide sea surface temperatures (SSTs) in the mid-1970s. Wintertime (December through March) polar-front jet stream positions in the North Pacific will be presented for six moderate-to-very-strong El Niño events — three before the winter of 1975-76 (1965-66, 1968-69, 1972-73) and three after (1982-83, 1986-87, 1991-92). The wintertime El Niño jet stream patterns before 1975-76 were similar across the North Pacific, and the patterns after 1975-76 were also similar. However, composites of the two sets are very different, revealing a significant interdecadal shift in the polar-front jet stream during El Niño events. Jet stream positions before 1975-76 were north of the wintertime mean jet stream pattern but have been south of the mean jet since 1975-76.

The jet stream composites suggest that changes in the overall level of SSTs can have dramatic effects on the wavelength of the mean jet stream pattern across the Pacific. The trough axis remained fixed at 130°E in the western Pacific before and after 1975-76. However, the jet stream ridge axis during El Niño events shifted westward to 150°W longitude before 1975-76 and eastward to 120°W after 1975-76. The connection between changes in SSTs and the subsequent effect on upper-air longwave patterns will be discussed, along with probable impacts of these jet stream shifts on California rainfall.

Long-Term Changes in the Equatorial Pacific Trade Winds

Allan J. Clarke and Anna Lebedeva

Abstract

Past work (Cane and Sarachik 1977; Li and Clarke 1994) has shown that surface zonal equatorial wind stress, zonally integrated from one side of the Pacific to the other, is the key variable for estimating long-term El Niño behavior in the eastern Pacific. The long-term behavior of this key variable is difficult to determine directly, because of the paucity of equatorial wind observations and because of false trends in the wind data introduced by gradual changes in measurement methods. However, surface pressure data generally do not suffer from these false trends, and theory suggests that this key wind variable is linearly related to the difference (Δp) of surface atmospheric pressure between the eastern and western equatorial Pacific. We used detrended COADS pressure in the eastern and western equatorial Pacific and post-1960 detrended Florida State University equatorial wind stress zonally averaged across the Pacific to verify this relationship. Pressure difference and zonally averaged equatorial zonal wind stress (τ) were highly correlated ($r = -0.85$), and the regression also showed that advection of zonal momentum contributes substantially to the momentum balance in the equatorial atmospheric boundary layer. Further, hindcasts of eastern equatorial Pacific sea surface temperature suggested that τ from Δp was more accurate than τ from winds even since 1960, when wind data are more plentiful.

Using the Δp time series as a proxy for zonally integrated wind stress suggests that the equatorial trades strengthened during the 1920s and 1930s, weakened from the mid-1940s to late 1950s, strengthened during the 1960s, and have weakened rapidly since. This pattern is qualitatively consistent with the long record of sea surface temperature measurements at Puerto Chicama (Peru). The more recent rapid weakening is consistent with trends in several physical variables reported previously by others. The long-term changes affect El Niño/La Niña intensity and contribute significantly to sea level change on the western coast of the Americas. A proxy record of eastern Pacific sea surface temperature from coral (Dunbar *et al* 1994) suggests that such long-term (decade and longer) weakening and strengthening of the Pacific equatorial trades has occurred before major anthropogenic greenhouse gas release and at least back to 1600 AD.

References

Cane, M.A., and E.S. Sarachik. 1977. Forced baroclinic ocean motions: II. The linear equatorial bounded case. *Journal of Marine Research* 35:395-432

Dunbar, R.B., G.M. Wellington, M.W. Colgan, and P.W. Glynn. 1994. Eastern Pacific sea surface temperature since 1600 AD: The $\delta^{18}O$ record of climate variability in Galapagos corals. *Paleoceanography* 9:291-315.

Li, B., and A.J. Clarke. 1994. An examination of some ENSO mechanisms using interannual sea level at the eastern and western equatorial boundaries and the zonally averaged equatorial wind. *Journal of Physical Oceanography* 24:681-690.

In: C.M. Isaacs and V.L. Tharp, Editors. 1996. *Proceedings of the Twelfth Annual Pacific Climate (PACLIM) Workshop, May 2-5, 1995.* Interagency Ecological Program, Technical Report 46. California Department of Water Resources.

Recent Trends in the Climate of the Tropical Pacific Region

Nathan J. Mantua and Nicholas E. Graham

Abstract: Observations of climate variables in the tropical Pacific region are examined for the period 1970-1994. We look at a variety of climate variables, including upper ocean temperatures, surface wind stress, precipitation, and the Southern Oscillation Index (SOI) and find evidence for two distinct decadal-scale warmings in the tropical Pacific ocean-atmosphere climate system during this period. The first warm epoch began shortly after 1976 and has been studied at some length. The more recent warming began in 1990 and persisted through the end of 1994 and is only now being examined in detail. We find distinct differences between the characteristics of the decadal-scale climate warmings and those commonly associated with the extreme phases of the El Niño/Southern Oscillation (ENSO) cycle. We interpret the decadal-scale warmings to be indicative of a multi-year time scale mode of coupled climate variability upon which the inter-annual ENSO cycle evolves.

In this paper we present an analysis of some aspects of the tropical Pacific climate variability for the years 1970 through 1994. Upper ocean temperature records indicate two relatively distinct multi-year climate warmings in the tropical Pacific region during this period. Additional measures of tropical climate variability, including the Southern Oscillation Index, an index of precipitation in the central equatorial Pacific, and an index of the surface wind stress across the equatorial Pacific Basin, exhibit multi-year time-scale variability that is physically coherent with that observed in the upper ocean temperatures. The purpose of this work is to document the large-scale features of these multi-year climatic warmings. We offer possible explanations for the origin of the warmings and discuss some of the broader-scale implications of multi-year climatic changes in the tropical Pacific region.

Based on our subjective interpretation of the indices shown in Figure 1, the first climatic warming in the tropical Pacific region occurred soon after the end of 1976 and the second appeared early in 1990. In addition to strong interannual variability, each index exhibits mostly negative values from 1970 to 1976 and mostly positive values after 1990.

The strategy we adopted involves comparing and contrasting the two climatic warmings by computing difference maps for the average fields in the "warm" period minus those in the preceding "cold" period. The warm/cold designations are taken to be relative terms. We subjectively define the initial warm period as January 1977 through December 1982 and the preceding cold period as January 1971 through December 1976. We define *WARMING1* to be the differences between average anomaly

In: C.M. Isaacs and V.L. Tharp, Editors. 1996. *Proceedings of the Twelfth Annual Pacific Climate (PACLIM) Workshop, May 2-5, 1995.* Interagency Ecological Program, Technical Report 46. California Department of Water Resources.

fields from 1977-1982 and those from 1971-1976. We define the most recent warm period as January 1990 through December 1994, preceded by the relatively cold period of January 1983 through December 1989. The *WARMING2* fields are, thus, the differences between the average anomalies from 1990-1994 and those from 1983-1989.

After computing the warming maps, we attempted to objectively estimate the portion of the multi-year climate changes that exhibit characteristics associated with the extreme phases of the ENSO cycle. We focused on spatial structure and coherence in the surface wind and SST anomaly fields, using a singular value decomposition (SVD) analysis. We found that each of the multi-year climatic warmings defined in the study had significant projections onto what we defined as a *pure ENSO* pattern. Our analysis also revealed that each of the climatic warmings exhibited features that do not project onto the pure ENSO patterns and, thus, are not commonly associated with variability in the ENSO cycle.

Data and Analysis Strategy

Datasets used in this study are monthly mean fields of the upper ocean and troposphere for the tropical Pacific region (loosely defined as 100°E to 70°W, 30°S to 30°N). Unless otherwise noted, each dataset spans the period from January 1970 through December 1994. The fields we analyzed are:

- SST fields from the Climate Analysis Center (January 1970 to October 1981) and from the optimally interpolated SST product produced by Reynolds and Smith (1994) from November 1981 through December 1994. These fields have been regridded to a 10° longitude by 2° latitude resolution.
- Expendable bathythermograph temperature profiles on a 5° longitude by 2° latitude grid, with vertical levels at 0, 20, 40, 60, and 80 meters depth. The XBT data span January 1970 through June 1993.
- The Southern Oscillation Index from the Climate Analysis Center.
- The Florida State University surface pseudo-wind stress analysis for the tropical Pacific (Legler and O'Brien 1988).
- Estimated oceanic precipitation rates from channels 1, 2, and 3 of the microwave sounding unit (Spencer 1990) for January 1979 through May 1994 and from satellite-derived outgoing longwave radiation (Griffith *et al* 1978) from June 1974 through December 1982. An OLR index from the Climate Analysis Center covering June 1974 through December 1994 is used in Figure 1. The MSU data are on a 2.5° grid in latitude and longitude. The OLR fields are on a 5.625° grid in latitude and longitude.

Our data coverage for all variables is complete for 1979 through June 1993. Coverage of the entire 1970-1994 period is realized only in the SST and pseudo-stress and pseudo-wind divergence fields.

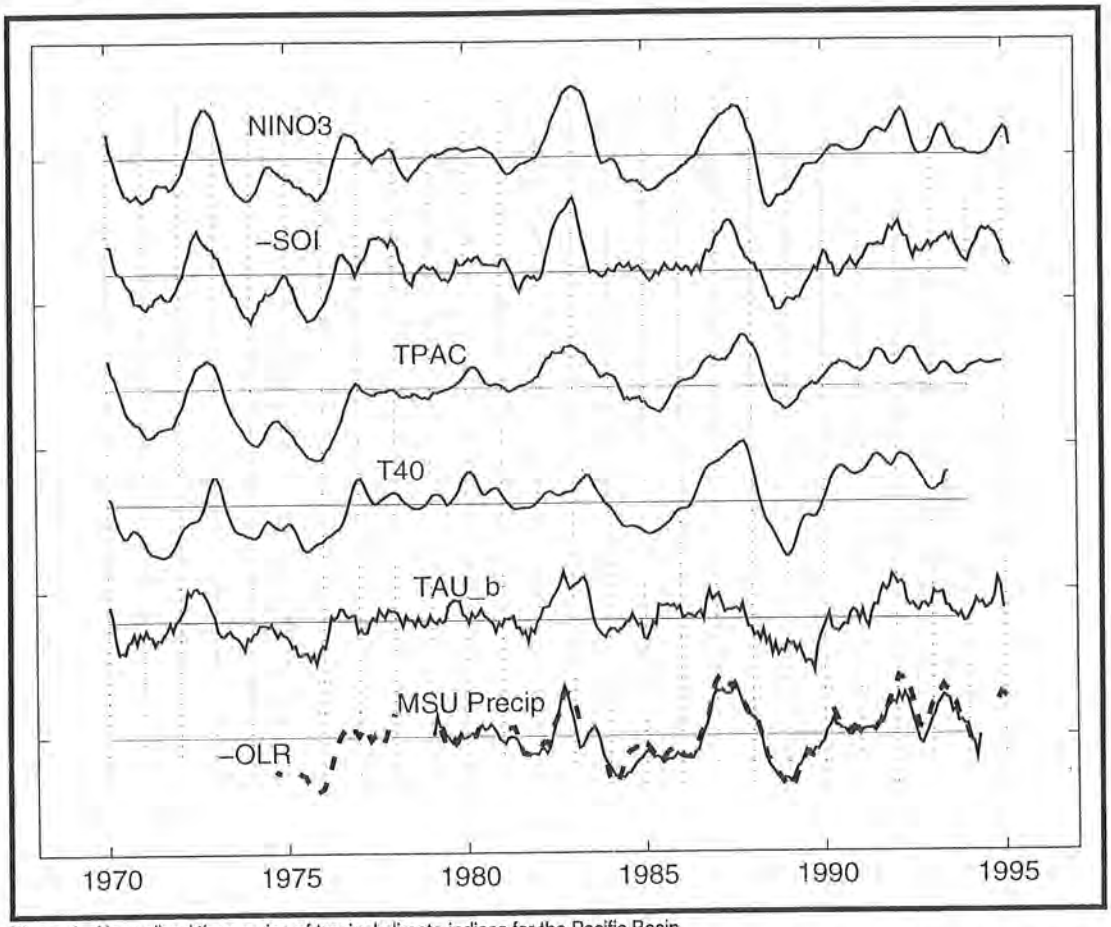

Figure 1 Normalized time series of tropical climate indices for the Pacific Basin.
Indices are plotted as anomalies from the mean of the record shown. A 5-month running mean has been applied for display purposes. The light solid lines are the zero lines for individual indices.

Indices of Tropical Climate Variability

Each time series in Figure 1 has been normalized by its monthly varying standard deviation. *NINO3* is the average SST anomaly in the eastern equatorial Pacific region (5°S-5°N, 150°W-90°W). This time series shows the strong interannual variability associated with the ENSO cycle, notably the warm extremes in 1972-73, 1982-83, 1986-87, 1991-92, 1993, and 1994-95 and the cold extremes in 1970-71, 1973-74, 1975-76, 1984-85, and 1988-89.

The SOI is defined as the normalized sea level pressure anomaly at Tahiti minus that at Darwin, Australia. The SOI is shown here with its sign reversed so that positive values now correspond to periods with an anomalously weak sea level pressure gradient between Tahiti and Darwin and, thus, a general weakening of the easterly Trade Wind flow between

those two locations. The SOI is highly correlated with NINO3 and the two indices depict much of the same interannual behavior (Table 1).

Table 1
CORRELATIION COEFFICIENTS FOR SELECT INDICES OF TROPICAL CLIMATE VARIABILITY

Index	SST1	FUS1	NINO3
FSU1	0.88		
NINO3	0.93	0.82	
SOI	-0.76	-0.82	-0.70

SST1 is the expansion coefficient for the leading SST singular vector from the SVD analysis.
FSU1 is the expansion coefficient for the leading wind stress singular vector.
NINO3 and SOI are as defined in the text.

Note that while NINO3 has returned to near zero values between the brief warm episodes from 1990 to 1994, the SOI has remained negative. The 5 consecutive years of negative SOI is an exceptional feature in the climate record for at least the past century.

TPAC is the average SST anomaly for the entire tropical Pacific region (from 23.5°S to 23.5°N and all longitudes within the Pacific Basin). The TPAC time series reflects the interannual warmings and coolings associated with the ENSO (*ie*, NINO3) and the longer period, broader scale, warming of the entire tropical Pacific in the period 1990-1994.

Similar variability is shown by T40, which is the average subsurface temperature anomaly at 40 meters depth for the entire tropical Pacific Basin (23.5°S to 23.5°N).

The zonal wind stress variability in the equatorial belt across the Pacific Basin is depicted by TAU_b, the average zonal wind stress anomaly from 10°N to 10°S, 120°E to 80°W. Precipitation variability in the central equatorial Pacific, from 160°W to 160°E, 10°N to 10°S, is depicted by the two time series labeled MSU and the negative OLR[1].

In general, all of the indices in Figure 1 exhibit similar variability: repeated negative values from 1970 to 1976 interrupted by the warm ENSO conditions in 1972 and 1973, near zero values from 1977 to 1981, strong interannual variability from 1982 to 1989, and persistent positive values superimposed on weak to moderate interannual variability from 1990 through 1994.

Difference Maps for the Tropical Climate Warmings

In this section, we present difference maps to highlight the multi-year time-scale features of the tropical Pacific climate changes from 1970 through 1994.

1 Low values of OLR correspond to cooler "top-of-the-atmosphere" emission temperatures. Emission temperatures are well correlated with cloud top altitudes, which are in turn related to precipitation rates in the tropics.

SST and Wind Stress

Figure 2 shows the difference maps (warm-cold) between the average SST and FSU pseudostress fields for the two climate warmings. Changes in average SST fields from the 1971-1976 cool period to the 1977-1982 warm period (Figure 2a) exhibit a symmetric pattern of warming over most of the tropical Pacific. The region of warmer SST is flanked by two

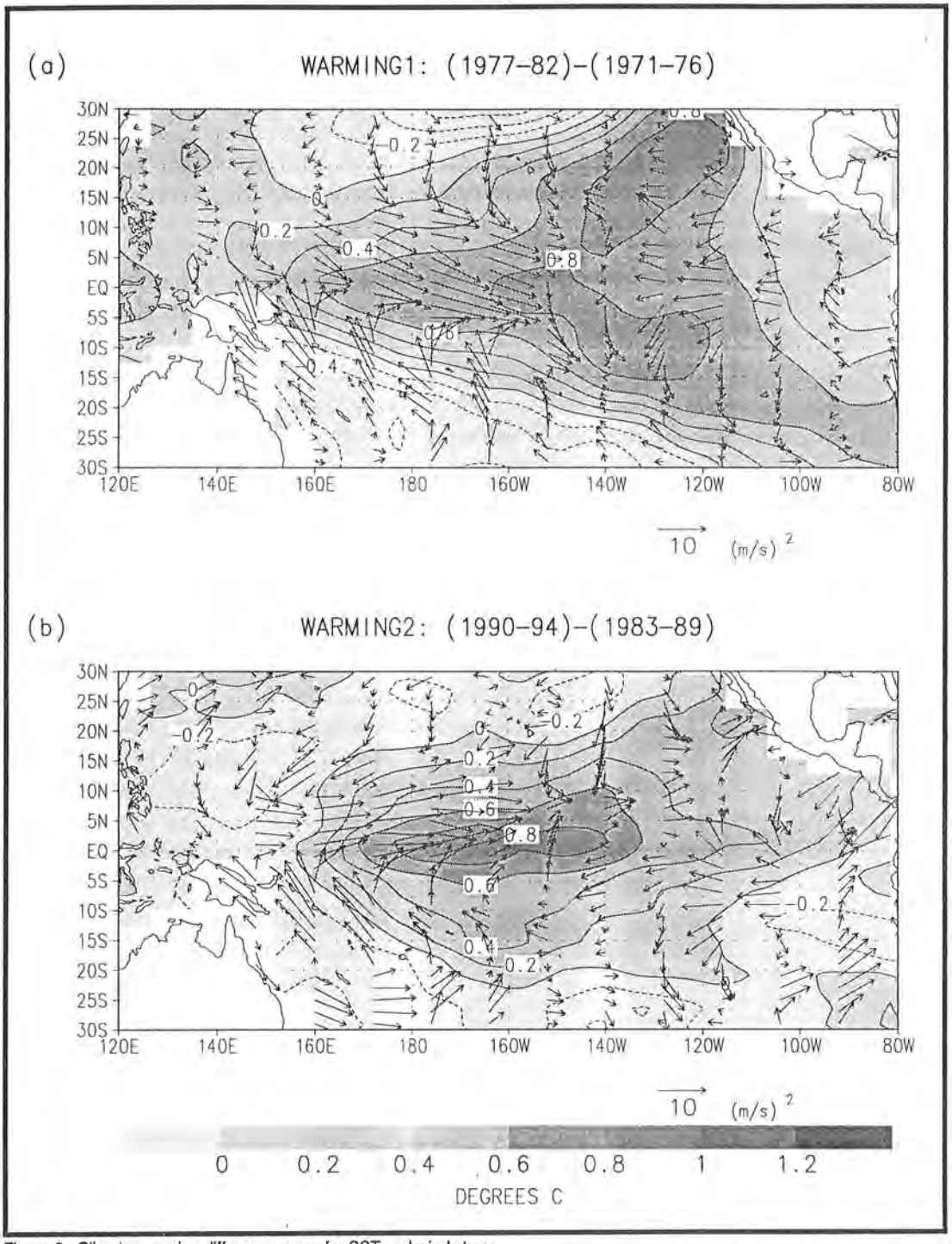

Figure 2 Climate warming difference maps for SST and wind stress.
Panel (a) shows SST and wind stress changes for *WARMING1*; panel (b) shows SST and wind stress changes for *WARMING2*. The shading interval is 0.2°C.

regions of mostly subtropical SST cooling in the western Pacific. The peak warming exceeds 0.8°C and is confined to longitudes between 160°W and 120°W.

Most of the area of warmer SST exceeds 0.4°C. Large changes in the average wind stress fields from 1971-1976 to 1977-1982 include:

- A region of westerlies (or weakened easterlies) in the central equatorial Pacific 165°E-150°W, 5°S-10°N;
- Enhanced easterlies in the eastern equatorial Pacific near 130°W-100°W, 5°S-10°N; and
- A band of enhanced southeasterly wind stress in the southwestern tropical Pacific covering the region from the east coast of Australia to 160°W.

The largest pseudo wind stress changes are O(10 m^2/s^2), which corresponds to wind speed changes of about 1 to 2 m/s.

Figure 2b shows SST and wind stress difference maps from the relatively cool period of 1983-1989 to the warm period of 1990-1994. The greatest SST increases in *WARMING2* are in a narrow equatorial belt between the Dateline and 140°W. The amplitude in this region is about 0.8°C. The warming in the central equatorial Pacific is accompanied by positive SST differences over most of the central Pacific.

To the west and poleward of the peak warming region are relatively weak negative SST changes. The largest cooling values are in the range of -0.2° to -0.4°C. A second region of negative SST change is located in the equatorial cold tongue region off the coast of South America. A look at a 45-year (1950-1994, not shown) index of the cold tongue SST reveals that from 1990 to 1994, SST in the cold tongue region has been very near the long-term (1950-1979) climatology. This suggests that *WARMING2* negative SST differences in the eastern equatorial Pacific may best be described as a return to long-term climatology after the extreme warm years associated with the 1982-83 and 1986-87 warm ENSO events. Like those for *WARMING1*, the *WARMING2* changes in the wind stress field (Figure 2b) are largest in the west-central equatorial Pacific, from 140°E to 150°W, 5°S to 10°N, where a change to more westerly flow is evident.

The change to more westerly flow in the western equatorial Pacific appears to be connected to the development of a near-symmetric cyclone pair in the western half of the basin (Figure 2b). There is also a region of enhanced easterly wind stress anomalies in the eastern equatorial Pacific.

Precipitation and Surface Wind Divergence

Difference maps for precipitation and surface wind divergence fields are shown in Figure 3. Divergence fields have been constructed by taking the divergence of a monthly set of pseudo-winds derived from the Florida State University (pseudo) wind stress records. Thus, the wind divergence data cover the complete period of interest. The precipitation fields do not

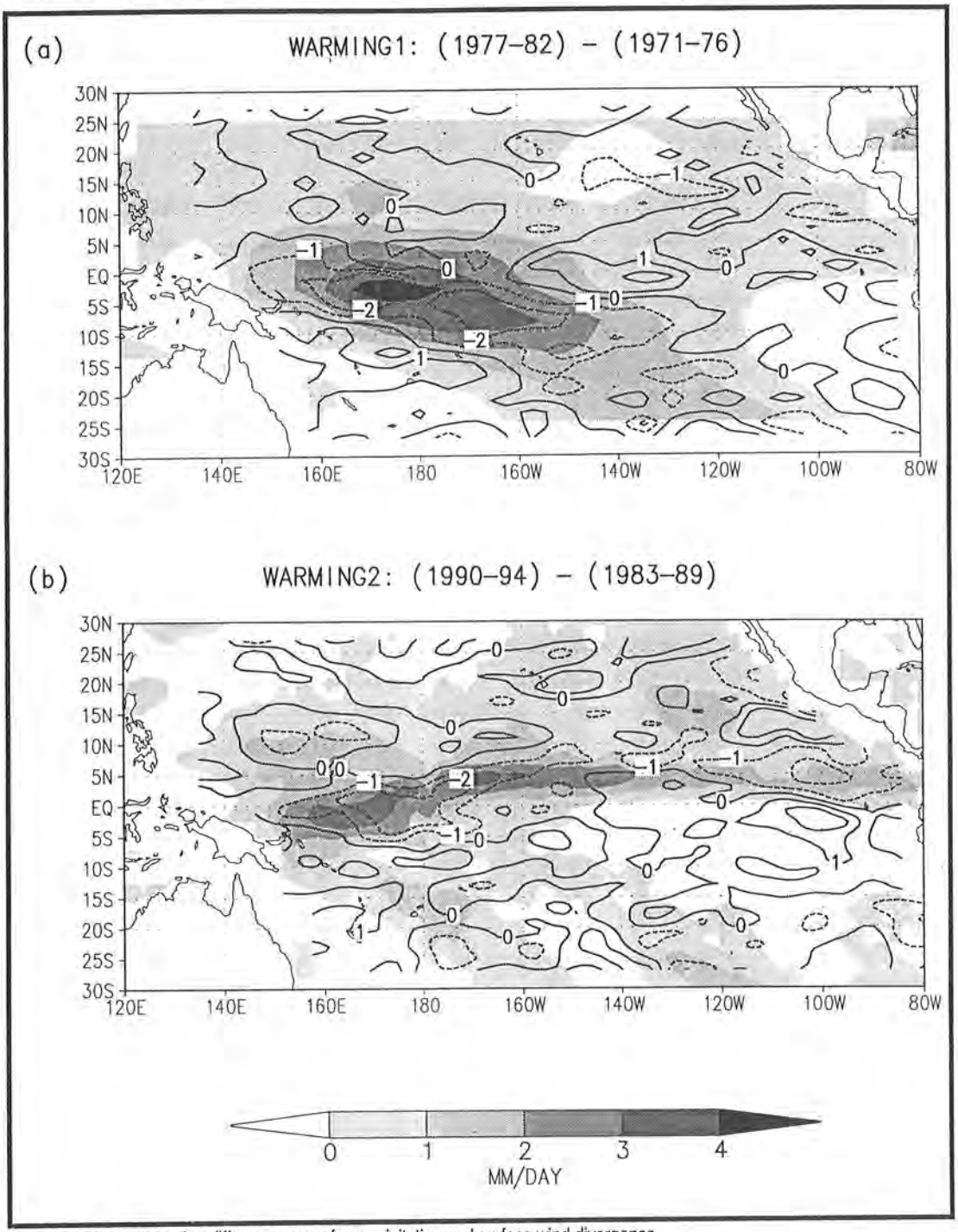

Figure 3 Climate warming difference maps for precipitation and surface wind divergence.
Panel (a) shows the difference maps for *WARMING1*; panel (b) shows difference maps for *WARMING2*.
The shading interval is 1 mm/day for the precipitation changes. The contour interval is $1*10^{-6}s^{-1}$ for the wind divergence.
Dashed contour lines are for negative values; solid contour lines are for positive values.

afford complete temporal coverage of the 1970-1994 period. However, major features in the precipitation difference maps are well reproduced by those in the surface wind divergence fields. Thus, we are confident that precipitation change signals associated with each of the climate warmings are being captured by the available precipitation data.

The precipitation fields shown in Figure 3a are derived from OLR. (Note that the OLR data begin in June 1974 and end in December 1982.) The largest changes in OLR-derived precipitation[2] from the cool period of June 1974 through December 1976 to the relatively warm period of 1977 through 1982 are focused along the general region of the South Pacific Convergence Zone (SPCZ).

Increases of more than 3 mm/day in precipitation are in the southeastward slanted band that begins near the equator at 160°E and ends near 10°S, 160°W. The distribution of enhanced surface wind convergence, depicted as changes in surface wind divergence of –2 to –3 $*10^{-6}$ s^{-1}, for the full 1971-1976 to 1977-1982 period of interest are essentially co-located with the OLR-derived increases in precipitation near the SPCZ. A general trend of increased precipitation over most of the tropical Pacific is also featured in Figure 3a.

The changes in precipitation shown in Figure 3b are derived from the Microwave Sounding Unit. The MSU data used to construct Figure 3b cover January 1983 through April 1994. As in Figure 3a, there is a change to increased precipitation over most of the tropical Pacific in *WARMING2*.

Increases in MSU precipitation from 1983-1989 to 1990-1994 are largest in the region near the equator between 160°E and the Dateline. Increases in this area are 2 to 3 mm/day. A narrow band of increased precipitation stretches to the west of the central equatorial maxima along a strip near the southernmost climatological position of the Intertropical Convergence Zone (ITCZ). Increases in surface wind convergence, shown by the dashed contours in Figure 3b, for the full period of 1983-1989 to 1990-1994 are essentially co-located with the MSU precipitation difference field for the abbreviated period, both in the central equatorial Pacific and along the ITCZ.

The spatial signatures of the *WARMING1* and *WARMING2* precipitation changes are distinct. The *WARMING1* precipitation increases are focused along the climatological position of the SPCZ; those for *WARMING2* are centered in the central equatorial Pacific and along the narrow line just to the north of the Equator, which is near the southernmost location of the ITCZ. Spatial features in the wind divergence fields are consistent with those in the satellite-derived precipitation.

2 To convert OLR to precipitation rates, we derived a regression coefficient from the overlapping OLR and MSU indices for the region 160°E-160°W, 10°S-10°N. The conversion factor is equal to -5.9 W/m^2 per mm/day precipitation.

Subsurface Ocean Temperatures

Figure 4 shows temperature differences at 40 meters depth. The *WARMING1* and *WARMING2* temperature difference maps for the tropical Pacific at 20, 40, 60, and 80 meters depth exhibit the same large-scale features, so we show only the 40-meter maps.

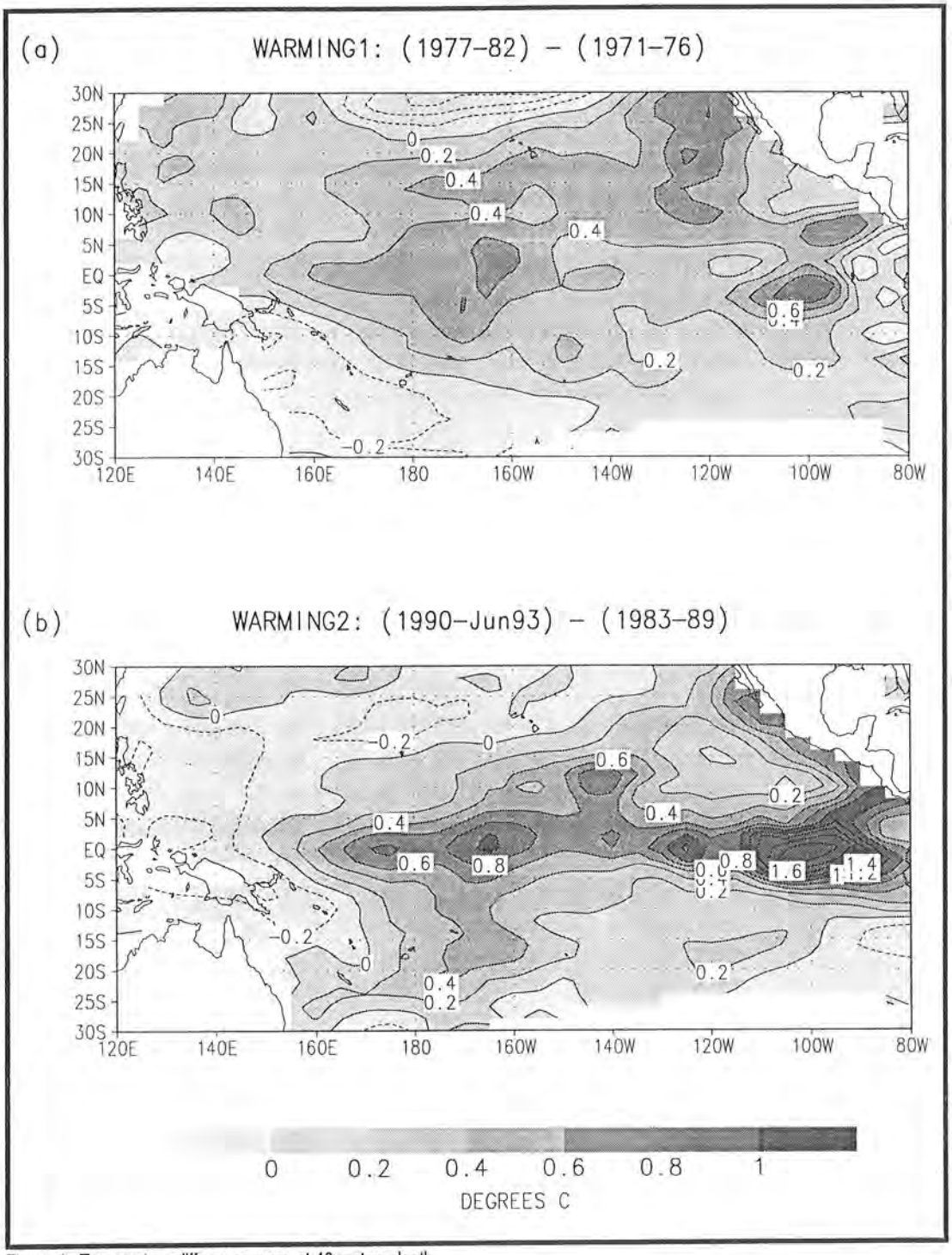

Figure 4 Temperature difference maps at 40 meters depth.
Panel (a) shows the difference maps for *WARMING1*; panel (b) shows the difference maps for *WARMING2*. The shading interval is 0.2°C.

The outstanding feature in Figure 4a is the change to warmer temperatures throughout most of the tropical Pacific region. Temperature increases of near 0.4° to 0.6°C cover much of the tropical Pacific Basin, with a small area of 0.8°C warming in the eastern equatorial Pacific. Two relatively small regions of SST cooling are located in the central and western subtropical and extratropical Pacific. For *WARMING1*, the spatial distribution of temperature change at 40 meters depth is similar to that at the ocean surface (compare Figures 2a, 4a).

The 40-meter temperature changes for *WARMING2* are shown in Figure 4b. Unlike the constancy evident between the surface and subsurface temperature changes for *WARMING1*, subsurface temperature changes for the post-1990 warming exhibit features distinctly different from those at the ocean surface. In Figure 4b, the peak warming of 0.8°C at 40 meters depth is in the eastern equatorial Pacific and in a small, separate region near 170°W, again on the equator. There is also a hint of a coastal maxima in the warmer upper ocean temperatures along the west coast of the Americas from the Baja Peninsula to the equatorial regions of South America.

Interpreting the Climate Changes: Are They ENSO Residuals?

This section focuses on the question: To what extent do the climate warmings of the late 1970s and 1990s look like a persistent warm episode of the ENSO cycle? We attempted to address this question using a statistical analysis tool that objectively identifies modes of covariability in pairs of datasets.

Theoretical and numerical modeling studies have found that ENSO is inherently dependent on coupling between sea surface temperature and surface winds (Hirst 1986; Zebiak and Cane 1987; Battisti 1988; Schopf and Suarez 1988). Mantua and Battisti (1995) have shown that the spatial structure of the leading SST-wind stress mode of covariability produced by so-called intermediate coupled ocean-atmosphere models of the tropical Pacific is similar to that found for the observations from 1975 to 1993. Here, we reproduce Mantua and Battisti's singular value decomposition (SVD) analysis of the observed SST and FSU wind stress for the slightly longer period of 1970-1994. The products of the SVD analysis allow construction of a monthly record of what we now define as the *pure ENSO* variability in observed climate from 1970 to 1994. (For details of the SVD analysis, see Wallace *et al* 1992 and Bretherton *et al* 1992.)

Time series of the SST and wind stress variability in the SVD-defined pure ENSO are shown in Figure 5. These time series are highly correlated (r=0.88), and each is highly correlated with traditional indices of ENSO variability (*ie*, NINO3 and the SOI; Table 1).

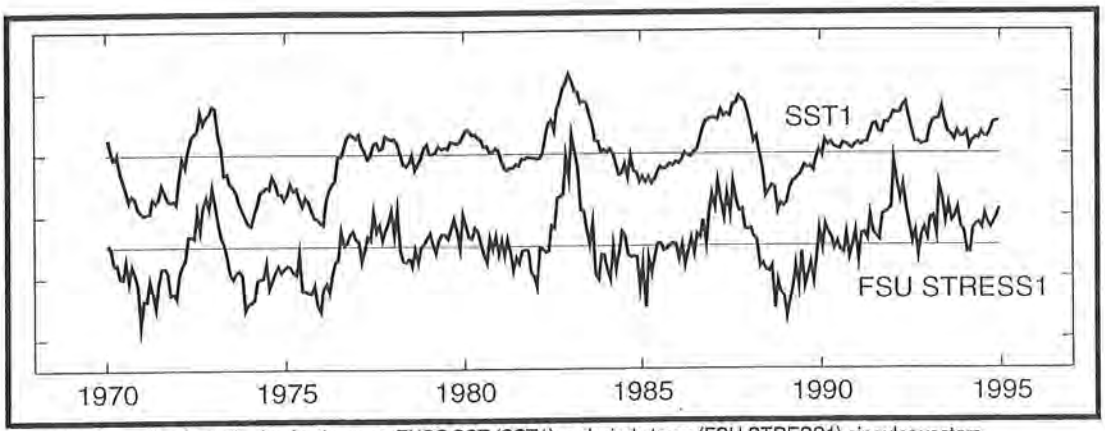

Figure 5 Normalized amplitudes for the *pure ENSO* SST (SST1) and wind stress (FSU STRESS1) singular vectors. Light solid lines are the zero lines for each time series.

Our *pure ENSO* SST and wind stress pattern, which emerges as the leading singular vector pair from the SVD analysis, is shown in Figure 6a. The amplitude of the wind stress and SST pattern represents the projection of the full *WARMING1* SST and wind stress difference map onto the normalized *pure ENSO* pattern (compare Figures 6a, 2a). The ENSO-like warming in Figure 6a is greater than 0.8°C in the central and eastern equatorial Pacific. The residual fields, that is, the total *WARMING1* SST and wind stress differences (Figure 2a) minus the ENSO projection (Figure 6a), are shown as the *non-ENSO* changes in Figure 6b. Notable features in Figure 6b include the large region of U-shaped warming with local maxima in the western equatorial Pacific and in the northeast and southeast subtropical Pacific. The region of greatest warming is west of the Baja Peninsula at 20°N-25°N, 135°W-120°W. The weakened northeasterly wind stress at 160°E-160°W, 5°N-20°N, and the enhanced easterlies in the eastern equatorial Pacific are also notable features in the non-ENSO fields for *WARMING1*.

Results from the pure ENSO projection onto the *WARMING2* SST and FSU wind stress fields are shown in Figure 7a. The amplitude of the *WARMING2* ENSO projection is about half that of *WARMING1* (compare Figures 6a, 7a). The *WARMING2* non-ENSO SST and wind stress changes, shown in Figure 7b, are largest in a region of SST warming in the central equatorial Pacific and in a region of SST cooling in the eastern Pacific from the equator to 20°S. The *WARMING2* non-ENSO wind stress changes in Figure 7b depict a region of weakened northeasterlies between 150°E and 170°W, from the equator to 15°N, and a region of enhanced easterly flow between 150°W to 110°W, from the equator to 15°S.

The non-ENSO components of the two climate warmings share more similarities in wind stress than in sea surface temperature. Both *WARMING1* and *WARMING2* non-ENSO components exhibit enhanced easterlies in the eastern equatorial Pacific and weakened northeasterlies

in the central Pacific between the equator and 15°N. The relatively strong ENSO projection in *WARMING1* may be understood as a relaxation toward climatological mean conditions after the repeated cold extremes in the ENSO cycle from 1970 to 1976. On the other hand, the weaker ENSO projection in *WARMING2* may be interpreted as a result of the

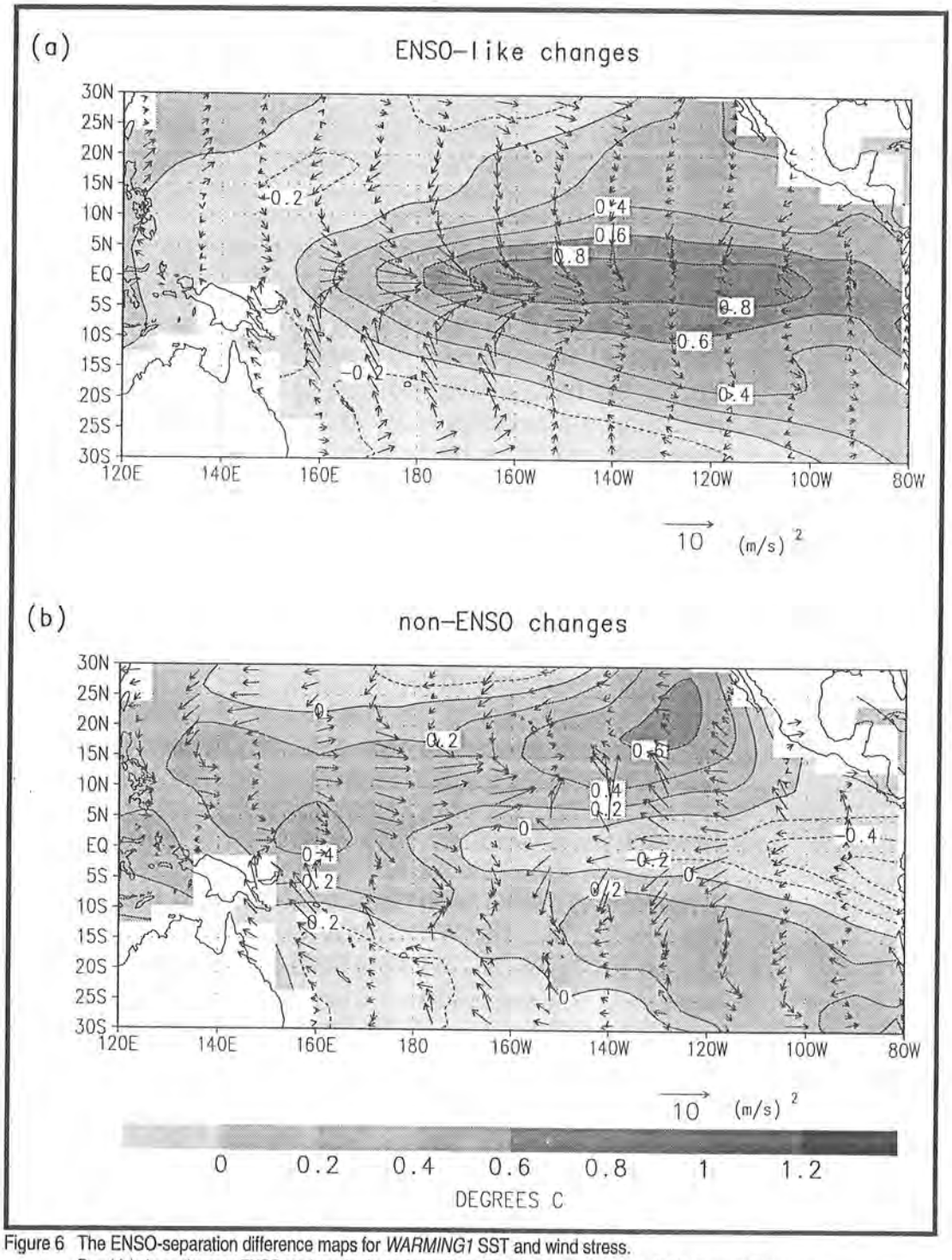

Figure 6 The ENSO-separation difference maps for *WARMING1* SST and wind stress.
Panel (a) shows the pure ENSO mode projections of the *WARMING1* SST and wind stress fields shown in Figure 1a.
Panel (b) shows the *WARMING1* non-ENSO changes in SST and wind stress, which are computed as the residual of the full and ENSO projection *WARMING1* changes. Scaling is the same as that for Figure 1.

moderate positive ENSO projections for 1983-1989 and 1990-1994, with the latter period being slightly larger.

Results from this analysis suggest that a significant portion of the *WARMING1* and *WARMING2* changes in SST and wind stress are not well described as a shift to a persistent canonical warm ENSO climate state.

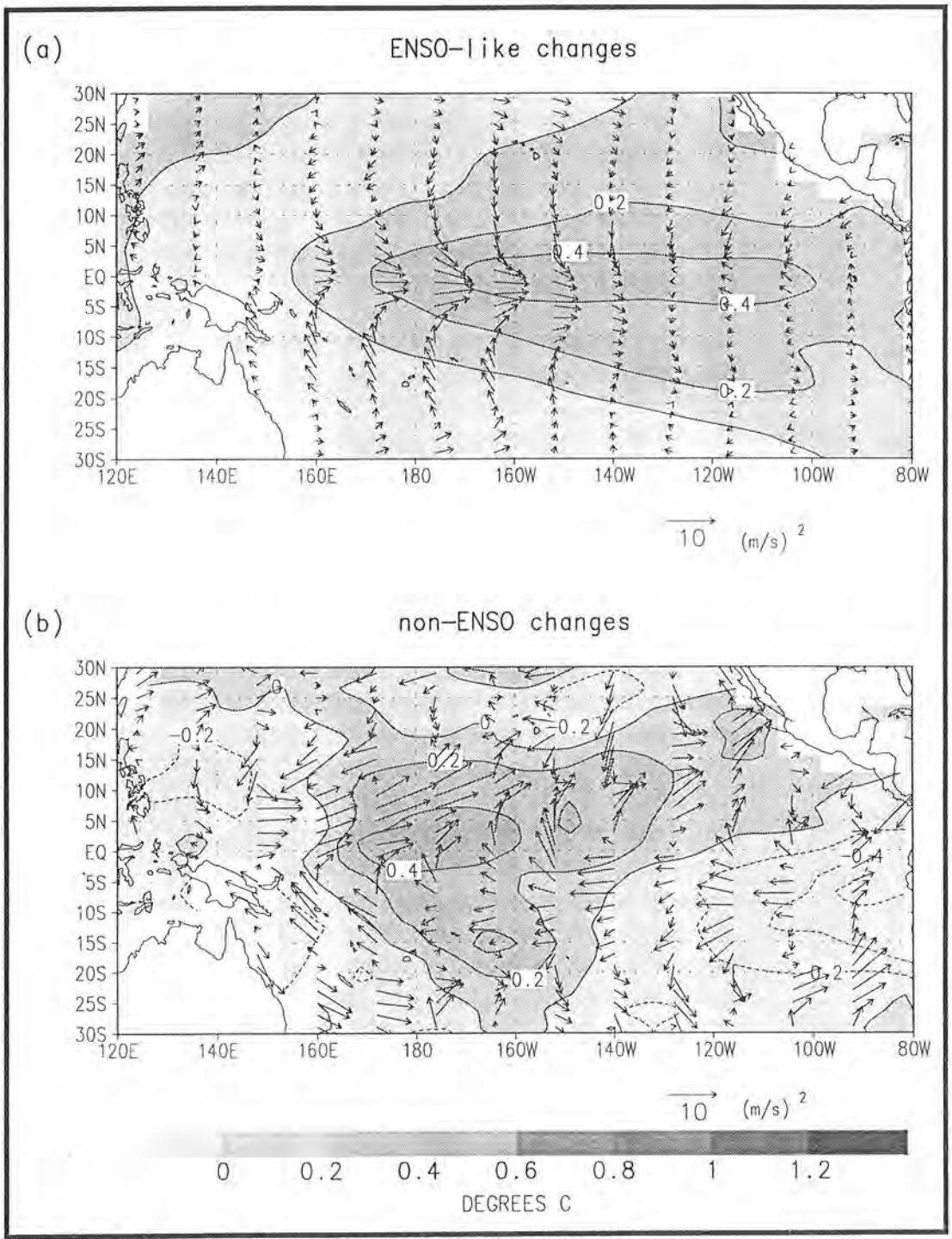

Figure 7 The ENSO-separation difference maps for *WARMING2* SST and wind stress.
Panel (a) shows the pure ENSO mode projections of the *WARMING2* SST and wind stress fields shown in Figure 1a.
Panel (b) shows the *WARMING2* non-ENSO changes in SST and wind stress, which are computed as the residual of the full and ENSO projection *WARMING2* changes. Scaling is the same as that for Figure 1.

Summary and Discussion

In this study, we present evidence for two multi-year climate warmings in the tropical Pacific region in the period of record from 1970 to 1994. The first multi-year change to a warmer tropical climate took place soon after 1976; the second took place near the beginning of 1990. Difference maps for the periods before and after the climate warmings depict large-scale, coherent changes in the upper ocean and troposphere over much of the tropical Pacific region. We have attempted to distinguish between features of the two climate warmings and those associated with ENSO-related climate variability. Our analysis suggests that, although a significant portion of the multi-year climate changes project onto ENSO anomaly patterns, important large-scale climate shifts remain that appear to be unrelated to the ENSO cycle. If our ENSO-separation technique is valid, these results argue for the presence of large-scale, low-frequency, but non-ENSO-like, modes of climate variability in the tropical Pacific region.

The non-ENSO aspects of the climate warmings examined in this study have their largest signatures in the west-central equatorial Pacific and in the off-equatorial eastern tropics. In the northern hemisphere, a band of warm SST and weakened northeasterly wind stress connects the two local maxima of SST warming, located near the Dateline and near the west coast of the Baja Peninsula. Near the equator, the strength of the basin-mean easterly Trade Winds is reduced. Concurrent with the weakened mean easterlies are relaxations in the east-west slope of the near- equatorial thermocline. We hypothesize that the collection of climate changes in the tropical Pacific region are indicative of either a new quasi-equilibrium climate state in the tropical Pacific region or an interdecadal mode of climate variability that is distinct from the interannual ENSO. In either case, we see compelling evidence for coherent large-scale changes in the tropical climate occurring at decadal time scales. For example, a weakening of the zonal near-equatorial winds leads to a relaxation in the equatorial thermocline slope. A flattening of the equatorial thermocline would likely allow an eastward expansion of the warm pool SST that is being continually opposed by the easterly wind-driven currents and upwelling. As the warm pool expands eastward into the central equatorial Pacific, the area of frequent intense tropical convection and precipitation also expands to the east. This, in turn, alters large-scale tropical circulation. In many respects, interactions of this type are understood to be fundamental to the instability mechanism for the ENSO cycle.

In the previous scenario, the classic development of the interannual ENSO (like, for example, that in the canonical Rasmussen and Carpenter (1982) ENSO event) does not take place. Instead, the slow time scale climate warming persists, in some sense leading to a "new" climatological basic state in the tropical Pacific. Superimposed upon this new, warmer, climate state is variability in the interannual ENSO cycle. Results from

previous studies suggest that a change in character of the ENSO cycle, in time and/or space, is likely to result from changes in the climatological basic state of the tropical climate system (Battisti and Hirst 1989; Wang 1995). We have conducted a simple experiment that demonstrates this phenomenon with the use of the Zebiak-Cane (Zebiak and Cane 1987, hereafter "ZC") coupled ocean-atmosphere model, a tool that has demonstrated skill at both simulating and predicting the ENSO cycle.

Figure 8a is a 200-year time series of NINO3 produced by the ZC model when linearized about the climatological basic state fields — which include the observed mean thermocline depth, monthly mean SST, wind and wind convergence fields —from 1950 to 1979. The NINO3 variability clearly indicates the presence of an interannual oscillation with a dominant spectral peak at about 4 years (Figure 8c). In Figure 8b is a 200-year time series of NINO3 for the same model linearized about the climatological basic-state fields for 1980-1992, a "warmer" climatology than that of 1950-1979. The character of model variability as indicated by NINO3 has undergone a dramatic change to a broader spectrum of mostly shorter period oscillations, with a weak spectral peak centered near a period of 2 years.

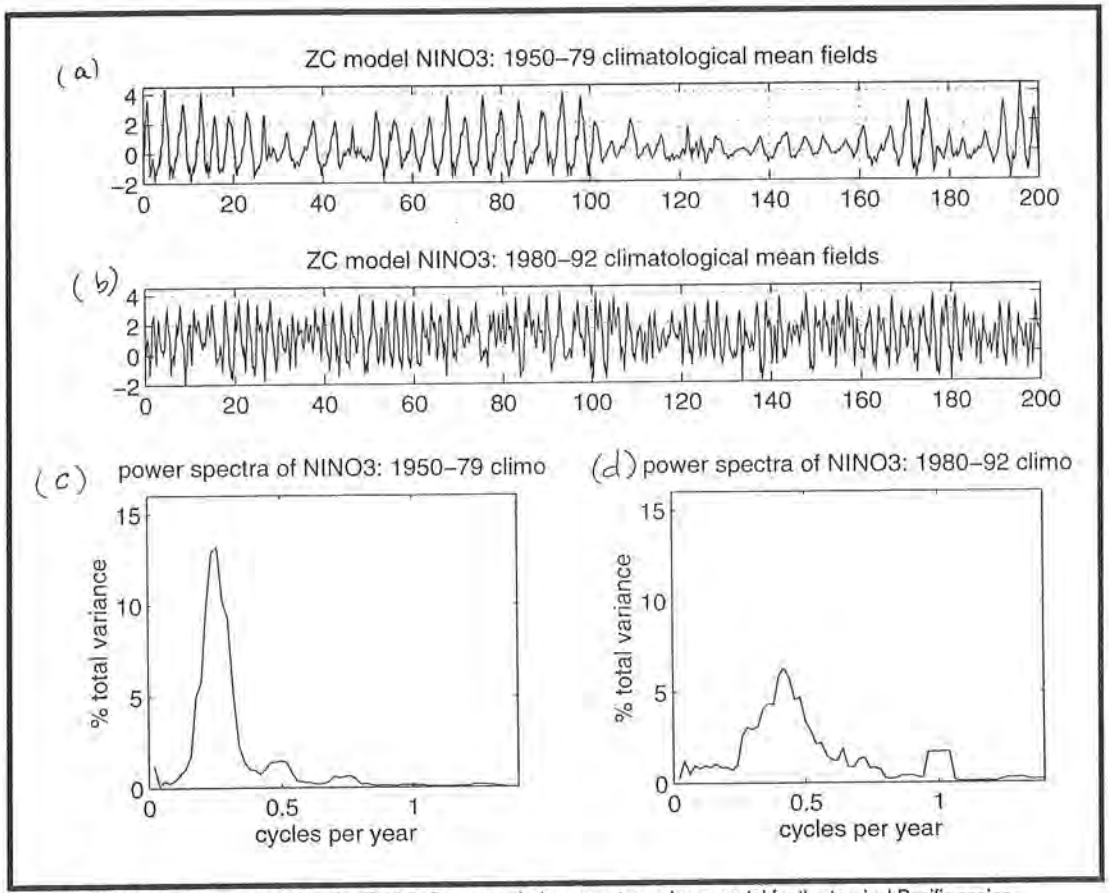

Figure 8 NINO3 indices produced by the Zebiak-Cane coupled ocean-atmosphere model for the tropical Pacific region.
Panel (a) is a 200-year time series of NINO3 from a version of the model that is linearized about the 1950-1979 climatological basic state.
Panel (b) is a 200-year time series of NINO3 from a version of the model that is linearized about the 1980-1992 climatological basic state.
Panel (c) shows the NINO3 power spectra for the 1950-1979 climatology simulation.
Panel (d) shows the NINO3 power spectra for the 1980-1992 climatology simulation.

A recent study by Wang (1995) documents decadal-scale changes in the temporal and spatial characteristics of the ENSO cycle. Wang attributes the variability in the ENSO cycle to decadal-scale variability in the climatological state of the tropical Pacific region. Our findings complement Wang's study by documenting the multi-year time scale climate changes observed between 1990 and 1994. We further speculate that changes in the character of the ENSO cycle are inherently linked to multi-year time scale modes of climate variability that may operate independently of the ENSO cycle. Models that demonstrate skill at reproducing key aspects of the ENSO cycle have thus far been incapable of reproducing multi-year off-equatorial or western equatorial climate variability such as that seen in our non-ENSO-like climate change fields (Figure 6b, 7b). These modeling results imply that the physics of the ENSO cycle differ from those essential to the longer time-scale mode of tropical climate variability documented in this study.

Acknowledgments

This study was supported by funding for the Scripps Institution of Oceanography Pilot Project for the International Research Institute for Climate Prediction (IRICP).

References

Battisti, D.S. 1988. The dynamics and thermodynamics of a warming event in a coupled tropical atmosphere-ocean model. *J. Atmos. Sci.* 45:2889-2919.

Battisti, D.S., and A.E. Hirst. 1989. Interannual variability in the tropical atmosphere-ocean system: Influence of the basic state and ocean geometry. *J. Atmos. Sci.* 46:1687-1712.

Bretherton, C.S., C. Smith, J.M. Wallace. 1992: An intercomparison of methods for finding coupled patterns in climate data. *J. Climate* 5:541-560.

Griffith, G.C., W.L. Woodley, P.G. Grube, D.W. Martin, J. Stout, D.N. Sikdar. 1978. Rain estimation from geosynchronous satellite imagery-visible and infrared studies. *Mon. Weather Rev.* 106: 1153-1171.

Hirst, A.C. 1986. Unstable and damped equatorial modes in simple coupled ocean-atmosphere models. *J. Atmos. Sci.* 43:606-630.

Legler, D.M., and J.J. O'Brien. 1988. Tropical Pacific wind stress analysis for TOGA. *IOC Time Series of Ocean Measurements*, IOC Technical Series 33, 4. UNESCO.

Mantua, N.J., and D.S. Battisti. 1995. A periodic variability in the Zebiak-Cane coupled ocean-atmosphere model: air-sea interactions in the western equatorial Pacific. *J. Climate* 8:2897-2927.

Rasmussen, E.M., and T.H. Carpenter. 1982. Variations in tropical sea surface temperature and surface wind fields associated with the Southern Oscillation/El Niño. *Mon. Wea. Rev.* 110:354-384.

Reynolds, R.W., and T.M. Smith. 1994. A high resolution global sea surface temperature climatology. Submitted to the *J. Climate*.

Schopf, P.S., and M.J. Suarez. 1988. Vacillations in a coupled ocean-atmosphere model. *J. Atmos. Sci.* 45:549-566.

Spencer, R.W. 1990. Global oceanic precipitation from the MSU during 1979-91 and comparisons to other climatologies. *J. Climate* 6:1301-1326.

Wallace, J.M., C.S. Bretherton, C. Smith. 1992. Singular value decomposition of sea-surface temperature and 500-mb height anomalies. *J. Climate* 5:1140-1156.

Wang, B. 1995. Interdecadal changes in El Niño onset in the last four decades. *J. Climate* 8:135-162.

Zebiak, S.E., and M.A. Cane. 1987. A Model ENSO. *Mon. Wea. Rev.* 115:2262-2278.

Analysis of Four Decades of High Elevation Climate Data

Mark Losleben

Abstract: Four decades of instrumented climate records at D1 on Niwot Ridge suggest that high elevation data are an important — and even unique — part of the full climate picture. High elevation data provide information on changing lapse rates as well as model verification for global warming, which is predicted to occur earliest in high latitudes and at high elevations. The D1 records show climatic trends that arguably support global warming, assuming that greater planetary wave amplitude is verification of warming. Lapse rates reflect conditions of air mass stability, atmospheric moisture, and could cover, which contribute to feedback processes involving temperature, precipitation, and snowpack. The D1 record shows a period, 1981-1985, when the lapse rate increased significantly, and this change was not detected by other data.

The D1 climate station is 2.7 kilometers east of the Continental Divide and 34 kilometers west of Boulder, Colorado, at an elevation of 3749 meters. The C1 climate station is 7 kilometers east of D1, at an elevation of 3018 meters. Both sites are on Niwot Ridge; D1 is in the alpine forest and C1 is in the subalpine forest.

Four decades, 1951-1994, of instrumented climate records on Niwot Ridge show:

- A decrease in fall temperatures (–0.044°C/yr), but no significant annual cooling (–0.009°C/yr);
- A daily average maximum:minimum temperature ratio that is relatively constant on a seasonal basis;
- A decreasing trend in the lapse rate (–0.012°C/km/yr) between 3749 and 3018 meters;
- A step-function decrease in winter pressure variability (19%) in the 1991-92 winter;
- A decrease in incident summer solar radiation (3 watts/m^2/yr) between 1971 and 1992, but an increase in 1965-1970 and in 1992-1994; and
- An annual precipitation increase of 11.04 mm/yr at 3749 meters, but no trend in annual precipitation at 3018 meters (Greenland 1994).

In: C.M. Isaacs and V.L. Tharp, Editors. 1996. *Proceedings of the Twelfth Annual Pacific Climate (PACLIM) Workshop, May 2-5, 1995.* Interagency Ecological Program, Technical Report 46. California Department of Water Resources.

The 1981-1985 "Cold Event"

Although there is no significant long-term trend in the 40-year temperature record at the 3749 meter site (D1), 1981-1985 is a notable cold period, averaging 3°C colder annually than in the rest of the record (Figure 1). This cold period is evident in the record for all seasons as well as in the maximum and minimum average daily values. A lower site, at 3018 meters (C1), also reflects this cold period, but less distinctly. At the lowest sites in the Colorado Front Range, Boulder and Longmont, this cold period is conspicuously absent.

The D1-Longmont lapse rate increased from an average of 6.3 to 7.6°C/km during the 1981-1985 period (Figure 2). The D1-C1 annual lapse rate increased about 1.5°C/km during this same time.

Surface solar insolation at both D1 and C1 declined steadily from 1971 to 1992 (Figure 3). Precipitation was enhanced slightly in the 1981-1985 period but was within the extremes of the 40-year record at both sites.

This cool period is not easily explained by reduced solar radiation nor increased cloudiness (as implied from the precipitation record and the lack of change in the temperature maximum: minimum ratio). A possible explanation may be a change in atmospheric circulation patterns during the 5-year period. Such changes could increase polar air mass frequency during 1981-1985 relative to the remaining record. However, air masses affect regions, and Boulder and Longmont did not cool during this period.

A possible explanation for this condition is that the two areas are dominated by elevationally different circulation patterns. The mountains of the Continental Divide near D1, dominated by west or northwest air flow, encourage a lee-developing cyclonic flow to develop over the eastern plains (Bresch and Reitter 1987), where Longmont and Boulder are located. This cyclonic tendency creates the potential for a southeasterly flow, and possible warm air advection, over the plains and at the same time a northwest flow and cold air advection over the mountains, only a few kilometers to the west.

In summary, the Niwot Ridge data suggest that high elevation climate data are an important part of the complete climate picture, both in model verification and for identification of changes that cannot be measured at low elevations alone.

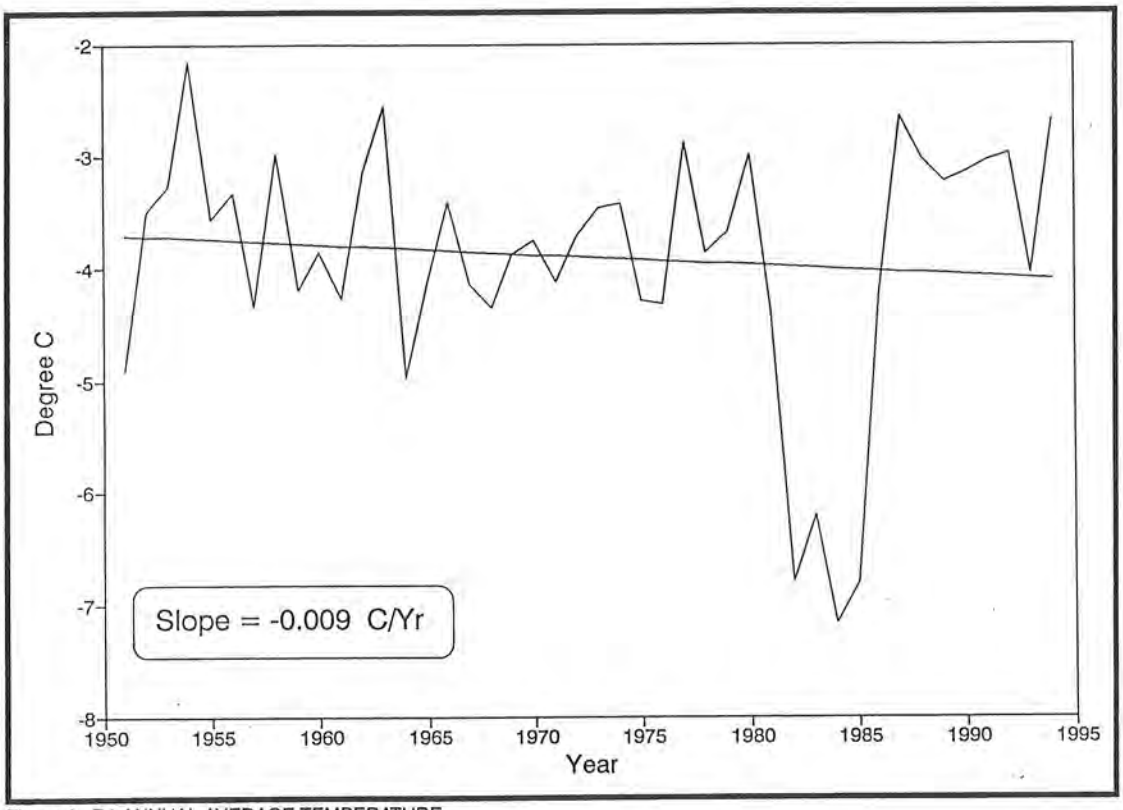

Figure 1 D1 ANNUAL AVERAGE TEMPERATURE

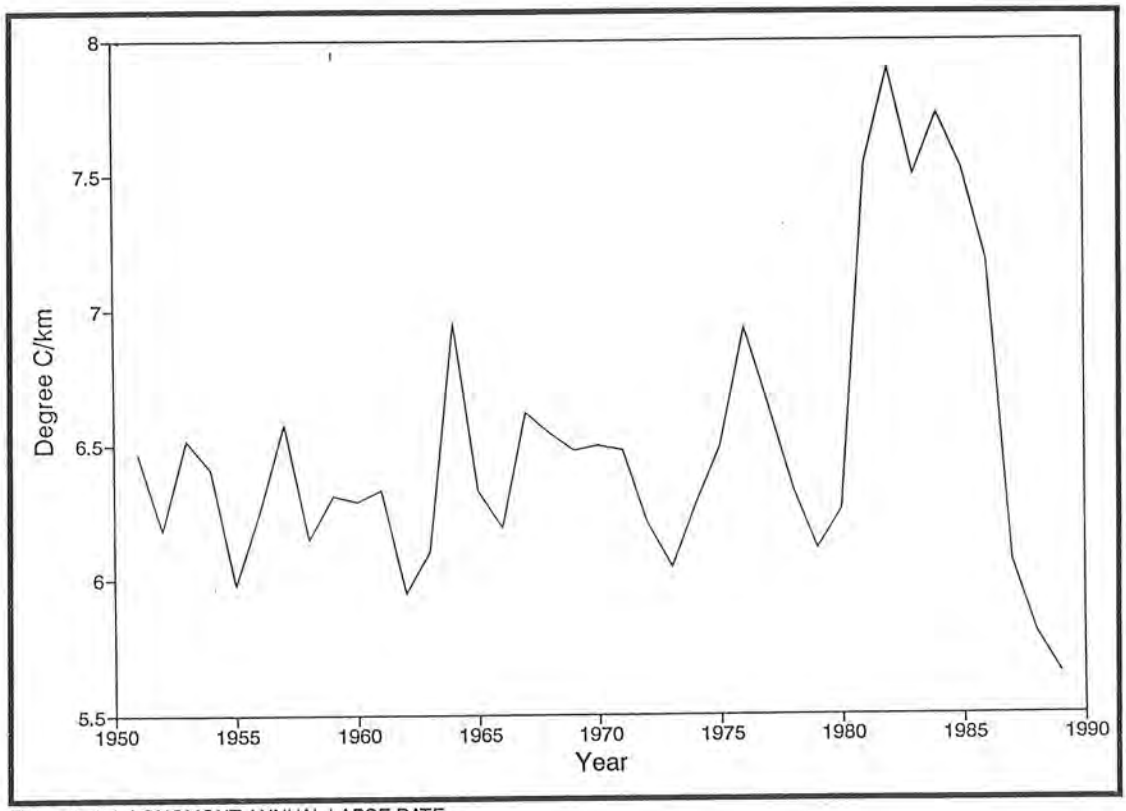

Figure 2 D1, LONGMONT ANNUAL LAPSE RATE

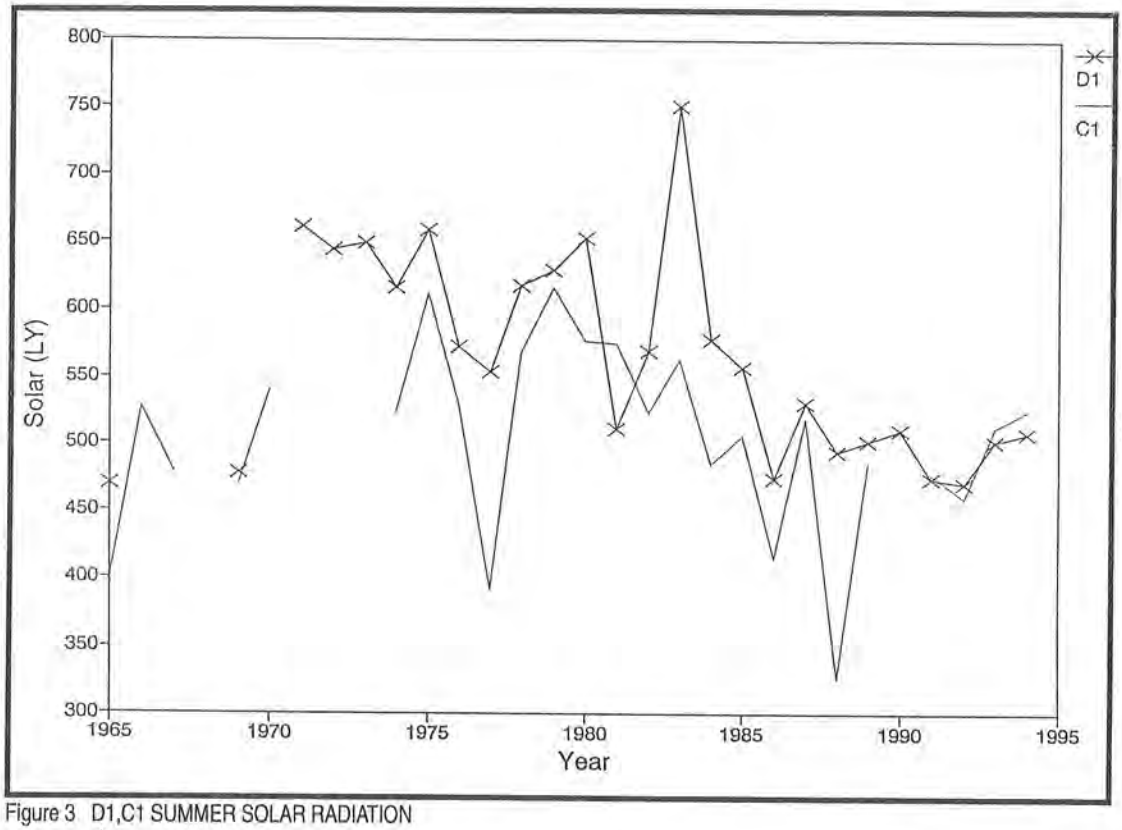

Figure 3 D1,C1 SUMMER SOLAR RADIATION

Future Study

Synoptic-scale classification or pressure grid correlation fields may verify whether or not changes in circulation occurred from 1981 to 1985. Establishment of the correlation between radiosonde and high elevation ground pressure and temperature data might also be valuable in augmenting the relatively few climate records at high elevations.

References

Bresch, J.F., and E.R. Reitter. 1987. Case study of unusual long-range sulfur transport episode. *American Meteorological Society* 26:315-321.

Greenland, D. 1994. A Decrease in Temperatures at High Elevations in the Colorado Front Range, USA. Unpublished report.

Relationships between Climate and Atmospheric Circulation in the Sonoran Desert Region

Connie A. Woodhouse

The goal of this research is to identify key features of atmospheric circulation that influence winter climate variability in the Sonoran Desert region. The relationship between winter climate and atmospheric circulation is investigated through the use of indices, which describe the principal features of circulation patterns. Principal questions addressed were:

- What atmospheric circulation patterns influence winter climate (precipitation and temperature) in the Sonoran Desert region?
- What circulation indices can be used to describe climate in this area?
- What are the relationships between climate and circulation as described by indices?
- How well do circulation indices explain variations in winter climate in the Sonoran Desert area?

The study area extends from 106°W to 118°W and from the United States/Mexico border to 37°N, encompassing southern California, the southern tip of Nevada, Arizona, and western New Mexico. Winter climate is described in terms of numbers of rainy days and average maximum temperatures at a network of 50 precipitation and 40 temperature stations throughout the study area.

A set of six circulation indices was compiled (Table 1). Existing indices used include the Southern Oscillation Index (NOAA Climate Analysis Center) and a sea surface temperature index from the equatorial Pacific (Kiladis and Diaz 1989; NOAA Climate Analysis Center). Indices specially constructed for this study include a modified Pacific North American index (after Yarnal and Diaz 1986), a cyclone frequency index, a southwestern trough index, and a Pacific high/southwestern low index.

In: C.M. Isaacs and V.L. Tharp, Editors. 1996. *Proceedings of the Twelfth Annual Pacific Climate (PACLIM) Workshop, May 2-5, 1995.* Interagency Ecological Program, Technical Report 46. California Department of Water Resources.

Table 1
CIRCULATION INDICES

INDEX	DESCRIPTION	SOURCE	INTERVAL
SOI	Southern Oscillation Index-sea level pressure; Tahiti - Darwin	Climate Analysis Center (CAC)	Seasonal
SST	Sea surface temperature from COADS data 4°N-4°S, 160°-80°W (1930-1979) 5°N-5°S, 190°-90°W (1980-1990)	Kiladis and Diaz (1989) CAC NINO3 index	Seasonal
PNA-modified	Pacific North American pattern; a measure of zonality across N. America. Location of pressure centers modified after Keables (1992) PNA3 pattern. PNA=1/3[-Z*(135°W, 35°N)+ Z*(100°W, 75°N)-Z*(70°W, 30°N)]	Constructed for this study	Monthly, Nov-Mar
Cyclone Freq	Cyclone frequency; Numbers of cyclones or low centers generated in, crossing though, or dissipating in study area, totalled for November-March.	Constructed for this study	Total winter
SWTROF	Southwestern trough; measure of intensity of low over the SW, in combination with high pressure over the Gulf of Alaska and the Great Lakes. SWTROF=1/3[-Z*(140°W, 50°N)+ Z*(115°W, 35°N)-Z*(80°W, 45°N)]	Constructed for this study	Monthly, Nov-Mar
PHSWL	Pacific high/southwestern low; measure of intensity of low over the SW, in conjunction with the longitudinal position of the Pacific high. PHSWL=Z*(115°W, 35°N)-longitude of the greatest 500mb height @ 30°N, 120°-160°W	Constructed for this study	Monthly, Nov-Mar

* Z=standardized 500mb height at each grid point.

Correlations between the precipitation and temperature station networks and different monthly and seasonal versions of the indices were performed to determine which index month, group of months, or season was most important to the two winter climate variables. Results are shown in Table 2. Precipitation from stations in New Mexico and the higher elevations of Arizona correlated better with winter SOI, but California and lower-elevation Arizona precipitation had a better correlation with previous fall SOI. Fall SOI was chosen for use in further analyses, because the lower elevation areas are most characteristic of the Sonoran Desert. No other indices had such marked regional differences. There were no correlations between the cyclone frequency index and rain days, nor between the PNA index and maximum temperatures.

Table 2
INDICES CORRELATED BEST WITH NETWORKS OF PRECIPITATION AND TEMPERATURE STATIONS

WINTER RAIN DAYS		MAXIMUM WINTER TEMPERATURE	
SOI	PREVIOUS FALL	SOI	PREVIOUS FALL
SST	WINTER	SST	WINTER
PNA	JFM AVERAGE	CYC FREQ	WINTER TOTAL
SWTROF	NDM AVERAGE	SWTROF	N-M AVERAGE
PHSWL	NDM AVERAGE	PHSWL	N-M AVERAGE

The sets of indices most important to precipitation and most important to temperature were entered into two separate, rotated principal components analyses (PCA), for the common period 1947-1990. In both cases, two components resulted, accounting for 76.5% of the total variance in rain day indices and for 78.6% of the total variance in temperature indices. In both PCAs, one component contained SOI, SST, and PNA (rain day indices only) indices and the other component contained the cyclone frequency (temperature indices only), southwestern trough, and Pacific high/southwestern low indices. For ease of identification, I named one component the "ENSO" component and the other the "Southwestern Low" component. Scores from the PCAs were saved and used to examine the spatial patterns and strength of the relationships between the climate variables and circulation indices.

Correlations were performed between the principal component scores and the network of precipitation and temperature stations. For precipitation, the areas of strongest correlations with the ENSO component scores are negative and in the lower Colorado River basin and southeastern California ($r = -0.63$). Weakest correlations, also negative, are in northeastern Arizona and northern New Mexico ($r = -0.38$). For the Southwestern Low component, areas of strongest correlation with precipitation are in western New Mexico and east-central Arizona and are negative ($r = -0.64$); areas of weakest correlations are in southern California and the lower Colorado River basin ($t = -0.20$). Correlations between temperature stations and the ENSO component graded from positive in southwestern New Mexico and southeastern Arizona ($r = 0.45$) to negative in stations on the California coast ($r = -0.30$). Temperature stations throughout central Arizona, southern Nevada, and California, except coastal and lower Colorado River basin areas, were strongly and positively related to the Southwestern Low component scores ($r = 0.64$ -0.81).

Component scores from each PCA were used in regression analyses to determine how well the set of six indices, as described by the two components, explain variations in winter precipitation and temperature in this area. The two components explain up to 65 percent of the variation in numbers of rainy days and up to 82 percent of the variation in maximum winter temperatures. The greatest amount of variation in rain days was explained in north-central New Mexico, with the least in southern Arizona and southern and coastal California ($r = 0.2$) (Figure 1). Variations in temperature were best explained in central and southern Arizona, and the least amount was explained along the California coast ($r = 0.4$) (Figure 2).

In summary, six circulation indices have been identified that describe circulation features important to winter climate in the Sonoran Desert region. Together, the set of six indices explains about 25 to 60 percent of the variations in number of winter rain days and about 60 to 80 percent of the variations in maximum winter temperatures in this region. These indices appear to be defining two types of circulation mechanisms that influence climate: ENSO/PNA, and presence of a low pressure center.

These two mechanisms likely are not independent. ENSO events, in particular, are quite variable and have been known at times to be characterized by the presence of a southwestern low (Keables 1992). The two patterns might better be described as a "typical" ENSO/positive PNA-type pattern and a reverse PNA-type pattern, characterized by a trough over the southwestern United States.

Literature Cited

Keables, M.J. 1992. Spatial variability of midtropospheric circulation patterns and associated surface climate in the United States during ENSO winters. *Physical Geography* 13:331-348.

Kiladis, G.N., and H.F. Diaz. 1989. Global climatic anomalies associated with extremes of the Southern Oscillation. *Journal of Climate* 2:1069-1090.

Yarnal, B., and H.F. Diaz. 1986. Relationships between extremes of the Southern Oscillation and the winter climate of the Anglo-American Pacific coast. *Journal of Climatology* 6:197-219.

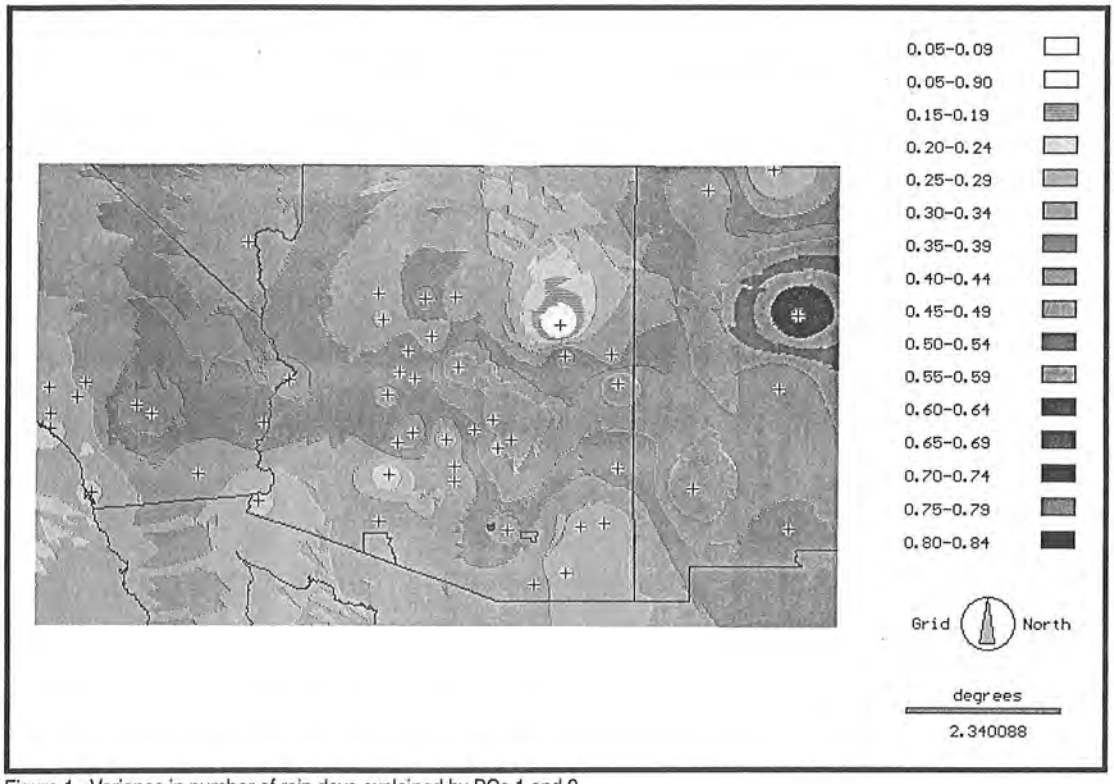

Figure 1 Variance in number of rain days explained by PCs 1 and 2.
Mapped values are r^2 values.

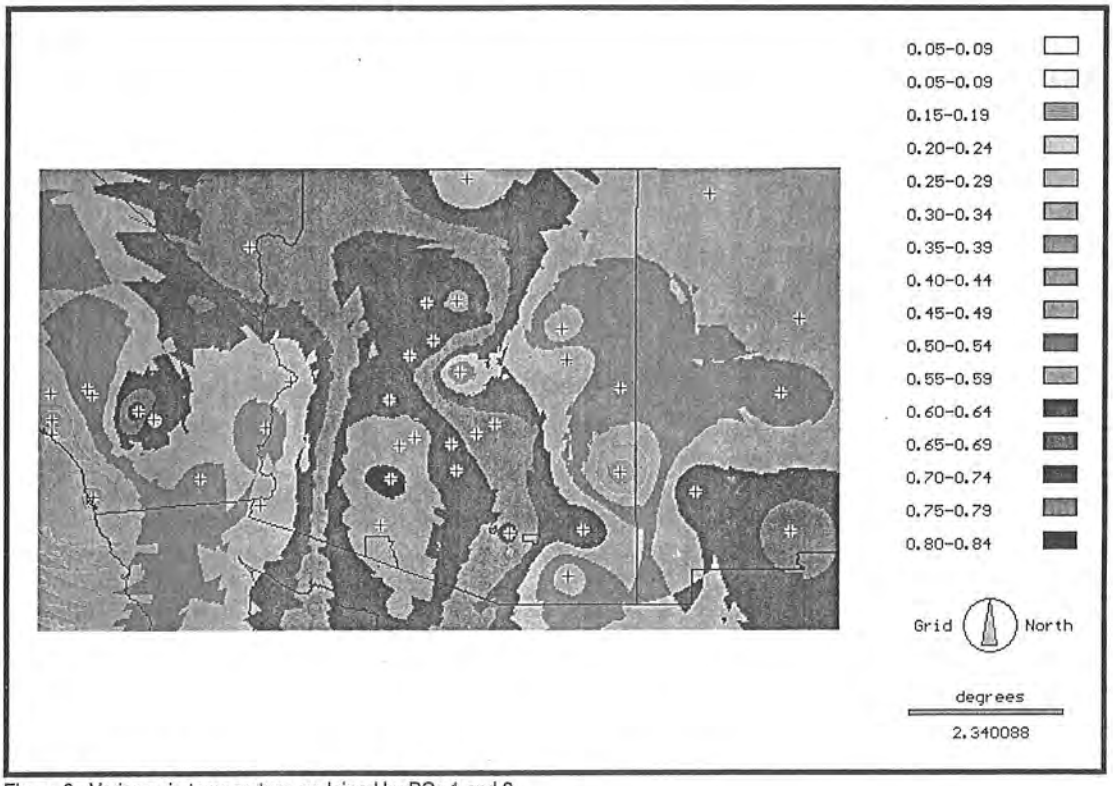

Figure 2 Variance in temperature explained by PCs 1 and 2.
Mapped values are r^2 values.

Geographic Patterns in the Lag of Temperature Response to Insolation for El Niño vs. La Niña Conditions

R.C. Craig, J.L. Betancourt, D.E. Jones

Abstract

The most important control on the annual cycle of temperature is insolation, with secondary influences from terms related to moisture, yet direct statistical analysis of the moisture-driven modulations (such as El Niño) of the response of temperature to insolation are not available. We have examined one aspect of the relationship between insolation and the instrumental record of maximum daily temperature — the lag between the two — at 252 stations in the western United States. We chose the lag (in days) that maximizes the cross correlation between these two variables. Three stations were chosen from each climate division in 11 western states, at low, intermediate, and high elevations, and 30 years of record (1961-1990) were examined.

We found geographic patterns in lag that reflect the effects of moisture as follows: (1) lag is largest in maritime settings, (2) lag is slightly larger in mountainous than in basin settings, and (3) lag is smaller in semiarid areas. The percentage variance explained by insolation is largest in the continental interior and smallest in maritime settings. The standard deviation of the residual of temperature from the insolation curve is largest in the Pacific Northwest and smallest in the southwestern deserts.

Inter-annual variations also tend to reflect the influence of moisture entrained by the jet streams. For example, the Pacific Northwest tends to be dry when the Southwest is wet, and vice versa, in concert with the positions and strengths of the polar and subtropical jet streams. This pattern of opposition is strongest during extreme phases of the southern oscillation. Stratifying our analysis by years of El Niño and La Niña, we find that during El Niño years lags are largest in the Southwest and during La Niña years, lags are largest in the Northwest. The difference in lag (computed as lag for an El Niño year minus the lag for a La Niña year) is largest in the Southwest and smallest in the Northwest. This difference ranges from about -20 to +30 days, a change of about 100% of normal.

We conclude that the difference in the lag reflects the shift in storm tracks with changing position and strength of the polar and subtropical jet streams. This lag can become a useful diagnostic tool for characterization of climates related to the two conditions.

In: C.M. Isaacs and V.L. Tharp, Editors. 1996. *Proceedings of the Twelfth Annual Pacific Climate (PACLIM) Workshop, May 2-5, 1995.* Interagency Ecological Program, Technical Report 46. California Department of Water Resources.

Decadal Patterns in Atmospheric Carbon Dioxide as Indicators of Changing Growth and Decay of Terrestrial Vegetation

Charles D. Keeling and Timothy Whorf

Abstract

Large-scale changes in the growth and decay of land plants can be deduced from trends in the concentration of atmospherics CO_2, after removing signals in the recorded data caused by oceanic and industrial disturbances to the concentration. Previously, we reported that atmospheric CO_2, on a global scale, showed a relationship to approximately decadal variations in surface air temperature, where variations in CO_2 concentration were expressed by an anomaly defined as the residual trend after removing the influence of the combustion of fossil fuels. Now, in our longest CO_2 records at Point Barrow, Alaska; Mauna Loa, Hawaii; and the South Pole; we discern patterns in the amplitude of the seasonal cycle of atmospheric CO_2 perhaps also related to changes in air temperature. Periods of warming at approximately decadal intervals since the late 1950s have been accompanied by increases in the amplitude of the seasonal cycle of atmospheric CO_2, a parameter that measures the metabolic activity of land plants on large spatial scales. We shall describe the relationship of changes in seasonal amplitude to decadal changes in CO_2 anomaly and temperature and then estimate what fraction of the CO_2 assimilated anomalously by plants during especially warm periods is sequestered in the terrestrial biosphere beyond the annual cycle. We shall also take note of a longer trend toward higher CO_2 amplitudes that may reflect an average increase in air temperature over the entire period of our CO_2 records.

Offshore Coho Salmon Populations near the Pacific Northwest and Large-Scale Atmospheric Events

David Greenland

Abstract: Catch of coho salmon off the coast of Washington and Oregon since 1925 appears to be related to large-scale events in the atmosphere, which in turn affect ocean currents and coastal upwelling intensities in the northeastern Pacific. At least two time scales of variation can be identified. The first is that of the El Niño/Southern Oscillation phenomenon giving rise to an irregular cycle of between 3 to 7 years. The occurrence of El Niños is associated with warm water anomalies off the coast and often with depressed salmon catches. The second time scale of variation seems to have a periodicity of about 20 years, although this is based on a limited dataset. This variation has been postulated to be related to the manner in which the subarctic ocean current operates; sometimes directing more nutrient-rich water into the Alaskan current, which moves it northward into the Alaskan gyre, while at other times guiding more nutrient-rich water southward into the Californian current off the shores of Washington and Oregon. During the former times, coho salmon catches tend to be low off the Washington and Oregon coasts, and the opposite also seems to hold true. The difference in these modes of the subarctic current may be related to long-term differences in the mode of operation of the atmospheric currents. The atmospheric currents may be quantitatively described by the use of teleconnective indices, which include: the Southern Oscillation Index and the Central North Pacific and Pacific North American. The values of these indices also have some explanatory power, at least in winter, over temperatures and precipitation values in the Pacific Northwest. This paper endeavors to describe how, if real, these atmospheric/oceanic effects are integrated and might affect the salmon catch. The possibility must also be considered that the atmospheric events are symbiotically related to the oceanic events and, further, that both may be enmeshed in even longer-term variability of climate.

Introduction

The story of salmon in the terrestrial-based freshwater aquatic ecosystems of the northwestern North American continent and the marine ecosystems of the north Pacific Ocean is a fascinating and multi-faceted one. Humans suffer from a lack of knowledge of many of the facets of the tale. One aspects that, until recently, has received little attention is the long chain of events that starts at one end with variations in the atmosphere and ends at the other with variability of population sizes of certain kinds of salmon. Climate is one factor that affects salmon population sizes either directly or indirectly in both the freshwater and marine phases.

This paper reviews some aspects of the effect of climate on salmon. These aspects occur on a variety of time scales. It then outlines a statistical

In: C.M. Isaacs and V.L. Tharp, Editors. 1996. *Proceedings of the Twelfth Annual Pacific Climate (PACLIM) Workshop, May 2-5, 1995.* Interagency Ecological Program, Technical Report 46. California Department of Water Resources.

This paper was first published under the title "Salmon Populations and Large Scale Atmospheric Events" in the *Proceedings of the 1994 Northeast Pacific Chinook and Coho Salmon Workshop. Salmon Ecosystem and Restoration: Myth and Reality.* November 7-10, 1994. Eugene, Oregon. American Fisheries Society. Western Division. It is republished here by permission.

relationship that appears to exist on an inter-decadal time scale between the population size of coho salmon as indicated by the catch of these fish off the coast of Washington and Oregon and the air temperature in parts of Oregon. An attempt to explain this relationship requires an examination of the large-scale variability and flow of air currents in the atmosphere of the western part of the Northern Hemisphere and the possibly related variation of ocean currents in the northeastern Pacific Ocean. Suggestions are made for further research that could provide new insight into these longer-term relationships.

Climate/Salmon Interactions in General

A cursory look at the literature reveals several important links between salmon population sizes and climatic variables. These links occur both directly and indirectly and at a variety of time and space scales.

An example of a small time scale link is the small time window of a matter of a few days during which juvenile salmon embark on their journey from the estuary to the sea. Adverse weather conditions, such as severe storms with high onshore winds, during this period could negatively impact survival. Spence and Hall (1994) have shown that the size of this window decreases from low to high latitudes. This fact makes storms and other potentially adverse climatic conditions in the higher latitude estuaries and river mouths particularly critical.

On a monthly time scale, it has been shown that while salmon are young, colder river water temperature slows growth and warmer water accelerates growth (Netboy 1980). However, a temperature increase in rivers generally reduces survival, because it may be associated with an increase in disease and fungal attacks in adults.

On a seasonal and annual time scale, there appear to be many climatic effects on salmon populations. The amount of water in rivers, as controlled by periods of high and low flow, is critical for salmon survival. Sharp (1992) claims that local salmon populations throughout the western continental United States have suffered from drought during 1976 to 1991. The relationship of salmon population size to El Niño conditions, which also occurs on this time scale, is treated more specifically below. Not many studies have been performed concerning the relationship between climate and salmon on decadal and century time scales. On a millennial time scale, there is limited and somewhat tenuous evidence to suggest that the inverse relationship of warmer climate and decreased salmonids, found on the El Niño-type time scale, may persist. Neitzel *et al* (1991) believe that during the Hypsithermal period of the Holocene, salmon were less plentiful in the Pacific Northwest.

One important point, which is often neglected, is that the fossil salmon record extends back to the Eocene (Pearcy 1992, p. 5). The implication of this is that at least some species of salmon have survived just about every conceivable extreme climate and type of climate variability the planet can offer or is likely to offer in the next century.

El Niños and Salmon

El Niño occurrences can impact salmon populations in a number of ways. During El Niños, anomalously warmer water is found off the coast of North America, and coastal upwelling and its associated nutrients are suppressed. There is evidence that the 1957-58 El Niño negatively affected salmon, giving rise, in 1960, to the lowest ocean landings off the continental United States coast since 1917 (Pearcy 1992). In addition, the lingering 1991-92 El Niño negatively affected salmon catch (Finley 1993). It has been established that years just following El Niño events generally tend to be years of low coho catches (Miller and Fluharty 1992).

One of the more spectacular and intense El Niño events was in 1982-83. During this event, salmon in the Pacific Northwest appeared to be stalled in estuaries before leaving for the sea because of the warmer water in the ocean. Salmon in the estuaries were subject to disease and predation, which decreased the populations. In addition, reduced primary productivity off the coast impacted both juvenile and adult coho salmon (Pearcy 1992). During this El Niño event, 58% of the adults predicted to return actually died in the ocean. The same El Niño markedly decreased growth and fecundity of the salmon of the year. Warm ocean temperatures off the Oregon coast shifted the center of distribution of juvenile coho northward to the coast of Washington.

Another feature of El Niños that does not seem to have received much attention is that they are often accompanied in the Pacific Northwest by warm, dry winters (Redmond and Koch 1991; Greenland 1994). Whether the lack of precipitation leads to stream discharge values low enough to affect salmon has not been investigated explicitly.

Interdecadal Relationships between Pacific Northwest Air Temperatures and Coho Salmon Catch off the Coast of Washington and Oregon

When temporally smoothed data are used for 1925 to 1985, there is a close inverse statistical relationship between PNW air temperatures and coho salmon catch off the coast of Washington and Oregon. This relationship was discovered by using the following steps.

Frances and Sibley (1991) had reported a close relationship between winter (November to March) air temperature at Sitka, Alaska, surface

water temperature at Langara Spit, Queen Charlotte Island, British Columbia, and the catch of pink salmon in the Gulf of Alaska. They had also reported an inverse relationship between the catch of pink salmon in the Gulf of Alaska and the catch of coho salmon off the coast of Washington and Oregon. Both relationships covered the period 1925 to 1985 and were found when the data were normalized and subjected to a 7-year weighted filter (Frances, pers. comm. 1994).

Given these relationships, I reasoned that an inverse relationship between air temperature in the Pacific Northwest and the catch of coho salmon catch off the coast of Washington and Oregon would be likely. I used a 5-year unweighted filter of the annual mean air temperatures at the H.J. Andrews Long-Term Ecological Research site, on the western slope of the Cascades in Oregon (44.2°N, 122.2°W). The filter was applied to values of Andrews temperatures, which were normalized to the long-term mean for 1925-1985. It has been shown elsewhere that Andrews temperatures are well related to those of western Oregon in general (Greenland 1994). Coho salmon catch data were extracted from the graphs of Frances and Sibley and a close inverse relationship was found (Figure 1). This relationship and time series suggest about a 20-year cycle in both PNW air temperature and coho salmon catch off the coast of Washington and Oregon. To attempt to explain this inverse relationship, we must explore the large spatial and long temporal aspects of atmospheric and ocean currents, as well as further thinking of Frances and Sibley and their colleagues.

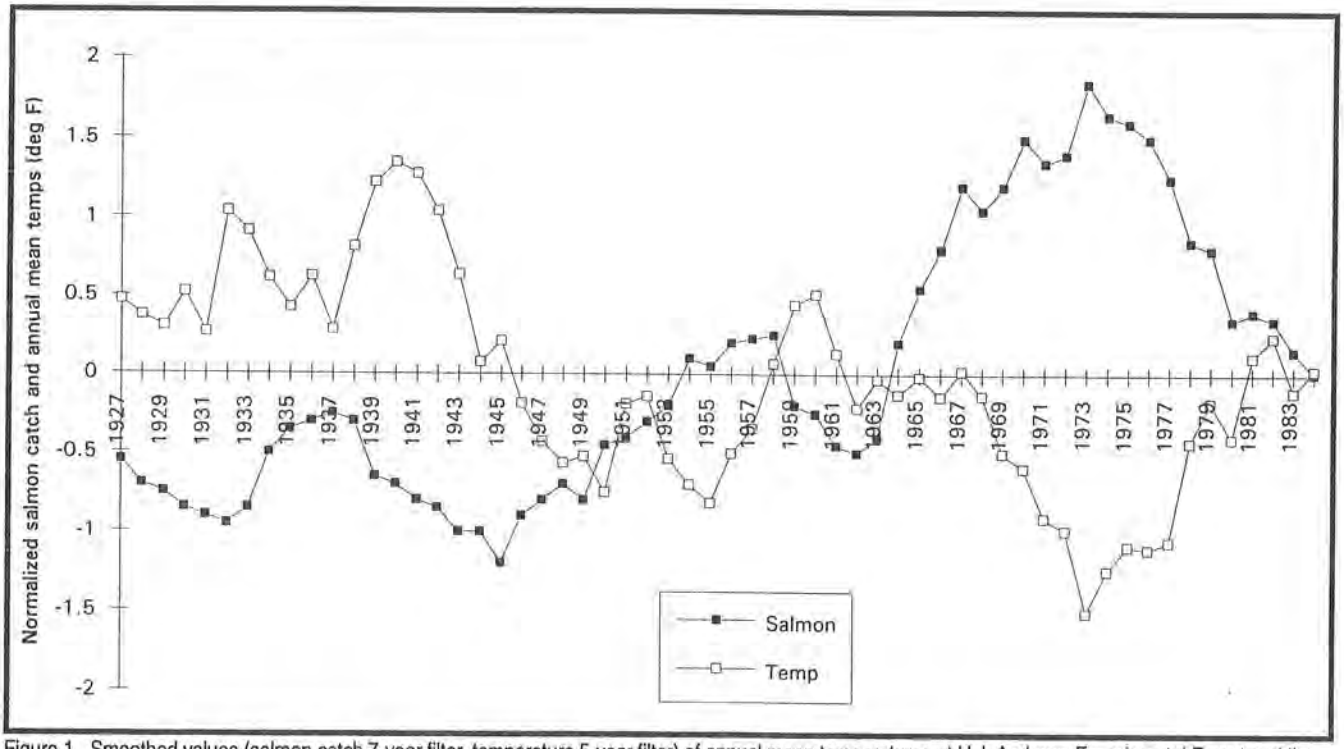

Figure 1. Smoothed values (salmon catch 7-year filter, temperature 5-year filter) of annual mean temperatures at H.J. Andrews Experimental Forest and the catch of coho salmon off the coast of Washington and Oregon, 1927-1983.

Large Spatial and Long Temporal Aspects of Atmospheric and Ocean Currents

It is well known that the currents of the atmosphere and ocean are related. Airflow over the surface of the ocean is one of the major driving forces of the ocean currents. Ocean flow in the eastern North Pacific is dominated by the Subarctic current and West Wind Drift, to its south, which together transport water eastward approximately between latitudes 40° and 50°N. This flow is driven by the westerly atmospheric flow at these latitudes. Toward the east of the ocean, the flow of these currents bifurcates. Part of it flows northward, as the Alaskan current, along the coast of British Columbia, and then westward along the southern coast of Alaska to form the Alaskan Gyre. Another part flows southward, forming the California current, part of which flows eastward, under the influence of the Trade Winds when it reaches about 20°N. The West Wind Drift, California current, and return westward flow of the North Equatorial current form part of the Central Pacific Gyre.

In two parts of these flows, nutrient-rich water can be brought from lower levels of the ocean by upwelling. Along the coast of the conterminous United States, this is achieved by application of the Coriolis force to coastal airflow (with a northerly component in summer) and coastal ocean current flow. The Coriolis force tends to deflect objects to the right of their path of motion in the Northern Hemisphere. This leads to offshore and divergent surface ocean flow which, in turn, draws the nutrient-rich water up from below. There is also upwelling on the northern side of the Subarctic current in the southern part of the Alaskan gyre. This upwelling is due to a process called Ekman pumping, which is caused by the change of flow direction of the faster velocity water near the surface compared to the slower velocity water at increasing depths in the ocean.

Winds in the atmosphere above the ocean are responsible for both the velocity of the ocean currents and their precise location from year to year and from decade to decade. They may also be responsible for the precise location of the bifurcation of the Subarctic current and the way in which quantities of nutrient-rich water are partitioned into the Alaskan and California currents.

The atmospheric currents of importance here are the winter flow of the mid-latitude westerly winds and, to a lesser extent, the flow of the easterly Trade Winds. At the surface of the Earth, the westerlies in winter are manifested by geostrophic air flow at the southern part of the Aleutian Low pressure system. In the upper air, at about 18,000-20,000 feet above the Earth's surface, the flow takes the form of long waves (parallel to the Earth's surface). The position and strength of the air flow in the waves is variable but on the average is characterized by a ridge of high pressure over the eastern Pacific sandwiched between a trough of low pressure in

the western Pacific, off the coast of Asia, and another trough over eastern North America and the western Atlantic Ocean (Barry and Chorley 1987, p. 136). The actual position and strength of the Aleutian Low and the position, degree of sinuosity (or amplitude of the waves), and strength of the flow in the upper air westerlies from year to year and from decade to decade is critical to controlling the flow and location of the ocean currents.

Climatologists have developed some simple indices to collapse a large amount of this atmospheric flow into a few numbers. The indices are sometimes called "teleconnective indices" since they help explain how pressure variations in one part of the hemisphere are related (teleconnected) to those in another part. The indices of use in this discussion are the Central North Pacific index (CNP), the Pacific North American index (PNA) and the Southern Oscillation Index (SOI). It should also be remembered that the strength of the teleconnective patterns is not necessarily stable over time.

The SOI is commonly used to measure the strength of the El Niño and the opposite La Niña phenomena. The SOI is measured as the mean sea level pressure difference between Tahiti and Darwin, Australia. Due partly to difficulty in terminology, it is becoming increasingly common to refer to "warm events" (which include El Niño) and "cold events" (which include La Niña). In the newer terminology "warm" and "cold" refer to the SSTs of the central Pacific Ocean.

Wallace and Gutzler (1981) were the first to introduce the PNA index. They characterized a strong winter PNA pattern as one associated with higher-than-normal temperature in the Pacific Northwest, resulting from a strong ridge of high pressure in the 700-millibar height field extending from the Pacific Northwest to Canada and Alaska. Wallace and Gutzler use a PNA index comprised of the pressure at four points on the latitude-longitude grid. The PNA index designed by Leathers *et al* (1991) and Leathers and Palecki (1992) following Yarnal and Diaz (1986) is the one used in this study. It uses a linear combination of standardized 700-mb geopotential height anomalies (Z*) at the grid points nearest the anomaly field centers. It is constructed as follows:

$$PNA = 1/3\{-Z^*(47.9°N,170.0°W)+ Z^*(49.0°N,111.0°W) -Z^*(29.7°N,86.3°W)\}$$

The PNA index describes the amplitude of the 700-mb flow pattern over the United States, which has a basic pattern of troughs of low pressure in the eastern Pacific and the eastern United States and a ridge of high pressure over the Rocky Mountain cordillera (see Leathers *et al* 1991, Figure 1). The meridional extreme of the pattern produces positive PNA values (and potentially more southwest winds over the Pacific Northwest), while the zonal extreme produces negative PNA values (and potentially

more west winds over the Pacific Northwest). Yarnal and Diaz (1986) demonstrated how strongly positive PNA and negative (reverse) PNA patterns are associated, respectively, with warm and cold El Niño/Southern Oscillation events and, in turn, with precipitation and temperature anomalies on the west coast of North America.

Cayan and Peterson (1989) designed the CNP index as being the mean sea level pressure over the region 35-55°N and 170°E-150°W. They show that streamflow in the west has correlations in the range 0.3-0.6 SLP with anomalies in the North Pacific. During times of a weak CNP, streamflows are high in Washington and Oregon. During times of a strong CNP, the polar front jet stream flows north of the Pacific Northwest, and below-average streamflow is observed. This is also often seen during El Niño events (see Cayan and Peterson 1989, Figure 9).

Interrelationships between the values of the SOI, PNA, and CNP indices have also been shown (Cayan and Peterson 1989). Significant correlations appear between the SOI and PNA during winter and spring; the SOI and CNP during winter; and the PNA and CNP during winter, spring, and fall. All of the synoptic studies indicate quite clearly the linkages between SSTs and particular pressure and teleconnective patterns in the Pacific Ocean and various aspects of climate on the West Coast and in the Pacific Northwest.

The HWFS Model and its Relationship to Atmospheric Flow

To explain the relationships between catches of Alaskan pink salmon and northern sea and air temperatures and the inverse relationship between catches of Gulf of Alaskan pink salmon and Washington/Oregon coho salmon, Frances and Sibley (1991) and Frances (1993) use a model suggested by Hollowed and Wooster (1991). For convenience, I call this the HWFS model, after the initials of all four investigators. According to this model, the inverse relationship in catch in the two ocean areas might be explained by the north or south movement of the divergence, or bifurcation, zone between the Alaskan and California current and the greater or lesser effect of the currents related to that north-south movement. The model is bimodal and postulates two states or modes of operation of the ocean currents. When the bifurcation zone is more to the north (HWFS Type A-West Coast), more cold, Subarctic current water is taken into the California current, and upwelling of nutrient-rich water off the Oregon and Washington coasts is enhanced. When the bifurcation zone is farther south (HWFS Type B-Alaska), more cold, Subarctic current water is taken into the Alaskan current, and water off the Oregon and Washington coasts is warmer.

Synthesis of Teleconnective Indices with the HWFS Model

The HWFS model may be placed in a larger atmospheric context by noting its relationship to the teleconnective index values discussed earlier (Figure 2). HWFS Type A-West Coast flow is associated with a high CNP value. This describes a weak Aleutian Low pressure, with winds coming more directly from the west across the Pacific at the latitudes of Washington and Oregon. This is consistent with a negative value of the PNA. The more northerly bifurcation of the Subarctic current pushes more water into the California current and gives rise to negative sea surface temperature anomalies. These conditions are not generally consistent with intense El Niño conditions. HWFS Type B-Alaska flow is associated with a low CNP value. This describes a strong Aleutian low pressure and enhanced southwesterly winds in the northeast Pacific. It is associated with meridional upper air flow and a positive PNA value. The more southerly Subarctic current bifurcation enhances northward ocean flow into the Alaskan current, giving rise to positive SST anomalies in the eastern part of the northeast Pacific. These conditions are consistent with results of El Niño events.

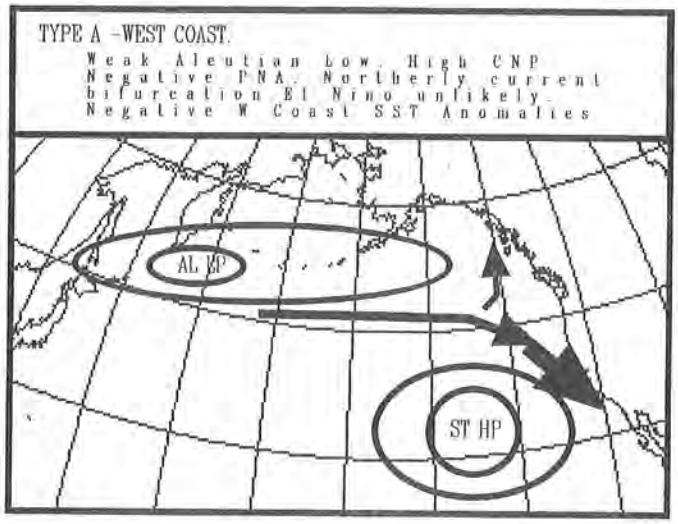

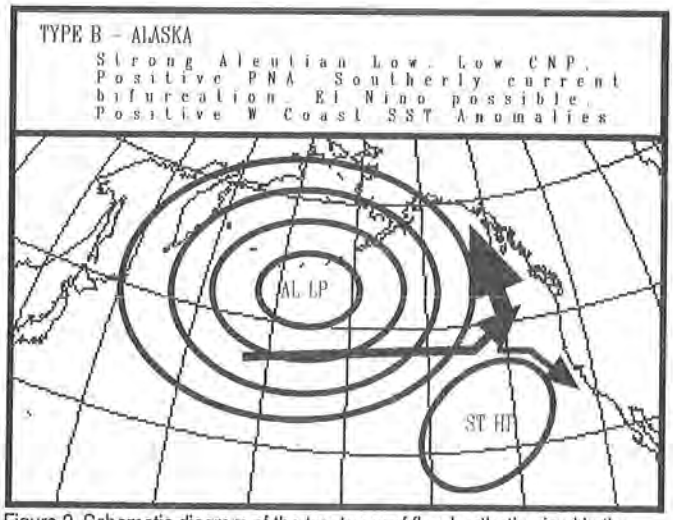

Figure 2. Schematic diagram of the two types of flow hypthothesized in the HWFS model and its associated atmospheric and oceanic events. Thick black lines schematically represent isobars of surface atmospheric pressure. Shaded arrows schematically represent the flow of the subarctic current and its partitioning into either the Alaskan current or the California current.

Hollowed and Wooster (1991) and Frances (1993) have suggested that El Niños are related to the change of state between Type A and Type B flow. They suggest that over the last 60 years, the switch from Type A mode to Type B mode has always occurred at the time of significant El Niño events (*eg*, 1925/26, 1940/41). This relationship, if true, is worthy of further investigation.

Further Research and Concluding Comments

There is a large amount of research to be completed before the ideas discussed here can be finalized and confirmed by observational data. Some of the more important research tasks include:

- Examine individual El Niños and salmon catch off Washington and Oregon with respect to the entire available salmon catch record and the intensity values of individual El Niños.
- Examine in more detail the exact biophysical processes leading to the decrease of salmon population size during El Niño years.
- Further identify the variability of the bifurcation of ocean water flow from the central north Pacific into the Alaskan and California currents. Possible tools for doing this include: an examination of ocean temperature, salinity, and other flow-identifying data from ocean weather ship P; and use of remote sensing imagery.
- Recalculate the PNW air temperature/coho salmon catch using the more representative climate divisional air temperature records of the National Weather Service and a temporally coherent salmon catch data series updated into the mid-1990s.
- Extended these analyses to look for relationships between salmon catch and the teleconnective indices. Jamir *et al* (1994) have started work on this.
- Test the hypothesis that intense El Niño conditions occur more often under HWFS Type B mode than under Type A mode.
- Study the flip-over between the HWFS Type A to Type B mode and vice versa. In particular, investigate the role, if any, of El Niño events in this and the relationship of the mode change to known major step functions in atmospheric flow, such as occurred in 1976 (Trenberth 1990).

If the HWFS model is confirmed, we need to ask:

- How is it effected by long-term climate change at scales longer than the interdecadal scale?
- What feedbacks are there from the ocean to the atmosphere and vice versa, and how do they operate?

With respect to the second question, Namias has pointed out, in a whole series of papers (*eg*, Namias 1969), the importance of the two-way interaction between the Pacific Ocean and the atmosphere above it. This needs to be taken into account in a more time-specific framework with respect to the HWFS model.

If the results of these and other investigations confirm the existence of interdecadal cycles related to the atmospheric and ocean current operation, such confirmation will have important management implications for the salmon resource. Not the least, it will be important to cast any management plans within a framework of interdecadal natural variability, which may also have some predictability. Possibly more important is

to further examine the historical and paleo record to further establish the strength of the variability and possibility of forecasting it in the future.

Acknowledgment

Preparation of this paper was supported in part by Cooperative Agreement PNW 92-0221 from the Pacific Northwest Research Station of the U.S. Forest Service and Long-Term Ecological Research Grant BSR-9011663 from the National Science Foundation.

I am grateful to Robert Frances of the School of Fisheries at the University of Washington for sharing some of his original data and unpublished notes on the HWFS model.

References

Barry, R.G., and R.J. Chorley. 1987. *Atmosphere, Weather, and Climate.* 5th Ed. Routledge, London. 460 pp.

Cayan, D.R., and D.H. Peterson. 1989. The influence of North Pacific Circulation on streamflow in the west. Pages 375-397 in *Aspects of Climate Variability in the Pacific and Western Americas.* Ed. D.H. Peterson. American Geophysical Union. 445 pp.

Francis, R.C. 1993. Climate change and salmonid production in the North Pacific Ocean. Pages 33-42 in *Proceedings of the Ninth Annual Pacific Climate (PACLIM) Workshop.* California Department of Water Resources.

Francis, R.C., and T.H. Sibley. 1991. Climate change and fisheries: What are the real issues? *The Northwest Environmental Journal.* 7:295-307.

Finley, C. 1993. Low coho return may halt '94 ocean season. *The Oregonian* Nov. 18.

Greenland, D. 1994. The Pacific Northwest regional context of the climate of the H.J. Andrews Experimental Forest Long-Term Ecological Research Site. *Northwest Science.* 69(2)81-96

Hollowed, A.B., and W.S. Wooster. 1991. Year class variability of marine fishes and winter ocean conditions in the northeast Pacific Ocean. *ICES Variability Symposium.* Paper No. 33. Session 3.

Jamir, T.V., A. Huyer, W. Pearcy, J. Fisher. 1994. The influence of environmental factors on marine survival of Oregon hatchery coho. Pages 115-138 in *Salmon Ecosystem Restoration: Myth and Reality.* Proceedings of the 1994 Northeast Pacific Chinook and Coho Salmon Workshop. Eugene, Oregon, November 7-10, 1994. (Mary Louise Keef, Ed.). Oregon Chapter, American Fisheries Society, P.O. Box 722, Corvallis, OR 97339.

Leathers, D.J., B. Yarnal, M.A. Palecki. 1991. The Pacific/North American teleconnection pattern and United States climate. Part I: Regional temperature and precipitation associations. *Journal of Climate.* 4(5):517-528.

Leathers, D.J., and M.A. Palecki. 1992. The Pacific/North American teleconnection pattern and the United States climate. Part II: Temporal characteristics and index specification. *Journal of Climate.* 5:707-716.

Miller, K.A., and D.L. Fluharty. 1992. El Niño and variability in the northeastern Pacific salmon industry: implications for coping with climate change. Pages 49-88 in M.H. Glantz. (Ed.). *Climate Variability, Climate Change and Fisheries.* Cambridge University Press. New York. 450 pp.

Namias, J.1969. Seasonal interactions between the North Pacific Ocean and the atmosphere during the 1960s. Monthly Weather Review. 97(3):173-192.

Netboy, A. 1980. The Columbia River Salmon and Steelhead Trout: Their Fight for Survival. University of Washington Press. Seattle. WA.

Neitzel, D.A., M.J. Scott, S.A. Shankle, J.C. Chatters. 1991. The effect of climatic change on stream environments: The salmonid resource of the Columbia River basin. The Northwest Environmental Journal. 7:271-293.

Pearcy, W.G. 1992. Ocean Ecology of North Pacific Salmonids. University of Washington Press, Seattle. WA. 179 pp.

Redmond, K.T., and R.W. Koch. 1991. Surface climate and streamflow variability in the western United States and their relationship to large scale circulation indices. Water Resources Research. 27:2381-2399.

Sharp, G. 1992. Fishery catch records, El Niño / Southern Oscillation, and longer term climate change as inferred from fish remains in marine sediments. Pages 379-417 in H.F. Diaz and V. Markgraf (Eds.). El Niño: Historical and Paleoclimatic Aspects of the Southern Oscillation. Cambridge University Press. Cambridge. 476 pp.

Spence, B.C., and J.D. Hall. 1994. Analysis of spatio-temporal variation in the migration timing of coho salmon (Oncorhynchus kisutch) smolts and implications of climate change. Abstract. Oregon Chapter. American Fisheries Society. 30th Annual Meeting. Sunriver, OR. 16-18 February. p.19.

Trenberth, K.E. 1990. Recent observed interdecadal climate changes in the northern hemisphere. Bulletin of the American Meteorological Society. 71(7):988-993.

Wallace, J.M., and D.S. Gutzler. 1981. Teleconnections in the geopotential height field during the Northern Hemisphere winter. Monthly Weather Review. 109:784-812.

Yarnal, B., and H.F. Diaz. 1986. Relationships between extremes of the Southern Oscillation and the winter climate of the Anglo-American Pacific Coast. Journal of Climatology. 6:197-219.

Decadal Variation in the Trans-Pacific Migration of Northern Bluefin Tuna (*Thunnus thynnus*) Coherent with Climate-Induced Change in Prey Abundance

Jeffrey Polovina

Abstract

Bluefin tuna (*Thunnus thynnus*) are highly prized by both recreational and commercial fishermen. In the Pacific, northern bluefin tuna spawn only in the western Pacific, with a portion of the juveniles migrating to the eastern Pacific. Indices of the relative abundance of bluefin tuna in the western and eastern Pacific show decadal variation in the proportion of bluefin making trans-Pacific migrations out of the western Pacific. Periods of reduced bluefin migration to the eastern Pacific occur when a key prey of bluefin, Japanese sardine (*Sardinops melanosticta*), are abundant in the western Pacific and distributed offshore. Bluefin migration increases when sardines are relatively scarce and contracted to coastal waters.

In: C.M. Isaacs and V.L. Tharp, Editors. 1996. *Proceedings of the Twelfth Annual Pacific Climate (PACLIM) Workshop, May 2-5, 1995.* Interagency Ecological Program, Technical Report 46. California Department of Water Resources.

Chronic and Catastrophic Influences of the Environment on the Population Dynamics of the Common Fishes

Paul E. Smith

Abstract

Seasonal, interannual, decadal and centennial influences on population dynamics have been described for several species. It now seems possible to interpret environmental changes that initiate population change in terms of the chronic changes due to temperature, for example. Catastrophic changes, rapid transport of large surface volumes, for example, that cause massive expatriation of species are difficult to accommodate in typical fisheries models. It is also recognized that predictive approaches will require precise information at low time resolution for chronic changes and crude information at high time resolution to detect catastrophic events.

In: C.M. Isaacs and V.L. Tharp, Editors. 1996. *Proceedings of the Twelfth Annual Pacific Climate (PACLIM) Workshop, May 2-5, 1995.* Interagency Ecological Program, Technical Report 46. California Department of Water Resources.

A 10-Year Time Series of Zooplankton Anomalies off the British Columbia Coast

David L. Mackas

Abstract

Zooplankton biomass and species composition have been sampled since 1985 at a set of standard locations off Vancouver Island. From these data, I have estimated multi-year average seasonal cycles and time series of anomalies from these averages. Amplitude and timing of the seasonal cycle differ between shelf and offshore locations. Minimum biomass is in winter (about 1-2 g/m^{-2} dry weight) and in all sub-regions. Maximum is in late spring on the continental shelf (7-8 g/m^{-2}) and in mid- to late summer seaward of the shelf-break (6-7 g/m^{-2}). The summer-autumn decline of herbivorous copepod biomass on the inner and middle parts of the shelf occurs during a period of sustained high food supply (3-8.5 mg/m^{-3} chl *a*) and is evidence for rapid advective export of surface-layer zooplankton from the continental shelf during the summer upwelling season. Most of the dominant taxa show interannual anomalies that are both statistically and ecologically significant. The zooplankton anomalies last rather a long time (0.3-5 years, depending on taxonomic group) and are larger along and seaward of the continental shelf break than on the continental shelf. They also occur throughout the span of the time series (not notably stronger in El Niño years). Both time scale and phasing of the anomalies suggest coupling to a longer-term change in North Pacific atmosphere/ocean conditions starting about 1988.

In: C.M. Isaacs and V.L. Tharp, Editors. 1996. *Proceedings of the Twelfth Annual Pacific Climate (PACLIM) Workshop, May 2-5, 1995.* Interagency Ecological Program, Technical Report 46. California Department of Water Resources.

Physical, Chemical, and Biological Characterization of Water Year Types in the San Francisco Bay Estuary

Peggy W. Lehman

Abstract

Twenty-three years of physical, chemical, and biological data were used to characterize conditions associated with wet, normal, dry, and critical water year types in the upper San Francisco Bay estuary. Data were collected monthly from October 1970 to September 1993 at 26 stations throughout the upper estuary. Eighteen physical and chemical variables were used to characterize environmental conditions. The biological community was described using phytoplankton chlorophyll *a* concentration and community composition. Environmental variables varied by a maximum of 124% about the long-term mean among water year types and was higher for streamflow (124%) than nutrient concentrations (33%) and water temperature (6%). Higher variation about the long-term mean was associated with phytoplankton chlorophyll *a* concentration and community composition, which varied by 150-175%. Differences among water year types were not consistently related to streamflow, but the greatest difference between water year types usually occurred for wet and critical years. Evaluation of water year data enabled an interdecadal view of the environmental and biological variability in the upper San Francisco Bay estuary.

In: C.M. Isaacs and V.L. Tharp, Editors. 1996. *Proceedings of the Twelfth Annual Pacific Climate (PACLIM) Workshop, May 2-5, 1995.* Interagency Ecological Program, Technical Report 46. California Department of Water Resources.

Climate-Related Long-Term Faunal Changes in a California Rocky Intertidal Community

James P. Barry, Charles H. Baxter, Sarah E. Gilman

Abstract

The effects of gradual climate change (*ie*, multi-decadal) on biological communities are not well understood for most natural systems, owing principally to the lack of quantitative observations in early studies. Although coastal communities respond rapidly to environmental perturbations, the protracted effects of climate change should be evident as concomitant shifts by species with similar environmental requirements. During periods of warming, species' ranges should migrate poleward. We resurveyed invertebrate species on an intertidal transect in central California, first established and surveyed in 1931, to assess shifts in community structure. Changes in the invertebrate fauna along the transect between 1931-1933 and 1993-1994 indicate that species' ranges shifted northward, consistent with predictions of change associated with climate warming. Of 45 invertebrate species, abundances of eight of nine southern species increased, and five of eight northern species decreased. No trend was evident for cosmopolitan species. Annual mean shoreline ocean temperatures at the site increased by 0.75°C during the past 60 years, and mean summer maximum temperatures from 1983-1993 were 2.2°C warmer than during 1921-1931.

In: C.M. Isaacs and V.L. Tharp, Editors. 1996. *Proceedings of the Twelfth Annual Pacific Climate (PACLIM) Workshop, May 2-5, 1995.* Interagency Ecological Program, Technical Report 46. California Department of Water Resources.

California Water Conditions in 1995

Maurice Roos

From 1987 through 1992, California endured 6 consecutive years of drought for the second time this century. The drought was broken in most parts of the state by a wet year in 1993, in which runoff was 125 percent of average. But 1994 was again critically dry, with runoff only 40 percent of average statewide, raising fears that the drought had resumed. The "drought watch" of 1994 was finally washed out to sea by two large floods (January and March), which made 1995 one of the wettest years this century and refilled all but a couple of California's major reservoirs. This paper provides information on water conditions and flooding in 1995 and some comparisons with previous years. Figure 1 is a location map.

Water Supply

Water year 1995 began without any real surprises, except that November (which was a good precipitation month, about 130 percent of average) was relatively cold with much snow in the mountains. By the end of December, estimated statewide seasonal precipitation (since October 1, the beginning of the water year) was around 90 percent of average and northern Sierra precipitation was about 95 percent of average. Then came a record January. Three months this year had triple normal precipitation: January, March, and June. June doesn't matter much for water year totals, because its average precipitation is less than 2 percent of the annual total. But January and March are wet months and the excess rainfall produced substantial flooding. Sandwiched between was a dry February with about 35 percent of average precipitation in the northern Sierra (Figure 2). Table 1 gives statistics for 1995 and the three previous water years.

Sacramento River unimpaired runoff was 33.9 million acre-feet for water year 1995, based on preliminary data. This is the second wettest in a record beginning in 1906; the record was set in 1983, when runoff was 37.7 MAF. The next two highest years were 1907 (33.7 MAF) and 1982 (33.3 MAF).

The four major rivers of the San Joaquin River region (Stanislaus, Tuolumne, Merced, and San Joaquin above Friant Dam) had an estimated 12.4 million acre-feet of runoff, making 1995 the third wettest year of record, exceeded by 1983 (15 MAF) and 1906 (12.43 MAF). Runner-up wet years were 1969 (12.3 MAF), 1907 (11.8), and 1982 (11.4 MAF).

In: C.M. Isaacs and V.L. Tharp, Editors. 1996. *Proceedings of the Twelfth Annual Pacific Climate (PACLIM) Workshop, May 2-5, 1995.* Interagency Ecological Program, Technical Report 46. California Department of Water Resources.

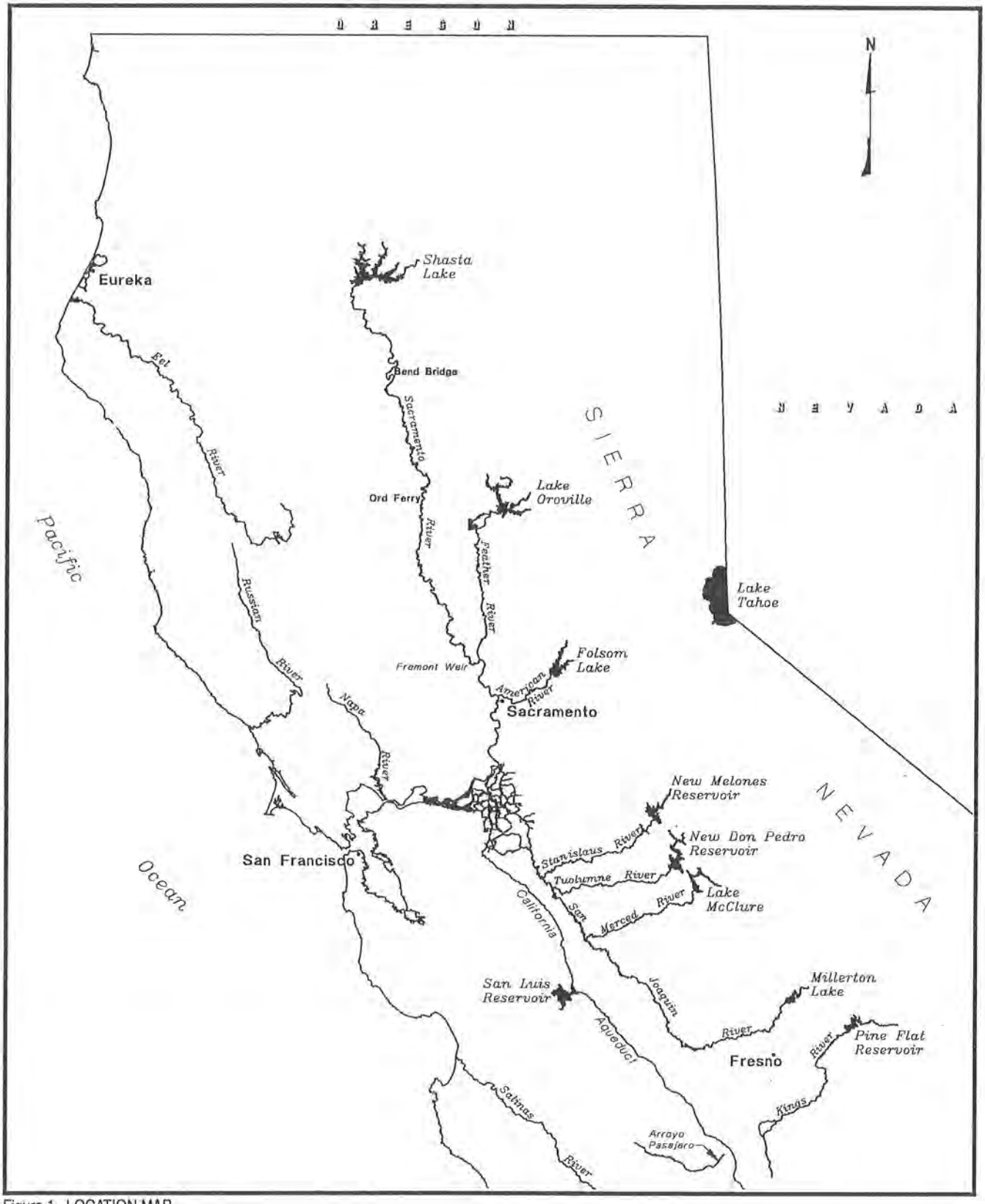

Figure 1 LOCATION MAP

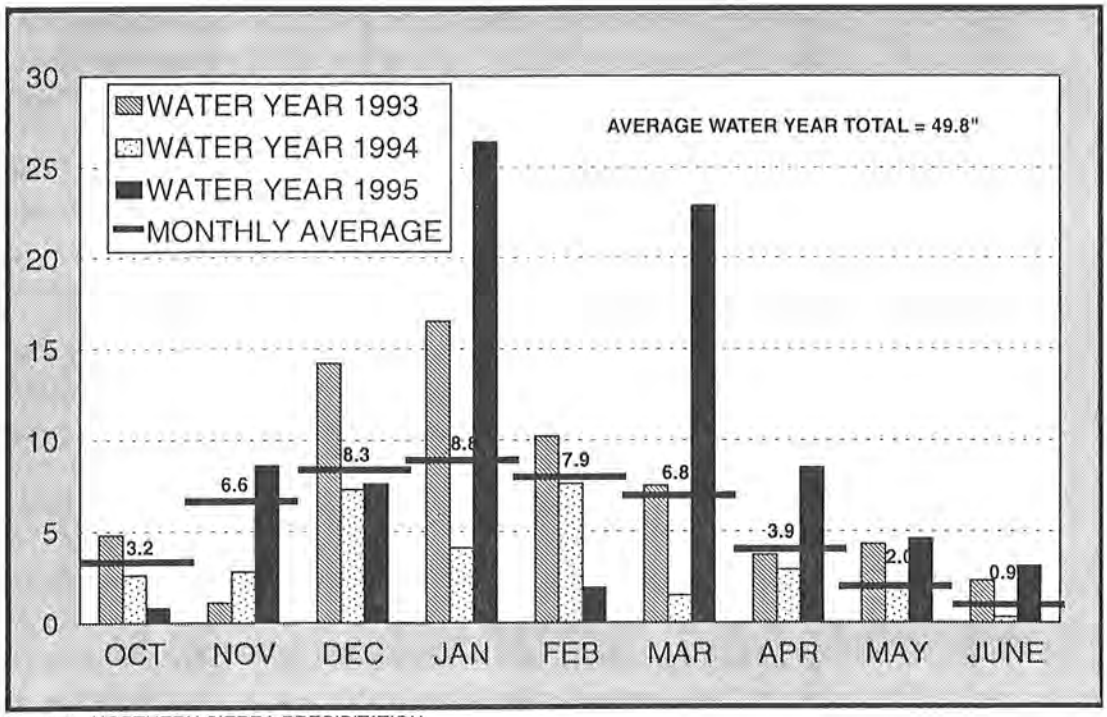

Figure 2 NORTHERN SIERRA PRECIPITATION
Eight-Station Average, in Inches

Table 1
WATER YEAR COMPARISONS

Percent of Average (unless noted)

	1995	1994	1993	1992
Statewide Statistics				
Precipitation	165	65	140	85
April 1 Snowpack	175	50	150	60
Runoff	180	40	125	45
Reservoir Storage, September 30	130	73	111	58
Reservoir Storage (MAF)	(28.1)	(15.9)	(24.0)	(12.7)
Regional Statistics				
Northern Sierra Precipitation	171	64	131	72
(8-Station Index, inches)	(85.4)	(31.8)	(65.1)	(36.0)
Sacramento River				
Unimpaired Runoff	184	42	120	48
Unimpaired Runoff (MAF)	(33.9)	(7.8)	(22.2)	(8.9)
San Joaquin River				
Unimpaired Runoff	214	44	144	45
Unimpaired Runoff (MAF)	(12.4)	(2.5)	(8.3)	(2.6)

Northern Sierra precipitation is second wettest since the record began in 1922.
Sacramento River unimpaired runoff is second wettest since the record began in 1906. WY 1983 was wetter and WY 1907 was just slightly less than 1995.
San Joaquin River unimpaired runoff is third wettest since the record began in 1906. WY 1983 was much wetter and 1906 was slightly wetter.

Snowmelt season runoff during April through July was also heavy in 1995. Preliminary figures show about 13.4 million acre-feet, 201 percent of average in the Sacramento River system and 8.0 MAF, 213 percent of average on the San Joaquin River. Three years exceeded this year's San Joaquin region volume of snowmelt: 1906 (9.2 MAF), 1969 (9.1 MAF), and 1983 (8.7 MAF). The same was true on the Sacramento River, with the three larger snowmelt years being 1907 (13.45 MAF, nearly the same), 1952 (nearly 13.7 MAF), and 1983 (also about 13.7 MAF).

In the 1987 PACLIM workshop, a trend of decreasing snowmelt runoff in Northern California was first brought to this group's attention (Roos 1987). That work was refined in a Western Snow Conference paper (Roos 1991) for the Sacramento River Index and for the combined two high elevation Kings and San Joaquin rivers in the southern Sierra. When snowmelt runoff (April-July) is expressed as a percentage of water year runoff, there was a decreasing trend of -0.13 percent per year on the Sacramento River system and -0.09 on the San Joaquin plus Kings rivers over the 1906-1990 period. Extrapolating the trend in the 1991 paper to 1995 would yield about 33 percent for Sacramento River unimpaired runoff and about 68 percent on the two southern Sierra rivers. The 1906-1990 average was 38 percent on the Sacramento and 72 percent on the San Joaquin plus Kings.

In view of the tremendous snowmelt runoff in 1995, one would assume the ratio to total water year runoff would be up. For the Sacramento River, the ratio of April-July runoff to water year runoff was 13.4/33.9 = 40 percent. This ratio is better than the 35 percent in 1994 and the same as in 1993, but it is not much more than the average of 38 percent for 1906-1990.

For the sum of the San Joaquin and Kings rivers, also reported on in the previous reference, preliminary 1995 April-July runoff was 5.0 million acre-feet, 69 percent of the water year total of 7.3 MAF. That is less than the 74 percent in both 1993 and 1994, but it is not far out of line from the mild decline noted in the 1991 paper. One can expect ups and downs from year to year in the percentage of water year runoff being discharged in April through July. This year's fraction, although above the trend line, is not as high as percentages of many past years. So it remains to be seen whether the trend toward a decreasing fraction of snowmelt runoff is changing.

The 1995 Floods

It seems that about twice a decade, some region of California gets hit with a major flood. In 1995, it was somewhat unusual that we had two periods of substantial flooding that embraced most of the state at one time or another.

In the January 1995 storms, the Coast Ranges north of San Francisco and the upper Sacramento Valley were hit particularly hard. On the

Russian River, in 3 days stages jumped from relatively low levels to nearly as high as the record-breaking February 1986 flood. On the Napa and Eel rivers, water levels were not quite as high as in 1986 but were well over flood stage.

The upper Sacramento River flood in January was generated from uncontrolled side-stream inflow from the area below Shasta Dam. Inflow to Shasta Lake exceeded 100,000 cubic feet per second twice during the week of storms but was almost completely stored. Flood levels in the upper Sacramento Valley exceeded 1986 at some stations but were less than the larger March 1983 flood. Farther downstream, peak levels were much less than the record levels of February 1986 — by about 4 feet at Fremont Weir and at Sacramento. Runoff from major Sierra rivers was not that unusual and mostly stored at the reservoirs. Peak inflow was about 68,000 cubic feet per second at Folsom Lake on the American River and nearly 120,000 cfs at Lake Oroville on the Feather River. Releases from the Oroville complex to the Feather River were only 5,000 cfs later in January, compared to 150,000 cfs in 1986.

As the January series of storms began, major reservoir storage in Northern California was quite low, because 1994 had been extremely dry. Much of the large flood runoff volume was stored in the reservoirs. Statewide storage increased nearly 8 million acre-feet during January, from 75 percent to 104 percent of average. February was quite dry, with a much slower storage increase, but by the time the March series of storms began, many reservoirs were approaching allowable flood limits. Thus, once heavy runoff began, major releases had to be made from the reservoirs, adding to the volume of downstream flow in the floodway system. During the March flood, releases from Oroville and Folsom dams were boosted to around half the rated capacity of downstream channels; later in the storm, releases from Shasta Dam reached the rated Sacramento River channel capacity of 79,000 cubic feet per second for a short time. Oroville releases peaked at 87,000 cfs and Folsom releases reached 50,000 cfs. Because of less side-flow from other uncontrolled tributaries, peak March flows in the upper Sacramento Valley were a little less than in January. In the lower system at Fremont Weir, near Sacramento, stages were about 1 foot higher than in January due to more tributary reservoir releases but were still within design capacities. To help control Sacramento River levels in the Sacramento metropolitan area, 22 of the 48 gates in the Sacramento Weir were opened.

The March floods produced a new record peak on the Salinas River and, based on flood marks, exceeded the 1986 peak on the Napa River by nearly 2 feet. They also produced high water above warning stage on the lower San Joaquin River. Arroyo Pasajero flows, which collapsed the Interstate 5 bridge crossing near Coalinga, probably were close to a 100-year event.

Storms at the end of April produced another strong Sacramento River rise and renewed weir overflow into the bypasses in early May. Oroville releases went up to 60,000 cfs. Overflow depths at Fremont Weir reached 2.5 feet on May 4, considerably more than the 1 foot of overflow in May 1983, the last time the weir overflowed into Yolo Bypass in May.

In conclusion, the 1995 winter storms were unique with respect to the breadth of unusually heavy precipitation statewide. The major flood control works of the Sacramento and San Joaquin Valley handled all the rain and runoff quite well. The main problems occurred on the smaller streams and on unregulated or partially regulated rivers, especially in the North Bay and Central Coast regions. Intense local convective storms within the broader wet circulation did overload small streams and storm drainage facilities and produced some rare recurrence statistics.

I do wish to add something on the American River operation, which produced much anxiety but no real threat. Peak inflow to Folsom Lake was estimated to be 68,000 cfs in the January storm period, 74,000 cfs in March, and about 52,000 cfs in early May. Corresponding peak releases at Nimbus Dam were about 30,000, 50,000 and 22,500 cfs. The peak daily inflows were 51,000, 55,000, and 38,000 cfs. The peak 3- and 5-day rates were in March, with about 44,000 and 36,000 cfs average inflow. These rates are about the 5-year exceedence level; in other words, to be expected in about 20 percent of the years.

Comparing the peak 5-day 1995 volume of 0.4 million acre-feet to the 100-year flood volume of nearly 1.5 MAF is sobering (Figure 3). The 100-year volumes are those derived in the Corps of Engineers' current American River flood control studies (USCE 1987, 1991). The February 1986 flood was computed to have a 5-day unimpaired volume of 1.27 MAF. Actual peak 5-day inflow to Folsom in 1986 was 1.1 MAF. We should not get a false sense of security from how well the major floodflows on the American River were handled in 1995.

Figure 4 compares peak 1995 flood stages with other floods. The 1995 data are preliminary, mostly based on real-time radio telemetry. Final stages based on recorded data may be slightly different.

San Joaquin River Snowmelt Flood

It is probably only every 10 years on average that there is a serious snowmelt flood problem in the San Joaquin River and the southern Sierra. This year was big and snowmelt was delayed. Normally, about three-quarters of the April-July runoff has occurred by mid-June; this year only 57 percent of the volume had melted at that time.

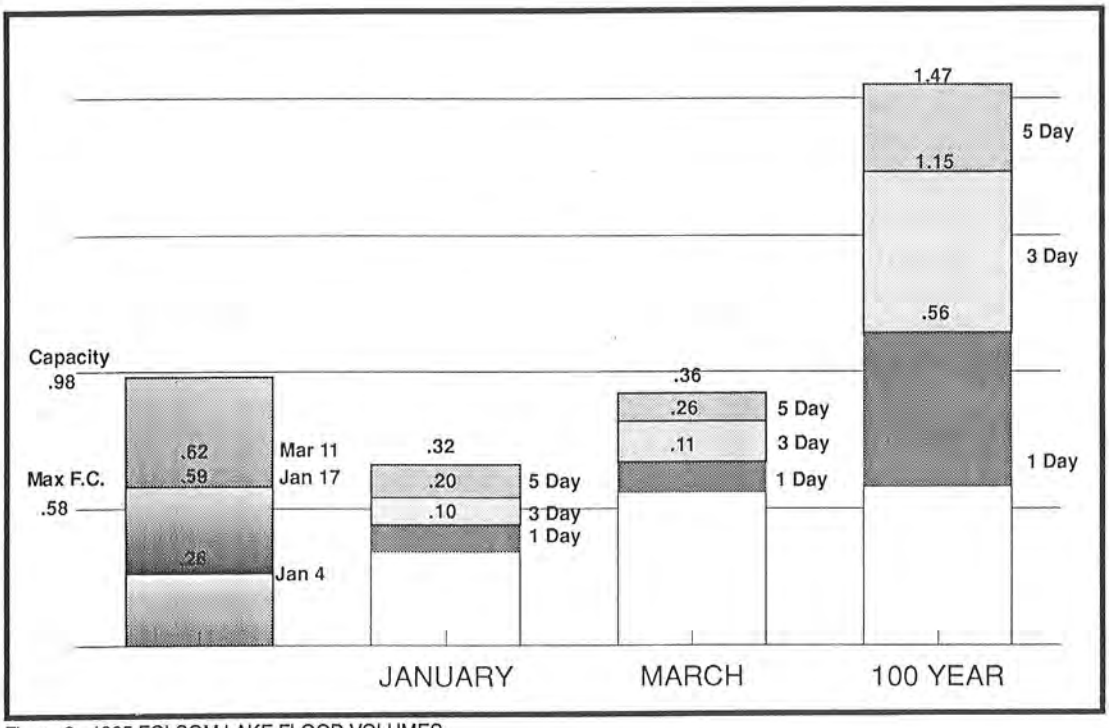

Figure 3 1995 FOLSOM LAKE FLOOD VOLUMES
Volumes in million acre-feet.

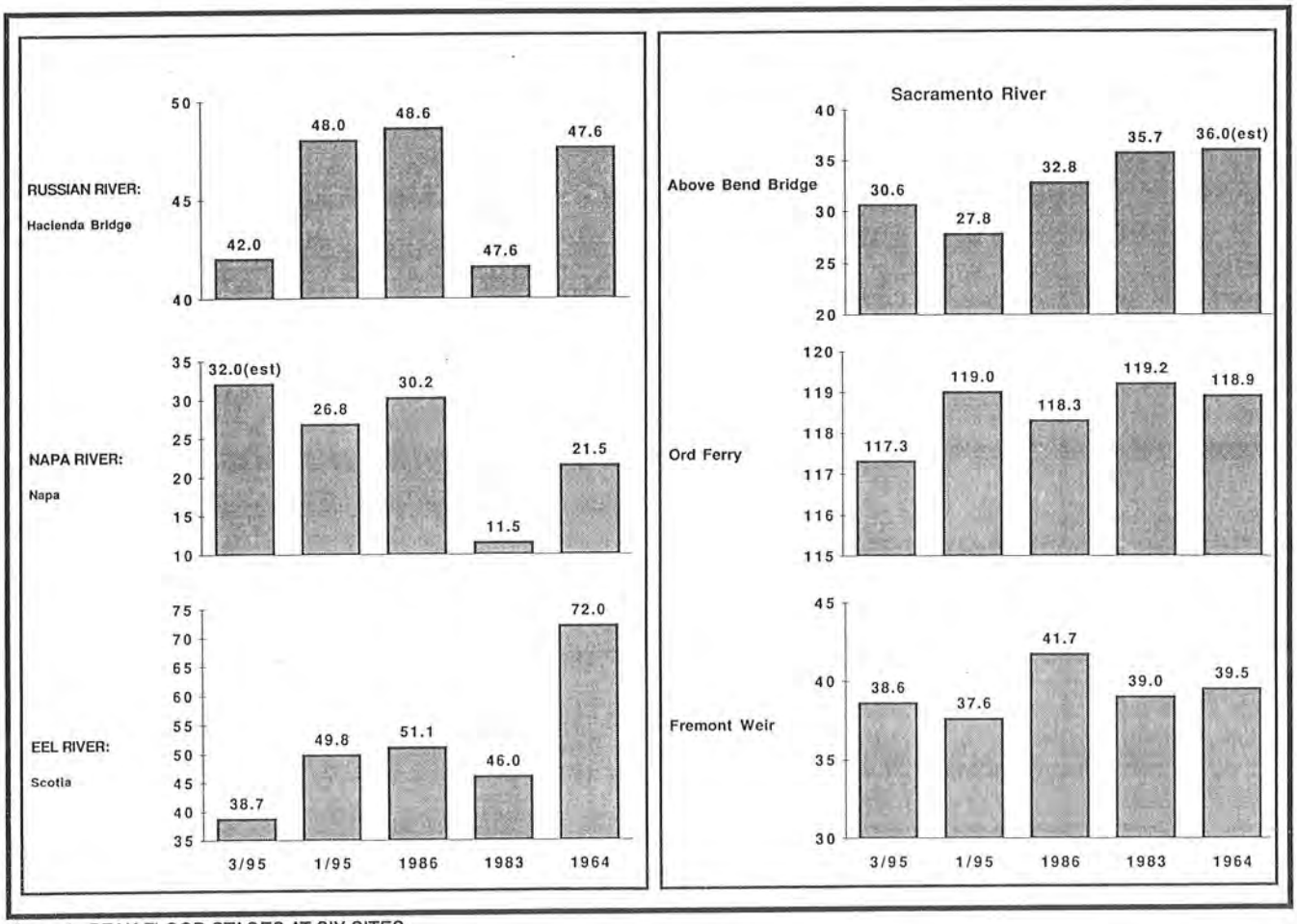

Figure 4 PEAK FLOOD STAGES AT SIX SITES

In a wet year, major reservoir operators on the San Joaquin River system try to just barely fill their reservoirs somewhat after the snowmelt peak as runoff begins receding. If they fill too soon, there is the risk of uncontrolled spill from a late-season runoff surge. If they are too low, there may not be enough volume to fill at the end of the season, with accompanying loss of power, water supply, and carryover storage for a possible following dry year. It is a difficult balance. Because of the relatively low runoff in mid-June, doubts were expressed about the forecasted volume of snowmelt. (Historical data show that delays in melting often result in lesser amounts.) Sometimes an appreciable amount of melt is delayed into August. Hence, Department of Water Resources forecasters (and others) began to lower projected total amounts for the season by 5 to 10 percent on the high elevation watersheds. Then, a late-June hot spell showed that perhaps the originally estimated volume was still there, and runoff forecasts (which were being updated weekly) were revised upward. However, reservoir releases had been curtailed in mid-June, and San Joaquin River levels had dropped. Many farmers then planted annual crops on the flood plain.

Continued warm mountain weather into July brought a new surge of snowmelt, with daily runoff peaks from the higher elevation Tuolumne through Kings river basins, which approached or matched earlier peaks. We believe the final snowmelt surge on July 9 was caused by a warm windy night in the high Sierra, which slowed the normal night radiation cooling (Figure 5). There were also some thunderstorms the previous day.

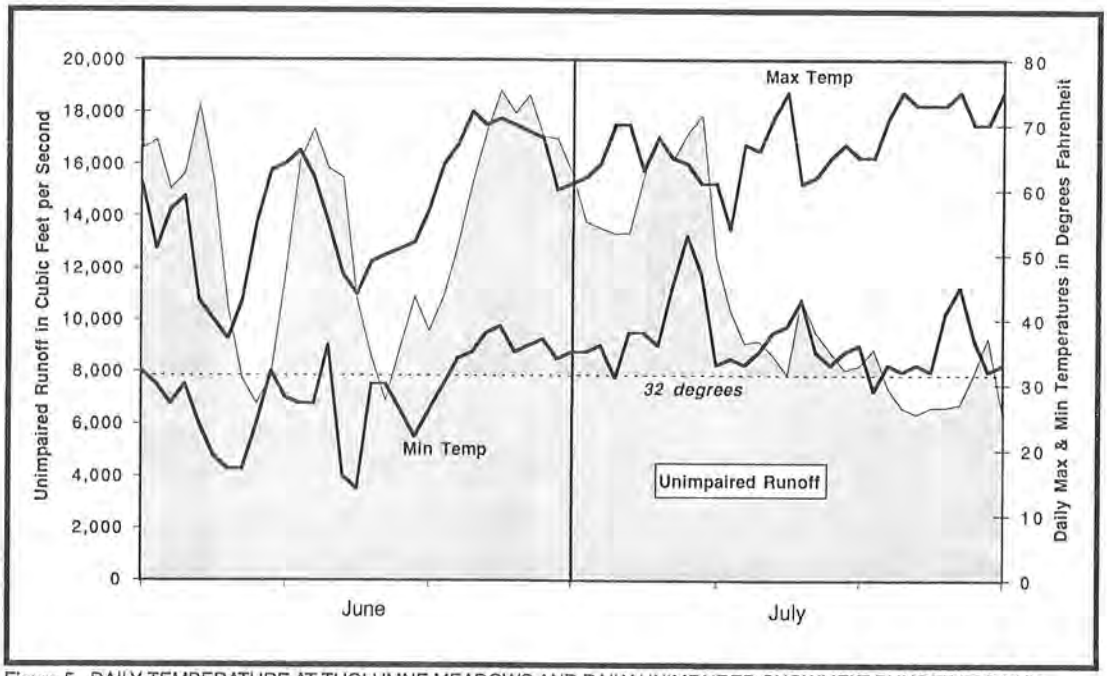

Figure 5 DAILY TEMPERATURE AT TUOLUMNE MEADOWS AND DAILY UNIMPAIRED SNOWMELT RUNOFF FOR THE TUOLUMNE RIVER IN 1995
Tuolumne Meadows is at 8,600-foot elevation.

By now, most reservoirs were nearly full and operators reacted by increasing downstream releases. The releases were within safe flood-carrying levels but did flood some of the newly planted crops. Forecasting and reservoir operations are being reviewed to see if we could have done better. The experience of another very wet year with unusually late snowmelt is extremely valuable for future operations.

There was a lot of water for the San Joaquin River system to handle in 1995. Things would have been worse earlier in the spring if we had not entered the year with rather low reservoir storage — about 70 percent of average, compared to nearly 150 percent on October 1, 1995. New Melones reservoir storage recovered from 16 percent full last year to about 73 percent this year. New Melones stored all the excess flow of the Stanislaus this year. The excess flows came from the Tuolumne, Merced, upper San Joaquin, and Kings rivers.

The bottom line is that the San Joaquin River reservoir and floodway system did its job with the enormous runoff this year, preventing a lot of damage. Nevertheless, it was not a perfect operation, and some forecasting and operations improvements can be made. Review of what happened can be helpful in devising slightly better strategies for minimizing downstream damage the next time.

References

Roos, M. 1987. Possible changes in California snowmelt patterns: Pages 22-31 in *Proceedings, Fourth Pacific Climate Workshop*, Pacific Grove, CA.

Roos, M. 1991. A trend of decreasing snowmelt runoff in Northern California. Pages 29-36 in *Proceedings of the 1991 Western Snow Conference*, Juneau, AK.

U. S. Army Corps of Engineers. 1987. *Folsom Dam and Lake, American River, Water Control Manual.* Plate 27. Sacramento District.

U.S. Army Corps of Engineers. 1991. *American River Watershed Investigation.* Volume 2, Appendix K, Chart 4. Sacramento District.

Recent Winters in the Western United States and Relationship to ENSO Patterns

Kelly T. Redmond

Abstract

In the mountainous western United States, winter weather has consequences for the entire year, especially with respect to the use of water. For most of the past 6-8 years, drought has been a persistent feature of the climate. This has in turn had substantial impacts on a wide variety of human and natural systems, including the arrangements by which water is allocated and the salmon population in the Pacific Northwest. The past four winters, years have seen more or less constant El Niño conditions; the corresponding winter snowpack patterns show differences and similarities with each other consistent with behavior over the past 60 years. The past decade will be examined with a new tool, the Standardized Precipitation Index developed by Tom McKee at Colorado State University, designed to supplement or replace the Palmer Drought Index. This index is capable of portraying the simultaneous behavior of climate elements on different time scales. (For example, it is possible to be in short-term deficit, mid-term excess, and long-term deficit, all at the same time.)

In: C.M. Isaacs and V.L. Tharp, Editors. 1996. *Proceedings of the Twelfth Annual Pacific Climate (PACLIM) Workshop, May 2-5, 1995.* Interagency Ecological Program, Technical Report 46. California Department of Water Resources.

Changes in the Hydrometeorological Regime in the Pacific Southwest

John J. Vaccaro

Abstract

Selected hydrometeorological (HM) data for the Pacific Northwest and atmospheric and North Pacific sea-surface temperature (SST) data are examined for three successive periods that are subsets of the historical record to estimate if their characteristics have changed. The HM data consist of monthly and water year precipitation totals for 50 sites in western Washington and streamflow averages for 112 sites in Washington, Oregon, and Idaho. The atmospheric information consists of the Southern Oscillation Index (SOI), Pacific North America Index (PNA), measures of the east-west and north-south components of geostrophic flow, and 700-mb height data. The atmospheric and SST data were examined because the HM regime is coupled to atmospheric circulation.

The water year subsets of the record were identified as pre-1947 (pre), 1947-1976 (base), and post-1976 (post). Means were calculated for the water year (October-September), the runoff season (March-August), the winter season (October-February), and a baseflow season (August-September). Differences in means and ratios of the means between the pre/post and the base periods were then examined for changes.

All but two water-year and winter-season means decreased compared to the base period, indicating a spatially consistent and distinct change in the HM regime during winter for the pre/post periods. For the runoff season, precipitation at most sites decreased for the pre period and increased for post period, indicating two different HM regimes during these periods. For both pre/post periods, water-year precipitation decreased because of decreased winter precipitation; however, the post-period water-year values did not decrease as much because of more precipitation in the runoff season. The water-year discharge for 97 of the 112 sites was less than the base period for both pre/post periods. Of the 15 sites with increased discharge, 14 were in a well-defined region and 13 had increases only for the post period. Winter-season streamflow decreased at all but 11 sites. Except for sites with increased annual discharge, means also decreased for the runoff season.

Changes in the SOI and PNA from the base period were generally similar to those of the HM data. Negative values of the SOI for the post period were more persistent than those in the historical record. Changes in the PNA were reflected in both atmospheric flow components. The 700-mb data display trends and differences between the base and post periods that are generally associated with warmer and drier conditions. SSTs have a significant long-term trend, and there have been large changes in monthly values between the base and post periods. These changes in atmospheric and SST data are clearly linked to and have influenced changes in the HM regime. Together, these changes suggest that an HM regime occurred during the post period that had not occurred in the historical record analyzed in this study: a regime with increased runoff-season precipitation over part of the Pacific Northwest and decreased water-year precipitation and streamflow over all but one region.

In: C.M. Isaacs and V.L. Tharp, Editors. 1996. *Proceedings of the Twelfth Annual Pacific Climate (PACLIM) Workshop, May 2-5, 1995.* Interagency Ecological Program, Technical Report 46. California Department of Water Resources.

River Salinity Variations in Response to Discharge: Examples from Western United States During the Early 1900s

David Peterson, Michael Dettinger, Daniel Cayan, Jeanne DiLeo, Caroline Isaacs, Larry Riddle, Richard Smith

ABSTRACT: Major controls on river salinity (total dissolved solids) in the western United States are climate, geology, and human activity. Climate, in general, influences soil-river salinity via salt-balance variations. When climate becomes wetter, river discharge increases and soil-river salinity decreases; when climate becomes drier river discharge decreases and soil-river salinity increases. This study characterizes the river salinity response to discharge using statistical-dynamical methods. An exploratory analysis of river salinity, using early 1900s water quality surveys in the western United States, shows much river salinity variability is in response to storm and annual discharge. Presumably this is because river discharge is largely supported by surface flow.

Introduction

Climate is one of the most important causes of variations in river (or stream) chemistry in the western United States. Other important factors include geology and human activity. How is climate connected to river salinity? Perhaps the most direct link is through river-basin salt-balance variations (*eg*, Ghassemi, Jackeman, and Nix 1995). Assume, initially, that the long-term mean soil and river salinity in natural systems is in a dynamic balance mostly controlled by river basin long-term mean precipitation. Salt stored in soils is generally increased by atmospheric deposition, evapo-concentration, and salt production via biotic and abiotic soil-forming processes including rock and mineral weathering and is generally decreased by flushing with fresh runoff or precipitation. If the climate becomes dryer on time scales ranging from months (see below) to millennia, the slow buildup of soil salt during the extended dry periods may exceed the intermittent flushing of salts during the less frequent wet periods. The soil-river system becomes more saline. Alternatively, if the climate becomes wetter, the soil-river system becomes less saline. In this simple conceptual model, the soil-river basin salt balances are controlled by the rate of flushing and, thus, by decreases or increases in precipitation (and all of the other complicating factors are assumed to be secondary). Climate controls salt dynamics largely through the rates of salt removal. Our ability to recognize climatic driven salinity variations may ultimately be controlled by the intersection of time scales at which flushing transits the system, the time scale of climatic forcing, and finally, the time scales of observational time series. A more complex model than

In: C.M. Isaacs and V.L. Tharp, Editors. 1996. *Proceedings of the Twelfth Annual Pacific Climate (PACLIM) Workshop, May 2-5, 1995*. Interagency Ecological Program, Technical Report 46. California Department of Water Resources.

our simple conceptual model would include feedback. For instance, with increasing precipitation/runoff and decreasing soil salinity, the rates of salt supply from weathering may also increase but less so than the rates of removal. In this paper, the utility of statistical-dynamical models is explored and an example of the role of water storage and time scales in salinity response is presented.

A long-term goal of our research is to better understand natural soil-river salinization processes and thereby to gain a broader perspective for interpreting artificial salinization processes. The north-south climate gradients in the west provide a natural laboratory with generally low salinities in the humid northwest and high salinities across the arid southwest. Presumably, with sufficient time, if this north-south climate gradient were reversed, the salinity regimes would also qualitatively reverse (increasing salinity in the northwest and decreasing salinity in the southwest). However, the responses of the soil-river salinities to changes in precipitation would not be instantaneous.

Statistical-dynamical methods have been used to study stream chemistry in response to variations in discharge (Whitehead *et al* 1986) as well as suspended sediment concentrations (Lemke 1991). One of our interests is to gain insight into the response of soils to regional differences in precipitation by analyzing the salinity-discharge responses of a wide range of river basins. A long-term goal is to understand the nature of the correlation between stream and soil salinity. We emphasize that the results given here are preliminary not only because of the simplified conceptual model used, but also because they are generally limited to analysis of annual cycles; analysis of longer and/or additional time series ultimately will be essential for building confidence in the results.

In the present analysis, our depiction of river chemistry is restricted to consideration of the concentration of total dissolved solids or salinity. As a further simplification, we selected the earliest, and therefore the least human influenced, statewide water quality surveys by the U.S. Geological Survey for California, Oregon, and Washington from about 1906 to 1912. Also, effects of mineralogical differences across this western region were not considered in this study.

Data and Methods

Early this century, water quality surveys were made in numerous river basins (Figure 1) in California (Van Winkle and Eaton 1910), Oregon (Van Winkle 1916b) and Washington (Van Winkle 1916a). In general, 100mL samples were collected each day, and 10 days of samples were combined as a composite sample for analysis of total dissolved solids and major ion composition (Dole 1909). Similarly, discharge was reported as 10-day mean values by combining daily observations.

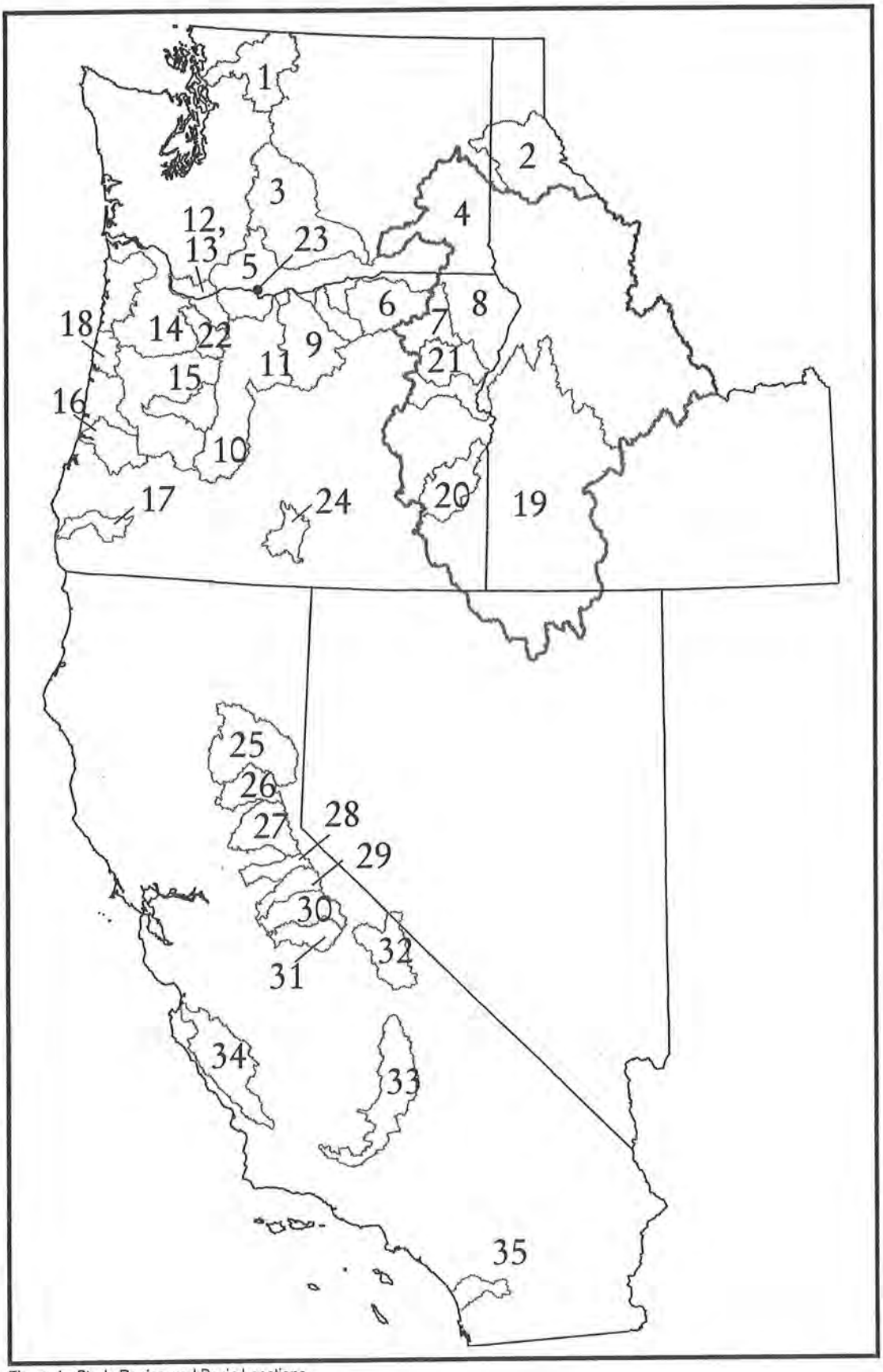

Figure 1 Study Region and Basin Locations
See Table 1 for names of river basins.

In the few instances with missing values, data were filled in by interpolation. Most discharge values were transformed as the log (base e) because salinity typically shows a more linear relationship to the log discharge than to discharge. Data treatment also included removal of the mean discharge and salinity.

Statistical models with discharge as the input or driving variable and salinity as the output or response variable were fitted according to:

$$y(t) = b_0u(t) + b_1u(t\text{-}1) + b_2u(t\text{-}2) + \ldots + e(t) \quad (1)$$

where y is salinity; u is discharge; t is present time; t-1 is a one-time internal (10-day) delay between input and output; t-2 is a two-time interval (20-day) delay between input and output with succeeding (t-x) at 10-day intervals; the b's are the response coefficients at various delays; and $e(t)$ is uncorrelated noise (Ljung 1987, 1991). Best fits were obtained for these models using the instrumental variable routines from MATLAB (Ljung 1991).

Results and Discussion

Most of the model results were identified using only one water year of 10-day mean values. Therefore, the parameter estimates (Table 1) are preliminary and the goodness-of-fits have not been tested on independent series.

The results are encouraging, with a mean correlation between observation and modeled values of 70%, and informative. To illustrate the usefulness of this kind of analysis, we selected the results of only two river basins for discussion. One of the basins, Umatilla River at Umatilla, shows a close discharge-salinity relationship; the other, Deschutes River at Moody, is an example of a weak relationship between discharge and salinity. Results for the Umatilla River are shown first, followed by those for the Deschutes River.

Umatilla River

Flow in the Umatilla River at Umatilla (Table 1) is characterized by low base flow and a high response to winter and spring precipitation and snowmelt (Figure 2). This response presumably indicates that water storage within the basin (and flow delays associated with such storage) is relatively small.

Under these presumed limited-storage conditions, the constant three coefficient model(b_0, b_1, b_2) captures about 90% of the variance (Table 1). However, a bias in the residuals (observed minus simulated values) indicates the model slightly overestimates concentrations (by about 10%) during annual rising discharge and underestimates (by about 10%) during falling discharge (Figure 3). This annual bias is probably due, in part, to saline irrigation water discharged into the river during summer (Van Winkle 1914a).

Table 1
DISCHARGE-SALINITY RESPONSE MODEL PARAMETERS AND STATISTICS

River and Location	Year	Observed Mean Discharge m^3s^{-1}	Observed Mean Salinity mgL^{-1}	Model Parameters b_0	b_1	b_2	b_3	Standard Deviation of Residual mgL^{-1}	Correlation Coefficient between Observed and Simulated	Range Between Base and Peak Discharge (% of Mean Discharge)
Washington, Oregon, and Adjacent States										
1 Skagit, Sedro Wolley	1910-11	449	48	-5.3	-28	0	0	11	0.12	145
3 Yakima, Prosser	1910-11	148	128	-20	-17	-7.6	0	24	0.90	330
4 Snake, Burbank	1910-11	1,870	131	-16	-3	-10	0	16	0.88	300
6 Umatilla, Yoakum	1911-12	29	100	-6.3	-2.7	-2.0	0	17	0.72	380
Umatilla, Umatilla	1911-12	25	188	-33	-10	-7.3	0	25	0.95	380
7 Grande Roude, Elgin	1911-12	54	98	-5.5	0	0	0	9.6	0.74	360
8 Wallowa, Joseph	1911-12	4.6	64	-0.2	0	0	0	3.0	0.50	310
9 John Day, McDonald	1911-12	165	142	-9.6	-4.9	-2.6	0	17	0.82	1,800
John Day, Dayville	1911-12	14	166	-25.7	0	0	0	20	0.87	360
10 Deschutes, Moody	1911-12	198	92	0	+7.8	0	0	6.5	0.39	140
Deschutes, Bend	1911-12	37	66	0	0	0	+7.0	4.9	0.24	59
11 Crooked, Prineville	1911-12	14	223	-2.7	-1.1	-0.6	0	37	0.89	350
12 Sandy, Brightwood	1911-12	24	49	-1.4	-1.9	-0.8	-1.8	3.3	0.95	220
13 Bull Run, Bull Run	1911-12	22	30	-3.2	-1.7	-0.5	-1.7	4.3	0.78	460
14 Willamette, Salem	1911-12	679	51	-3.1	-0.8	0	0	6.5	0.59	490
15 McKenzie, Springfield	1911-12	127	48	-7.2	-1.8	-0.5	-1.2	2.8	0.93	300
16 Umpqua, Elkton	1911-12	160	68	0	-2.5	0	0	5.1	0.48	380
17 Rogue, Tolo	1911-12	105	71	0	-5.1	2.3	0	5.2	0.66	350
18 Siletz, Siletz	1911-12	46	42	-0.04	0	0	0	5.1	0.41	600
19 Snake, Weiser	1911-12	621	220	-17	-13	-11.5	-16.7	21	0.84	300
20 Owyhee, Owyhee	1911-12	44	230	-6.7	-12.7	-7.9	-8.1	35	0.89	510
21 Powder, North Powder	1911-12	10	193	0	-7.9	0	0	36	0.50	450
22 Clackamas, Cazadero	1911-12	75	50	-8.1	-3.9	-1.6	0	3.7	0.91	280
23 Columbia, CascadeLocks	1910-11	6,700	91	0	0	-4.6	-6.5	9.5	0.62	220
Columbia, Cascade Locks	1911-12	5,610	98	-3.6	-16.8	0	0	8.1	0.87	290
24 Chewancan, Paisley	1911-12	4	85	-5.5	0	0	0	7.7	0.52	530
California										
25 Feather, Oroville	1906	275	99	-9.1	-3.6	6.6	0	11	0.83	360
26 Yuba, Smartville	1906	140	84	-3.3	-11	0	0	11	0.86	360
27 American, Fair Oaks	1906	298	80	-0.2	-4.4	-5.1	0	8.3	0.87	1,200
28 Mokelumne, Clements	1906	56	76	-7.4	-3.2	-4.1	0	15	0.76	370
29 Stanislaus, Knights Ferry	1906	302	83	-9.1	-15	0	0	27	0.48	210
30 Tuolumne	1906	136	73	0	0	-8.8	-5.3	16	0.80	350
31 Merced	1906	130	66	0	0	-12	-4.0	16	0.60	220
32 Owens, Charles Butte	1906	8.7	339	-45	-0.1	0	0	30	0.52	200
33 Kern, Bakersfield	1906	89	128	-15	-20	0	0	30	0.78	520
34 Arroyo Seco, Soledad	1906	12	281	-23	-9.5	-10	0	44	0.90	960
35 San Luis Rey, Pala	1906	143	320	-13	0	0	0	34	0.61	1,900

As expected for the simple conceptual model presented in the Introduction, total dissolved solids decrease with increasing discharge and, indeed, the response shows an approximately first-order exponential decrease in salinity with increase in discharge (Figure 4). An example of hysteresis in a salinity-discharge cycle is where the salinity response differs depending on whether discharge is increasing or decreasing (Figure 5). Much of this hysteresis was captured by the statistical-dynamical model (as indicated by similar departures of observed and simulated salinities from a smooth exponential decrease in concentration with increase in discharge). We believe an important mechanism for hysteresis is that the early seasonal flushing flows (rising discharge limb) carry more concentrated salts than the later flows (falling discharge limb).

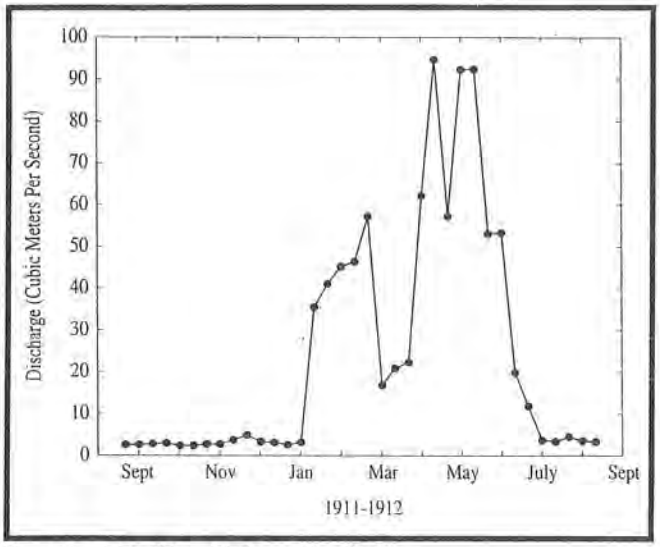

Figure 2 10-Day Mean Discharge Umatilla River, Umatilla, Oregon, 1911-1912

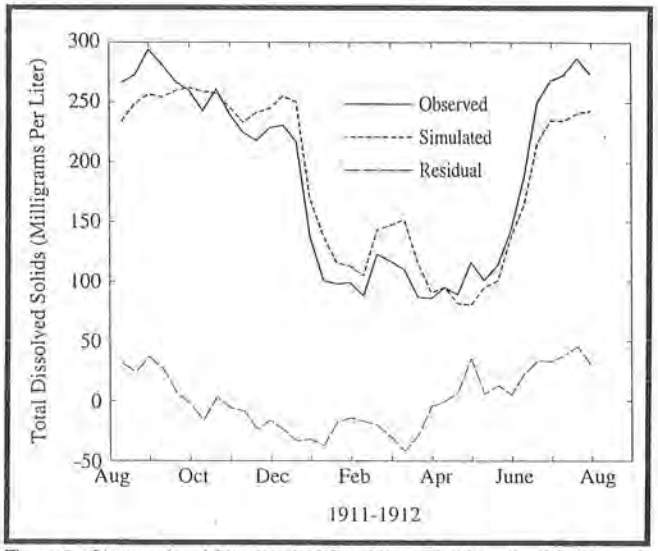

Figure 3 Observed and Simulated 10-Day Mean Total Dissolved Solids and the Residuals (Observed minus Simulated), Umatilla River at Umatilla, 1911-1912

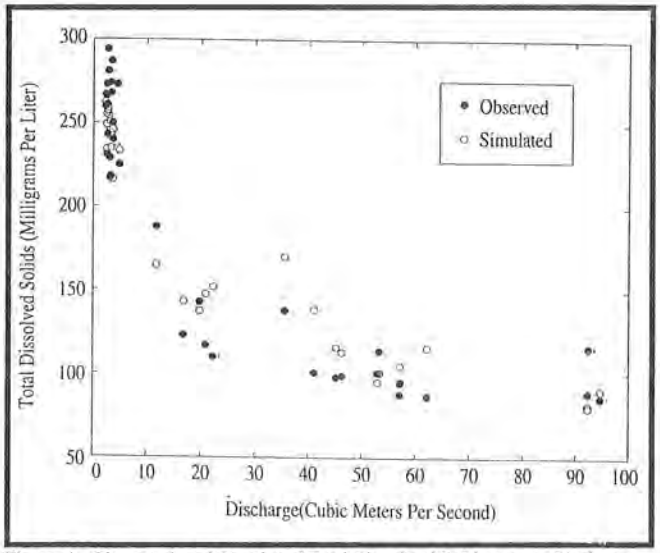

Figure 4 Observed and Simulated Total Dissolved Soids versus Discharge, Umatilla River at Umatilla, 1911-1912

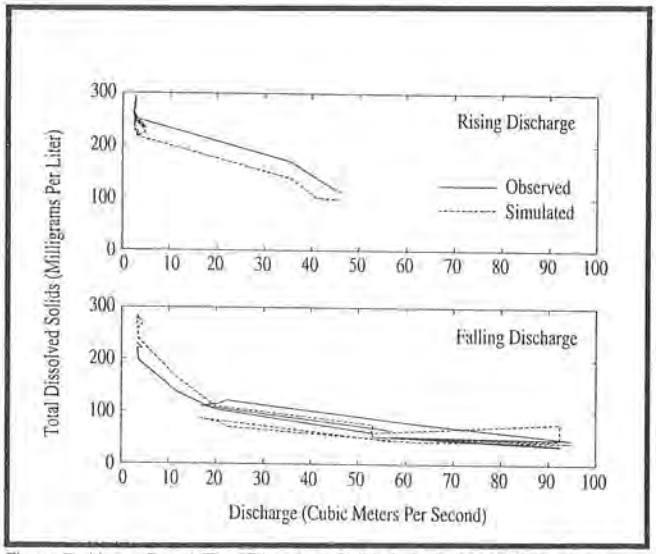

Figure 5 Upper Panel: Total Dissolved Solids in Relation to Rising Annual Discharge.
Lower Panel: Total Dissolved Solids in Relation to Falling Discharge, Umatilla River at Umatilla, 1911-1912

Deschutes River

In the Deschutes River system (Table 1), water storage in the soils and basalts underlying the basin dampen and delay the pulse of moisture input associated with winter precipitation (Shelton 1985). Thus, in contrast to the Umatilla River at Umatilla, the Deschutes River at Moody shows a high base flow relative to the winter-spring peak flows (Figure 6). For example, in the Umatilla River (1911-1912), base flow is about 20 times less than peak flows, whereas in the Deschutes River, base flow was about half the peak flows.

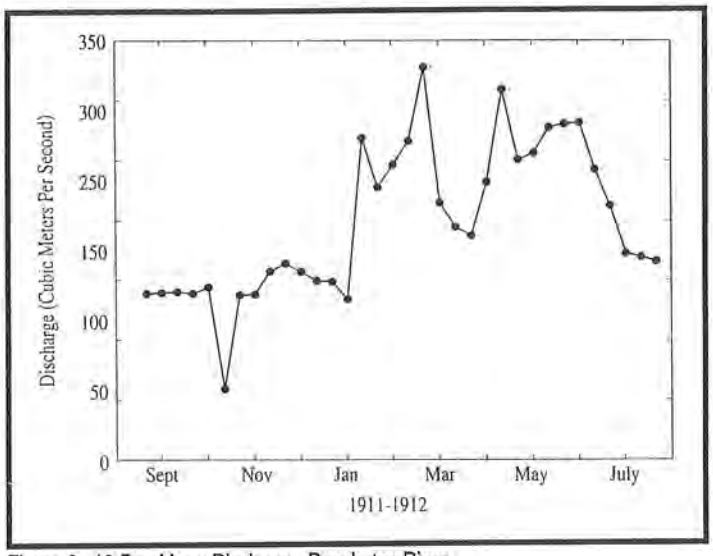

Figure 6 10-Day Mean Discharge, Deschutes River, Moody, Oregon, 1911-1912

The sensitivity of total dissolved solids concentrations to variations in discharge is low in the Deschutes River; in fact, total dissolved solids concentrations tend to increase with increasing discharge (Figure 7). We conclude that the poor correlation (correlation coefficient of 0.39) of observed and simulated total dissolved solids (Figure 8) is probably a result of dampening of salinity variations that "parallels" the dampening of discharge variations in this basin. Slow transit of subsurface storage within this basin, causes base flow and, indeed, the lion's share of streamflow to undergo considerable damping, mixing and homogenization. Consequently, the discharge time scale of variation in this basin is probably at least annual and the salinity time scale is longer still (from the looks of Figure 8). Neither the model nor the 350-day time series is adequate to fit the slow variations in discharge and salinity that characterize this basin.

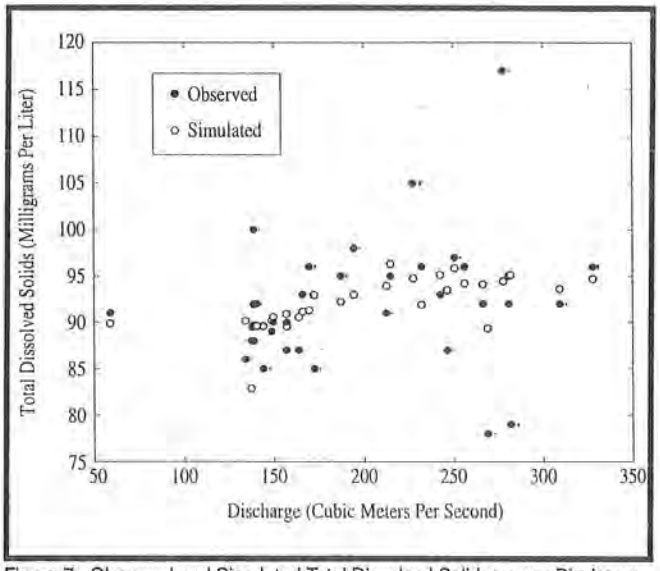

Figure 7 Observed and Simulated Total Dissolved Solids versus Discharge, Deschutes River at Moody, 1911-1912

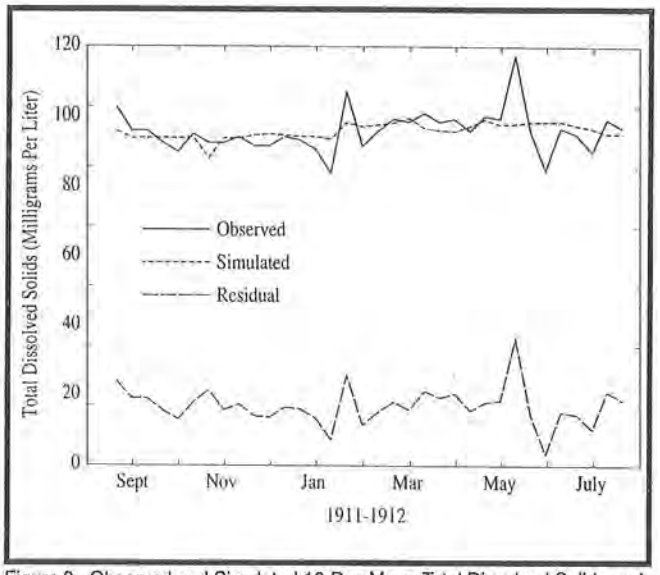

Figure 8 Observed and Simulated 10-Day Mean Total Dissolved Solids and the Residuals (Observed minus Simulated), Deschutes River at Moody, 1911-1912

Conclusion and Future Research

In the western United States, much river-salinity variability is in response to storm and annual variations in discharge, presumably because discharge is largely supported by surface flow. Basins with large storage and high base flow, such as the Deschutes River, are exceptions to this generalization. Also, however, not all basins with low base flow show a strong response of salinity to discharge.

Although considerable work needs to be done, statistical-dynamical modeling methods appear to offer an efficient way to characterize the complex variations in riverine chemistry, including river basin salt-balance phenomena. The preliminary success of the models is encouraging, but we need to compare the results with observations from other years. Further, the analysis of model parameters should be normalized to runoff (discharge per unit area). Also, a more complete evaluation of model parameters should include analysis of effects of the length of record and observational errors associated with inadequate sample collection, storage, and analysis as well as climatic (*eg*, snowpack) and human (*eg*, reservoirs) influences. Finally, discharge-response characteristics probably also vary for the different major ions. The Deschutes River example suggests that multiple-input models, with surface and subsurface discharge, may be needed.

Acknowledgment

Data and manuscript preparation of Lucenia Thomas and reviews of Marc Sylvester and Jim Thomas are appreciated.

References

Dole, R.B. 1909. *The Quality of Surface Waters in the United States, Part I: Analyses of Waters East of the 100th Meridian.* U.S. Geological Survey Water Supply Paper 236. pp. 9-26.

Ghassemi, F., A.J. Jackeman, H.A. Nix. 1995. *Salinization of Land and Water Resources: Human Causes, Extent, Management and Case Studies.* CAB International, Wallingford, UK. 26 pp.

Lemke, K.A. 1991. Transfer function models of suspended sediment concentration. *Water Resources Research* 27:293-305.

Ljung, L. 1987. *System Identification: Theory for the User.* Prentice-Hall. Inglewood Cliffs, NJ. 519 pp.

Ljung, L. 1991. System Identification: A Toolbox User's Guide for use with Matlab™ Inc. The MathWorks. Natick, MA. 204 pp.

Shelton, M.L. 1985. Modeling hydroclimatic processes in large watersheds. *Annals of Association of American Geographers* 75:185-202.

Van Winkle, W., and F.M. Eaton. 1910. *The Quality of the Surface Waters of California.* U.S. Geological Survey Water Supply Paper 237. Government Printing Office. Washington, DC. 142 pp.

Van Winkle, W. 1914a. *Quality of the Surface Waters of Washington.* U.S. Geological Survey Water Supply Paper 339. Government Printing Office. Washington, DC. 105 pp.

Van Winkle, W. 1914b. *The Quality of the Surface Waters of Oregon.* U.S. Geological Survey Water Supply Paper 363. Government Printing Office. Washington, DC. 137 pp.

Whitehead, P.G., C. Neal, S. Seden-Perriton, N. Christophersen, S. Langen. 1986. A time series approach to modeling stream acidity. *Journal of Hydrology* 85:281-303.

Reconstructing 20th Century Flood Patterns in Havasu Creek, Arizona, Using Historical and Dendrochronologic Data

Theodore S. Melis and William M. Phillips

Abstract

Havasu Creek is the second largest tributary of the Colorado River in Grant Canyon. Perennial streamflow in the creek seldom exceeds 2 m^3/s, but it supports an important riparian habitat as well as unique travertine pools and waterfalls that attract over 20,000 tourists annually. Havasu Canyon is also home to over 400 members of the Havasu Tribe. Despite a long history of habitation and recreation in Havasu Canyon, streamflow records for Havasu Creek are extremely limited, making flood prediction difficult. Historical accounts and photographs indicate that Havasu Creek experienced frequent, large floods in both winter and summer during the late 19th and early 20th centuries. The largest flood was in January 1910. Between about 1940 and 1990 mainly smaller summer floods occurred. In September 1990, the largest flood in Havasu Creek since 1935 and possibly 1910 was generated by intense thunderstorms. The 1990 flood had a peak discharge of about 575 m^3/s, caused severe damage to Supai, Arizona, scoured hundreds of ash trees (*Fraxinus* sp.), and altered many pools and waterfalls along Havasu Canyon. Smaller floods also occurred in July 1992 and February 1993. Dendrochronologic data indicate that most ash trees along Havasu Creek germinated after 1940, with a peak in recruitment during the late 1960s and early 1970s. This recent peak likely reflects disturbance by humans rather than effects of flooding. The recent flood pattern resembles the more dynamic flood regime of the first third of the 20th century. Trends in annual frequency of 24-hour precipitation >25 mm within four nearby precipitation records follow the historical pattern of flooding in Havasu Canyon.

In: C.M. Isaacs and V.L. Tharp, Editors. 1996. *Proceedings of the Twelfth Annual Pacific Climate (PACLIM) Workshop, May 2-5, 1995.* Interagency Ecological Program, Technical Report 46. California Department of Water Resources.

An 800-Year Paleoflood Record from the Sacramento Valley, California

Roger Byrne and Donald Sullivan

Abstract

Four cores recovered from Little Packer Lake in Glenn County, California, have provided a paleoflood record for the past 800 years. Little Packer Lake (unofficial name) is an oxbow lake on the west bank of the Sacramento River, some 16 miles north of Colusa. Sediments of the lake are fine-grained (clay and silt) and show an alternating sequence of dense (flood) and less dense (non-flood) layers on x-radiographs. The same alternation is also clearly evident in magnetic susceptibility profiles; flood deposits have high magnetic susceptibilities and non-flood deposits have low susceptibilities. Chronological control is provided by Lead 20 for the past 100 years and conventional radiocarbon dates for the earlier period. The sequence of flood deposits in the top 2 meters of the record shows a reasonable agreement with the known history of floods during the past 150 years. At least three major flood events are indicated for AD 1400-1525, although these dates may have to be revised when more dates become available.

In: C.M. Isaacs and V.L. Tharp, Editors. 1996. *Proceedings of the Twelfth Annual Pacific Climate (PACLIM) Workshop, May 2-5, 1995.* Interagency Ecological Program, Technical Report 46. California Department of Water Resources.

Can Lake Sediments Provide a Record of Tropical Storms? The Case of Laguna de Juanacatlan, Jalisco, Mexico

Roger Byrne, Douglas Allen, Eric Edlund, Clare Polansky

Abstract

Laguna de Juanacatlan is a small (15 hectare) lake in the State of Jalisco, Mexico. Its sediments are predominantly varved and thereby offer the potential of a high resolution paleoclimatic record. In 1990, three ~10 meter cores were recovered from the lake, the longest of which produced a basal date of 7,400 BP (uncalibrated). Two of three cores taken in about 10 meters of water show the same basic stratigraphy. The third core, taken on the edge of the lake, is only minimally varved. Of particular interest in all three cores is the irregular presence of dense laminae 2 to 4 times thicker than the normal summer? laminae. We hypothesize that these dense layers are the result of above-average erosion in the watershed during tropical storms. To test this hypothesis, we collected data on tropical storms in the area for the period 1921-1990. Preliminary analysis indicates that the dense layers are indeed storm-induced. A reconstruction for the 7,400-year period indicates that at least five major storms affected the area between 7,000 BP and 3,000 BP; one major storm between 3,000 BP and 1,000 BP; and four major storms between 1,000 BP and the present.

In: C.M. Isaacs and V.L. Tharp, Editors. 1996. *Proceedings of the Twelfth Annual Pacific Climate (PACLIM) Workshop, May 2-5, 1995.* Interagency Ecological Program, Technical Report 46. California Department of Water Resources.

Influence of Climatography on Rainfall Thresholds for Initiation of Debris-Flows on the California Coast

Raymond C. Wilson

Abstract

Since 1986, the U.S. Geological Survey and National Weather Service have operated a warning system for debris flows triggered by severe rainstorms in the San Francisco Bay region. The NWS tracks storm systems as they approach the region, forecasts precipitation, and observes rainfall with a network of radiotelemetered rain gauges (ALERT). The USGS also monitors ALERT data and compares the observed and forecast rainfall to thresholds for debris-flow initiation. Both groups jointly assess debris-flow hazards and issue public advisories when rainfall conditions reach or approach critical levels.

Rainstorms in 1993 and 1995 triggered damaging debris flows in both northern and southern California, leading to speculation about expanding the present effort to a statewide warning system. While some elements of the warning system, such as weather forecasting, already operate on statewide scales, a key element is missing: a reliable set of threshold values of rainfall intensity and duration necessary for the initiation of debris flows in different regions of the state.

Rainfall/debris-flow thresholds depend on the thickness, character, and behavior of the hillslope materials, which, in turn, depend on the geology, topography, vegetation, and climate of the area. In the San Francisco Bay region, for example, more rainfall appears to be required to trigger debris flows in areas with high mean annual precipitation than in areas with low MAP. However, a study of historical data on rainfall and debris-flow occurrence in southern California, where MAP is roughly half that of the San Francisco Bay region, suggests that simply normalizing San Francisco Bay thresholds for MAP will produce threshold values that are much too low. The MAP is lower in southern California because storms are less frequent, in keeping with the general correlation of storm frequency with geographic latitude along the Pacific coast. The average rainfall amounts for individual storms, however, generally equal those of storms farther north and perhaps provide a better parameter for normalizing rainfall/debris-flow thresholds.

In: C.M. Isaacs and V.L. Tharp, Editors. 1996. *Proceedings of the Twelfth Annual Pacific Climate (PACLIM) Workshop, May 2-5, 1995.* Interagency Ecological Program, Technical Report 46. California Department of Water Resources.

Disturbance Climate in the Columbia River Basin

Sue A. Ferguson and Miriam R. Peterson

Abstract

Climatological events that disturb a landscape are important components in ecosystem processes. Modern ecosystem management plans now hope to incorporate knowledge of the spatial distribution and frequency of disturbance climate. The following describes a few analytic tools developed to help managers include disturbance climate in an ecosystem management plan for areas in the Columbia River Basin of the northwestern United States. In many cases, a geographic information system (GIS) was used to develop maps of disturbance climate patterns to overlay on other ecosystem maps like vegetation, soils, wildfires, animal habitat, *etc.*

Primary components of disturbance in the Columbia River Basin include blown-down trees, cold damage to infant plants, rain-on-snow floods, lightning fire ignition, drought stress, and frontal winds during fire season. Modeled surface winds for individual storms known to have blown down a large number of trees were compared against prevailing winds to determine blow-down potential. Simple algorithms were developed to determine cold-damage potential and rain-on-snow flood potential. These were applied to daily temperature and precipitation data to show the spatial pattern of cold-damage and rain-on-snow for three characteristic climate patterns. Automated lightning detection data were used to identify patterns of lightning strikes. "Dry" lightning was distinguished from "wet" using the Haines Stability Index to help determine characteristic weather patterns associated with lightning in the northwest. Lightning strike patterns were also compared with wildfire occurrence data. The Palmer Drought Severity Index was used to determine the historical frequency of 6- to 12-month drought periods and help identify the cause of drought for mountain, plain, basin, and plateau regions. McKee's Precipitation Deficit Index helped identify drought at varying spatial and temporal scales. A simple analysis of surface pressure changes was able to determine the frequency and severity of wind gusts that contribute to the spread of wildfire.

In: C.M. Isaacs and V.L. Tharp, Editors. 1996. *Proceedings of the Twelfth Annual Pacific Climate (PACLIM) Workshop, May 2-5, 1995.* Interagency Ecological Program, Technical Report 46. California Department of Water Resources.

Fire, Climate, and Vegetation: The Sedimentary Record of Fire in Montane Meadows, Sierra Nevada, California, USA

R. Scott Anderson and Susan J. Smith

Abstract

This abstract parallels one prepared for the NATO Workshop on Biomass Burning, Algarve, Portugal (October 1994).

Though knowledge of fire occurrence and weather pattern relationships has been used for many years by land managers in, for instance, prescribed fire planning, understanding of the relationship between Holocene climates and fire is just beginning to be investigated (*eg*, Clark 1988; Swetnam and Betancourt 1990). We are investigating this relationship in a major mountain range in California, examining charcoal and pollen content in sediments of montane meadows to compare paleo-fire and paleo-vegetation (thus, climate) sequences for the Holocene. We have been using Jim Clark's (1988) thin-section technique, embedding the sediments with epoxy resin and examining detailed charcoal records at about 1-millimeter intervals. This methodology has allowed us to begin to reconstruct detailed local fire histories and to speculate on the broader implications of fire in the Sierra.

This research has implications for understanding former natural episodes of "biomass burning". Preliminary fire chronologies from eight locations demonstrate temporal correspondence for several periods in the past. Sedimentary charcoal abundance is high at most locations from about 8700 to 9200 YBP, very low from about 4500 to 8700 YBP, and high once again for the last about 4500 years. Our working hypotheses suggest that the lower abundance of charcoal (thus fire) during the early to middle Holocene resulted from lowered biomass and fire carrying capacity in Sierran forests. Changes in climate during the later Holocene allowed greater conifer forest development, with an increase in biomass and greater fire. Climatic variability, such as the late to middle Holocene establishment of ENSO conditions in the eastern Pacific, may also have been important.

References

Clark, J.S. 1988. *Nature* 334:233-235.

Swetnam, T.W., and J.L. Betancourt. 1990. *Science* 249:1017-1020.

In: C.M. Isaacs and V.L. Tharp, Editors. 1996. *Proceedings of the Twelfth Annual Pacific Climate (PACLIM) Workshop, May 2-5, 1995.* Interagency Ecological Program, Technical Report 46. California Department of Water Resources.

Changes in Mass Balance of South Cascade Glacier, North Cascades, 1959 to 1994

Steven M. Hodge, Robert M. Krimmel, Edward G. Josberger

Abstract: Annual, winter, and summer mass balance measurements at South Cascade Glacier in the North Cascade Mountains of Washington State constitute a continuous time series 36 years long, from 1959 to 1994. The glacier net balance, the difference between the winter balance (total accumulation) and summer balance (total ablation), decreased abruptly in 1977, from an average of –0.09±0.90 m/yr for 1959-1976, to –1.02±0.71 m/yr for 1977-1994. The decrease in this average, –0.91 m/yr, exceeded its standard deviation (1s) for both periods. However, an even more statistically significant decrease occurred in the winter balance, which averaged +3.00±0.60 m/yr for 1959-1976, but only +2.27±0.46 m/yr for 1977-1994, the decrease in the average clearly exceeding either standard deviation. The summer balance does not show any significant abrupt change, averaging –3.09±0.55 m/yr before 1977 and –3.27±0.55 m/yr after, but linear fits to the data show that since the late 1970s the summer balance has been decreasing about 0.045 m/yr, about three times faster than the winter balance has been increasing. These results suggest that the winter snowpack in the Washington Cascades underwent an abrupt decrease between 1976 and 1977, and has remained at about the new lower level since 1977. This decrease appears to have occurred because of a change in conditions that prevented snow from accumulating, rather than because of a change in total regional winter precipitation. The long-term trends at South Cascade Glacier are decreased winter accumulation and increased summer ablation, neither of which is conducive to glacier growth, so the trend in the Pacific Northwest is clearly away from an ice-age type of climate at the current time. The data also demonstrate that a glaciologically significant long-term change in snow precipitation can occur rapidly, in as short an interval as 1 year, much more rapidly than changes in temperature.

South Cascade Glacier is a small valley glacier near the crest of the North Cascade Range in north-central Washington State (Figure 1). It is at the head of the South Fork of the Cascade River, a tributary to the Skagit River. It lies in a coastal, maritime climate where winter precipitation, mostly in the form of snow, is heavy and can exceed 4.5 meters annually. Although the glacier is only about 2 km^2 in area, it occupies about 34 percent of a north-facing basin and, thus, is larger and lies at a lower elevation than most other glaciers in the region.

Since 1959, the U.S. Geological Survey has measured winter, summer, and net mass balances at this glacier. These data, one of the longest such records on any glacier outside Europe, are shown in Figure 2. The results are published in annual data reports; for example, Krimmel (1993).

The winter balance is the net snow accumulated above the previous summer surface at the end of the winter season, which usually occurs in late April or early May on South Cascade Glacier. It is not the same as total winter snowfall, nor necessarily total annual snowfall, since some winter precipitation can occur as rain and some snowfall can occur in the summer. Nevertheless, it is equivalent to, and somewhat representative

In: C.M. Isaacs and V.L. Tharp, Editors. 1996. *Proceedings of the Twelfth Annual Pacific Climate (PACLIM) Workshop, May 2-5, 1995.* Interagency Ecological Program, Technical Report 46. California Department of Water Resources.

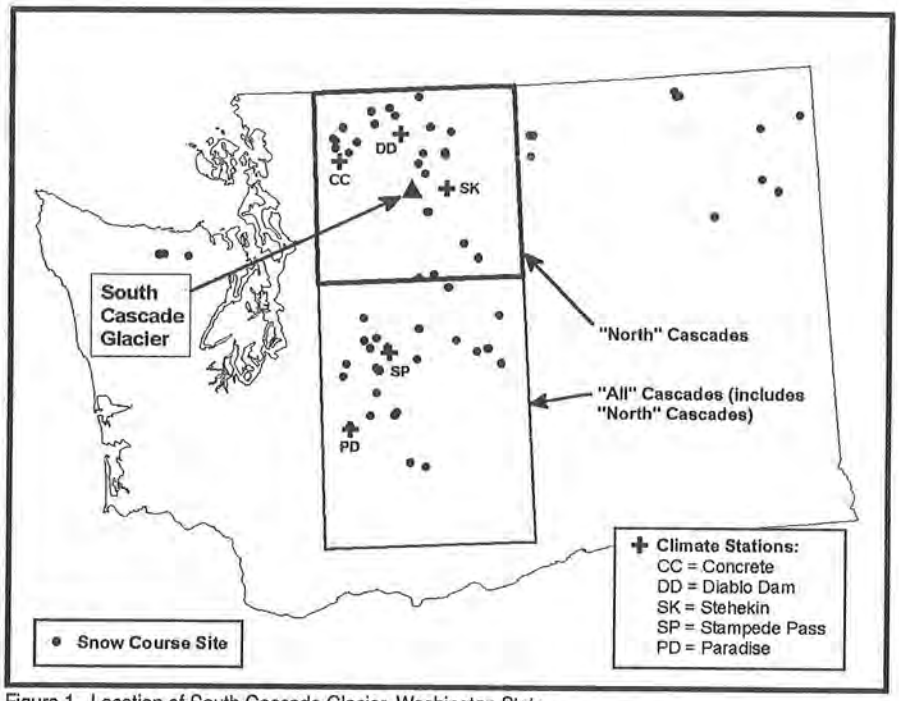

Figure 1 Location of South Cascade Glacier, Washington State.
The USDA snow course sites and NCDC climate stations used in this paper are also indicated.

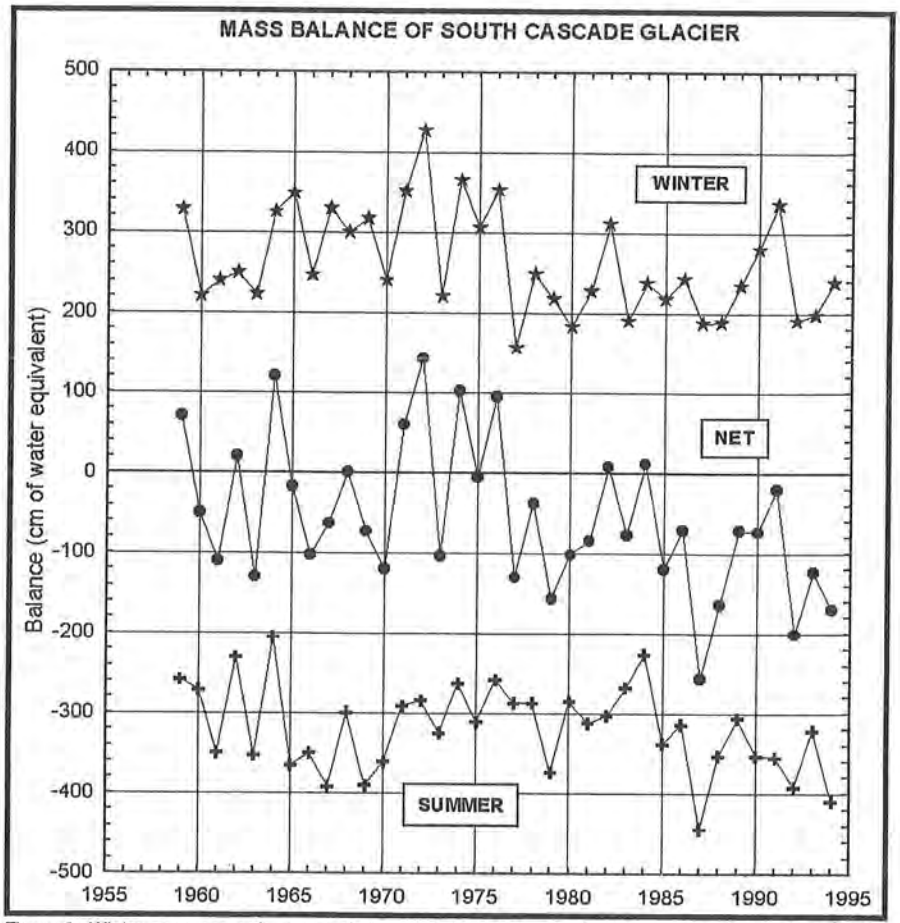

Figure 2 Winter, summer, and net mass balance of South Cascade Glacier, measured since 1959 by the U.S. Geological Survey.
This is one of the longest such records (36 years) on any glacier outside of Europe.

of, the total amount of water in the regional high-elevation snowpack at the end of winter. The net balance is the net change in total mass of the glacier between two successive summer surfaces, which are formed at the end of each melt season, usually sometime in October. The summer balance is the difference between the two: winter minus net. All balance values are averaged over the glacier area and expressed in units of depth of water equivalent. The data are assigned to the calendar year in which the melt season ends; the winter balance thus represents accumulation that commenced during the fall of the previous calendar year. Errors depend upon the year but typically are 0.1-0.2 meters/year.

Analysis and Interpretation

The net mass balance of South Cascade Glacier decreased abruptly in 1977, from an average of –0.09±0.90 meters/year for 1959-1976 to –1.02±0.71 meters/year for 1977-1994. The decrease in the average, –0.93 meters/year, exceeded its standard deviation (1σ) for both periods. However, an even more statistically significant decrease occurred in the winter balance, which averaged +3.00±0.60 meters/year for 1959-1976 but only +2.27±0.46 meters/year for 1977-1994. The decrease in the average, –0.73 meters/year, clearly exceeded either standard deviation. The summer balance does not show any significant abrupt change: it averaged –3.09±0.55 meters/year for 1959-1976 and –3.27±0.55 meters/year for 1977-1994. Since 1977, the net balance of South Cascade Glacier was positive in only 2 years, but only by a small amount (about +0.01 meters/year).

These results are more readily evident when the data are normalized as standard deviates (the departure of a value from the average, divided by the standard deviation). The standard deviates in Figure 3 were computed using the entire time series. The thick horizontal lines are the average standard deviate computed separately for the periods 1959-1976 and 1977-1994. The thick dashed lines are linear fits to the post-step data; these were added because this is a better approximation to the trend after the step, especially for the winter and net balance.

The winter balance underwent predominantly a step decrease between 1976 and 1977 and has been increasing slowly since 1977, about +0.015 meters/year. On the other hand, the summer balance does not show a similar step change. Instead, since the late 1970s it has been decreasing about –0.045 meters/year, about three times faster than the winter balance has been increasing. The net balance of South Cascade Glacier has, thus, continued to decrease slowly since 1977.

This abrupt change is, fortuitously, now in the middle of the complete South Cascade Glacier mass balance time series, with 18 years of data on either side of it. Thus, this change is not an artifact caused by unequal sampling periods.

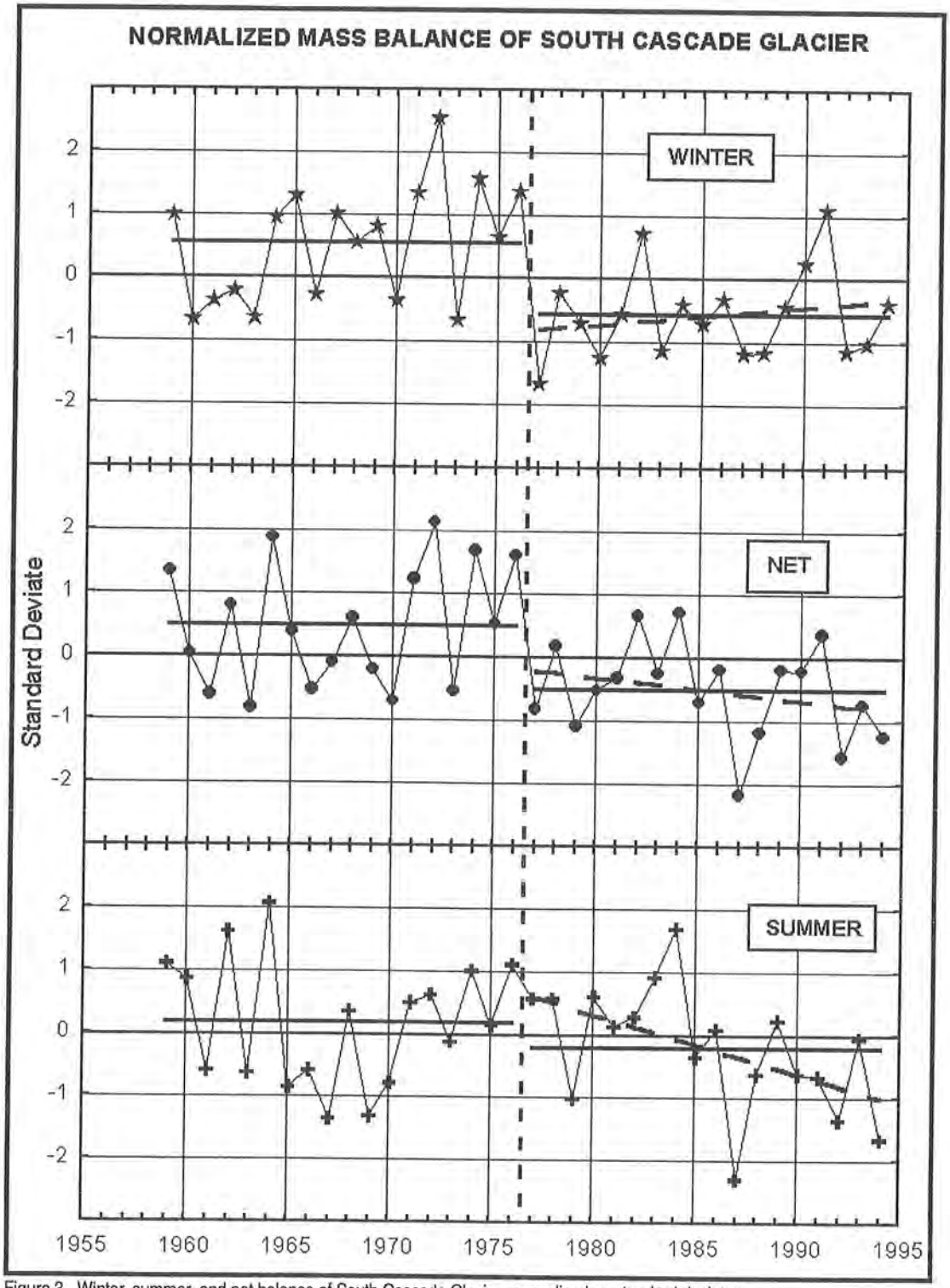

Figure 3 Winter, summer, and net balance of South Cascade Glacier, normalized as standard deviates.
Standard deviates are computed relative to the average for the entire data record. Average values before and after an assumed step change between 1976 and 1977 are shown as thick horizontal lines. Linear fits to the post-step data are shown as thick dashed lines.

These results are consistent with similar ones found from a large number of other environmental variables elsewhere in the Pacific Northwest (Ebbesmeyer *et al* 1991), including snowpack measurements made at USDA snow course sites (Dracup *et al* 1994). Figure 4 shows average snowpack at the end of March for all snow courses in the Washington Cascades (the "all Cascades" region defined in Figure 1) for the same period, 1959-1994, as the South Cascade Glacier balance measurements. All sites not having sufficient data to cover this period were excluded. The data were obtained from the Snow Survey Program, U.S. Department of Agriculture, Portland, Oregon. A step change between 1976 and 1977 is readily apparent in the overall snowpack.

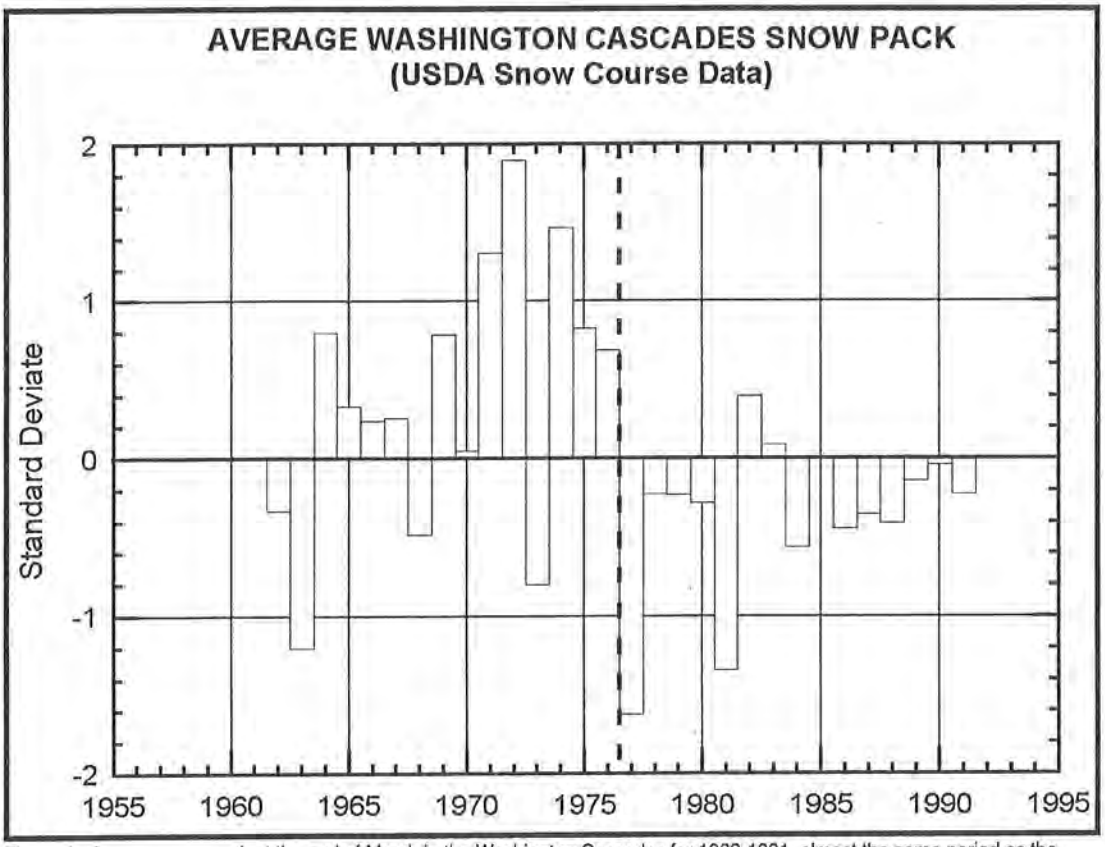

Figure 4 Average snowpack at the end of March in the Washington Cascades for 1962-1991, almost the same period as the South Cascade Glacier balance measurements.
Data are from USDA snow courses; sites that were used are shown in Figure 1.

Figure 5 shows the same data processed with techniques similar to those used for the mass balances, with the average value before and after the 1976-1977 step shown as thick horizontal lines. The data were filtered in various ways, by elevation, by "north" versus "all" Cascades, and by "March-only data" versus "all months of data". In all cases, a step decrease in 1977 is evident in the snow course data.

Accumulation and ablation on a temperate maritime glacier such as South Cascade Glacier are usually considered to be related primarily to regional winter precipitation and summer temperature, respectively (Paterson 1981). Figures 6-9 show average winter and summer temperature

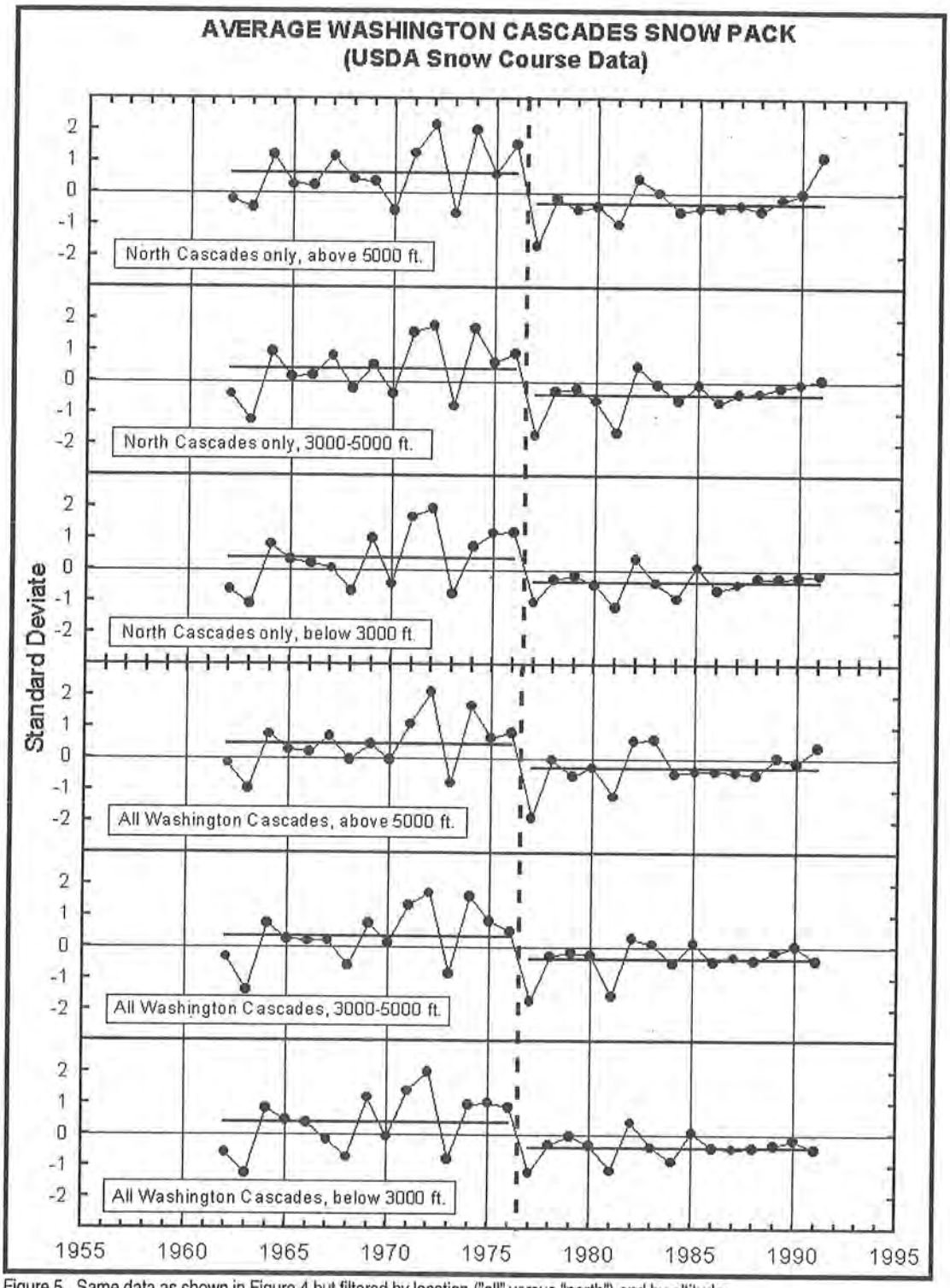

Figure 5 Same data as shown in Figure 4 but filtered by location ("all" versus "north") and by altitude.
Average values before and after an assumed step between 1976 and 1977 are shown as thick horizontal lines.

and precipitation for five climate stations: Paradise, Stehekin, Stampede Pass, Diablo Dam, and Concrete. These stations were selected because they are relatively close to South Cascade Glacier in either altitude or horizontal distance. Figures 6-9 also show regionally-smoothed data for

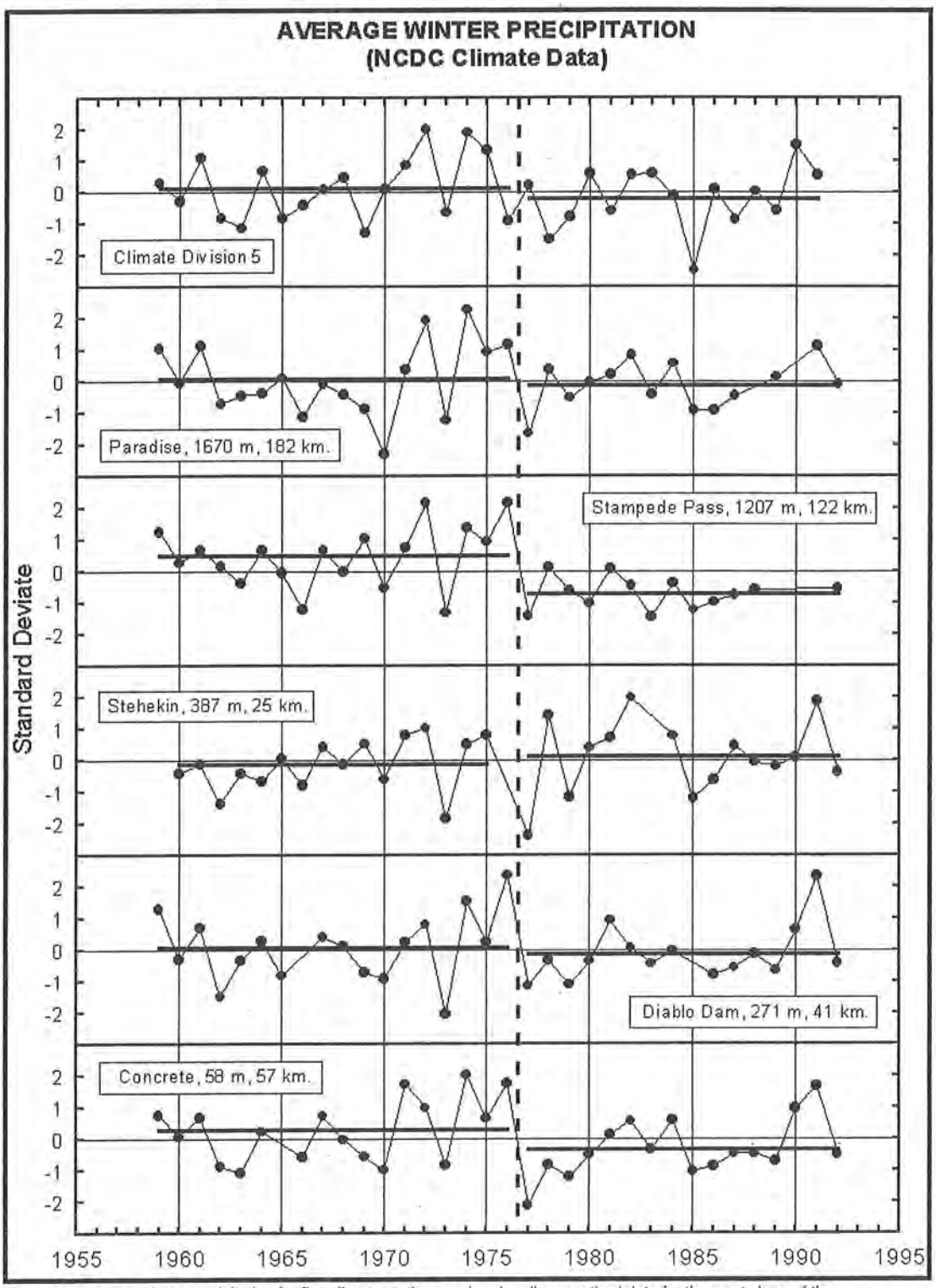

Figure 6 Average winter precipitation for five climate stations and regionally-smoothed data for the west slope of the North Cascades (Climate Division 5).
Altitude (m) and distance (km) from South Cascade Glacier are indicated after each station name.
Locations of the five climate stations are shown in Figure 1.

the west slope of the North Cascades (climate division 5). The data are from the National Climate Data Center, files TD-3200 (climate station data) and TD-9640 (climate division data). Daily values of climate station data and monthly values of climate division data were averaged to give

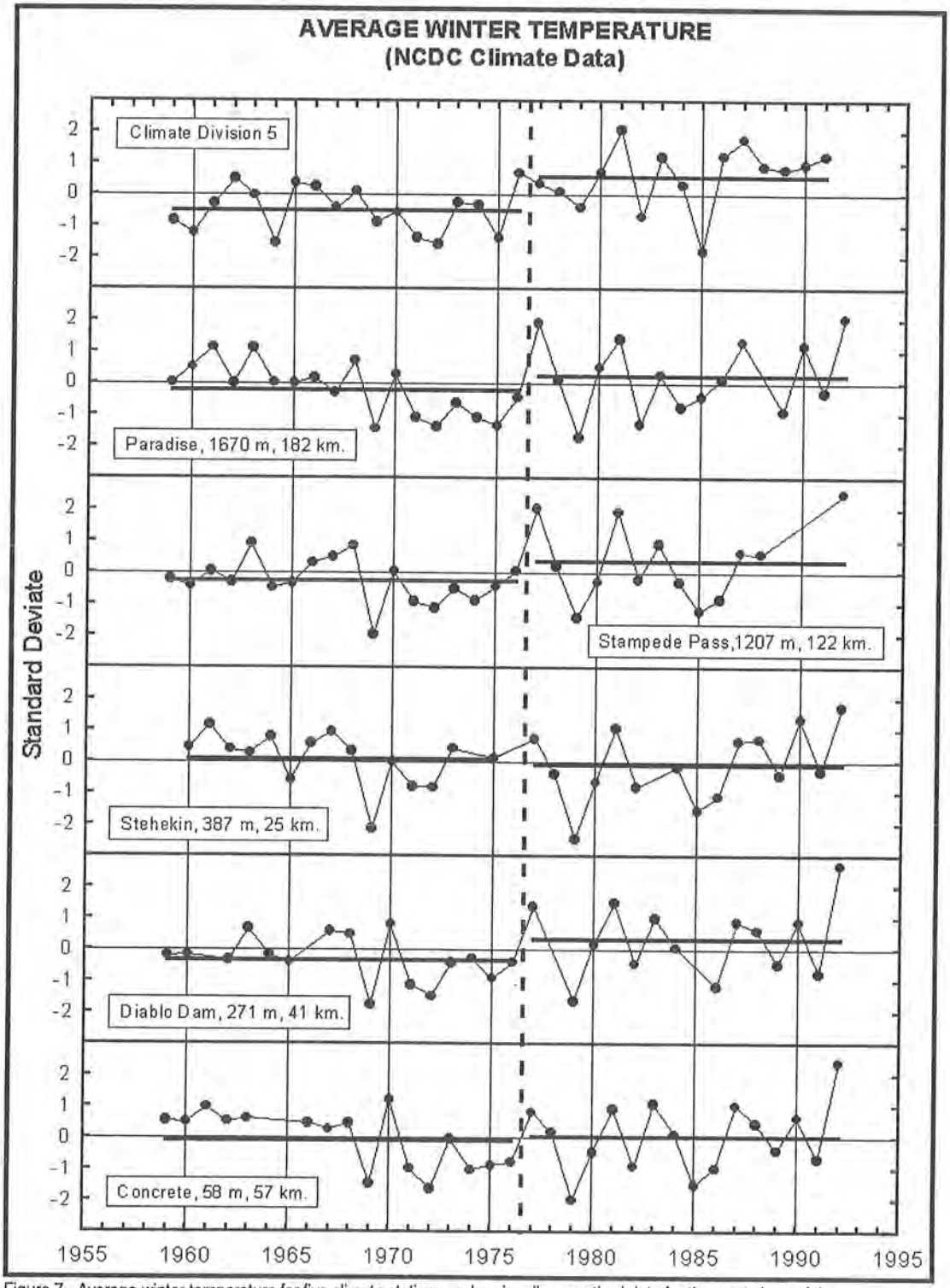

Figure 7 Average winter temperature for five climate stations and regionally-smoothed data for the west slope of the North Cascades (Climate Division 5).
Altitude (m) and distance (km) from South Cascade Glacier are indicated after each station name.
Locations of the five climate stations are shown in Figure 1.

winter and summer means for each year. Winter was defined as November through April, and summer was defined as May through October — the same periods as the balance seasons on South Cascade Glacier.

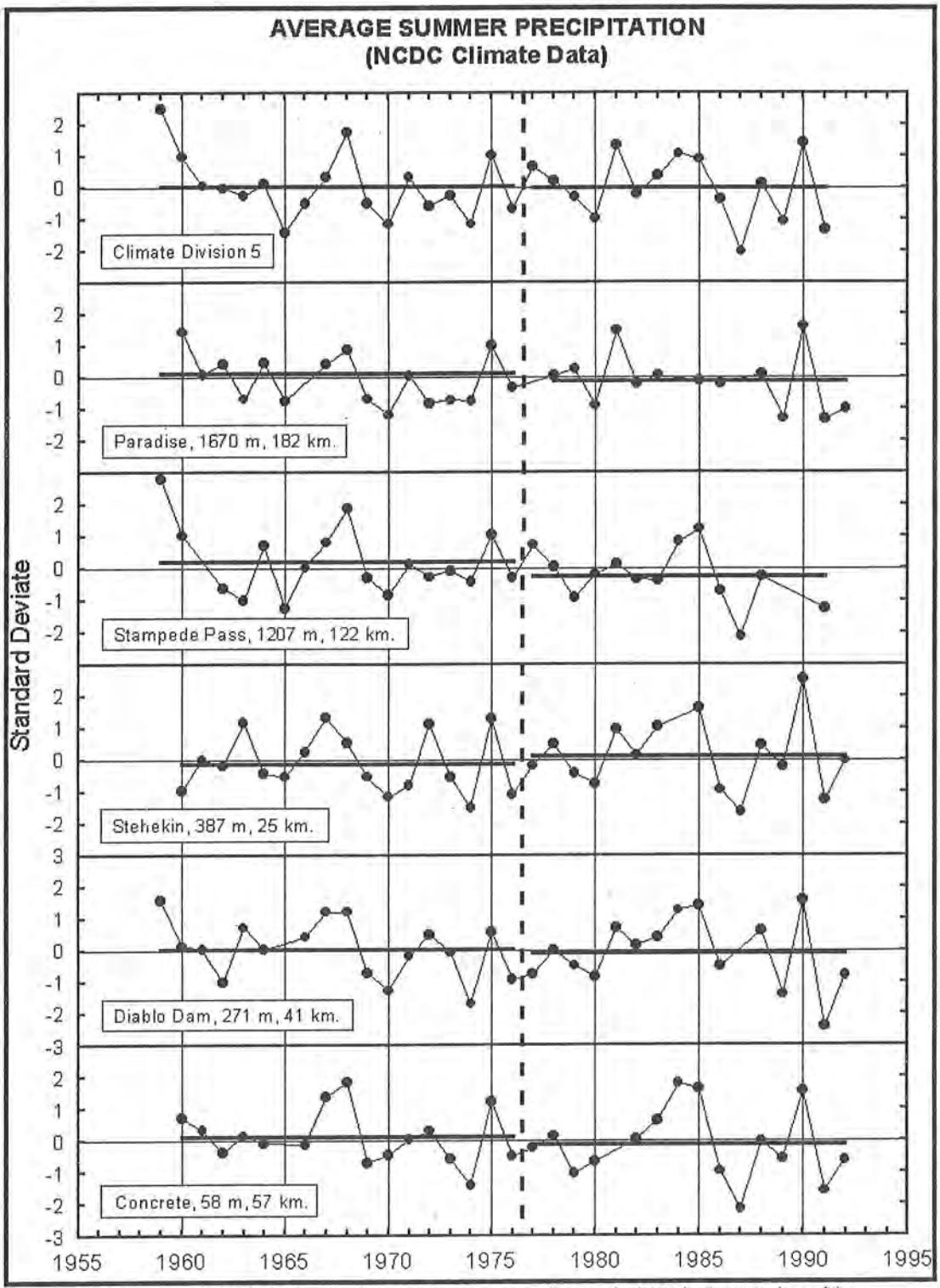

Figure 8 Average summer precipitation for five climate stations and regionally-smoothed data for the west slope of the North Cascades (Climate Division 5).
Altitude (m) and distance (km) from South Cascade Glacier are indicated after each station name.
Locations of the five climate stations are shown in Figure 1.

Even though only constant values were fitted to the data, to maintain consistency with Figures 3 and 5, it is clear that in all cases the average temperature, both in winter and in summer, has been increasing since 1977, and in most cases more rapidly in summer than in winter. This is

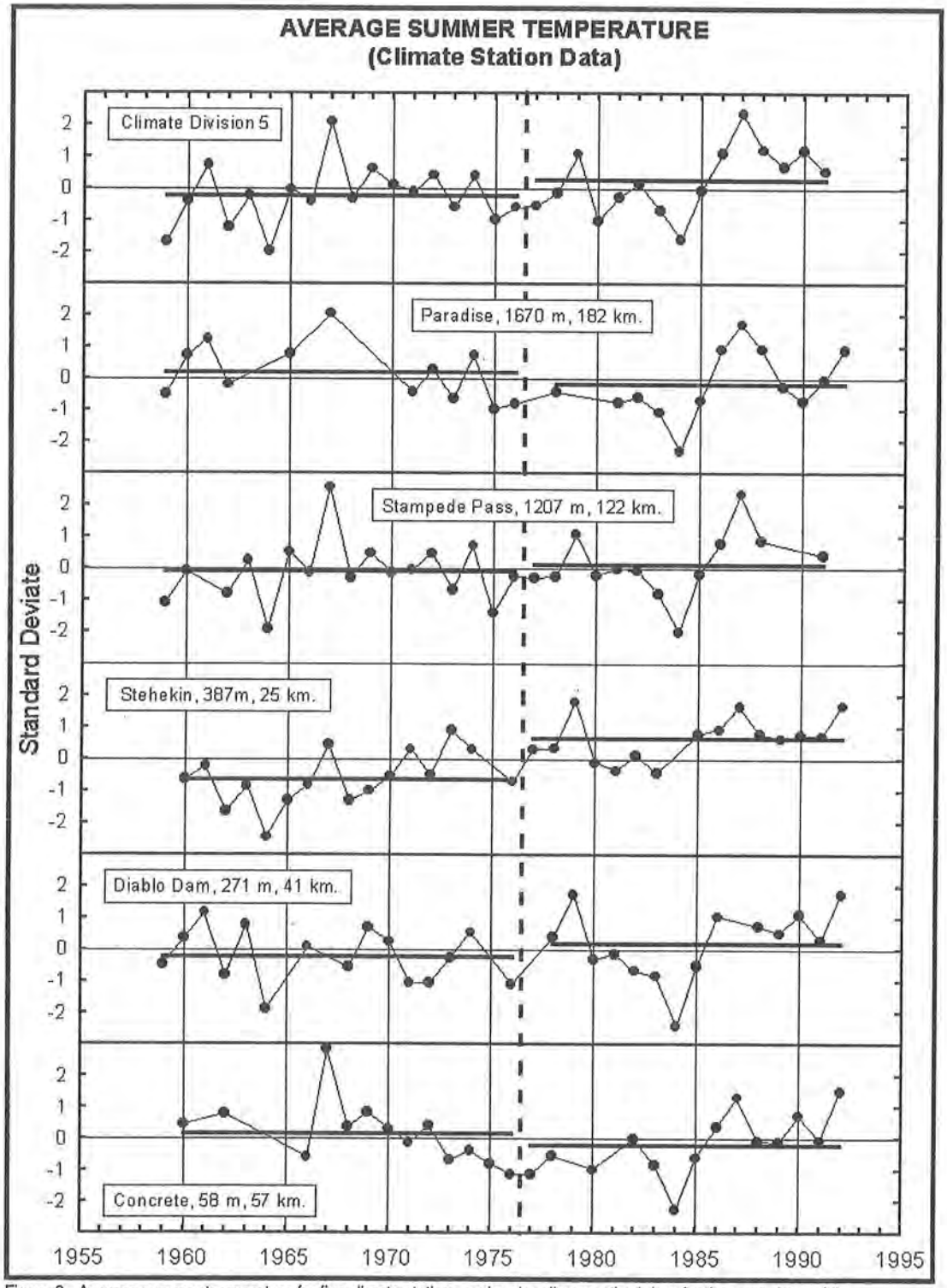

Figure 9 Average summer temperature for five climate stations and regionally-smoothed data for the west slope of the North Cascades (Climate Division 5).
Altitude (m) and distance (km) from South Cascade Glacier are indicated after each station name.
Locations of the five climate stations are shown in Figure 1.

consistent with our observations of steadily decreasing summer balance on South Cascade Glacier since 1977 and supports the concept that the summer ablation on a glacier in a temperate maritime regime is coupled to the regional summer temperature. However, except for Stampede Pass, the average winter precipitation does not show any evidence for a step-like change similar to that observed in the South Cascade Glacier winter mass balance or the snow course measurements, so the link between winter snow accumulation and regional winter precipitation is not as clear.

Discussion

Winter snowpack precipitation in the Washington Cascades, as indicated by either snow course or glacier mass balance measurements, underwent an abrupt decrease between 1976 and 1977, and has remained at about the new lower level since 1977. However, because this same decrease is not evident in the climate station winter precipitation, which is total precipitation regardless of form (rain or snow), it appears that the snowpack in the Washington Cascades must have decreased because a change in conditions prevented snow from accumulating.

Rising winter temperatures could be one such condition, since they would cause not only more precipitation to fall as rain rather than snow but also more mid-winter melting of snow (enough to cause runoff, not just refreezing). However, the fact that a step change occurred only in winter snow accumulation and not in regional winter temperature indicates that either other processes are involved or the overall mechanism is simply very sensitive to small perturbations, too small to be evident in regional climate data.

Neither of the trends observed at South Cascade Glacier, decreased winter accumulation or increased summer ablation, is conducive to glacier growth. The present trend is clearly away from an ice-age type of climate.

More important, however, regardless of the cause of observed trends, the data clearly demonstrate that a glaciologically significant long-term change in snow precipitation can occur very rapidly — in as short an interval as 1 year, much more rapidly than changes in temperature. Similar conclusions about extremely rapid transitions in accumulation rate from glacial to interglacial conditions, possibly in as little as 1 to 3 years, have been deduced from deep ice cores recently drilled in Greenland (Alley *et al* 1993).

Mass balance measurements on a glacier are, in effect, a direct measure of the particular combination of climate conditions, whatever they may be, that lead to or away from an ice-age type of climate. Our data indicate that such "glacial climate" can vary rapidly.

Conclusions

- Winter snowpack in the Washington Cascades underwent an abrupt decrease between 1976 and 1977 and has remained at about the new, lower level since 1977.
- This decrease occurred because of a change in conditions that prevented snow from accumulating, rather than because of a change in total regional winter precipitation.
- The long-term trends at South Cascade Glacier are decreased winter accumulation and increased summer ablation. Neither is conducive to glacier growth, so the current trend in the Pacific Northwest is clearly away from an ice-age type of climate.
- A glaciologically significant long-term change in snow precipitation can occur rapidly — in as short an interval as 1 year — much more rapidly than changes in temperature.

References

Alley, R.B., D.A. Meese, C.A. Shuman, A.J. Gow, K.C. Taylor, P.M. Grootes, J.W.C. White, W. Ram, E.D. Waddington, P.A. Mayewski, G.A. Zielinski. 1993. Abrupt increase in Greenland snow accumulation at the end of the Younger Dryas event. *Nature* 362:527-529.

Dracup, J.A., J.P. Sample, P.M. Wells. 1994. Climate induced change in the standard deviate of snow depth and water equivalent. Pages 9-16 in *Proceedings of the 62nd Annual Western Snow Conference*, April 1994, Santa Fe, New Mexico.

Ebbesmeyer, C.C., D.R. Cayan, D.R. McLain, F.H. Nichols, D.H. Peterson, K.T. Redmond. 1991. 1976 step in the Pacific climate: Forty environmental changes between 1968-1975 and 1977-1984. Pages 129-141 in *Proceedings of the Seventh Annual Pacific Climate (PACLIM) Workshop*, April 1990. J.L. Betancourt and V.L. Tharp, editors. California Department of Water Resources, Interagency Ecological Studies Program Technical Report 26.

Krimmel, R.M. 1993. *Mass Balance, Meteorological, and Runoff Measurements at South Cascade Glacier, Washington, 1992 Balance Year.* U.S. Geological Survey Open-File Report 93-640, 38 pp.

Paterson, W.S.B. 1981. *The Physics of Glaciers*. Second edition. Pergamon Press, Oxford, United Kingdom.

Interannual to Decadal Time-Scale Variations in Glacier Mass Balance

Roy A. Walters

Abstract

The mass balance of glaciers depends on the seasonal variation in precipitation, temperature, and insolation. For glaciers in western North America, these meteorological variables are influenced by the large-scale atmospheric circulation over the northern Pacific Ocean. The purpose of this study is to gain a better understanding of the relationship between mass balance at glaciers in western North America and the large-scale atmospheric effects at interannual and decadal time scales. This study investigates large-scale similarities between glaciers using exploratory data analysis, rather than examining the relationship between mass balance at a single glacier, and local and nonlocal forcing. This study is an extension of a previous study (Walters and Meier, AGU Monograph 55, 1989), which used empirical orthogonal function (EOF) analysis to bring out the large-scale similarities and differences in glacier behavior as recorded in the mass balance time-series. Once the EOF extraction is finished, the mode amplitude time-series are correlated with climatological variables, a procedure that emphasizes interannual variability. Results from this study are similar to those of the previous study, which had shorter time series available (20 years of simultaneous data at seven glaciers). Both glacier balances and EOFs show strong correlations with large-scale variations in seasonal 700-mb height anomalies and sea level pressure and weaker correlations with Southern Oscillation Index and Pacific North American index. These results support the conclusion that the largest modes in the EOF analysis have succeeded in capturing the synoptic-scale similarities in the datasets and showing that the response of the individual glaciers is more highly dependent on large-scale atmospheric conditions than on local-scale meteorological differences. The decadal scale variability is coherent over the southern set of glaciers in Washington State and British Columbia. Although the data are noisy, response of the northern set of glaciers in Alaska appears out of phase with response of the southern glaciers. This suggests that the decadal-scale variability in the glaciers is related to similar variability in pressure anomalies rather than to any basin-scale coherent process.

In: C.M. Isaacs and V.L. Tharp, Editors. 1996. *Proceedings of the Twelfth Annual Pacific Climate (PACLIM) Workshop, May 2-5, 1995.* Interagency Ecological Program, Technical Report 46. California Department of Water Resources.

The Little Ice Age: Glacier Variations and Climate Since AD 1250

Stephen C. Porter

Abstract

During the past hundred years, mountain glaciers throughout the world have retreated significantly from moraines built during the previous several centuries. In the 1930s, Francois Matthes of the U. S. Geological Survey concluded that the moraines represent the greatest advances of glaciers since the end of the last glacial age, some 10,000 years earlier, and informally referred to this late Holocene interval of expanded ice cover as the Little Ice Age.

In favorable situations, glacier time series having a resolution of about 10 years can be developed that span the past few centuries. In the European Alps and Scandinavia, reliable historical data about glacier variations (paintings, lithographs, sketches, maps, written documents, photographs) span the last 2-4 centuries, but for most of the world such data are restricted to the past 100 years. Dendrochronology can provide high-resolution dating at sites where glaciers terminated below the tree line, but often this approach provides only minimum ages for glacier recession during all or part of the last 6 centuries. Crustose lichens can be used to date moraines closely (about 10 years) in areas of rapid growth (*eg*, Alps, Cascade Range, Canadian Rockies), but slow lichen growth rates limit dating resolution in polar and subpolar latitudes. Results are most reliable where the three approaches can be combined (*eg*, European Alps) and where subfossil and living trees provide close dendrochronological and calibrated 14C age control prior to historical time.

The onset of the Little Ice Age, based on moraines in the Alps, Scandinavia, and northwestern North America, dates to the middle 13th century. Crop failures in Iceland and expanding sea-ice cover in the North Atlantic at that time also indicate progressive cooling, while in mainland Europe, wind storms and sea floods increased markedly. As summers became cooler and wetter, grain failed to ripen, wheat prices rose, and famine became pervasive. In England, the life expectancy fell by 10 years within only a century.

There was a brief respite during the 1500s when conditions became more equable, but by the end of that century, glaciers were again advancing, heralding the main phase of the Little Ice Age. By the early 1600s, many glaciers reached their greatest postglacial extent. Farms were overrun by advancing ice in the Alps, in Iceland, and in Scandinavia. During the worst years of that century, sea ice completely surrounded Iceland, and Denmark Strait was blocked by ice in the summer. In 1615 the cod fishery in the Faeroe Islands failed due to increasing ice cover. The hard winters of the Little Ice Age are clearly depicted by contemporary artists who painted with stark realism the snowy landscapes, frozen rivers, and stormy skies of northern Europe.

The decade of 1810-1819 was the coldest in Europe since the 17th century, and it witnessed renewed advances of glaciers to new maxima in the Alps. The erratic weather of the 19th century led to further crop failures, rising grain prices, epidemics, and famines and resulted in large-scale emigration, especially to North America. By the middle of the century, however, rising temperature led to widespread retreat of glaciers and sea ice, signaling the end of the Little Ice Age.

In: C.M. Isaacs and V.L. Tharp, Editors. 1996. *Proceedings of the Twelfth Annual Pacific Climate (PACLIM) Workshop, May 2-5, 1995.* Interagency Ecological Program, Technical Report 46. California Department of Water Resources.

Glacier fluctuations of the Little Ice Age are unrelated to orbital forcing and show no obvious correlation with solar variations. However, their decadal-scale pattern resembles the succession of major sulfur-emitting volcanic eruptions that lowered mean tropospheric air temperatures by 0.4-1.0°C for up to several years.

References for Further Reading:

Davis, P.T., and G. Osborn (eds). 1988. Holocene glacier fluctuations. *Quaternary Science Reviews* 7:113-242.

Grove, J.M. 1988. *The Little Ice Age.* London, Methuen.

Kasser, P., and W. Haeberli (eds). 1981. *Switzerland and Her Glaciers, From the Ice Age to the Present.* Berne, Kümmerly and Frey.

Ladurie, E.L. 1971. *Times of Feast, Times of Famine: A History of Climate Since the Year 1000.* New York, Doubleday.

Nesje, A., and T. Johannessen. 1992. What were the primary forcing mechanisms of high-frequency Holocene glacier and climatic variations? *The Holocene* 1:79-84.

Orombelli, G., and S.C. Porter. (1982). Late Holocene fluctuations of Brenva Glacier. *Geografia Fisica e Dinamica Quaternaria* 5:14-37.

Porter, S.C. 1981. Glaciological evidence of Holocene climatic change. Pages 82-110 in T.M. Wigley, M.J. Ingram, G. Farmer (eds), *Climate and History.* Cambridge, Cambridge University Press.

Porter, S.C. 1986. Pattern and forcing of Northern Hemisphere glacier variations during the last millennium. *Quaternary Research* 26:27-48.

Röthlisberger, F. 1987. *10,000 Jahre Gletschergeschichte der Erde.* Aarau, Verlag Sauerländer, 416 pp.

The Terrestrial Paleorecord of Climate Change over the Past Thousand Years in the Canadian Rockies

Brian H. Luckman

Abstract

High alpine environments provide a variety of paleorecords based on physical (glaciers, glacio-lacustrine sedimentation) and biological systems (tree rings, tree-line fluctuations). These records have varying temporal resolution and contain different climate-related signals but, in concert, provide a more comprehensive reconstruction of past climates than is possible from any single archive. The glacier record, which has been the traditional reference source in this area, is discontinuous and abbreviated because the classic 18th and 19th century "Little Ice Age" moraines represent the most extensive Holocene glacier event in this area. Evidence of a less extensive glacier advance between AD 1140 and 1370 is found at three glaciers, and there is fragmentary less-precisely dated evidence of glacier events in the mid-16th and early 17th centuries at some sites. The dendrochronological records routinely cover the past 300-400 years but include millennial chronologies in three species. These records show strong regional suppression in ring-width series corresponding to the early 18th, mid-19th and late 20th century glacial events plus periods in the mid-14th, mid-15th, and late-16th/early 17th centuries for which little well-dated glacial evidence is available. Glacio-lacustrine sediment records show strong evidence for the glacial event in the 13th century at Bow Lake and for a mid-15th century event at Moose Lake. Studies of snag populations at three sites show relatively abrupt periods of dieback of treeline populations associated with the late 16th and 17th centuries that are presently unexplained.

Although there is strong evidence for a Little Ice Age glacial event, it is much more difficult to recognize this event in the more continuous dendrochronological and glacio-lacustrine records. Taken together, the data provide evidence of multiple glacial events in the last 1000 years which, although poorly resolved prior to AD 1700, generally indicate a pattern of progressively more extensive glacial advances culminating in the 18th and 19th centuries. The concept of a "Medieval Warm Period" and "Little Ice Age" as distinctive climatic intervals of several centuries' duration is clearly a gross oversimplification, as glacier advances and intervening warmer periods occurred throughout the last millennium.

In: C.M. Isaacs and V.L. Tharp, Editors. 1996. *Proceedings of the Twelfth Annual Pacific Climate (PACLIM) Workshop, May 2-5, 1995.* Interagency Ecological Program, Technical Report 46. California Department of Water Resources.

Variability in a Radiolarian Time Series and Its Relationship to Climate

Amy L. Weinheimer and Daniel R. Cayan

Abstract: Recently, paleoceanographers have been challenged to produce reliable proxies of climate variables that can be incorporated into climate models. In developing proxies using time series of annual radiolarian species fluxes from Santa Barbara Basin, we identify groups of species associated with years of extreme sea surface temperatures and sea level heights. The relative fluxes of warm and cool species are generally inversely related in 1914-1991 and fairly reliably reflect SST in 1955-1991. However, these groups do not reflect SST in 1914-1954, even though their fluxes continued to be inversely related. Species associated with high and low sea level height exhibit a similar pattern. Analysis of species structure indicates variability within the system and no evidence of assemblages from surrounding provinces dominating the species structure at any time. Failure of the proxies in 1914-1954 may be due to changes within the California Current System or in the biologic response to hydrographic conditions, or it may indicate a problem with our chronology of the varves.

Predicting climate and climate change through modeling is important to both science and economics. Climate varies over time scales of years to centuries and can shift abruptly or change gradually. Low frequency changes over the past century have been attributed to both anthropogenic effects and to natural variability of the climate system (Bloomfield and Nychka 1992; Keeling *et al* 1992; Wigley and Raper 1990). To separate these sources of observed change, we need to know magnitude and frequency of natural climate variability. However, instrumental records are short relative to the important time scales of variability (decadal-century; Bloomfield and Nychka 1992). Instrumental records used to develop and validate climate models span, at most, 150 years. One way to extend instrumental records and provide time series for validation of models is to use natural records (*ie*, tree rings, ice cores, corals, sediment). These longer records also contain a history of the full range of climate variability, with several realizations of decade and longer scale changes not available in instrumental records. Until we have records with sufficient realizations of this variability, our understanding of the causes of climate change is limited.

Over the past century, global temperatures have been increasing. Initiation of this "global warming" coincides with the industrial revolution, prompting the hypothesis of the greenhouse effect. Alternatively, the warming may be an expression of low frequency, natural variability. To separate natural and anthropogenic effects, we need a history of climate prior to instrumental records with which we can put changes of the past century into context with respect to natural variability. Extending the

In: C.M. Isaacs and V.L. Tharp, Editors. 1996. *Proceedings of the Twelfth Annual Pacific Climate (PACLIM) Workshop, May 2-5, 1995*. Interagency Ecological Program, Technical Report 46. California Department of Water Resources.

instrumental records with the marine record can be done mainly with corals or sediment. Reconstructions of temperature and salinity from corals have been successful (Dunbar *et al* 1994; Linsley *et al* 1994). However, large, long-lived corals used in paleoclimate reconstructions are restricted to tropical latitudes, and a major source of climate forcing is in the mid-latitudes (Latif and Barnett 1994).

Environmental conditions are also recorded continuously in marine sediments. Ideally, with seasonal deposition of sediment and low oxygen bottom waters, annual layers of sediment are preserved. These conditions exist in the Santa Barbara Basin in the Southern California Borderland (Koide *et al* 1972; Soutar and Crill 1977). Annual laminations are preserved in this sediment throughout the Holocene (Kennett, Baldauf, *et al* 1994). Seasonal runoff of terrigenous material during winter, alternating with biogenic siliceous material in spring and summer, generates a layered pattern in the sediment. These varves (one year of sediment composed of one dark and one light layer) are preserved because the low oxygen water entering the basin excludes burrowing animals from the bottom of the basin. In addition to its ideal depositional environment, the geographic location of Santa Barbara Basin lies at a center of action for both oceanic and atmospheric circulation patterns (Davis 1976). Cross correlations of California regional sea surface temperatures with North Pacific SST and Northern Hemisphere 700mb heights show coherence and teleconnections between Santa Barbara Basin and the North Pacific Basin and North America.

There has been some debate over how well records from Santa Barbara Basin represent the California Current. However, several studies show that these records reflect basinwide oceanic and atmospheric conditions (Miller *et al* 1994; Lange *et al* 1990; Weinheimer and Cayan 1994). In fact, recent results from the longest cores taken in Santa Barbara Basin, those of the Ocean Drilling Program, suggest that paleoceanographic changes over the past 20ky in the basin are linked, probably by atmospheric coupling, to similar events in the Atlantic Ocean (Kennett and Ingram 1995). There is strong evidence that its sedimentary record contains multiple proxies of Pacific-wide fluctuations in oceanic and atmospheric conditions (Pisias 1979; Lange *et al* 1990; Weinheimer 1994). In this region, changes in oceanic circulation and water masses strongly influence SSTs, planktonic assemblages and productivity (Lange *et al* 1990; Pisias 1978). Typically, during periods of high sea level pressure over the Central North Pacific, southward flow of the California Current is strong, resulting in low SST, low sea level height (SLH), high productivity, and cool water planktonic assemblages in Santa Barbara Basin. These conditions reverse with low pressure over the Central North Pacific. Results presented here are the latest in developing the radiolarian component in the Santa Barbara Basin sediment as proxies of instrumental records used in measuring climate-induced fluctuations in the California Current.

Methods

Varved sediments in the Santa Barbara Basin were collected by boxcore (SBBC 9110 1302-2; 34°12.9'N, 120°03.2'W, 588m). A vertical slab of the boxcore was sampled at annual resolution using a contact print of an x-radiograph as a template, and the surface area of each annual sample measured. The >45 µm siliceous fraction was extracted, and a known volume was analyzed for radiolarians, identifying 300-500 specimens, per year. Annual accumulation rates (no.cm^{-2} y^{-1}) were calculated for the total radiolarian assemblage (Figure 1) and for each species from 1914 to 1991.

We developed a different approach in grouping species into climatically indicative units than we have used in the past. Previously, we grouped species according to their water mass affinity (*ie*, Weinheimer and Cayan 1994). Although these "environmental" groups reflected regional to hemisphere scale climatology, we wanted more objective definitions of the groups. Since we know radiolarians with cold and warm affinities are found in Santa Barbara Basin sediment, we chose two instrumental records reflecting cold and warm conditions in the California Current System (SST and SLH) to compare to species accumulation rates. We used annually averaged, 5-degree-gridded monthly mean SST from 30-40°N, 135-120°W (Parker and Jackson 1995), to derive the annual regional SST time series. The sea level height record is a composite of annually averaged Los Angeles monthly detrended sea level height (1924-1991) from the Permanent Service for Mean Sea Level dataset and annually averaged San Francisco monthly sea level height (1914-1923) in Cayan *et al* (1991). Although these records have monthly resolution,

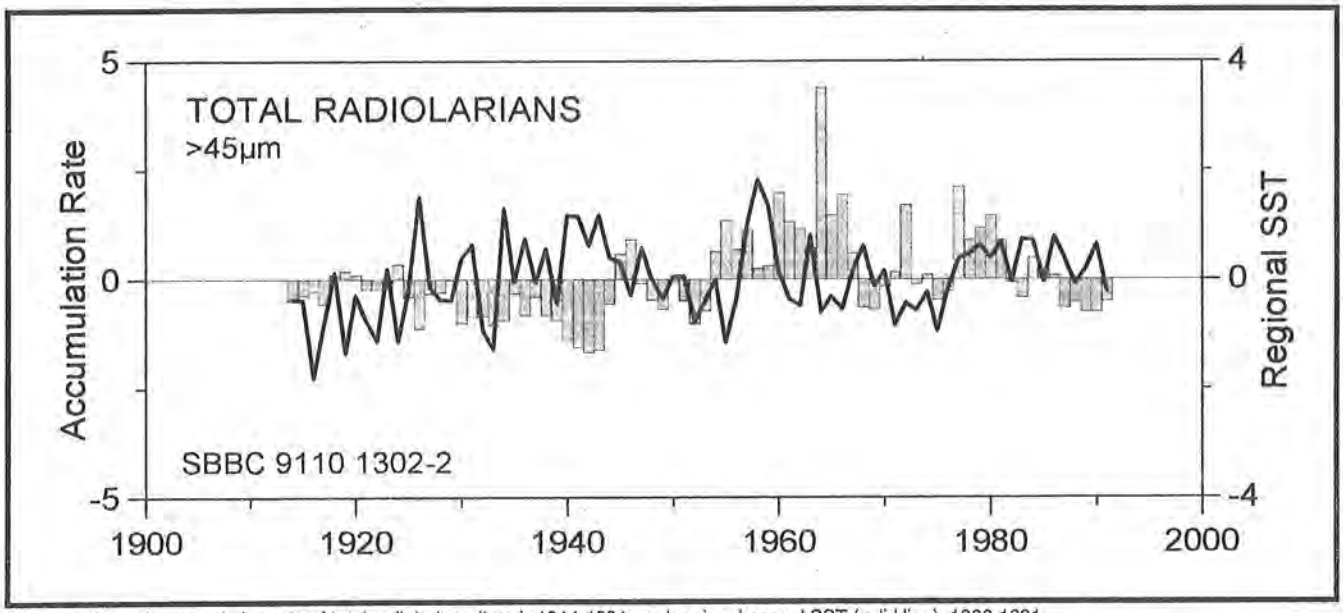

Figure 1 Annual accumulation rate of total radiolarians (bars), 1914-1991, and regional annual SST (solid line), 1900-1991. Both time series are shown as standard anomalies taken over the period illustrated.

we chose to annually average them to match the scale of resolution available in the sedimentary record. Whether the deposition of radiolarians in the Santa Barbara Basin is episodic, occurring within one season or another, as in diatoms (Grimm *et al* in press) is not presently known. Half of the time series was used to develop these proxies (1955-1991) and the other half for validation (1914-1954). Species associated with warm SST were identified by comparing, using t-tests, their average flux for the 12 years with the warmest winter SSTs in 1955-1991 to their average flux in the balance of the years between 1955 and 1991. Similarly, species associated with cool SSTs were identified in the 12 coolest winters. Four categories of species resulted: category 1 contains species with higher flux in the 12 years with the warmest winters; category 2 contains species with lower flux in the 12 years of warmest winters; category 3 contains species with higher flux in 12 years of coolest winters; and category 4 contains species having lower flux in the 12 years of coolest winters. This procedure was repeated for spring, summer, and fall. We summed the accumulation rates for species with similar responses to SST (*ie*, species with higher fluxes in years with warmest seasons, *etc*) to generate the four time series in Figure 2; the same was done for SLH (Figure 3). No species is represented more than once in the paired SST or SLH time series.

Conceivably, a cosmopolitan type species might have high flux during both cool and warm years. Although a few species, for example, had high fluxes in years with warm season(s) and low fluxes in years with cool season(s), only one species exhibited high fluxes for both warm and cool years. This species was not included in further analyses. No species was associated with both high and low SLH. In cases in which a species had high flux in years of warm (cool) seasons and low flux in years of cool (warm) seasons, it was grouped with species that had high fluxes in warm (cool) years. The same method was used for the SLH groups.

Results

As a first evaluation of the relationship between radiolarian flux and hydrographic conditions, we compared the total flux to regional annual SST (Figure 1). Decadal trends in flux and SST after 1950 resemble each other but do not appear closely related prior to 1950. This change in relationship to SST may reflect a problem with our chronology or a change in the response of the radiolarians to SST. If the cause is biological, then evidence of change, such as in the species present, should coincide with the shift in response to SST around 1950. We investigated the possibility of a biological effect using the Spearman rank correlation (Sokal and Rolf 1969) to measure interannual similarities in assemblages.

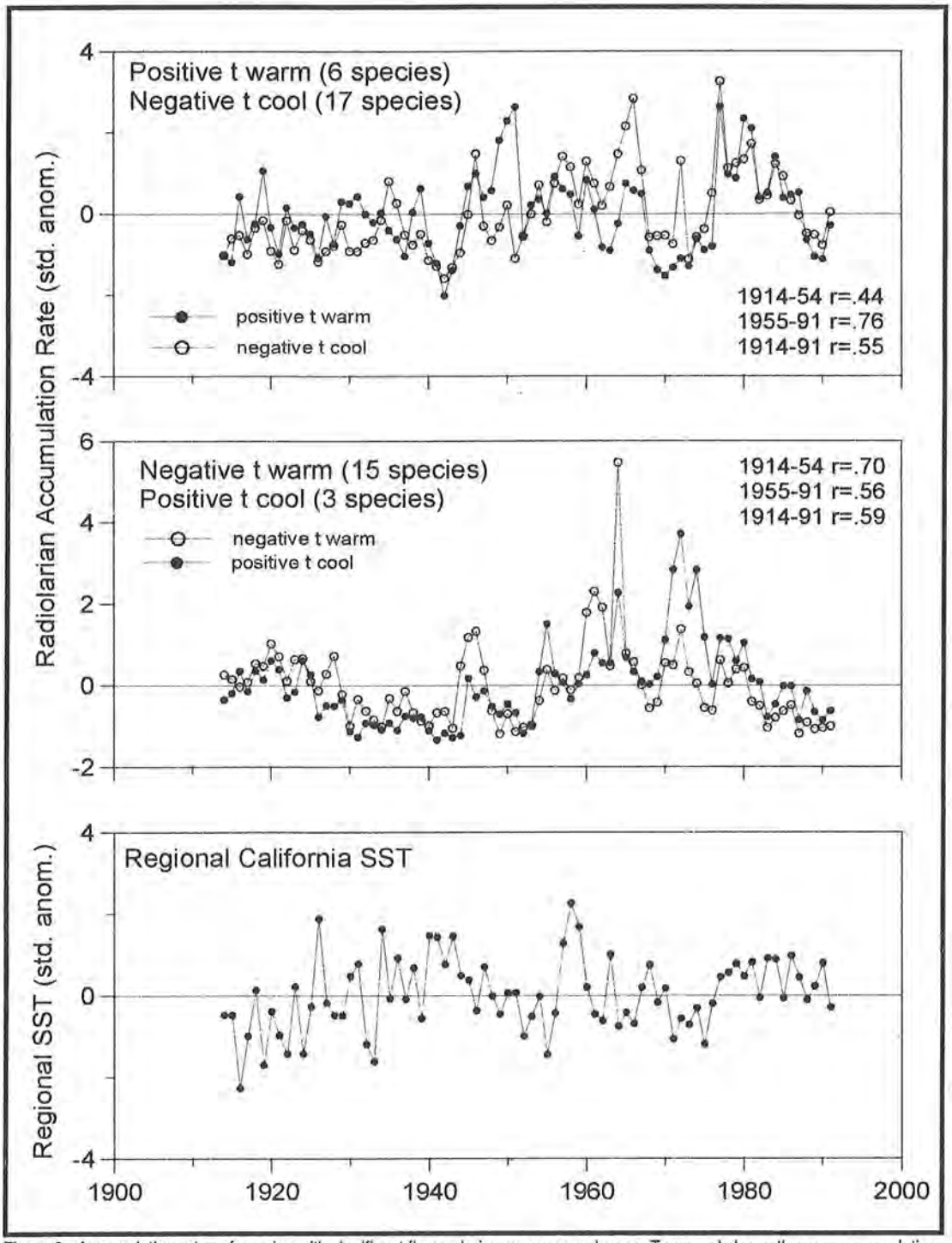

Figure 2 Accumulation rates of species with significant fluxes during warm or cool years. Top panel shows the sum accumulation rate of "warm" species with higher fluxes during warm years (positive t warm) and with lower fluxes in cool years (negative t cool). Middle panel shows the sum accumulation rate of "cool" species with lower fluxes during warm years (negative t warm) and higher fluxes during cool years (positive t cool). The number of species comprising each time series is in parentheses and correlation coefficients for each pair of time series is in the respective panel. SST is in the bottom panel. All data are standard anomalies calculated over the period illustrated.

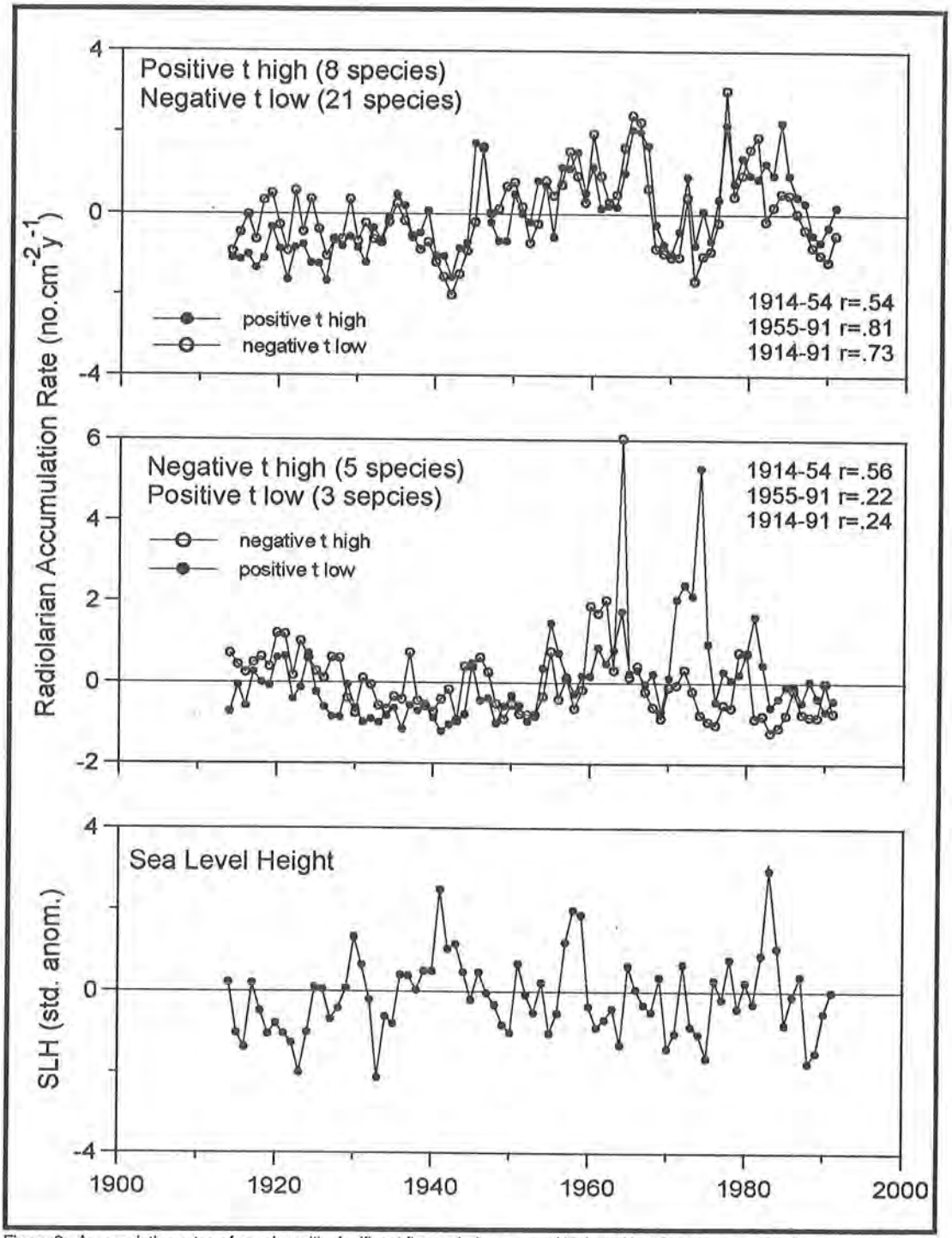

Figure 3 Accumulation rates of species with significant fluxes during years of high and low SLH. Top panel is the accumulation rate for "high" sea level species with higher fluxes in high SLH years (positive t high) and lower fluxes in low SLH years (negative t low). Middle panel shows the accumulation rate for low, SLH species with lower fluxes in high SLH years (negative t high) and higher fluxes in low SLH years (positive t low). The number of species used in each time series is in parenthesis and correlation coefficients between pairs are listed in both panels. SLH in the bottom panel is a composite of San Francisco (1914-1923) and Los Angeles (1924-1991) SLHs. All data are standard anomalies calculated over the period illustrated.

Species Structure

Consistency in species structure over a geographic region can be used to delimit oceanic ecosystems (McGowan and Walker 1985). Conversely, change in species structure over time or space can indicate a geographic shift in a boundary in time or transgression of a boundary in space. As a measure of species structure, we used the Spearman rank correlation (Sokal and Rolf 1969) of species abundance where a rank of 1 indicates identical species rank structure, 0 indicates no similarity, and –1 indicates inverse structure. The average coefficient for each year (Figure 4) ranged from r=0.51-0.87 (mean=0.83, r significant at 95%=0.251). Although there was some interannual variability in species structure, the correlations suggest no major shift in species structure. Years with lower coefficients tended to be associated with El Niño and warm years (1942, 1943, 1957, 1965, 1986) and, generally, years in the second half of the time series had slightly lower average coefficients than the first half. This suggests that faunas from different provinces may have been introduced to the California Current system during El Niño or warm events, and also perhaps more frequently since the 1950s.

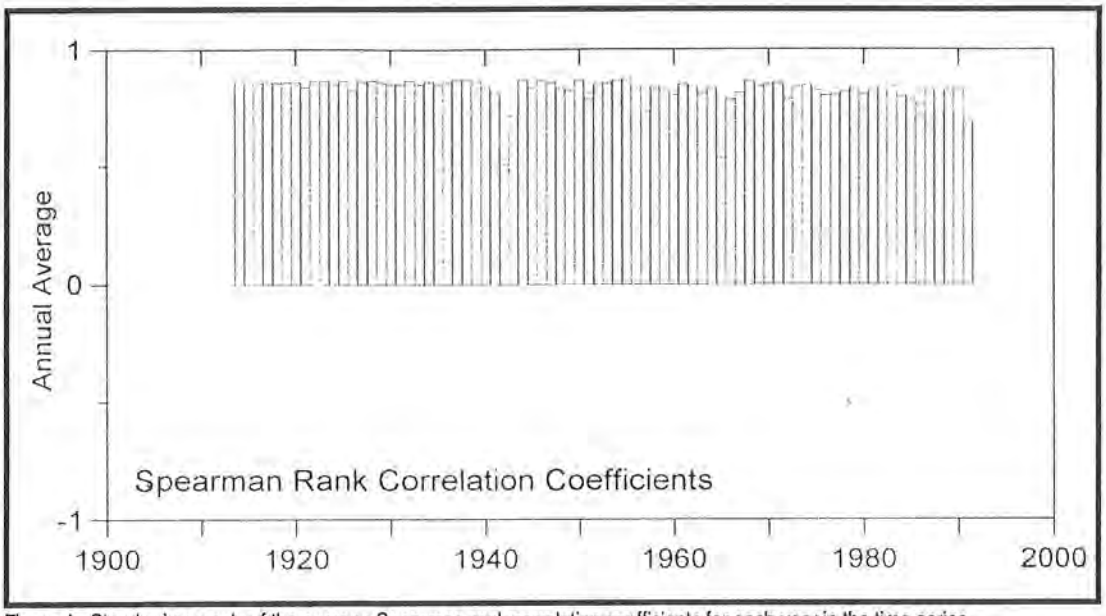

Figure 4 Standard anomaly of the average Spearman rank correlation coefficients for each year in the time series.

Class Accumulation Rates

The high correlation between series in each pair illustrated in Figures 2 and 3 shows, for example, that species with warm affinities (low flux during cool years or high flux during warm years) respond similarly to environmental conditions. Correlations for 1914-1954 are generally as high as for 1955-1991, indicating that the species in each pair of series represents a coherent unit. Since the series in each pair are so similar, we summed their ARs to form four classes: warm and cool based on SST and high and low based on SLH.

Class Percents

An obvious feature of the percent warm and cool class time series (Figures 5 and 6) is their inverse relationship, maintained in both the developmental (1955-1991, r = -0.77) and independent (1914-1954, r = -0.89) periods. The SLH classes are also inversely related but not as dramatically (r = -0.69 and -0.76, respectively). Even though the warm and cool classes were defined using extreme SSTs, the correlations with SST generally are not significant, with percent cool correlating better to SST than percent warm (Table 1). The percents of high and low SLH class also correlate poorly to the instrumental SLH record. Interestingly, not only do the SST and SLH classes validate, in spite of their lack of agreement to instrumental records, but the SST classes are more disparate in 1914-1954 than in 1955-1991.

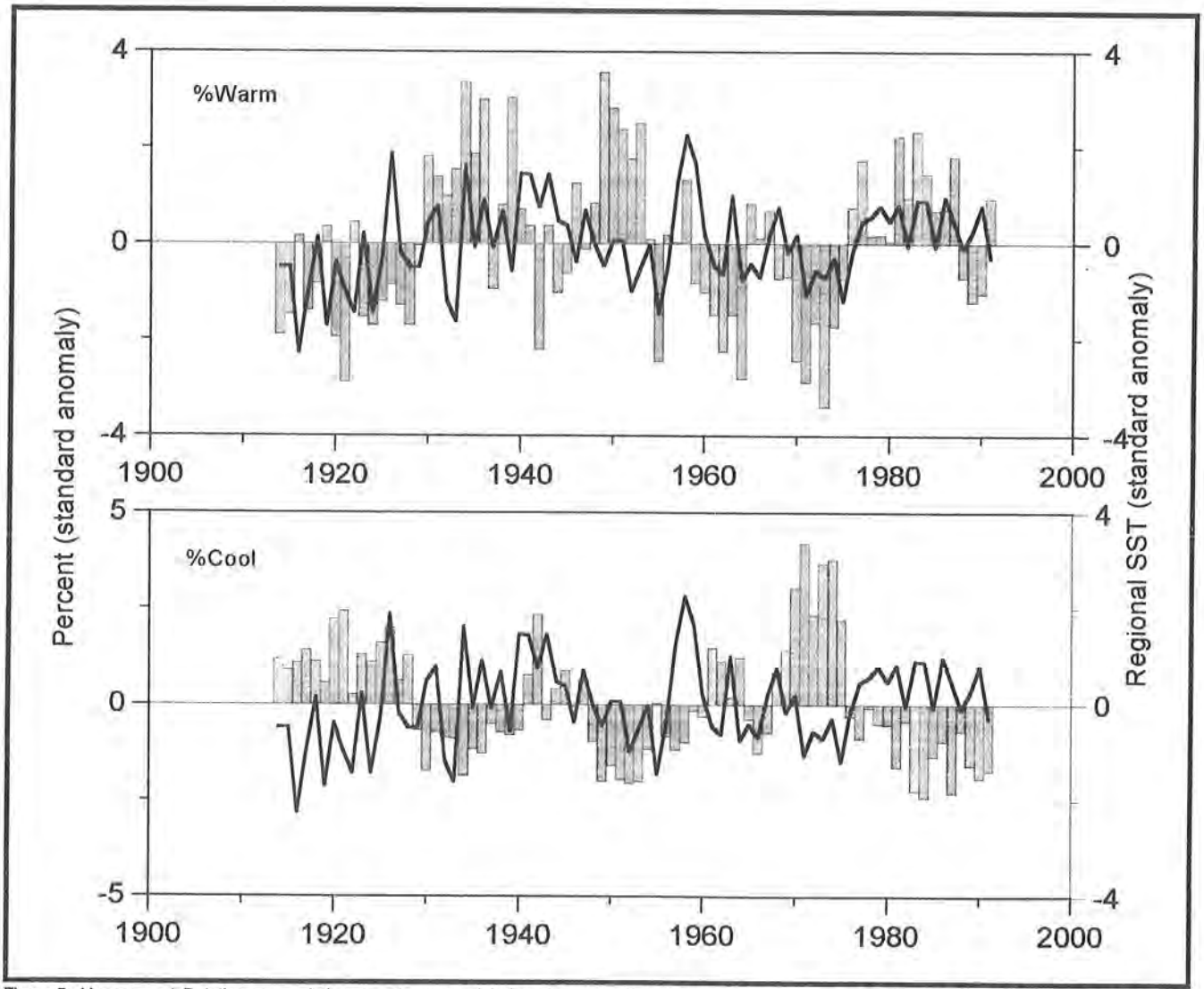

Figure 5 Upper panel: Relative accumulation rate of warm radiolarians (species with high fluxes in warm years or low fluxes in cool years) (bars) and the regional SST (solid line).
Lower panel: Relative accumulation rate of cool radiolarians (species with low fluxes in warm years or high fluxes in cool years) (bars) and the regional SST (solid line). All data are standard anomalies calculated over the period illustrated.

Neither fluxes of the SST or SLH classes (Figures 2, 3, 5, and 6) show a pattern related to the years of low Spearman rank correlation coefficients; therefore, it is unlikely that species entering during El Niños contribute much to the SST or SLH class fluxes, and perhaps they constitute a third discernible group within the radiolarian assemblage.

We hypothesize that the warm and high SLH classes of radiolarians would increase with SST and SLH, respectively. In general, fluxes follow this pattern, but during about 1930-1950, they are opposite to what we expect. The same is true for the cool and low SLH radiolarians, suggesting a problem with the chronology or a change in the relationship between the instrumental and the biological records. We doubt the chronology is off by more than plus or minus a few years, and it would have to be off by a decade or so to make the radiolarian and instrumental records fit.

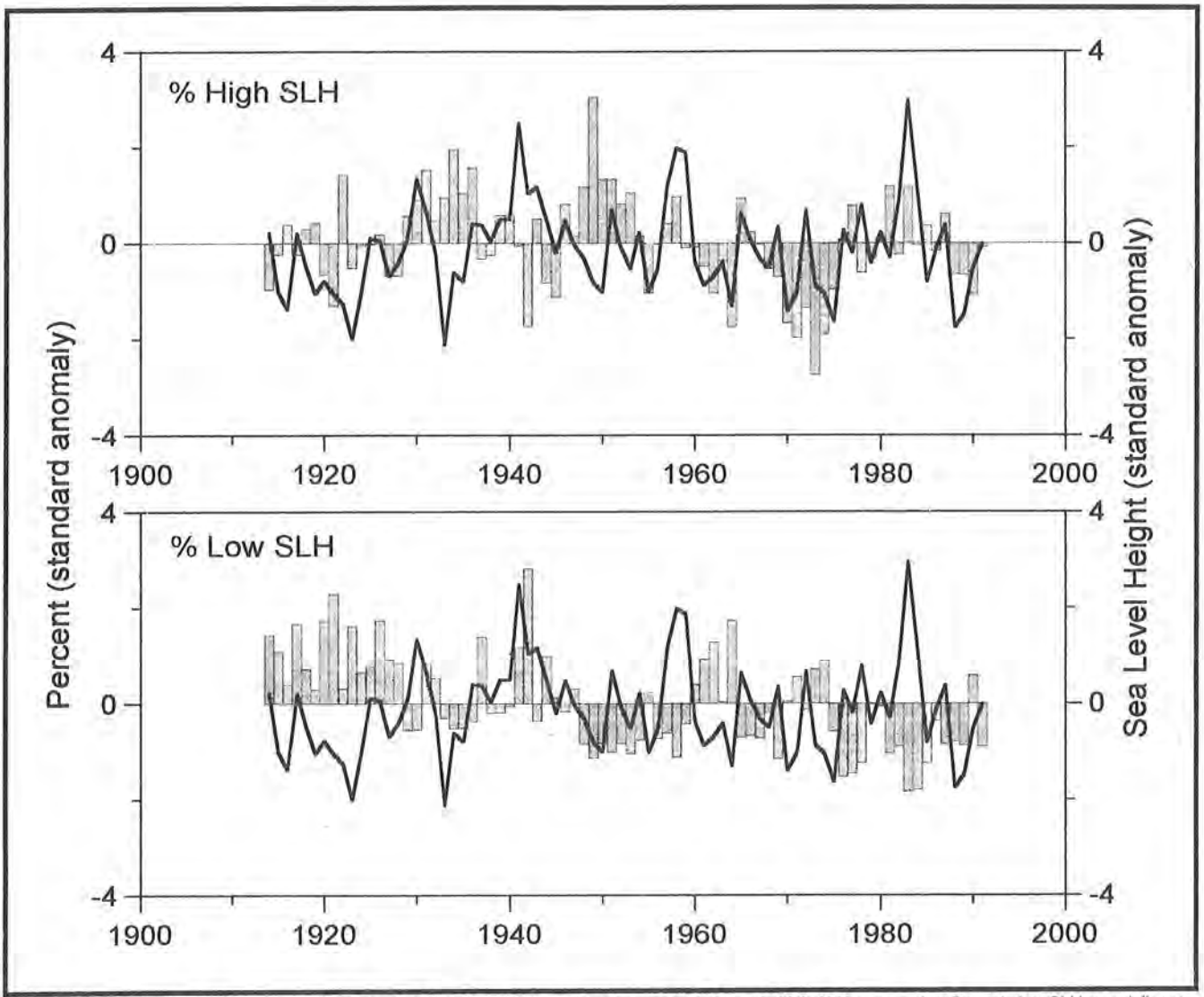

Figure 6 Upper panel: Relative accumulation rate of high SLH radiolarians (species with high fluxes in high SLH years or low fluxes in low SLH years) (bars) and annual SLH (solid line).
Lower panel: Relative accumulation rate of low SLH radiolarians (species with low fluxes in high SLH years or high fluxes in low SLH years) (bars) and annual SLH (solid line). All data are standard anomalies calculated over the period illustrated.

Table 1
CORRELATION COEFFICIENTS FOR PERCENT SST AND SLH RADIOLARIAN GROUPS ON SST AND SLH FOR THE YEARS USED TO DEVELOP THE GROUPS (1955-1991), THE VALIDATION PERIOD (1914-1954), AND THE ENTIRE TIME SERIES (1914-1991)

Years	% Warm on % Cool	% Warm on SST	% Cool on SST
1914-1954	-0.89	0.03	-0,03
1955-1991	-0.77	0.53	-0.61
1914-1991	-0.80	0.14	-0.29
Years	**% High on % Low**	**% High on SLH**	**% Low on SLH**
1914-1954	-0.50	-0.08	0.02
1955-1991	-0.76	0.58	-0.53
1914-1991	-0.69	0.23	-0.23

Alternatively, the hydrography during 1930-1950 may have been anomalous, and the typical interpretation of SST and SLH as indicators of flow in the California Current System is inadequate.

Conclusions

Sediment from Santa Barbara Basin contains several records for modeling (paleo)climate. Promising results from analysis of the annual radiolarian record indicate that they may represent a multivariate history of climate. We have some optimism that total radiolarian accumulation rate generally reflects regional SST of decadal time scales, providing a general history of the California Current System. It is not clear, however, whether SST is truly the environmental variable controlling radiolarian density or whether it is just a surrogate for some other mechanism(s). Typically, warm SSTs prevail when the California Current is sluggish, upwelling is diminished and more water from the south and west enters the system. Since radiolarian density off California increases offshore and southward, similar to the pattern of SST, we expect their flux to increase with SST. Although the fluxes of total, percent warm, and percent cool reflect SST fairly well from 1950-1991 and 1914-1930, during 1930-1950 the relationship of flux to SST is opposite what we expect. The mismatch in 1930-1950 raises questions whether the radiolarian and SST relationship changes through time or whether the chronology of the core is inaccurate. The internal consistency of the radiolarian classes suggests that either some external force (not reflected in the SST record) is influencing the radiolarian flux or that the chronology is wrong, but this would require shifting the dates ±10 years to make the fluxes fit the instrumental record. We doubt this is entirely the case, based on correlations between this core (SBBC 9110 1302-2) and several others from Santa Barbara Basin. Distinct layers in the cores make

correlations fairly straight forward, and multiple cores provide us many expressions of the varves from which to interpret the age.

If we accept that the chronology is accurate within a few years, then the radiolarian distributions in 1930-1950 with respect to the instrumental records is opposite to what our hypothesis predicts. Assuming the instrumental records reflect the oceanography of the California Current System, there should be evidence in the species structure indicating a definite shift in the assemblage. Measuring species structure with Spearman rank correlation coefficients does not reveal any changes until the late 1930s, several years after the mismatch begins, and the coefficients are only slightly lower than average. Although the species structure apparently did not change, groups of species can be identified that are inversely related through time, which shows that there was some variability in species structure. The Spearman rank correlation is not sensitive enough to detect these subtle changes in relative flux (rank) within a large assemblage of species with fairly constant ranks.

In future research, we will investigate the period of 1930-1950 to determine the character of the mismatch between the biological and instrumental records. By analyzing in greater detail the species composition for these two decades and correlating between the radiolarians and instrumental records at various lags, we should be able to better evaluate this period.

Bibliography

Bloomfield, P., and D. Nychka. 1992. Climate spectra and detecting climate change. *Climatic Change* 21:275-287.

Davis, R. 1976. Predictability of sea surface temperature and sea level pressure anomalies over the North Pacific Ocean. *J. Phys. Oceanogr.* 6:249-266.

Dunbar, R.B., G.M. Wellington, M. Colgan, P.W. Glynn. 1994. Eastern Pacific climate variability since 1600 AD: Stable isotopes in Galapagos corals. *Paleoceanogr.* 9(2):291-315.

Grimm, K.A., C.B. Lange, A.S. Gill. In press. Biological forcing of hemipelagic sedimentary laminae: evidence from ODP Site 893, Santa Barbara Basin, California. *J. Sed. Res.*

Keeling, C.D., T.P. Whorf, M. Wahlen, J. van der Plicht. 1992. Interannual extremes in the rate of rise of atmospheric carbon dioxide since 1980. *Nature* 375(6533):666-670.

Kennett, J.P., J.G. Baldauf, *et al.* 1994. Proc. ODP, Init. Repts., 146 (Pt. 2), College Station, TX (Ocean Drilling Program). 92 pp.

Kennett, J.P., and B.L. Ingram. 1995. A 20,000-year record of ocean circulation and climate change from the Santa Barbara Basin. *Science* 377:510-514.

Koide, M.A., A. Soutar, E.D. Goldberg. 1972. Marine geochronology with 210Pb. *Earth Planetary Sci. Lett.* 14:442-446.

Lange, C.B., S.K. Burke, W.H. Berger. 1990. Biological production off southern California is linked to climatic change. *Climatic Change* 16:319-329.

Latif, M., and T.P. Barnett. 1994. Causes of decadal climate variability over the North Pacific and North America. *Science* 266:634-637.

Linsley, B.K., R.B. Dunbar, G.M. Wellington, D.A. Mucciarone. 1994. A coral-based reconstruction of Intertropical Convergence Zone variability over Central America since 1707. *J. Geophys. Res.* 99(C5):9977-9994.

McGowan, J.A., and P.A. Walker. 1985. Dominance and diversity maintenance in an oceanic ecosystem. *Ecological Monographs* 55(1):103-118.

Miller, A.J., D.R. Cayan, T.P. Barnett, N.E. Graham, J.M. Oberhuber. 1994. Interdecadal variability of the Pacific Ocean: Model response to observed heat flux and wind stress anomalies. *Climate Dynamics* 9:287-302.

Parker, D.E., and M. Jackson. 1995. The standard GISST data sets: Versions 1 and 2. Pages 50-51 in *Workshop on Simulations of the Climate of the Twentieth Century using GISST.* C.K. Folland and D.P. Rowell, editors. Hadley Centre for Climate Prediction and Research CRTN 56.

Pisias, N.G. 1978. Paleoceanography of the Santa Barbara Basin during the last 8000. *Quat. Res.* 10:366-384.

Pisias, N.G. 1979. Model for paleoceanographic reconstructions of the California Current during the last 8000 years. *Quat.* Res. 11:373-386.

Sokal, R.R., and F.J. Rolf. 1969. *Biometry.* Freeman and Company, San Francisco. 776 pp.

Soutar, A., and P.A. Crill. 1977. Sedimentation and climatic patterns in the Santa Barbara Basin during the 19th and 20th centuries. *Geol. Soc. Am. Bull.* 88:1161-1172.

Weinheimer, A.L. 1994. Radiolarian and diatom fluxes in two California Borderland basins as indices of climate variability. Ph.D. Dissertation, University of California, Santa Barbara, California. 117pp.

Weinheimer, A.L., and D.R. Cayan. 1994. Radiolarian flux in the Santa Barbara Basin as an index of climate variability. Pages 107-118 in *Proc. 11th Annual Pacific Climate (PACLIM) Workshop.* C.M. Isaacs and V.L. Tharp, editors. Calif. Dept. of Water Resources, Interagency Ecol. Stud. Prog. Report 40.

Wigley, T.M.L., and S.C.B. Raper. 1990. Natural variability of the climate system and detection of the greenhouse effect. *Nature* 344:324-327.

Evidence for Changes in Large-Scale Upwelling in the California Current over the Past 700 Years

Tim R. Baumgartner and John Southon

Abstract

Bidecadal radiocarbon measurements on tree rings provide a detailed series of ^{14}C activities at isotopic equilibrium with atmospheric CO_2. This terrestrial series reflects the variable production of ^{14}C in the atmosphere, resulting from variability in cosmic-ray flux, and is used for calibration of the atmospheric ^{14}C ages to dendrochronological ages. The ^{14}C ages of oceanic materials are subject to an additional complication. This is because oceanic radiocarbon ages depend not only on simple exchange with the atmosphere but also on regional variations induced by ocean circulation related to climate change. Most marine environments do not permit development of a comparable series of ^{14}C ages with which to compare the terrestrial tree ring series. However, we have recently begun work on such a series using material from the varved sediments of the Santa Barbara Basin off southern California. We are dating samples of the pelagic pteropod *Limacina helicina*, which lives in the upper 100 meters of the water column and which is sufficiently abundant in these sediments to provide material for AMS dating of intervals as short as 5 years. The varve chronology, although still not perfectly accurate, permits age calibration to within 10 years. We now have a nearly continuous record of ^{14}C dates representing the age of the water over the upper 100 meters. This record now extends from AD 1260 to 1900 and is resolved into intervals that vary from 5 to 20 years. The time series of ocean-terrestrial age differences (the regional ocean-reservoir ages) of contemporaneous samples exhibits variability over centennial time scales that cannot be explained by a constant rate of ventilation of deeper waters. The relative age of the water was oldest at about AD 1450. The ocean reservoir ages show an increase prior to 1450 and a progressive decrease with time after 1450. Although there may be other explanations, we believe this trend is principally the result of changes in large-scale upwelling of water from below 500 meters. These changes were probably also associated with changes in the intensity of the California Current. If this is true, the large-scale upwelling along the eastern boundary of the North Pacific gyre during the past millennium appears to have been at its most intense around AD 1450. The period between 1450 and 1900 appears to have experienced a long-term decrease in pumping of deeper/older water toward the surface.

In: C.M. Isaacs and V.L. Tharp, Editors. 1996. *Proceedings of the Twelfth Annual Pacific Climate (PACLIM) Workshop, May 2-5, 1995.* Interagency Ecological Program, Technical Report 46. California Department of Water Resources.

On the Strength of the California Current: A Record from the Southern Baja California Margin

Juan Carlos Herguera, Tim Herbert, Vicente Ferreira Bartrina

Abstract

To characterize the strength of the flow of the California Current, we searched in the southern Baja California continental margin, the southernmost site affected by its relatively cool and less saline waters. We retrieved several cores from a silled basin, also known as Cuenca San Lazaro or Soledad, located at 25°10'N) with a sea-floor depth of 540 meters. This basin collects biogenic sediments that record the variations in the strength of the cooler flow of the California Current from the north and of the warmer tropical waters from the south. The laminated nature of the record preserves information with an annual to interannual periodicity of the dynamics of this boundary. It is precisely during El Niño years when records show the strongest sea surface temperature anomalies for the whole North American coast, comparable in size only to the equatorial thermal anomalies. This thermal contrast is also a marked feature in the annual variations of the SSTs for this site, one of the highest observed seasonal thermal contrast off the North American shores affected by the current. Our study site is further characterized by high levels of primary productivity, mostly a consequence of the advection of the cold nutrient-rich California current waters and associated upwelling processes, which are responsible for the production and high export of organic matter, opaline and calcite shells to the sea-floor. Here we present some preliminary results based on the fluxes of planktic foraminifera and the paleotemperature determinations derived from the alkenone biomarker in organic extracts from the sediment, known as the U^{k}_{37} reconstruction method.

In: C.M. Isaacs and V.L. Tharp, Editors. 1996. *Proceedings of the Twelfth Annual Pacific Climate (PACLIM) Workshop, May 2-5, 1995.* Interagency Ecological Program, Technical Report 46. California Department of Water Resources.

Oceanographic Variability at Clipperton Atoll Since the 1880s: Stable Isotopic Evidence from Massive Corals

Braddock K. Linsley and Robert B. Dunbar

Abstract

Clipperton Atoll (10°18'N, 109°13'W), lies within the eastern Pacific elongated warm water pool centered at 10°N and is situated at the boundary of the North Equatorial Counter-Current (NECC) and westward-flowing eddy currents moving away from Central America. This area is on the periphery of the influence of ENSO's warm events, with SSTs anomalies averaging +1°C. The stable SST field drives convection in the eastern Pacific intertropical Convergence Zone, resulting in rainfall that exceeds 3 meters/year. Fifteen coral cores were collected from massive heads of *Porites lobata* in April 1994 for the purpose of reconstructing oceanographic and climatic conditions at this open ocean site in the eastern Pacific. The colonies were all growing near the outer edge of a 10-13 meter terrace surrounding the atoll. The four longest coral cores from different heads extend back into the 1880s, even with the exceptionally high growth rates, which average 2.2 centimeters/year.

Sub-annual $\delta^{18}O$ and $\delta^{13}C$ analyses were performed on selected cores at intervals of about 10 to 20 samples per year, and annually averaged samples were analyzed on three cores to examine long-term trends back to the 1880s. Calibration of the isotopic data was performed using *in situ* and satellite derived SSTs. MSS estimated precipitation, monthly cloud cover, and wind fields, and a salinity climatology. The annual 1-2°C range in SST appears to be accurately record by the $\delta^{18}O$ composition of these corals with only a small effect of salinity or the $\delta^{18}O$ (sub-seawater). The long-term $\delta^{18}O$ annually-averaged records all demonstrate that SST in this region has been generally stable for the past 120 years with the exception of the last 10 years, which show a 0.5°C warming in concordance with SST data and the more frequent occurrence of ENSO events. For $\delta^{13}C$, the subannual sampling reveals that $\delta^{13}C$ minima coincide with $\delta^{18}O$ minima, with the most depleted values occurring at the end of the dry season when SST is at a maximum. This correlates with the initiation of the low density portion of annual skeletal growth. The annually averaged $\delta^{13}C$ data reveal generally stable $\delta^{13}C$ values from the 1880s until the mid-1960s, when a >1‰ trend toward depleted values occurs that continues through April 1994. The origin of this $\delta^{13}C$-depleted trend is unclear. CZCS data reveal that tradewind-induced coastal upwelled waters from central Mexico extend west past Clipperton. We hypothesize that this change in coral $\delta^{13}C$ is the result of increased westward advection of upwelled coastal waters and decreased influence of the NECC at Clipperton.

In: C.M. Isaacs and V.L. Tharp, Editors. 1996. *Proceedings of the Twelfth Annual Pacific Climate (PACLIM) Workshop, May 2-5, 1995.* Interagency Ecological Program, Technical Report 46. California Department of Water Resources.

Oxygen Isotope Analysis of Corals from the Gulf of California and the Gulf of Panama: Application and Implications for Coral-Based Paleoclimate Reconstructions

William A. Jones, Robert B. Dunbar, Gerard M. Wellington

Abstract

Coral-based reconstruction of past variability of sea surface conditions is improving our understanding of the tropical ocean-atmosphere system. We present oxygen isotope records from corals collected near the tip of Baja California (Baja) and the Gulf of Panama (Saboga). The Gulf of California experiences a large annual range in temperature related to seasonal upwelling and the influence of the California Current. The Gulf of Panama experiences a large range of temperature and salinity related to the seasonal migration of the intertropical Convergence Zone that produces wind-induced upwelling early in the year and a pronounced wet season from May to December. The isotope records are calibrated with COADS, GEDEX, interpolated Reynolds, AVHRR, and site observations of sea surface temperature. Salinity and proxy salinity data developed from rainfall and river discharge records are used to calibrate the Saboga coral. Seasonal and monthly calibration of the Baja coral attests to the presence of a strong annual temperature cycle, but annually averaged data exhibit limited correlation with temperature. Poor constraint of annual and interannual variability of the isotopic content of the Gulf of California water contributes to the weak annual correlation. The bimonthly Saboga record correlates strongly with salinity (r^2=0.72) and proxy salinity (r^2=0.66) and moderately with annual salinity (r^2=0.45). Temperature is not significant at $p<0.05$ in calibrations using both salinity and temperature as dependent variables but is weakly correlated (r^2=0.2) with temperature as the only dependent variable after applying a water correction term. Most, but not all, ENSOs appear in both records as a depletion in the annual maximum isotopic values. The catastrophic 1982-83 event is absent from the Saboga record. A strong coherence between records from the Gulf of Chiriqui (>300 kilometers away) and Uraba Island, Gulf of Panama (>60 kilometers) indicates that the corals are recording regional signals in addition to local reef conditions. The Saboga coral exhibits a strong coherence to the interannual Panama rainfall measured at Barro Colorado Island. Each record shows a trend toward drier conditions since the early 1950s. A 20-year isotope record from a Pleistocene coral taken from a marine terrace near the Baja coral exhibits similar annual variability as the modern coral and the possible occurrence of two ENSO events. There is evidence in both records of a step (*eg*, Ebbesmeyer 1991) toward more positive isotope values occurring in the mid-1970s, but we do not argue for interpretation as a climatic "state" shift.

In: C.M. Isaacs and V.L. Tharp, Editors. 1996. *Proceedings of the Twelfth Annual Pacific Climate (PACLIM) Workshop, May 2-5, 1995.* Interagency Ecological Program, Technical Report 46. California Department of Water Resources.

Integrating Varve and Tree-Ring Time Series for Southern California Climate Reconstruction: A 20th Century Outlook

Franco Biondi, Carina B. Lange, Kimberly Cobb, Wolfgang Berger

Abstract

Our objective is to combine terrestrial and oceanic records for reconstructing West Coast climate. Tree rings and marine laminated sediments provide high-resolution, accurately dated proxy data on the variability of climate and on the productivity of the ocean and have been used to reconstruct precipitation, temperature, sea level pressure, primary productivity, and other large-scale parameters. We present here the latest Santa Barbara basin varve chronology for the twentieth century as well as a newly developed tree-ring chronology for Torrey pine (*Pinus torreyana* Parry ex Carr). Varve thickness was measured both visually and using an image analysis system on the same set of X-radiographs. The year-to-year variation in total varve thickness is mostly a function of the light layer thickness (summer deposition). Interestingly, the linear trend caused by sediment compaction was observed in the total and dark layer thicknesses only; there was no significant trend in the light layer. The Torrey pine chronology is well correlated with other tree-ring chronologies for Southern California. The correlation with local and regional climatic parameters suggests that the dark layers within Santa Barbara varves are mostly related to local rainfall, whereas tree-ring indices reflect regional precipitation. Additional studies are underway to assess the response of varve and tree-ring records to variability in sea surface temperature and coastal sea level height.

In: C.M. Isaacs and V.L. Tharp, Editors. 1996. *Proceedings of the Twelfth Annual Pacific Climate (PACLIM) Workshop, May 2-5, 1995.* Interagency Ecological Program, Technical Report 46. California Department of Water Resources.

Synoptic Dendroclimatology: A Process-Based Approach for Linking Tree-Ring Information to Atmospheric Circulation over the Pacific and Western North America

Katherine K. Hirschboeck, Fenbiao Ni,
Michelle L. Wood, Connie A. Woodhouse

Abstract

Synoptic dendroclimatology uses dated tree rings to study and reconstruct climate from the viewpoint of the climate's weather components and their relationship to atmospheric circulation. This approach defines a connection between large-scale circulation and ring-width variation at local sites using correlation fields, composite maps, indexing, and other circulation-based methodologies. Correlation fields between ring widths at a site and gridded geopotential heights represent "circulation response patterns" (CRPs). Composite circulation maps of individual high or low growth "signature" years can be compared with CRPs. We constructed CRPs and circulation composite maps for two tree-ring localities in the western United States that have a sensitivity to winter climate: a chronology from central Oregon, and a regional average chronology from northern New Mexico. Results show that high and low tree growth at the two sites are associated with two totally different large-scale prior-winter circulation patterns. In Oregon, growth is enhanced by lower-than-normal 500-mb pressure heights over the Gulf of Alaska. The composite map for high-growth years depicts the same pattern, while the composite for low-growth years is an inverse of the CRP. The correlation and composite maps for northern New Mexico depict a circulation relationship that is completely different from the Oregon site. High growth is correlated with a belt of North Pacific Ocean lower-than-normal 500-mb heights that extends into the southwest. Low-growth years are dominated by a strong ridge over the lower southwest.

In: C.M. Isaacs and V.L. Tharp, Editors. 1996. *Proceedings of the Twelfth Annual Pacific Climate (PACLIM) Workshop, May 2-5, 1995.* Interagency Ecological Program, Technical Report 46. California Department of Water Resources.

Atmospheric Circulation Patterns Associated with Tree Growth Anomalies in the Central and Southern Sierra Nevada Mountains

Gregg M. Garfin

Abstract

Previous authors (Graumlich 1993; Hughes and Brown 1992; LaMarche 1974) have discussed long-term fluctuations of climatic parameters reconstructed from tree rings sampled in the Sierra Nevada. In this work, I examine patterns of atmospheric circulation associated with tree growth anomalies at mid-to-high altitudes (2000-3500 meters). Although atmospheric circulation patterns associated with past tree growth anomalies cannot be unequivocally interpreted from the tree-ring record, knowledge of climatic controls over tree growth anomalies can lead to richer interpretations of the extensive dendrochronological resource from the Sierra Nevada.

In: C.M. Isaacs and V.L. Tharp, Editors. 1996. *Proceedings of the Twelfth Annual Pacific Climate (PACLIM) Workshop, May 2-5, 1995.* Interagency Ecological Program, Technical Report 46. California Department of Water Resources.

Climate-Driven Hydrologic Transients in Holocene Lake Records

Alison J. Smith, Joseph J. Donovan, Daniel R. Engstrom,
Emi Ito, Valerie Panek, Eric Gong

Understanding the link between climate and regional hydrologic processes is of primary importance in estimating the possible impact of future climate change and in the validation of climate models that attempt to simulate such changes. Two distinct problems need to be addressed:

- Quantitatively establishing the link between changes in climate and the hydrologic cycle, and
- Determining how these changes are expressed over differing temporal and spatial scales.

To solve these problems, our interdisciplinary group is studying important aspects of hydrology, paleolimnology, geochemistry, and paleontology as they apply to climate-driven hydrologic changes.

Detailed Holocene records of regional surface hydrology may be reconstructed in terms of both ground water flow and solute composition. We have chosen a region in the northern Midwest with a well-documented record of mid-Holocene climate change and a known history of drought during the 1930s, which can be used to calibrate the mid-Holocene record. The mid-Holocene period in the northern Midwest was characterized by decreased atmospheric precipitation and increased summer insolation, and by associated decreases in lake levels (COHMAP 1988). This change in climate state can also be viewed as a large-scale climate transient, with corresponding hydrologic transients in the region. By carefully selecting a lake in the region and carrying out a multifaceted study including isotope, trace metal, and ostracode ecological analyses as well as hydrologic modeling, we can reconstruct these climate-driven hydrologic transients and obtain estimates of past hydrologic conditions.

Elk Lake, Grant County, Minnesota (latitude 45°,52'; longitude 95°,48'), is on the prairie-forest border and is one of a chain of lakes in an outwash-filled valley system in the Alexandria Moraine near the town of Hoffman. It is a Mg-Ca-HCO_3 lake, high in sulfate, with a specific conductance of 950 µS/cm. Shallow ground water flow is controlled by topography and surface water stage. There are two shallow aquifers (<30 meters depth): the outwash aquifer, composed of glacial outwash sands

In: C.M. Isaacs and V.L. Tharp, Editors. 1996. *Proceedings of the Twelfth Annual Pacific Climate (PACLIM) Workshop, May 2-5, 1995.* Interagency Ecological Program, Technical Report 46. California Department of Water Resources.

and gravels (highly permeable); and the shallow till aquifer, composed of heterogeneous glacial till and lacustrine clay with thin discontinuous sand and gravel strata (moderately permeable). Only these shallow aquifers are thought to interact with the chain of lakes. Ground water flow here displays an unusual configuration: the area of lakes is flanked on both east and west sides by parallel perennial streams (the Chippewa and Pomme de Terre rivers) about 7 kilometers apart and at stage elevations that differ by about 20 meters. Therefore, a cross-gradient exists in shallow ground water flow (from the Chippewa to the Pomme de Terre), induced by the difference in stream stage. Nearly normal to this flow gradient is the unusual linear chain of lakes within the Elk Lake channel, interpreted to represent either a meltwater channel or a collapsed tunnel valley. The lake chain acts as a ground water and surface water drain, inducing flow from east to west (from the Chippewa to the Pomme de Terre). Baseflow increases downstream in both rivers, but at a greater rate in the Pomme de Terre, reflecting this cross flow. The zone of ground water discharge from the Elk Lake channel is accompanied by an increase in dissolved solids in the river, consistent with the chemical mixing of streamflow with the more mineralized ground water.

We are engaged in:

- Documenting and modeling the present lake/ground water interaction to determine the relative importance of ground water sources reaching Elk Lake today;

- Evaluating the ostracode paleoecological record in a 16-meter core recovered from the deepest part of Elk Lake, to obtain quantitative estimates of changes in solute composition and atmospheric precipitation; and

- Analyzing the trace metal chemistry and stable isotope composition of lake water, modern ostracode shells, and fossil ostracodes.

We have characterized ground water flow into and out of lakes in the chain using numerical modeling techniques (Figure 1). Results of steady-state simulation indicate that the lakes receive recharge from surrounding uplands (recharge from the till aquifer), whereas there is a component of flow between lakes induced by surface water stage differences (recharge from surface water). Under today's hydrologic conditions, the dominant flow component is the surface water: This is especially pronounced during high lake stage accompanying wet years of 20-year-period climatic cycles, when lakes will fill to spill elevations and their chemical concentrations tend to homogenize. At low stage (dry years), the lakes are coupled only by slow ground water flow, and lake chemistries have the opportunity to diverge under ground water control.

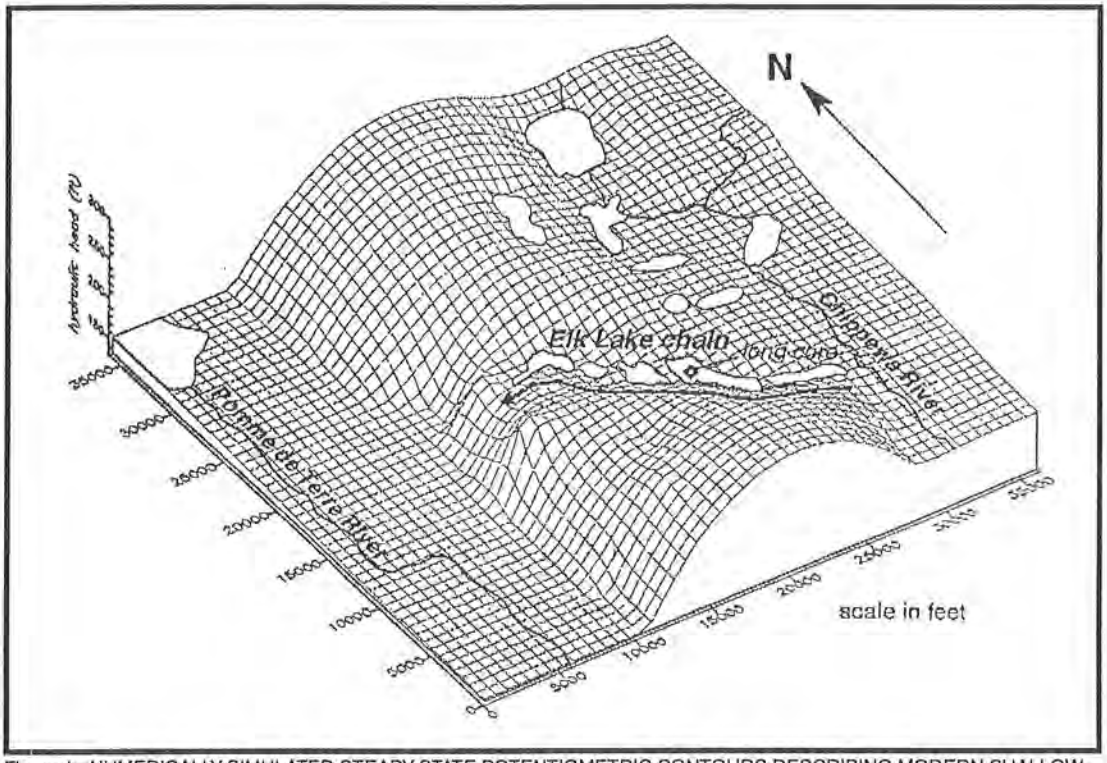

Figure 1 NUMERICALLY-SIMULATED STEADY-STATE POTENTIOMETRIC CONTOURS DESCRIBING MODERN SHALLOW GROUND WATER FLOW, ELK LAKE AREA, WESTERN MINNESOTA

Typical surface water sources, widespread over the last 2 years due to wet conditions, have Ca-Mg-HCO_3 dominance and are relatively low (<600 mg/L) in dissolved solids (TDS). Till ground water, on the other hand, is up to 2000 mg/L TDS, generally Mg-Ca-SO_4 dominant, at much higher pCO_2, and quite distinctive from the surface water signal. During wet years, the till ground water flow component is likely a small fraction of the current surface water flow through the lake chain. We are attempting to quantify the absolute fluxes using mixing models employing halide ions and by carbon and isotopic mass balance in Elk Lake. The till ground water fraction may have been relatively minor during "normal" (20-year) drought cycles. However, the till is sufficiently low in hydraulic conductivity so that only very low recharge rates would be required to sustain this ground water regime. Therefore, we hypothesize that the till fraction may have been a much more substantial fraction of the lake fluid mass balance during periods of extreme and sustained arid conditions, such as those documented in this region during the mid-Holocene.

Analysis of the core is near completion and reveals the solute evolution of the lake through time. The radiocarbon dates for the core are not yet available, but based on microfossil and sedimentological evidence, the full Holocene record is represented. Data from ostracode distributions (Figure 2) show how the lake changed from a dilute, Ca-Mg-HCO_3 lake of less than 500 mg/L TDS in the early Holocene (zone A) to a more concentrated lake, enriched in bicarbonate relative to calcium, and then underwent a distinct change in the pathway of solute evolution (zone B).

In mid-Holocene time, Elk Lake became a closed basin, saline lake, depleted in bicarbonate relative to calcium, with total concentrations of about 15,000 mg/L total dissolved solids (top of zone B). After mid-Holocene time, the lake returned to bicarbonate enrichment relative to calcium (zone C) and, finally, to the more dilute conditions characterized by the modern lake (zone D). The mid-Holocene change in solute path inferred from the ostracodes reflects changes in either ground water source or changes in ground water divides and catchments associated with increased evaporation.

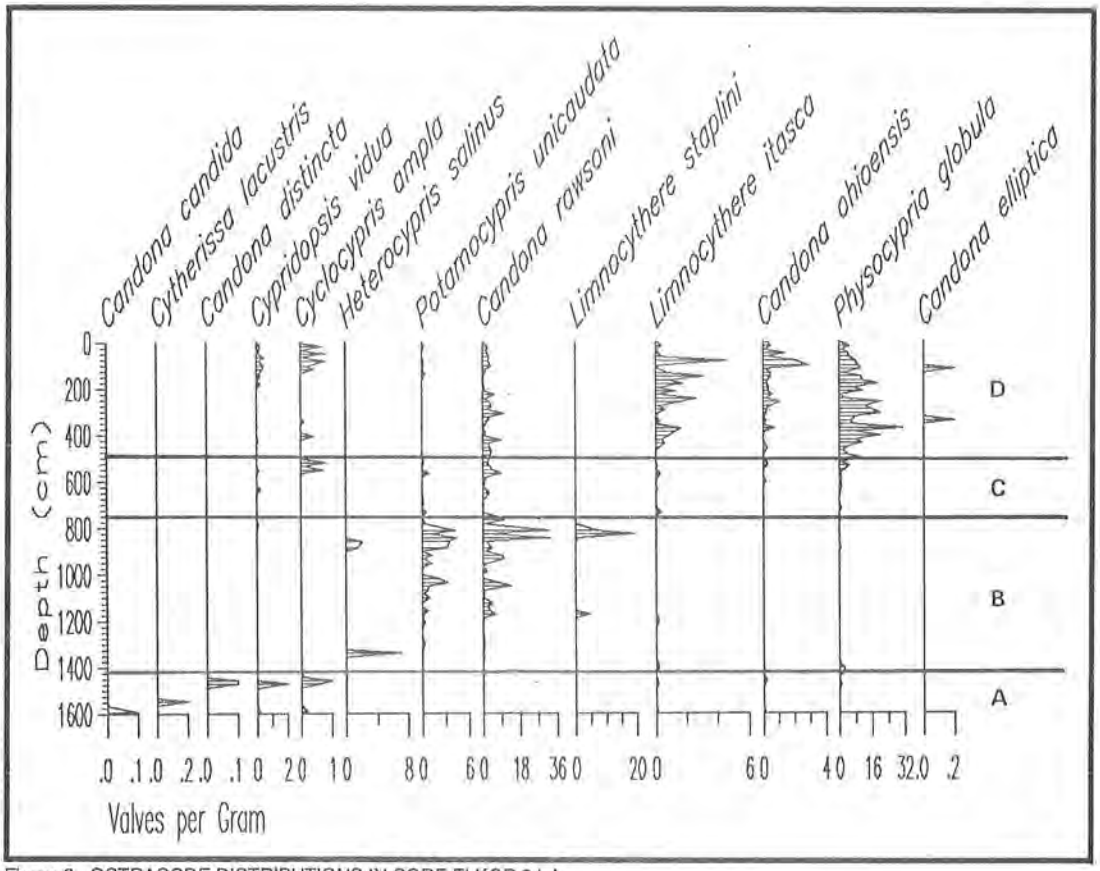

Figure 2 OSTRACODE DISTRIBUTIONS IN CORE ELKGR 94-A

The trace metal and oxygen-isotope data (Figure 3) clearly indicate a change in chemical composition of ground water inputs to Elk Lake during the mid-Holocene (zone B). The most arid intervals according to ostracode assemblages are marked by large negative excursions in $\delta^{18}O$ (5-10 per mil PDB) and large positive swings in Mg/Ca and Sr/Ca in the ostracode calcite. Although evaporative concentration could account for higher values for the trace metal ratios, the negative shifts in oxygen (and carbon) isotopes during arid phases are opposite those expected from greater evaporation and are far larger than any caused by increased temperature. Ground water supplying the lake during this period was characterized by ^{18}O less evolved from meteoric composition, and when considered with the ostracodes and the numerical modeling, suggests a

source in the ground water till fraction. The systematically lower values for Sr/Ca and Mg/Ca and higher values for ^{18}O in the late Holocene (zones D and E) characterize a ground water source enriched in calcium relative to strontium and magnesium and enriched in ^{18}O relative to source waters during the mid-Holocene.

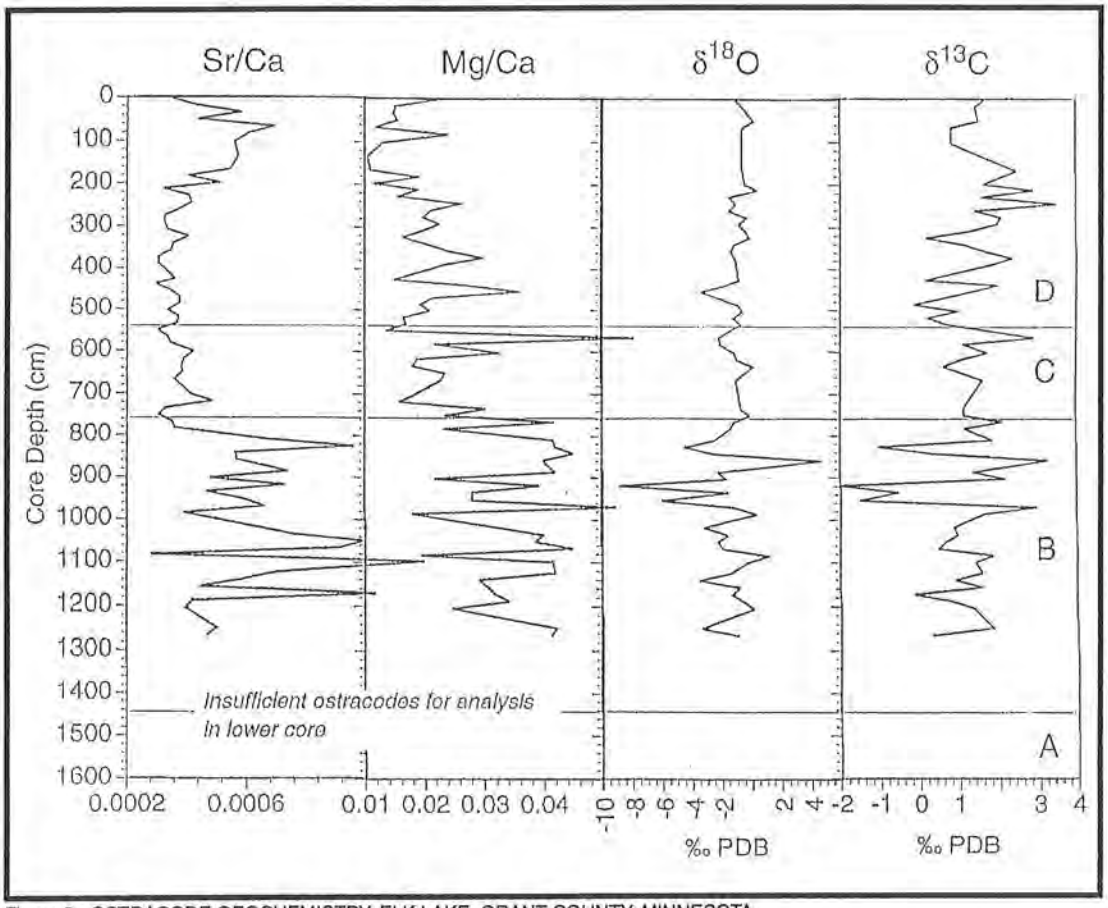

Figure 3 OSTRACODE GEOCHEMISTRY, ELK LAKE, GRANT COUNTY, MINNESOTA

Relatively few studies have attempted to link lake and ground water hydrochemical interaction over differing temporal and spatial scales. This attempt to capture the interactive nature of climate and the hydrologic cycle in detail will increase our understanding of the dynamic character of the two systems and provide a way to forecast future regional hydrologic responses to climate change.

Reference

COHMAP Members. 1988. Climatic changes of the last 18,000 years: Observations and model simulations. *Science* 241:1043-1052.

High-Resolution Record of Climate Change in the Owens Lake Basin, California, for the Period 52,500 to 12,500 YBP

Larry Benson, James Burdett, Michaele Kashgarian, Steve Lund, Robert Rye

Abstract: High-resolution ^{18}O and total inorganic carbon (TIC) studies of cored sediments from the Owens Lake Basin, California, indicate that Owens Lake was hydrologically open (overflowing) most of the time between 52,500 and 12,500 ^{14}C YBP. Desiccation of Owens Lake occurred between <15,500 and 13,700 ^{14}C YBP. Poor correspondence of ^{18}O and TIC variability in the time intervals 52,500 to 40,000 and 26,000 to <15,500 ^{14}C YBP indicates the occurrence of glaciation in the Sierra Nevada. Comparison of the Owens Lake $\delta^{18}O$ record and the lithic record of North Atlantic core V2381 indicates some degree of association. However, there does not appear to be any clear and simple relationship between iceberg discharge in the North Atlantic and variation in the hydrologic balance of Owens Lake. Numerous millennial-scale oscillations in the hydrologic balance of the Owens Lake surface-water system are absent from North Atlantic lithic and temperature records. The lack of a strong correspondence between North Atlantic climate records and the Owens Lake $\delta^{18}O$ record has two possible explanations: (1) the sequence of large and abrupt climate change indicated in North Atlantic records is not global in scope and is largely confined to the North Atlantic and surrounding areas, or (2) Owens Lake is located in a part of the Great Basin that is relatively insensitive to the effects of climate perturbations recorded in the North Atlantic region.

Introduction

Evidence for rapid oscillations in air and water temperatures during the last glacial period has been recognized in ice-core records from Greenland (Dansgaard *et al* 1993; Grootes *et al* 1993; Taylor *et al* 1993) and in sediment cores from the North Atlantic (Heinrich 1988; Bond *et al* 1992; Bond and Lotti 1995). The most recent Dansgaard-Oeschger cold event, the Younger Dryas, has also been documented in pollen records from western Europe, Maritime Canada, and southern New England and may be represented in pollen records from the Pacific Northwest (Wright 1989; Peteet 1995 and references therein). Layers of lithic fragments have been found in sediment cores from the North Atlantic. The thickest and most widespread of these layers (Heinrich layers) are rich in ice-rafted carbonate-rich debris and appear to be linked to the dynamics of the Laurentide ice sheet via iceberg discharge into the North Atlantic (Bond et *al* 1992; Bond and Lotti 1995; Broecker 1994; Andrews and Tedesco 1992; Broecker *et al* 1992; Andrews *et al* 1993). Five of the last six Heinrich events occurred at the end of progressive decreases in sea surface temperature and were followed by rapid increases in temperature (Bond *et al* 1993). Thus, Dansgaard-Oeschger cycles and lithic events are

In: C.M. Isaacs and V.L. Tharp, Editors. 1996. *Proceedings of the Twelfth Annual Pacific Climate (PACLIM) Workshop, May 2-5, 1995.* Interagency Ecological Program, Technical Report 46. California Department of Water Resources.

thought to be associated with major oscillations in atmospheric and sea-surface temperatures.

The causes and global extent of these climatic perturbations are not clear. Several authors have attempted to link proxy records of climate change from central China, the southeastern and western United States, the Chilean Andes, and New Zealand with Dansgaard-Oeschger cycles or Heinrich events (Porter and Ahisheng 1995; Grimm *et al* 1993; Allen and Anderson 1993; Phillips *et al* 1994; Clark and Bartlein 1995; Lowell *et al* 1995). Many of these studies lacked the resolution or age control to demonstrate unequivocally that climatic perturbations in the study areas were synchronous with North Atlantic climatic oscillations. In this paper, we compare a well-dated high-resolution proxy record of variation in the hydrologic balance of Owens Lake, California, with the timing of North Atlantic lithic events to examine whether abrupt changes in the hydrologic balance of a western Great Basin lake were synchronous with abrupt climatic oscillations in the North Atlantic region.

Climate and Hydrology of the Owens Lake Basin

Owens Lake is in the western part of the Great Basin at the southern end of Owens Valley, which lies between the central Sierra Nevada on the west and the Inyo-White mountain ranges on the east (Figure 1). During the historical period, Owens Lake was a hydrologically closed (endorheic) system. Consumptive use of water from the Owens River system began about 1870 (Lee 1912). At the time the Los Angeles aqueduct was completed in 1913, Owens Lake was about 10 meters deep (surface elevation about 1091 meters) and had a surface area of about 260 km^2. By about 1930, the lake had desiccated as the result of diversion of surface flow to the Los Angeles aqueduct (LADWP 1976).

Cool-season precipitation from North Pacific sources is dominant throughout the central Sierra Nevada. The paths of westerlies bringing moisture-laden air from the Pacific Ocean is an important determinant of the hydrologic balance of Owens Lake. The progression of maximum precipitation along the western flank of the Sierra Nevada is associated with southward movement of the mean position of the polar jet stream (Riehl *et al* 1954; Horn and Bryson 1960; Pyke 1972). A tendency for precipitation maxima to concentrate near the axis of the jet stream and for precipitation to decrease rapidly south of the axis and less rapidly north of the axis has been observed (Starrett 1949). During July and August, the westerlies weaken, and Pacific storm tracks move north of the Sierra Nevada. During this warm season, the Owens Valley receives only a small amount of moisture in the form of convective storms that originate in the Gulf of California. Because of the orographic effect of the Sierra Nevada, about 99% of the runoff reaching the Owens Basin originates in this mountain range (Hollett *et al* 1991).

Rock Types in Owens Lake Catchment Areas

The Sierra Nevada west of Owens Valley is composed of granitic and metamorphic rocks, and the Inyo-White mountains to the east are mostly composed of granites and sedimentary rocks (Hollett *et al* 1991 and references therein). Carbonate, in the form of calcitic marble, makes up fs20 % of Sierra Nevada bedrock in the Owens River drainage (Bateman 1965). Historically, little dissolved carbonate entered the Owens River from the arid Inyo-White drainage. In addition, the western drainage of

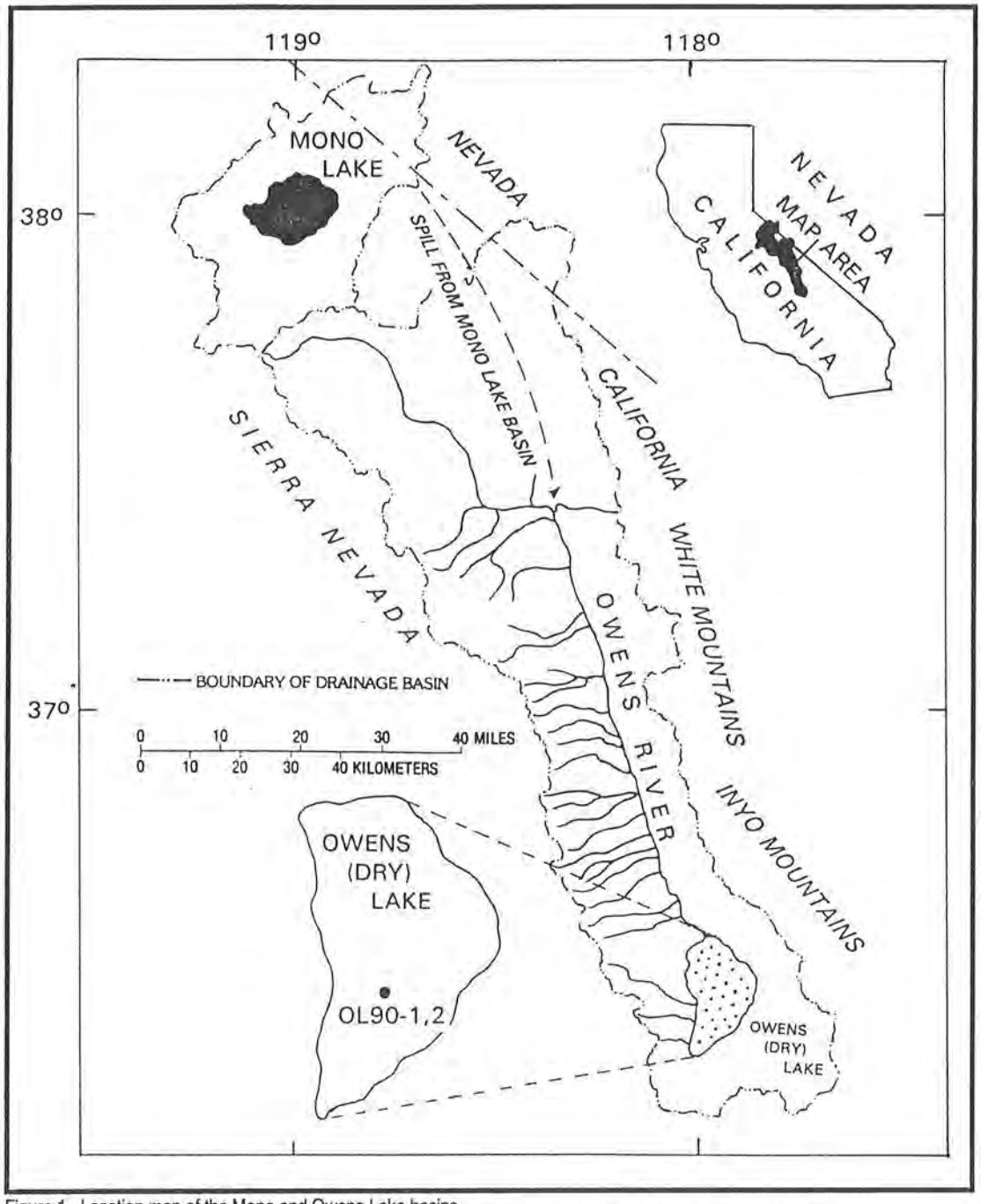

Figure 1 Location map of the Mono and Owens Lake basins.
Mono Lake is not thought to have spilled to the Owens Lake basin during the past 100,000 years.

the Inyo-White mountains appears to have remained unglaciated during the Wisconsin period (A.R. Gillespie and F.M. Phillips, personal communication, 1996). This suggests that little or no detrital carbonate was transported from the Sierra Nevada and Inyo-White mountains to the Owens Lake basin during past glaciations and that the Owens River contained little dissolved carbonate derived from the dissolution of carbonate bedrock.

Methods

In 1990, sediment cores OL90-1 (28.20 m) and OL90-2 (32.75 m) were obtained from the Owens Lake basin (Figure 1) using a truck-mounted split-spoon corer. The cores were stored in a refrigerated facility after collection. Age control for OL90-2 is based on 26 AMS ^{14}C determinations made on the total organic carbon (TOC) fraction of cored sediment (Figure 2). AMS radiocarbon dates were determined at the Lawerence Livermore National Laboratory Center for Accelerator Mass Spectrometry on bulk organic matter. Small aliquots of sediment (20-50 mg) were rinsed several times in an ultrasonic bath with deionized water to remove salts and also with 0.1N HCl to remove soluble carbonate from the sediment. The samples were then dried at 50°C in a vacuum oven. The procedure used for oxidation of bulk organic matter in pretreated sediment and subsequent reduction of CO_2 to filamentous graphite for AMS assay is described in Vogel *et al* 1987. Because carbonates make up <1% of the Sierra Nevada catchment area, we believe that the $^{14}C/C$ ratio of Owens River water approached the $^{14}C/C$ ratio of atmosphere CO_2 in the past; *ie*, the reservoir effect was small.

An age model for OL90-2 was obtained by fitting a second degree polynomial to the ^{14}C age-depth data (Figure 2). The ^{14}C chronology for OL90-1 was first obtained by correlating magnetic susceptibility peaks in OL90-1 and OL90-2 (Figure 3) and then using a correlation plot (Figure 4) to calculate an equivalent OL90-2 depth for OL90-1 samples. The ^{14}C age-depth polynomial for OL90-2 was then applied to OL90-1 samples. The Laschamp geomagnetic excursion, which has a K-Ar age of 46,600 ± 2400 cal YBP (Levi *et al* 1990 and references therein), was found at a depth of 28.0 meters in OL90-1 (Steve Lund, unpublished data). Our age model yields a ^{14}C age of 44,900 YBP at this depth. This is equivalent to a calendar age of 48,800 YBP (Edouard Bard, unpublished data).

About 650 sediment samples from the two cores were analyzed for $\delta^{18}O$ and TIC. Because carbonate makes <1% of the Sierra Nevada catchment area, we believe that detrital carbonates did not make up a significant part of the carbonate used in stable isotope analyses. The cores were sampled continuously except for the 5.36- to 16.00-meter interval of OL90-2. In this sediment interval, 1 centimeter was skipped between 2-centimeter-long samples. Each sediment sample (which integrates

between 20 and 100 years of record) was suspended in 40 milliliters of distilled-deionized water, centrifuged at 15,000 rpm, and the salty supernatant decanted. This procedure was repeated until conductivity of the supernatant was less than 3 times tap water. The samples were then freeze-dried and homogenized.

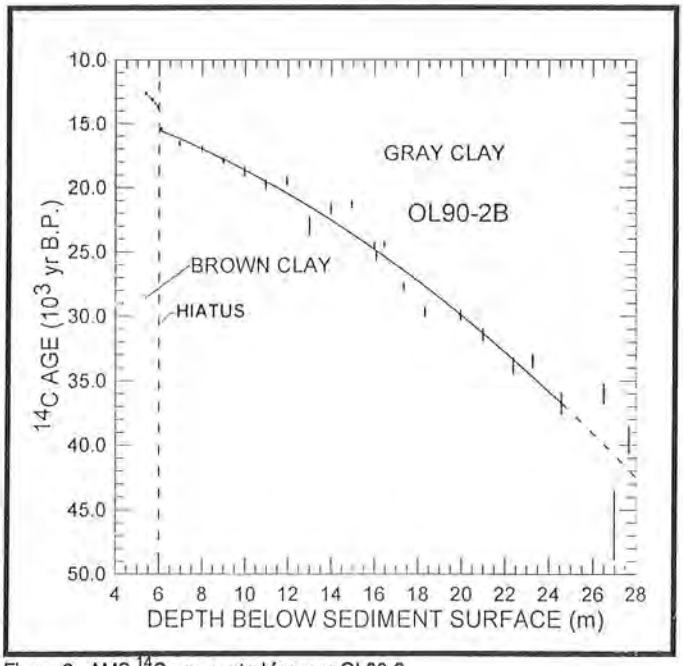

Figure 2. AMS ^{14}C age control for core OL90-2. The ^{14}C age polynomial was not fit to samples from depths greater than 25 meters.

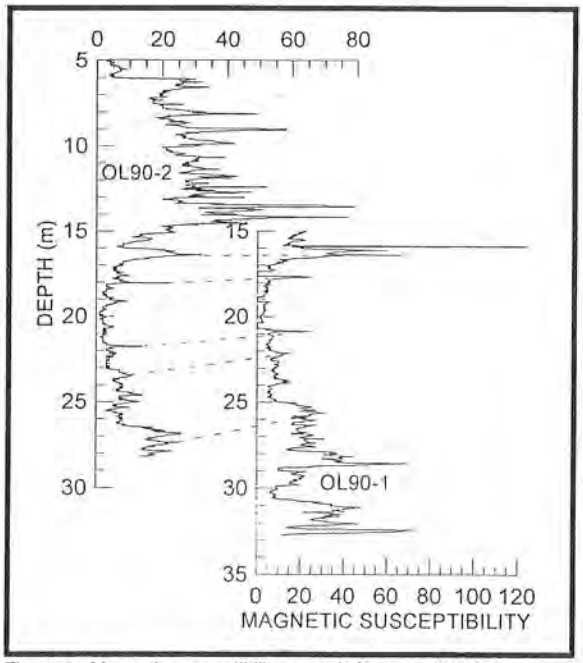

Figure 3. Magnetic susceptibility records for cores OL90-2 and OL90-1. Dashed lines indicate method of peak-to-peak correlation between these two records.

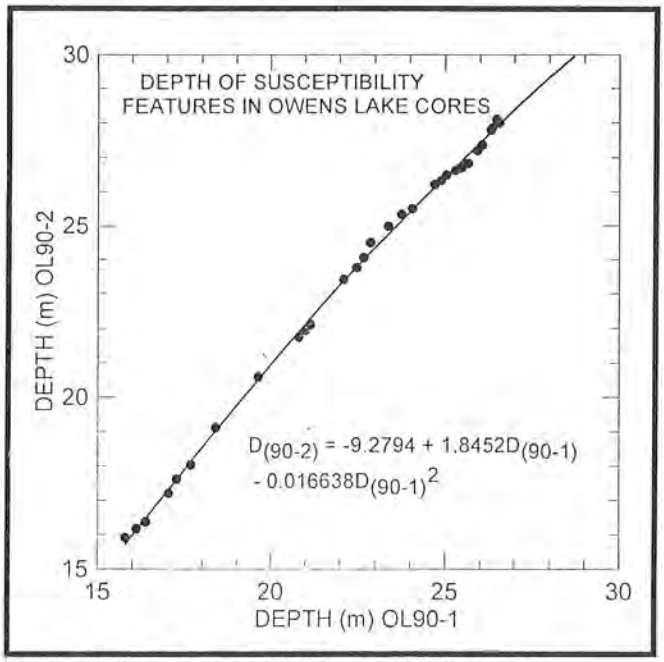

Figure 4. Depth-depth polynomial fit to susceptibility features in cores OL90-2 and OL90-1.

The ^{18}O values of the TIC were obtained in the following manner. Bulk samples were roasted in *vacuo* at 380°±10°C for 1 hour. Each sample was reacted individually for 10 minutes at 75°C. Evolved CO_2 was purified on a Kiel Automated Carbonate Extraction Device[1], introduced directly into a Finnigan MAT 251 triple collecting mass spectrometer, and analyzed for stable carbon and oxygen isotopes. Isotopic ratios of the samples were compared to a standard reference gas, and the differences were reported in standard delta notation (Craig 1957) vs. VPDB and VSMOW. Isotopic compositions of analyzed samples were normalized to a best-fit curve derived from repeated analyses of three NBS standards. Reported precisions were ±0.07‰ for $\delta^{13}C$ and ±0.10‰ for $\delta^{18}O$. Sample reproducibilities were 0.22±0.29‰ for $\delta^{13}C$ and 0.34±0.37‰ for $\delta^{18}O$ (103 samples). Data from samples with transducer pressures <150 μ and sample voltages <0.5 V were discarded. All samples that indicated anomalously high or low isotopic values were rewashed and rerun. A low isotope (^{18}O:^{16}O) ratio is referred to as isotopically light (more negative $\delta^{8}O$ value); a high isotope ratio is referred to as isotopically heavy. TIC was measured using a UIC Model 5012 CO_2 coulometer. Sample reproducibility was 0.015±0.012%C (27 samples). TIC analyses were performed on OL90-2 samples between 5.36 and 14.0 meters before and after the desalting process.

Variation in δ18O and TIC with Change in Hydrologic State and Balance

In terms of hydrologic state, a lake is either closed (endorheic) or open (overflowing). When Owens Lake is closed, the isotopic value of lake water at any instant represents a balance between isotopically light water entering the lake as inflow and on-lake precipitation ($\delta^{18}O_{d+p}$) and isotopically light water leaving the lake as evaporation. When hydrologic and isotopic steady states are achieved,

$$\delta^{18}O_L = \delta^{18}O_{d+p} - 10^3 \ln \alpha_{w->v}$$

where $\delta^{18}O_L$ is the $\delta^{18}O$ value of lake water and $10^3\ln\ \alpha_{w->v}$ is the time-averaged ^{18}O fractionation factor between liquid water (w) and water vapor (v) (Benson and White 1994; Benson *et al* 1996).

Data for $\delta^{18}O_{d+p}$ and $10^3\ln\ \alpha_{w->v}$ are not available for the existing Owens Lake surface water system; however, values of these two variables exist for surface water systems north of Owens Lake; for example, the $\delta^{18}O$ values of streams that flow into Mono Lake average about –16‰ (unpublished data of W.P. Patterson and C.N. Drummond); and $10^3\ln\ \alpha_{w->v} \approx$ –14‰ for waters evaporating from Pyramid Lake, Nevada (Benson and White 1994). Therefore, $\delta^{18}O_L \approx$ –2‰ during hydrologic closure, when

1 Use of tradenames in this paper does not imply endorsement by the U.S. Geological Survey.

hydrologic and isotopic steady states are achieved. This value is an approximation, valid only for the present-day climate, because the fractionation factor ($10^3 \ln \alpha_{w->v}$) is a function of relative humidity, the fraction of advected air in the boundary layer that overlies the lake, and the $\delta^{18}O$ value of advected air (Benson and White 1994). Values of these parameters in the late Wisconsin differed from present-day values. The above calculation indicates, however, that when a hydrologically closed Great Basin lake approaches an isotopic steady state, it becomes enriched in the heavy isotopes of oxygen.

When inflow (discharge) and on-lake precipitation (V_{d+p}) exceed evaporation (V_e), lake level rises and $\delta^{18}O_L$ decreases; when $V_e > V_{d+p}$, lake level declines and $\delta^{18}O_L$ increases until an isotopic steady state is achieved. The rate of change of $\delta^{18}O_L$ is a function of the rate of change in lake volume (V_L); the greater the rate of change in V_L, the greater the excursion in $\delta^{18}O_L$. Only large and rapid shifts in the hydrologic balance are recorded in the $\delta^{18}O$ values of carbonates precipitated from open waters of Owens. When Owens Lake overflowed, $\delta^{18}OL$ was primarily a function of the outflow:inflow (V_o:V_{d+p}) ratio (Benson *et al* 1996). Decrease in $\delta^{18}O_L$ accompanied increase in V_o:V_{d+p}. When the residence time of water in the Owens Lake basin approached zero, the value of $\delta^{18}O_L$ approached $\delta^{18}O_{d+p}$; *ie*, when $V_o \rightarrow V_{d+p}$, $\delta^{18}O_L \rightarrow \delta^{18}O_{d+p}$.

When the influx of detrital sediments is relatively constant, variation in the percentage of TIC tends to mirror variation in the $\delta^{18}O$ concentration of the TIC fraction. In a hydrologically-closed Na-HCO_3-dominated lake, all Ca that enters the lake precipitates as $CaCO_3$. When the lake overflows, however, some of the dissolved Ca in lake water is carried out of the basin by overflow; the greater the V_o:V_{d+p} ratio, the greater the loss of Ca. Therefore, if the flux of detrital sediments is relatively constant, high TIC amounts will parallel heavy $\delta^{18}O$ values and *vice versa*.

Results and Discussion

Variation in the Effective Wetness[2] of the Owens Lake Basin

The overall $\delta^{18}O$ record (Figure 5) indicates that Owens Lake overflowed much of the time between 52,500 and 12,500 ^{14}C YBP. High-frequency oscillations in $\delta^{18}O$ during this time are interpreted to indicate variations in the V_o:V_{d+p} ratio or brief oscillations in hydrologic state (closed $\leftrightarrow$ open). The highest overflow rates appear to have occurred between 13,200 and 12,500 ^{14}C YBP. Large amounts of TIC and heavy $\delta^{18}O$ values between

2 Effective wetness is a measure of change in the hydrologic balance of a lake. For a hydrologically closed lake, effective wetness is defined as the ratio of the surface area of a lake at time *t* divided by the mean historical surface area. For an overflowing lake, the theoretical surface areas at time *t* can be calculated by dividing the inflow volume by the evaporation rate. For Owens Lake to overflow, the effective wetness must be ≥2.4.

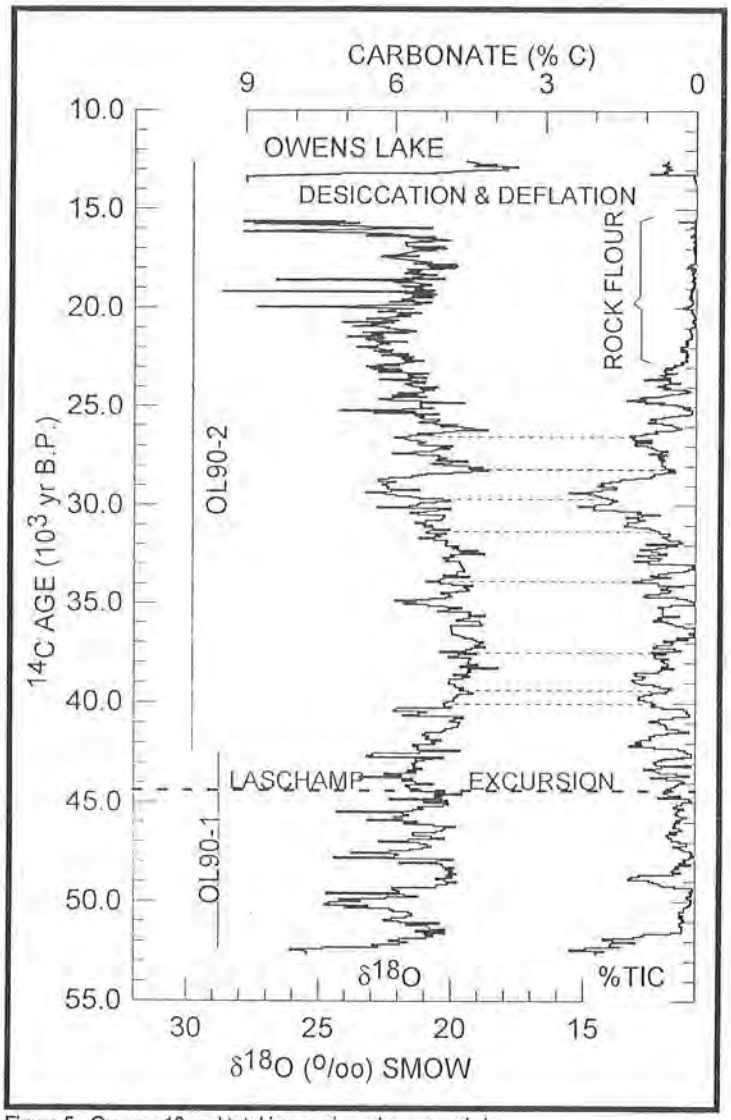

Figure 5. Oxygen-18 and total inorganic carbon records in cores OL90-2 and OL90-1 for the period 51,500 to 12,500 ^{14}C YBP. Thin dashed lines indicate correlations between both records between 40,000 and 26,000 ^{14}C YBP. The Laschamp excursion, which in France has been dated at 46,600±2400 cal YBP, was found at a depth equivalent to 44,900 ^{14}C YBP in core OL90-1.

31,000 and 29,000 ^{14}C YBP indicate a time of relatively low overflow and a greater frequency of closed-basin conditions[3].

Discontinuities in the depth-age distribution of Owens Lake sediments (Figure 2) indicate the existence of a sediment hiatus between <15,500 and 13,600 ^{14}C YBP. Sediments at the base of the hiatus are characterized by several features that indicate the occurrence of desiccation and deflation in the Owens Lake basin, including: (1) ≤1 centimeter of topography, (2) a 1- to 3-millimeter-thick lag deposit of coarse micaceous sand and frosted quartz grains, and (3) mudcracks. Soluble carbonate salts below this hiatus (Figure 6) document the former existence of a Na-CO_3 brine that diffused into the bottom of Owens Lake prior to its desiccation. Thus, the ^{14}C and salt data indicate that Owens Lake desiccated between <15,500 and 13,600 ^{14}C YBP and that deflation removed an unknown thickness of sediment from the dry lake bed.

First and second order variations in TIC and δ^{18}O can be associated for the period 40,000 to 26,000 ^{14}C YBP. The lack of association of TIC and δ^{18}O variability between 52,500 and 40,000 ^{14}C YBP and between 26,000 and 15,500 ^{14}C YBP indicates dilution and masking of the TIC signal by detrital sediments. We believe the detrital sediments were produced by glaciers located along the east flank of the Sierra Nevada; *ie*, in the summer months, glacially derived rock flour was transported to the Owens Lake basin by meltwater. The youngest rock flour event probably represents material derived from the Tioga and possibly Tenaya glaciations (Dorn *et al* 1987; Bursik and Gillespie 1993 and references therein). The oldest rock flour event may be a late stage of the Younger Tahoe glaciation (Blackwelder 1931; Phillips *et al* 1990).

3 Overflow during even the wettest of climates may have been seasonal. During winter, tunnels at the base of the glacier through which snowmelt and rock flour were transported would have frozen shut. The only water escaping the glacier during the winter season would have been water produced by subglacial melting.

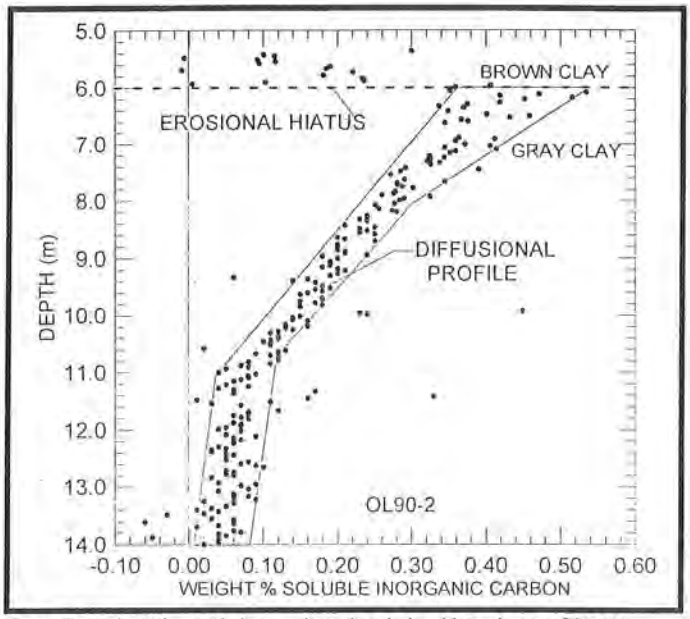

Figure 6. Weight % soluble inorganic carbon below hiatus in core OL90-2. Top of diffusion profile has been removed by deflation.

Values of $\delta^{18}O$ during the interglacial period (40,000 to 26,000 ^{14}C YBP) are generally lighter than during periods of glaciation, indicating that the intervening interglacial period was wetter than the glacial periods that preceded and followed the interglacial. Lack of intense glaciation between 40,000 to 26,000 ^{14}C YBP suggests that warm-season temperatures were high enough to melt and evaporate winter snow accumulations.

Comparison of the Owens Lake $\delta^{18}O$ Record with the V2381 Lithic Record

Bond *et al* (1993) have correlated proxy air temperature records (Dansgaard-Oeschger events) from the Summit ice core with proxy sea surface temperature records from North Atlantic sediment cores. The North Atlantic cores also contain intervals rich in ice-rafted lithic fragments, released from icebergs that had been discharged from the Laurentide ice sheet. The lithic intervals with the highest accumulation rates are called Heinrich events (Heinrich 1988). In their correlation, Bond *et al* (1993) demonstrated a link between iceberg discharge from the Laurentide ice sheet (evidenced by lithic layers) and variation in air and water temperature in the North Atlantic region; *ie*, five of the last six Heinrich events occurred at the end of progressive decreases in sea surface temperature and were followed by rapid increases in temperature.

The trajectory of the polar jet stream played a key role in the hydrologic balance of the Owens Lake basin during the Wisconsin glacial cycle. The presence of an ice sheet across Canada greatly affected the position and intensity of westerly flow, forcing the jet stream southward throughout the year (Kutzbach and Guetter 1986; Kutzbach 1987; Kutzbach *et al* 1993). During the Wisconsin glaciation, the Laurentide ice sheet underwent gradual expansion and contraction in response to external factors such as solar forcing, and it also may have experienced abrupt decreases in size resulting from its own internal dynamics (MacAyeal 1993). Some of the changes in the size and shape of the ice sheet may have been accompanied by a rapid shift of mean position of the polar jet stream over the Great Basin and a

concomitant change in the hydrologic balance of Great Basin lakes, including Owens. If the cold-warm oscillations documented in the North Atlantic sediment and ice records were linked to changes in ice-sheet size, we might expect changes in the hydrologic balance of Great Basin lakes to correlate with North Atlantic records of climate change.

To determine if the abrupt and large changes in climate recorded in North Atlantic ice and sediment cores affected the climate of the Great Basin, we attempted to correlate the Owens Lake hydrologic-balance proxy record ($\delta^{18}O$) with a North Atlantic lithic record from core V2381 (Figure 7; numbered warm Dansgaard-Oeschger events are also indicated). The lithic record, instead of the left-coiling *Neogloboquadrina pachyderma* proxy-temperature record, was chosen for comparison with the Owens Lake $\delta^{18}O$ record for two reasons: (1) the sea surface temperature record (based on the relative abundance of *N. pachyderma*) is not sensitive to extremely cold water temperatures, and (2) the lithic record may indirectly reflect changes in the size of the Laurentide ice sheet.

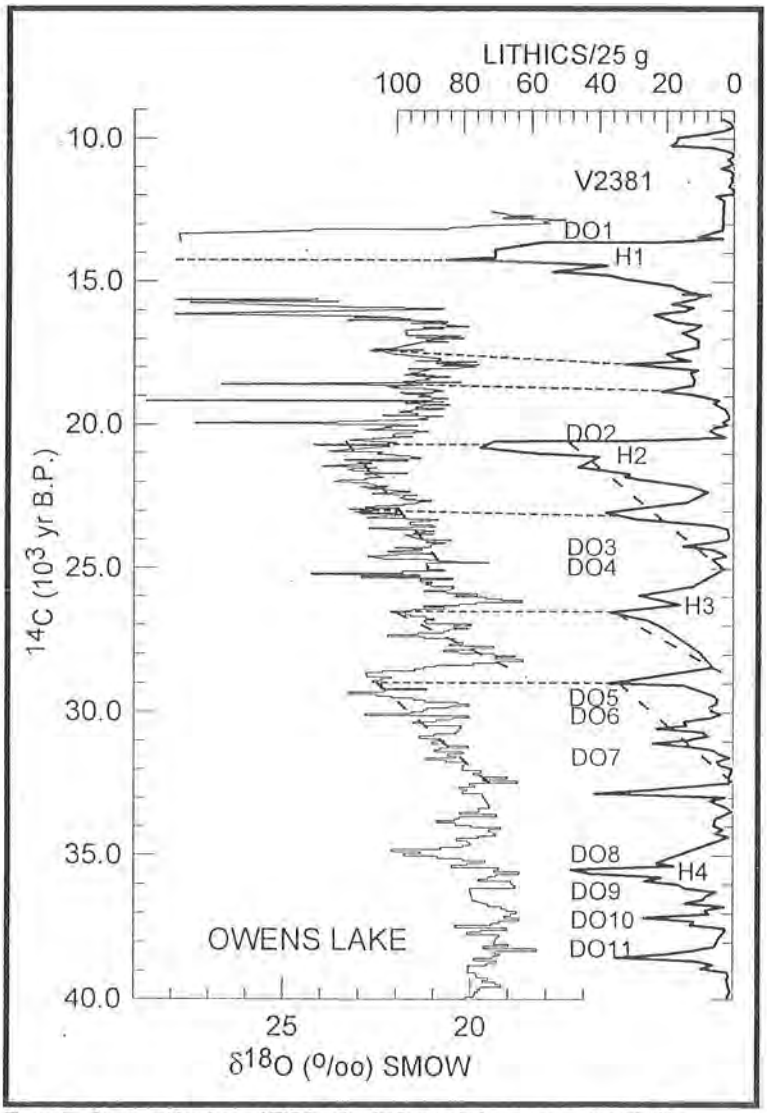

Figure 7. Oxygen-18 values of TIC fraction in Owens Lake cores compared with lithic record from North Atlantic core V2381.
H1-H4 indicate Heinrich events; DO1-DO11 indicate Dansgaard-Oescheger warm events. Thin dashed lines indicate attempts to associate lithic maxima with $\delta^{18}O$ minima; heavy dashed lines indicate trends in both records.

We were able associate trends of increasing iceberg discharge with decreases in effective wetness of the Owens Lake basin; for example, a generally decreasing trend in effective wetness corresponds to a period that features a series of successively larger lithic events bounded by Heinrich events H3 and H2. It also is possible to associate some of the major lithic events with decreases in effective wetness; for example, Owens Lake desiccated at the time of H1 (Figure 7). To the extent that these associations are correct, the data suggest that release of icebergs to the North Atlantic reduced the size of the Laurentide ice sheet, thereby allowing the mean position of the polar jet stream to shift northward over the Great Basin. However, there does not appear to be any clear or simple relationship between iceberg discharge in the North Atlantic and

variation in the hydrologic balance of Owens Lake. There are numerous millennial-scale oscillations in the hydrologic balance of the Owens Lake surface water system that are absent from North Atlantic lithic and temperature records (Figure 7).

The lack of a strong correspondence between North Atlantic climate records and the Owens Lake $\delta^{18}O$ record has two possible explanations: (1) the sequence of large and abrupt climate change indicated in North Atlantic records is not global in scope and is largely confined to the North Atlantic and downwind regions, or (2) the Owens Lake basin is in a region that is relatively insensitive to climate perturbations recorded in the North Atlantic region. For example, it may be that when the polar jet stream shifted northward in response to a reduction in ice-sheet size, its mean path remained south of the Owens Lake basin.

Conclusions

Between 52,500 and 12,500 ^{14}C YBP, the climate of the Owens Lake basin was often ≥2.4 times effectively wetter than during the historical period. Glaciers occupied the Sierra Nevada during the first third (52,500 to 40,000 ^{14}C YBP) and most of the last third (26,000 to <15,500 ^{14}C YBP) of this wet period. The lack of Sierran glaciers during the middle third (40,000 to 26,000 ^{14}C YBP) indicates that summers were relatively long and/or warm. A desiccation of Owens Lake that occurred between <15,500 and 13,700 ^{14}C YBP was followed by an extremely wet period (13,300 to <12,500 ^{14}C YBP).

Comparison of the Owens Lake $\delta^{18}O$ record and the lithic record of North Atlantic core V2381 indicates some degree of association. However, there does not appear to be any clear or simple relationship between climate records from the North Atlantic and a proxy hydrologic-balance record from the Owens Lake basin.

Acknowledgments

We are grateful to the following people for discussions regarding this manuscript: Gerard Bond of the Lamont-Doherty Earth Observatory; Alex Blum, Richard Marzolf, and James Gardner of the U.S. Geological Survey; Alan Gillespie and Douglas Clark of the University of Washington; Peter Clark of Oregon State University; John Andrews of the University of Colorado; Timothy Lowenstein of the State University of New York- Binghamton; and Fred Phillips of the New Mexico Institute of Mining and Technology. The radiocarbon work was performed in part under the auspices of the U.S. Department of Energy by Lawrence Livermore National Laboratory under contract W-7405-ENG-48. Other studies reported herein were funded by the Global Change Program of the U.S. Geological Survey.

References

Allen, B.D., and R.Y. Anderson. 1993. Evidence from western North America for rapid shifts in climate during the last glacial Maximum. *Science* 260:1920-1923.

Andrews, J. T., and K. Tedesco. 1992. Detrital carbonate-rich sediments, northwestern Labrador Sea: Implications for ice-sheet dynamics and iceberg rafting (Heinrich) events in the North Atlantic. *Geology* 20:1087-1090.

Andrews, J.T., K. Tedesco, W.M. Briggs, L.W. Evans. 1993. Sediments, sedimentation rates, and environments, SE Baffin Shelf and NW Labrador Sea 8 to 26 ka. *Canadian Journal of Earth Sciences* 31:90-103.

Bateman, P.C. 1965. Geology and tungsten mineralization of the Bishop District, California. *Geology Society of America Bulletin* 97:97-109.

Benson, L.V., L.D. White, R. Rye. 1996. Carbonate deposition, Pyramid Lake subbasin, Nevada: 4. The use of stable isotope values of carbonate deposits (tufas) to determine variability in the hydrologic balance of paleolake systems. *Palaeogeography, Palaeoclimatology, Palaeoecology* (in press).

Benson, L.V., and J.W.C. White. 1994. Stable isotopes of oxygen and hydrogen in the Truckee River-Pyramid Lake surface-water system. 3. Source of water vapor over Pyramid Lake, Nevada. *Limnology and Oceanography* 39:1945-1958.

Benson, L.V., L.D. White, R. Rye. 1996. Carbonate deposition, Pyramid Lake subbasin, Nevada: 4. The use of stable isotope values of carbonate deposits (tufas) to determine variability in the hydrologic balance of paleolake systems. *Palaeogeography, Palaeoclimatology, Palaeoecology* (in press).

Blackwelder, E. 1931. Pleistocene glaciation in the Sierra Nevada and Basin ranges. *Geological Society of America Bulletin* 42:865-922.

Bond, G., H. Heinrich, W. Broecker, L. Labeyrie, J. McManus, J. Andrews, S. Huon, R. Jantschik, S. Clasen, C. Simet, K. Tedesco, M. Klas, G. Bonani, S. Ivy. 1992. Evidence for massive discharges of icebergs into the North Atlantic ocean during the last glacial period. *Nature* 360:245-249.

Bond, G., W. Broecker, S. Johnsen, J. McManus, L. Labeyrie, J. Jouzel, G. Bonani. 1993. Correlations between climate records from North Atlantic sediments and Greenland ice. *Nature* 365:143-147.

Bond, G.C., and R. Lotti. 1995. Iceberg discharges into the North Atlantic on millennial time scales during the last glaciation. *Science* 267:1005-1010.

Broecker, W.S. 1994. Massive iceberg discharges as triggers for global climate change. *Nature* 72:421-424.

Broecker, W., G. Bond, M. Klas, E. Clark, J. McManus. 1992. Origin of the northern Atlantic's Heinrich events. *Climate Dynamics* 6:265-273.

Bursik, M.I., and A.R. Gillespie. 1993. Late Pleistocene glaciation of Mono Basin, California. *Quaternary Research* 39:24-35.

Clark, P.U., and P.J. Bartlein. 1995. Correlation of late Pleistocene glaciation in the western United States with North Atlantic Heinrich events. *Geology* 23:483-486.

Craig, H. 1957. Isotope standards for carbon and oxygen and correction factors for mass-spectrometric analysis of carbon dioxide. *Geochimica Cosmochimica et Acta* 12:113-149.

Dansgaard, W., S.J. Johnsen, H.B. Clausen, D. Dahl-Jensen, N.S. Gundestrup, C.U. Hammer, C.S. Hvidberg, J.P. Steffensen, A.E. Sveinbjornsdottir, J. Jouzel, G. Bond. 1993. Evidence for general instability of past climate from a 250-kyr ice-core record. *Nature* 364:218-220.

Dorn, R.I., B.D. Turrin, A.J.T. Jull, T.W. Linick, D.J. Donahue. 1987. Radiocarbon and cation-ratio ages for rock varnish on Tioga and Tahoe morainal boulders of Pine Creek, eastern Sierra Nevada, California, and their paleoclimatic implications. *Quaternary Research* 28:38-49.

Grimm, E.C., G.L. Jacobson Jr., W.A. Watts, B.C.S. Hansen, K.A. Maasch. 1993. A 50,000-year record of climate oscillations from Florida and its temporal correlation with the Heinrich events. *Science* 261:198-200.

Grootes, P.M., M. Stuiver, J.W.C. White, S. Johnsen, J. Jouzel. 1993. Comparison of oxygen isotope records from the GISP2 and GRIP Greenland ice cores. *Nature* 366:552-554.

Heinrich, H. 1988. Origin and consequences of cyclic ice rafting in the northeast Atlantic Ocean during the past 130,000 years. *Quaternary Research* 29:143-152.

Hollett, K.J., W.R. Danskin, W.F. McCaffrey, C.L. Walti. 1991. *Geology and Water Resources of Owens Valley, California.* U.S. Geological Survey Water-Supply Paper 2370. 77 pp.

Horn, L.H., and R.A. Bryson. 1960. Harmonic analysis of the annual march of precipitation over the United States. *Annals of the Association of American Geographers* 50:157-171.

Kutzbach. J.E. 1987. Model simulations of the climatic patterns during the deglaciation of North America. Pages 425-446 in: W.F. Ruddiman and H.E. Wright, Jr. (eds), *The Geology of North America.* Geological Society of America, K-3.

Kutzbach, J.E., and P.J. Guetter. 1986. The influence of changing orbital parameters and surface boundary conditions on climate simulations for the past 18000 years. *Journal of Atmospheric Science* 43:1726-1759.

Kutzbach, J.E., P.J. Guetter, P.J. Behling, R. Selin. 1993. Simulated climatic changes: Results of the COHMAP climate-model experiments. Pages 24-93 in: H.E. Wright, Jr., J.E. Kutzbach, T. Webb III, W.F. Ruddiman, F.A. Street-Perrott, P.J. Bartlein (eds), *Global Climates since the Last Glacial Maximum.* University of Minnesota Press, Minneapolis.

Los Angeles Department of Water and Power. 1976. *Increased pumping of the Owens Valley groundwater basin: Final Environmental Impact Report 2.* 125 pp.

Lee, C.H. 1912. *An Intensive Study of the Water Resources of a Part of Owens Valley, California.* U.S. Geological Survey Water-Supply Paper 294. 135 pp.

Levi, S., H. Audunsson, R.A. Duncan, L. Kristjansson, P.-Y. Gillot, S.P. Jakobsson. 1990. Late Pleistocene geomagnetic excursion in Icelandic lavas: Confirmation of the Laschamp excursion. *Earth and Planetary Science Letters* 96:443-457.

Lowell T.V., C.J. Heusser, B.G. Andersen, P.I. Moreno, A. Hauser, L.E. Heusser, C. Schluchter, D.R. Marchant, G.H. Denton. 1995. Interhemispheric correlation of late Pleistocene glacial events. *Science* 269:1541-1549.

MacAyeal, D.R., 1993. Binge/purge oscillations of the Laurentide ice sheet as a cause of the North Atlantic's Heinrich Events. *Paleoceanography* 8:775-784.

Peteet, D. 1995. Global Younger Dryas? *Quaternary International* 28:93-104.

Phillips, F.M., A.R. Campbell, G.I. Smith, J.L. Bischoff. 1994. Interstadial climatic cycles: A link between western North America and Greenland? *Geology* 22:1115-1118.

Phillips, F.M., M.G. Zreda, S.S. Smith, D. Elmore, P.W. Kubik, P. Sharma. 1990. Cosmogenic chlorine-36 chronology for glacial deposits at Bloody Canyon, eastern Sierra Nevada. *Science* 248:1529-1532.

Porter, S.C., and A. Zisheng. 1995. Correlation between climate events in the North Atlantic and China during the last glaciation. *Nature* 375:305-308.

Pyke, C.B. 1972. *Some Meteorological Aspects of the Seasonal Distribution of Precipitation in the Western United States and Baja California.* University California Water Resources Center Contribution 139.

Riehl, H., M.A. Alaka, C.L. Jordan, R.J. Renard. 1954. The jet stream. *Meteorological Monograph* 2:23-47.

Starrett, L.G. 1949. The relation of precipitation patterns in North America to certain types of jet streams at the 300-millibar level. *Journal of Meteorology* 6:347-352.

Stuiver, M., and P.J. Reimer. 1993. Extended ^{14}C Data Base and Revised CALIB 3.0 ^{14}C Age Calibration Program. *Radiocarbon* 35:215-230.

Taylor, K.C., G.W. Lamorey, G.A. Doyle, R.B. Alley, P.M. Grootes, P.A. Mayewski, J.W.C. White, L.K. Barlow. 1993. The "flickering switch" of late Pleistocene climate change. *Nature* 361:432-436.

Vogel, J.S., D.E. Nelson, J.R. Southon. 1987. ^{14}C background levels in an accelerator mass spectrometry system. *Radiocarbon* 29:323-333.

Wright, H.E. Jr. 1989. The amphi-Atlantic distribution of the Younger Dryas paleoclimatic oscillation. *Quaternary Science Reviews* 8:295-306.

A Late Pleistocene Paleohydrologic Record of Sierra Nevada Runoff from Owens Lake, California

J. Platt Bradbury

Abstract

A 323-meter (about 800,000 year) core of lake deposits beneath Owens Lake playa, Inyo County, California, contains a nearly continuous paleolimnological record based on diatom assemblages. The core chronology is anchored by the Matuyama/Brunhes magneto-stratigraphic boundary, by the Bishop ash near the base of the record, by the 500 ka Dibekkulewe ash at 224 meters, and by radiocarbon dates near the trop. Throughout most of its history, Owens Lake was characterized by freshwater diatoms, indicating a positive hydrologic input from the Owens River and overflow to lake systems downstream. Both benthic and planktic freshwater diatoms dominate in ashy and sandy sediments between 800 and 440 ka and suggest shallow, open-water environments in a basin where sedimentation and subsidence were approximately balanced. After 440 ka, freshwater planktic diatoms dominate, implying that the Owens basin became deeper, perhaps as a result of increased rates of tectonic subsidence. The stratigraphic distribution of saline benthic and planktic diatoms record comparatively short intervals when the lake was shallow and saline. Nevertheless, periodic overflow during these times prevented deposition of evaporites. According to a chronology based on sediment mass accumulation rates, the alternation of saline and freshwater diatom assemblages approximately tracks the progression of oxygen isotope stages recorded in marine deposits. Even-numbered isotope stages representing glacial conditions are matched by episodes where freshwater planktic diatoms dominate, indicating abundant precipitation in the Sierra Nevada in response to a southward shift of storm tracks originating in the North Pacific around the Aleutian Low.

In: C.M. Isaacs and V.L. Tharp, Editors. 1996. *Proceedings of the Twelfth Annual Pacific Climate (PACLIM) Workshop. May 2-5, 1995.* Interagency Ecological Program, Technical Report 46. California Department of Water Resources.

A Detailed 2,000-Year Late-Holocene Pollen Record from Lower Pahranagat Lake, Southern Nevada, USA

Peter E. Wigand and Martha L. Hemphill

Abstract

Preliminary analysis of 128 pollen samples and 7 radiocarbon dates from a 5-meter-long, 10-centimeter-diameter sediment core retrieved from Lower Pahranagat Lake (elevation 975 meters), Lincoln County, Nevada, gives us a rare, continuous record of vegetation change at 14-year intervals over the past 2,000 years. During this period, increasing *Pinus* (pine) pollen values with respect to *Juniperus* (juniper) pollen values reflect the increasing dominance of pinyon in southern Nevada woodlands during the past 2,000 years. Today, *Pinus* pollen values indicate that pinyon pine is more frequent in the southern Great Basin since the end of the Neoglacial 2,000 years ago. During the same time frame, a general decrease in Poaceae (grass) pollen values with respect to *Artemisia* (sagebrush) pollen values reflects the general trend of increasing dominance of steppe and desert scrub species with respect to grasses. Variations in these two species reflect not only the generally more xeric nature of climate during the past 2,000 years, but also periods of summer-shifted rainfall about 1,500 years ago that encouraged a period of both grass and pinyon expansion.

The ratio of aquatic to littoral pollen types indicates generally deeper water conditions 2,000 to 1,000 years ago and more variable, but predominately more marshy, conditions at the site during most of the past 1,000 years. Investigation of ostracodes from the same record by Dr. R. Forester at the USGS corroborates the pollen record by providing evidence of shifts between open and closed hydrologic systems, including lake, marsh, and even stream habitats. Analysis of an additional 10 meters of core recovered in the summer of 1994 with a basal date of 5,600 years ago promises to provide the highest resolution record of middle through late Holocene vegetation and climate history for southern Nevada.

In: C.M. Isaacs and V.L. Tharp, Editors. 1996. *Proceedings of the Twelfth Annual Pacific Climate (PACLIM) Workshop, May 2-5, 1995.* Interagency Ecological Program, Technical Report 46. California Department of Water Resources.

Response of Pacific Northwest Vegetation to Large-Scale Changes in Climate During the Last 100,000 Years

Cathy Whitlock and Patrick J. Bartlein

Abstract

Paleoclimatic variations in western North America depend on a hierarchy of temporal and spatial controls that can be examined using a combination of modeling studies and data synthesis. A particular record reflects the superimposition of multiple controls that operate on a variety of temporal and spatial scales; identification of these controls is not necessarily straightforward. The regional vegetation response to large-scale changes in the climate system of the last 21,000 years is used as a conceptual model to help explain earlier vegetation and climate at two localities. Carp Lake (Lat. 45°55'N, Long. 120°53'W, elevation 714 meters) provides a pollen record of the past about 75,000 years based on 12 radiocarbon ages and 11 tephra layers. The early Wisconsin period (about 75,000-68,000 years ago) supported mixed conifer forests indicative of cool, wet conditions. The early mid-Wisconsin (about 60,000-50,000 years ago) featured oak, hemlock, Douglas fir, and fir during a period of cool dry summers, cool wet winters, and higher-than-present summer insolation. The mid-Wisconsin (about 68,000-25,000 years ago) registered alternating pine forest and open pine-dominated parkland that imply cooler-than-present conditions. Little Lake (Lat. 44°10'N, Long. 123°35'W, elevation 217 meters) provides paleoenvironmental information for the past 42,000 years in the central Coast Ranges (Worona and Whitlock, in press). From about 42,000 to 24,000 years ago, open forest of pine, western hemlock, and fir indicate that summers were cooler and more humid than present.

In: C.M. Isaacs and V.L. Tharp, Editors. 1996. *Proceedings of the Twelfth Annual Pacific Climate (PACLIM) Workshop. May 2-5, 1995.* Interagency Ecological Program, Technical Report 46. California Department of Water Resources.

Multiple-Proxy Lacustrine Record of Moisture Transport over Western North America from 24,000 to 12,000 YBP, Lake Estancia, New Mexico

Bruce D. Allen, Roger Y. Anderson, Crayton J. Yapp

Abstract

Pluvial Lake Estancia in central New Mexico experienced large and rapid fluctuations in surface area and elevation during the build-up to and termination of the last glacial maximum (LGM). Due to continuous groundwater discharge, a minimum pool covering about 400 square kilometers was maintained in the central basin until about 12,000 years ago, ensuring a continuous depositional sequence even during low stands of the lake. Surface runoff from the surrounding drainage basin, resulting in high stands of the lake, is manifested by stream channels that terminate near the high shorelines and deltaic deposits in near-shore localities, by increased quantities of detrital quartz grains, and by growth pulses in populations of ostracodes in basin-center settings. Time-series of detrital quartz and ostracode-species abundance reveal several major episodes of stream discharge and freshening, separated by about 2,000 years, in the period 24,000-12,000 YBP. Mass balance calculations support the physical evidence for increased precipitation and input of surface water during freshening and expansion of the lake. Preliminary stable-isotopic and trace-metal ratios of ostracode valves from the interval 20,000-18,000 YBP indicate that climatic shifts toward effectively drier conditions occurred as rapidly as shifts toward increased precipitation. Changes in $\Delta 180$ suggest significantly different isotopic compositions for waters entering the lake during freshening and drawdown events, with more negative values corresponding to reduced surface runoff, lake drawdown, and a higher proportion of input to the lake from ground water. The sensitive response to fluctuations in climate by several independent proxies at Estancia show that transport of Pacific moisture over western North America changed dramatically during the last Ice Age, perhaps comparable to the large and rapid changes in climate documented from high-latitude ice and North Atlantic marine sediments for the LCM and its transitions.

In: C.M. Isaacs and V.L. Tharp, Editors. 1996. *Proceedings of the Twelfth Annual Pacific Climate (PACLIM) Workshop, May 2-5, 1995.* Interagency Ecological Program, Technical Report 46. California Department of Water Resources.

A Rock-Magnetic and Geomagnetic Secular Variation Record from Late-Pleistocene Lake Estancia, New Mexico

H.D. Rowe, J.W. Geissman, Bruce D. Allen, Roger Y. Anderson

Abstract

Exposed sediments of Late Pleistocene Lake Estancia contain a high resolution record of regional climate variability for the period about 12,000 to 32,000 years. A detailed rock-magnetic study is being performed on this well-dated, well-preserved sedimentary sequence to determine how the magnetic signature of sediments responded to regional climate change. A record of short-term geomagnetic field changes (secular variation) is also being constructed for use in correlating the climate record from Estancia with those from the west coast of North America and the Pacific Ocean. Samples were taken from the lake sequence exposed in two Holocene blowouts, near the lake basin center. Using lexan cubes, a sampling interval of 1.9 centimeters was established to obtain a record with a temporal resolution on the scale of decades. A long (7.7 meter) sedimentary sequence was sampled from one locality and DRM, ARM, and IRM data have been collected on this large suite. A shorter (3 meter) sequence is currently being sampled and analyzed. The relationship between X_{vol} and Depth in the sequence is useful for intrabasinal correlation. Along with X_{vol}, the variation in magnetic mineralogy, grain size, and grain abundance may indicate when and how quickly regional climate changes occurred. Rock-magnetic parameters indicate that the dominant magnetic carrier in these sediments is pseudo-single domain magnetic, though the magnetic mineral abundance is variable throughout the sequence. Thermal studies are underway to determine the role of Fe-sulfides as remanence carriers and lake environment indicators.

In: C.M. Isaacs and V.L. Tharp, Editors. 1996. *Proceedings of the Twelfth Annual Pacific Climate (PACLIM) Workshop, May 2-5, 1995*. Interagency Ecological Program, Technical Report 46. California Department of Water Resources.

The QBO, El Niño, and Tidal Resonance Model

Thor Karlstrom

The QBO and ENSO

The QBO winds in the lower stratosphere alternate from easterly to westerly regimes, with a mean period estimated by various researchers at about 26, 27, or 28 months (2.2-2.3 years). The winds originate earliest at the higher altitudes, have maximum velocity at an intermediate level, and dissipate gradually downward at a uniform rate of about 1 kilometer/month to disappear near the tropopause. Because these wave trains are initiated at higher altitudes and transgress time in downward propagation, one might suspect a forcing function at the top. However, similar stratospheric oscillations have been simulated in GCMs (general circulation models) based on the dynamic interplay of tropical tropospheric and oceanic parameters plus the *ad hoc* inclusion of the effects of equatorial eastward-moving Kelvin Waves and the slower westward-moving Rossby Waves, which evidently set up a delayed response oscillation (Takahashi and Boville 1992 in Coriolle *et al* 1993). GCMs expanded to include the effects of adiabatic processes (radiation, convection, precipitation, and latent heat) also simulate QBO-type waves in the stratosphere but without any *ad hoc* parameterization of equatorial wave forcing (Coriolle *et al* 1993). This suggests that such oscillations are inherent in the lower atmosphere/ocean system and are transmitted upward into the stratosphere by wave-breaking (momentum deposition). The amplitude of these simulated oscillations, however, is significantly less than the observed value, suggesting that an additional amplifying source may be missing in the model.

The GCMs designed to predict the recurrence of anomalously warm surface water, higher sea level, and downwelling in winter along the west coast of South America (El Niño) principally include the major oscillating pressure system of the tropics (the Southern Oscillation) and the interacting Kelvin/Rossby wave model. The Southern Oscillation largely determines temperature, precipitation, and wind changes in the tropics; the wave model facilitates the recurring eastward movement of warm surface water formed principally in the western Pacific. Correlation of El Niño with the Southern Oscillation has resulted in designation of the combined systems as ENSO. Failure of most ENSO models to predict some El Niños (Kerr 1993) has led to the suggestion that the erratic timing of El Niño is a function of a low-order transition to chaos through a series

In: C.M. Isaacs and V.L. Tharp, Editors. 1996. *Proceedings of the Twelfth Annual Pacific Climate (PACLIM) Workshop, May 2-5, 1995.* Interagency Ecological Program, Technical Report 46. California Department of Water Resources.

of frequency-locked steps created by nonlinear resonance forced by the annual cycle (Jin *et al* 1994; Tziperman *et al* 1994) and, thus, by implication unpredictable — on the way to chaos, but not quite.

Resonance Analysis

Since this analysis focuses on higher frequency components of the weather, I begin by placing them in context with lower-frequency elements of the tidal-resonance climatic model. Figures 1 through 6 are examples of paleoclimatic records suggesting in-phase relationships with the 556-year tidal cycle and its 2/1 (278-year), 4/1 (139-year), 6/1 (92.7-year), 12/1 (46.3-year), and 25/1 (22.2-year) resonances.[1] Figures 1, 4, 5, and 6 are slight modifications of figures presented in Karlstrom (1995); Figures 2 and 3 have not been previously published. The coefficient of correlation (R) shown in these and subsequent figures represents the percentage of match by inspection between paleoclimatic trend and cycle turning points.

The above resonance correlations suggest doubling, tripling, and redoubling of a forcing cycle, a phenomenon characteristic of a complex dynamic system in nonlinear transition to chaos, although linearity cannot be excluded at the present level of analysis.

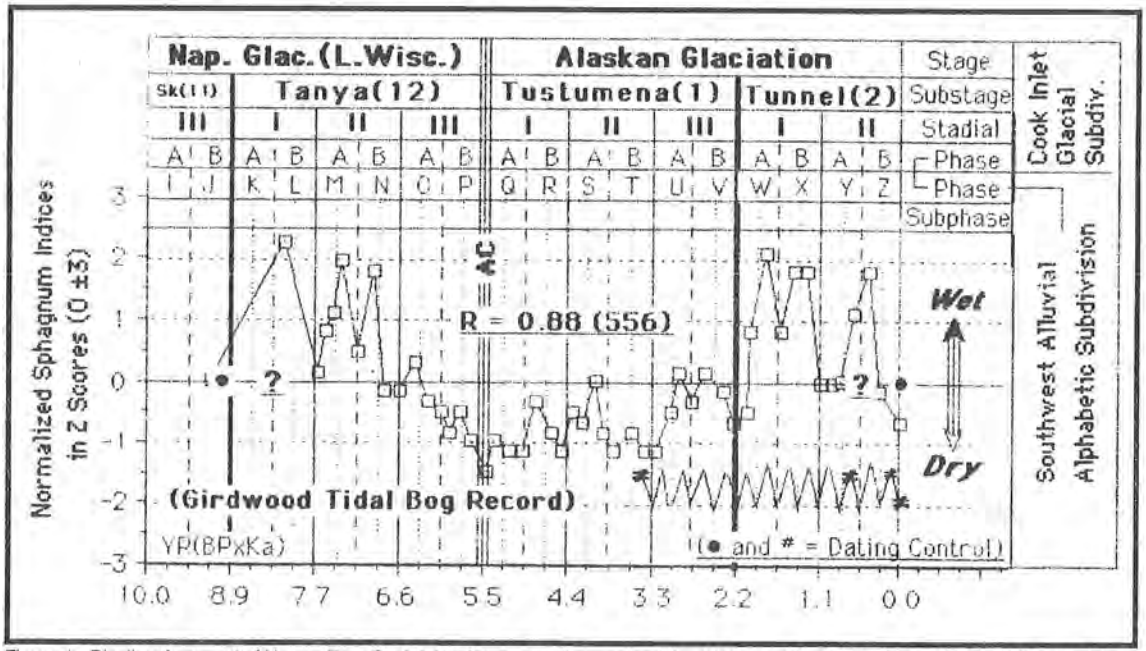

Figure 1 Bioclimatic record of Homer Bog, Cook Inlet, Alaska, on time-scale of the 1112-year Stadial Cycle and its 2/1 (556-year) Phase Cycle and 4/1 (278-year) Subphase Resonance. Pollen indices in Huesser (1965) time-calibrated by basal date listed in Karlstrom (1964). The higher frequency Girdwood Bog record is schematically plotted as interpreted climatically in Karlstrom (1961). Because of wider sampling intervals, Homer Bog shows the strongest tendency to oscillate in phase with the 556-year Phase Cycle and positions the driest post-glacial interval contemporaneous with the late Atlantic dry interval of Europe (see Figure 2). (AC = Altithermal Culmination)

1 The ratio indicates frequency change relative to the base cycle as 1; the resulting subharmonic resonance is identified by wavelength in the accompanying parentheses.

In Figure 1, Alaskan bioclimatic and chronstratigraphic evidence suggests the 556-year Phase Cycle and its double 2/1 (278-year) resonance.

In Figure 2, these resonances appear to be recorded in examples of European bog records with primary trends suggesting that the major post-glacial warm/dry interval of northern and central Europe were contemporaneous with that in North America, culminating between 6000 and 5000 YBP.

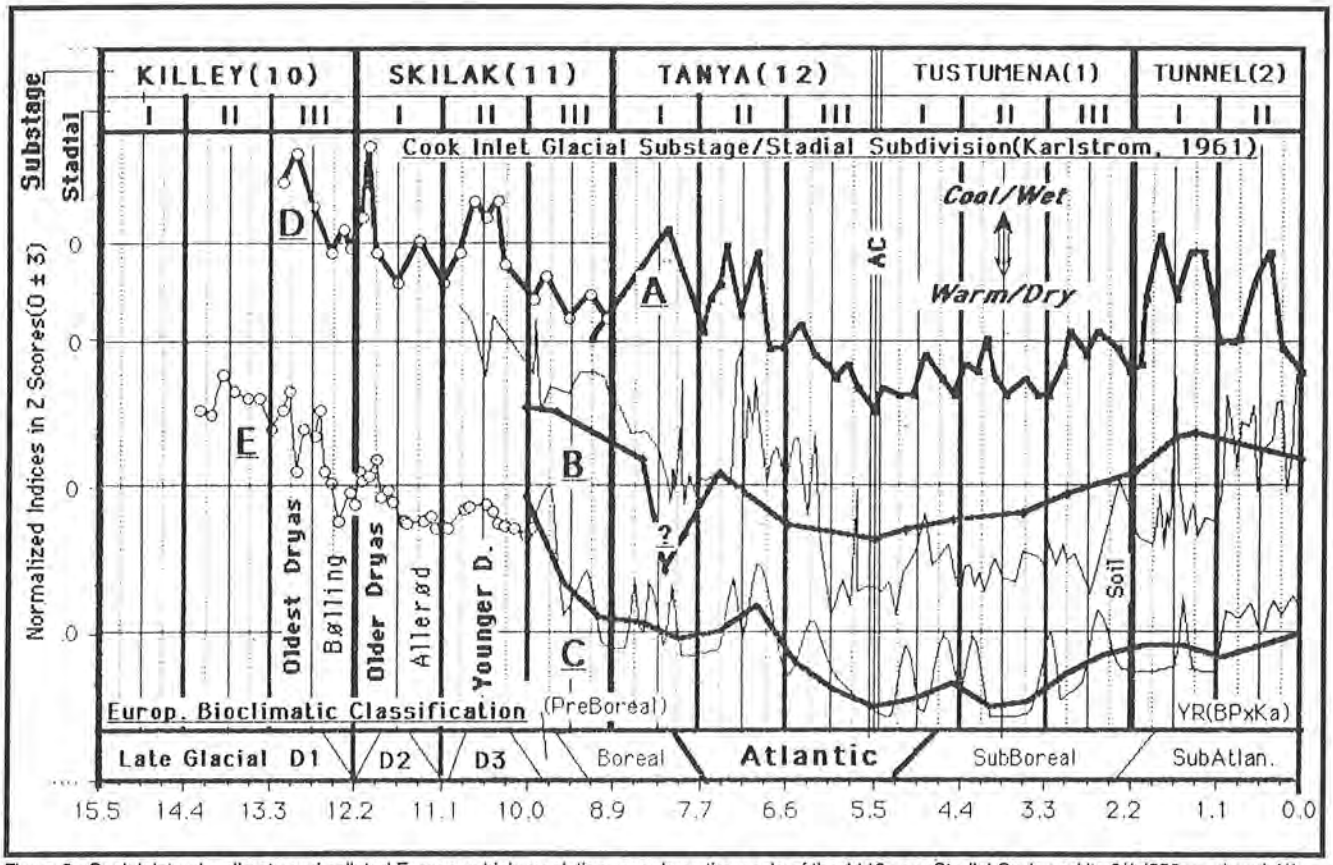

Figure 2 Cook Inlet paleoclimate and collated European high-resolution records on timescale of the 1112-year Stadial Cycle and its 2/1 (556-year) and 4/1 (278-year) resonances. A. Cook Inlet, Homer Bog (Figure 1); B. Agaröds Bog/hydrology of Sweden (Nilsson 1964); C. Alps timberline fluctuations (Beug 1982); D. Danish Bolling Bog (in Karlstrom 1961); and E. Swiss Wachseldorn Bog (Oeschger and others 1980) which, though more complacent (lower amplification of secondary oscillations), replicates with some fidelity the classic Late Glacial Dryas sequence of Denmark in D. Data used in constructing Alps record C are shown in Figure 3. (AC = Altithermal Culmination)

Figure 3 provides the data used in constructing the Postglacial timberline record of the European Alps.

In Figure 4, southwest dendroclimatic records suggest a regionally robust Event Cycle of 139-years, which represents doubling (2/1) of the 278-year Subphase Cycle and a redoubling (4/1) of the 556-year Phase Cycle.

In Figure 5, paleoclimatic records suggesting the 6/1 (92.7-year) and 12/1 (46.3-year) resonances seem to be directly related to solar activity as expressed in Sunspot Cycle length and could be either linear or nonlinear in origin.

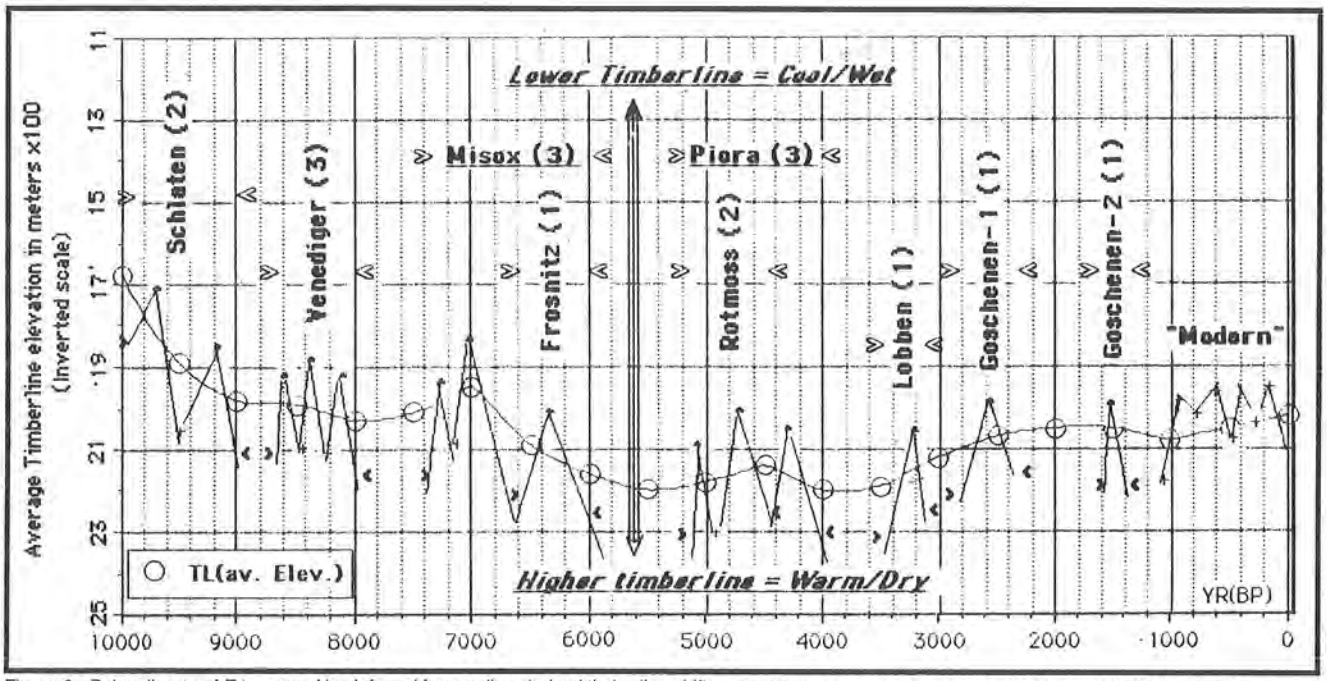

Figure 3 Paleoclimate of European Alps inferred from pollen-derived timberline shifts. From Paleoecological data summarized in Beug (1982). Main trends from averaged elevations of five curves reconstructed, respectively, for the Alps of Austria, France, Wallis, northern and south-central Switzerland. The superimposed named secondary cold phases (number of events shown in parentheses) are from various workers in different parts of the Alps. The plotted amplitudes of these radiocarbon-bracketed cold phases are relative and not to scale. "Modern" events after Patzelt (1980). Time-scale in years before present (1950). >–< = Bracketing radiocarbon dates.

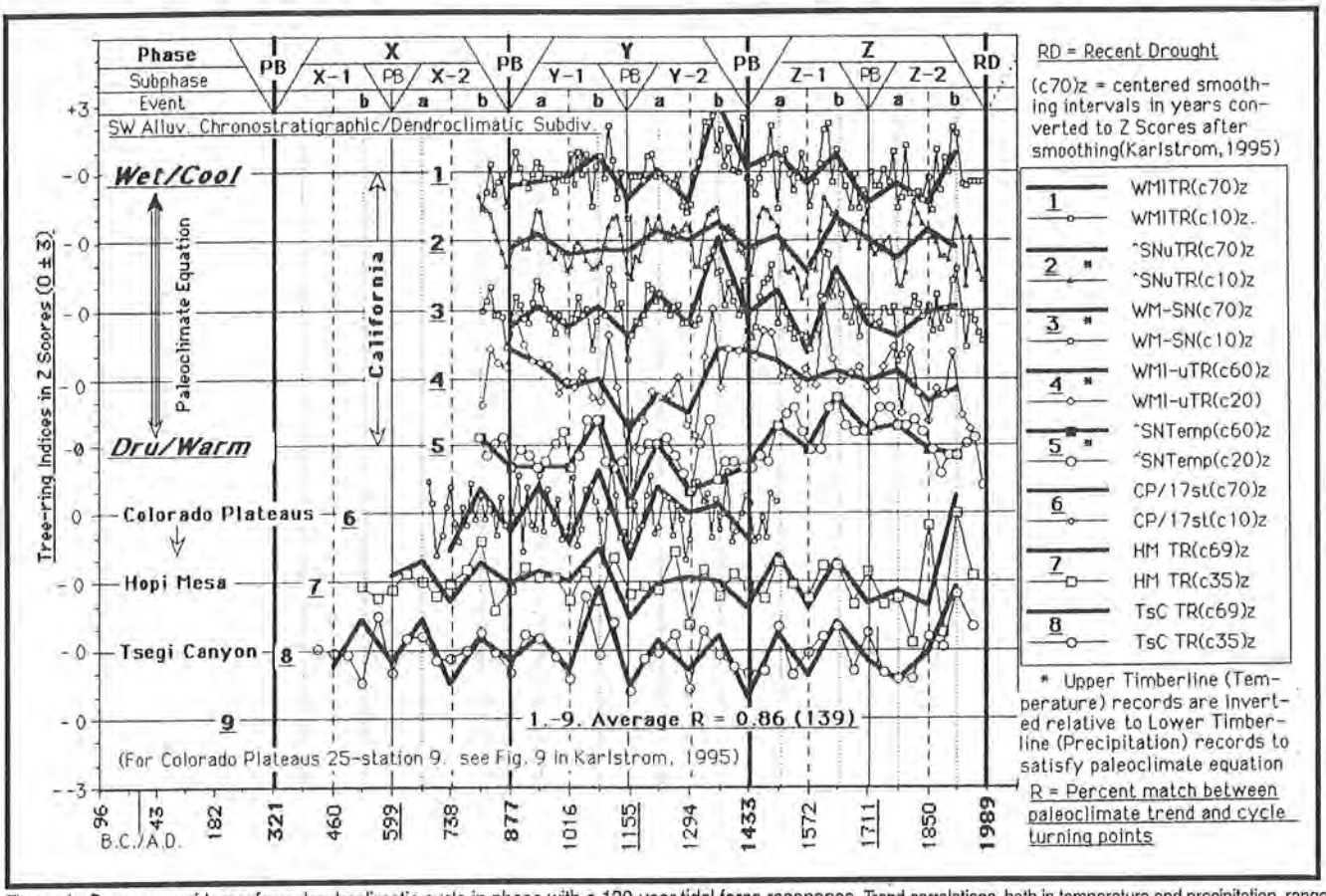

Figure 4 Summary evidence for a dendroclimatic cycle in phase with a 139-year tidal force resonance. Trend correlations, both in temperature and precipitation, range from 0.75 to >0.9, or within the range of correlations from tree-ring/ climate calibrations. This suggests that the cycle is real, regionally robust, and related to changing atmospheric dynamics and patterns. Similar half-cycle analyses of other records may define differing regional patterns and local responses, advancing understanding of climatic/biologic process. PB = point boundary (clustering of basal contact dates: Karlstrom 1988). 1: White Mountain, California, 10-year precipitation indices (Fritts 1967). 2: Sierra Nevada, California, 10-year temperature indices (Scuderi 1987). 3: 1 and 2 combined (precipitation and temperature). 4: White Mountain, California, 20-year precipitation and temperature indices (Lamarche 1974). 5: Sierra Nevada, California, 20-year temperature indices (Graumlich 1992). 6: Colorado Plateaus 17-station 10-year precipitation indices (Berry 1982). 7, 8, 9: Annual precipitation indices from Dean and Robinson (1978).

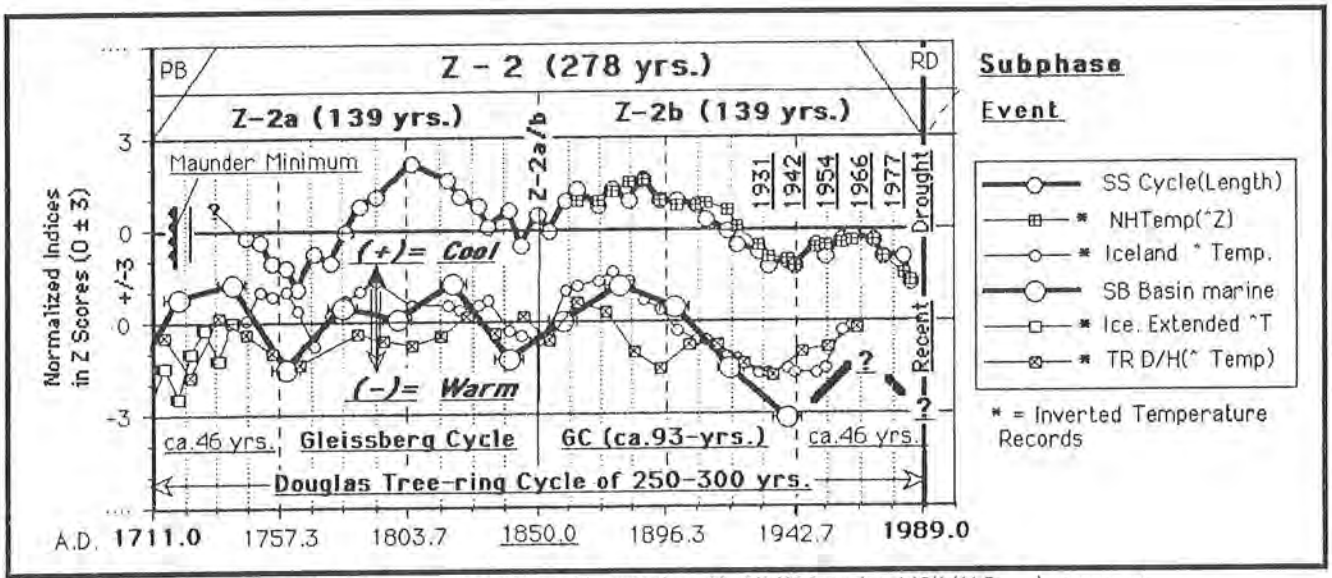

Figure 5 Sunspot and climate records on timescale of the 139-year Event Cycle and its 3/1 (46.3-year) and 12/1 (11.5-year) resonances. Sunspot, hemispheric temperature, and Iceland indices to 1745 from Friis-Christensen and Lassen (1991); extension of Iceland temperature record by indices from Bergthorsen (1969). Santa Barbara marine indices from Pandolfi and others (1980), and tree-ring-dated isotope indices from Epstein and Yapp (1976). Sunspots and collated climatic records appear to be related to the Tidal Resonance Model through in-phase relationships with the ~46-year resonance and its 2x Gleissberg Sunspot Cycle. Some tendency for sunspot-length and higher resolution climate records to oscillate in phase with the 11.5-year resonance.

In Figure 6, the 25/1 (22.2-year) resonance also appears to be directly related to solar activity but, in this case, with solar magnetism (the double Hale Sunspot Cycle). Thus, resonance could also be a function of either linear response or a fundamental fifth produced in a nonlinear transitional phase toward chaos. These apparent frequency-dependent correlations with both Sunspot length and Solar magnetism emphasize the potential complexity (and remaining uncertainty) of the mix of processes seemingly involved in tidal/solar influence on weather.

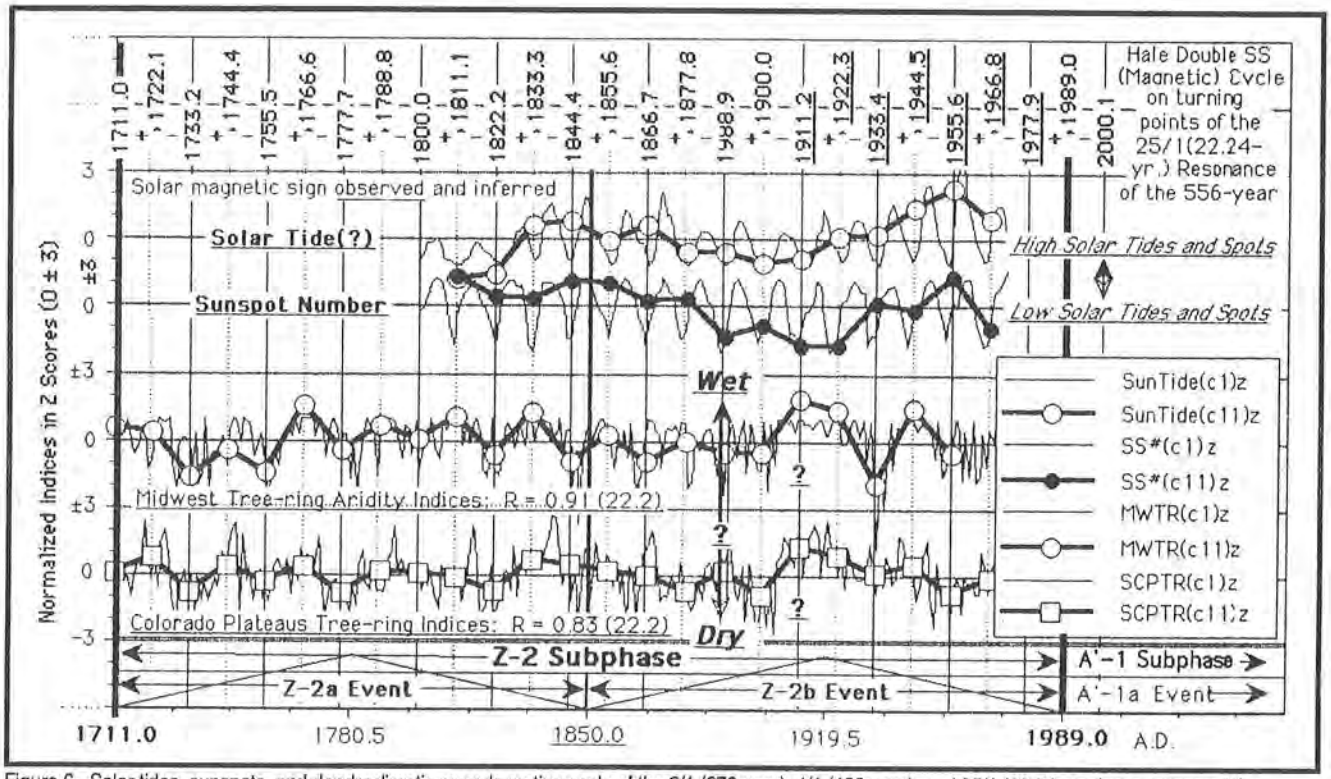

Figure 6 Solar tides, sunspots, and dendroclimatic records on timescale of the 2/1 (278-year), 4/1 (139-year), and 25/1 (22.24-year) resonances of the 556-year phase cycle. Annual indices of sunspots and solar tides from Wood in Gribbin (1976); of midwest tree-ring indices from Mitchell and others (1979) in Burroughs (1992); and of Colorado Plateaus tree-ring indices from Dean and Robinson (1978). Half-cycle smoothing on turning points of the 25/1 (22.24-year) resonance that is in phase with the average Hale double sunspot (magnetic) cycle. This, in turn, seemingly integrates solar/earth tidal phases with terrestrial climate through solar magnetic change (+ solar magnetism = generally increased earth rainfall).

In Figure 7, I extend analysis to higher frequencies by comparing two resonances of the tidal-force model that approximately match the mean period of the QBO as represented by indices derived from Figure 5.8 in Burroughs (1992). The 250/1 (2.22-year) resonance of the 556-year tidal cycle tests the repeated suggestion in the literature that the QBO may be the fifth resonance of the mean Sunspot Cycle (11.1 years). The slightly longer 240/1 (2.32-year) resonance is intrinsically much stronger in that it is a combination of resonance components divisible by all integers through 10, excepting the weak 7th and 9th. Figure 7 shows that the 250/1 resonance is evidently too short for consistent in-phase relationships with the QBO, whereas the 240/1 resonance appears to be strongly in phase with the QBO both in timing (as extrapolated over 500 years from AD 1433) and in average duration. Burroughs (1992) gives the mean period of the QBO as about 28 months. The 2.32 years (27.8 months) of the 240/1 resonance is essentially the same. Nonetheless, a much longer QBO record is required to more precisely define mean cycle length and to statistically exclude the possibility of fortuitous coincidence within the present short segment of record.

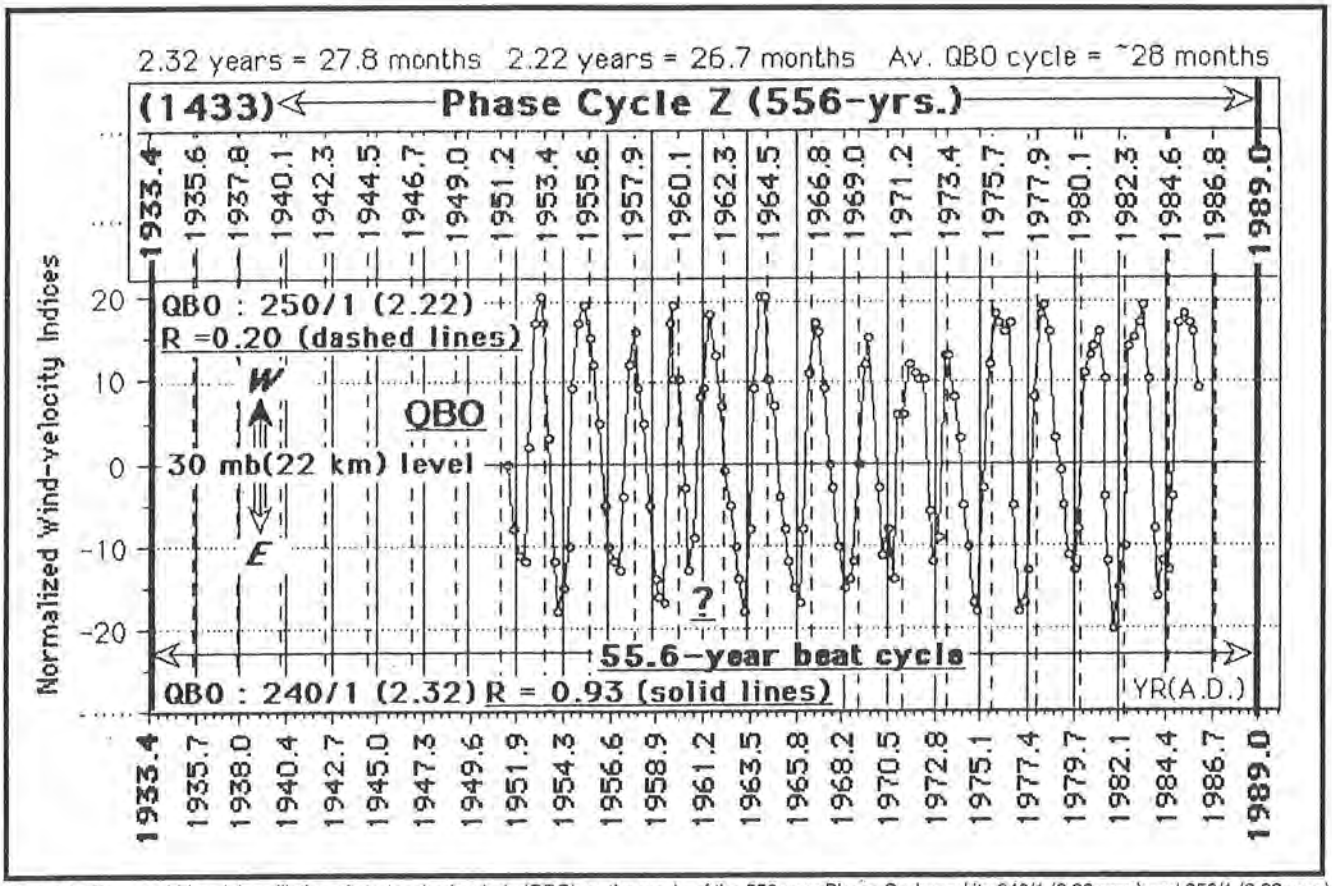

Figure 7 The quasi-biennial oscillation of stratospheric winds (QBO) on timescale of the 556-year Phase Cycle and its 240/1 (2.32-year) and 250/1 (2.22-year) resonances. The two resonances produce a beat cycle every 55.6 years when they return to phase, or ten times during each Phase Cycle. The 240/1 resonance appears strongly in phase with the QBO record; the 250/1 resonance (one-fifth of the average Sunspot Cycle) is evidently too short for consistent in-phase relationships with the QBO. Monthly indices from Figure 5.8 in Burroughs (1992) replotted at 3-month intervals.

In Figures 8 and 9, I extend analyses of these two resonances through correlation with Jones and Wigley's (1990) version of average global temperature. Whereas the 240/1 (QBO?) resonance may be weakly represented (Figure 8), no correlation in phasing is apparent with the 250/1(Sunspot) resonance (Figure 9). However, as graphed in Figure 9, the progressive decrease in Sunspot length toward the end of Phase Cycle Z is consistent with Friis-Christensen and Lassen's (1991) longer term correlation of decreasing Sunspot length with increasing global temperature — and evidently with the tidal resonance model as well (Figure 5).

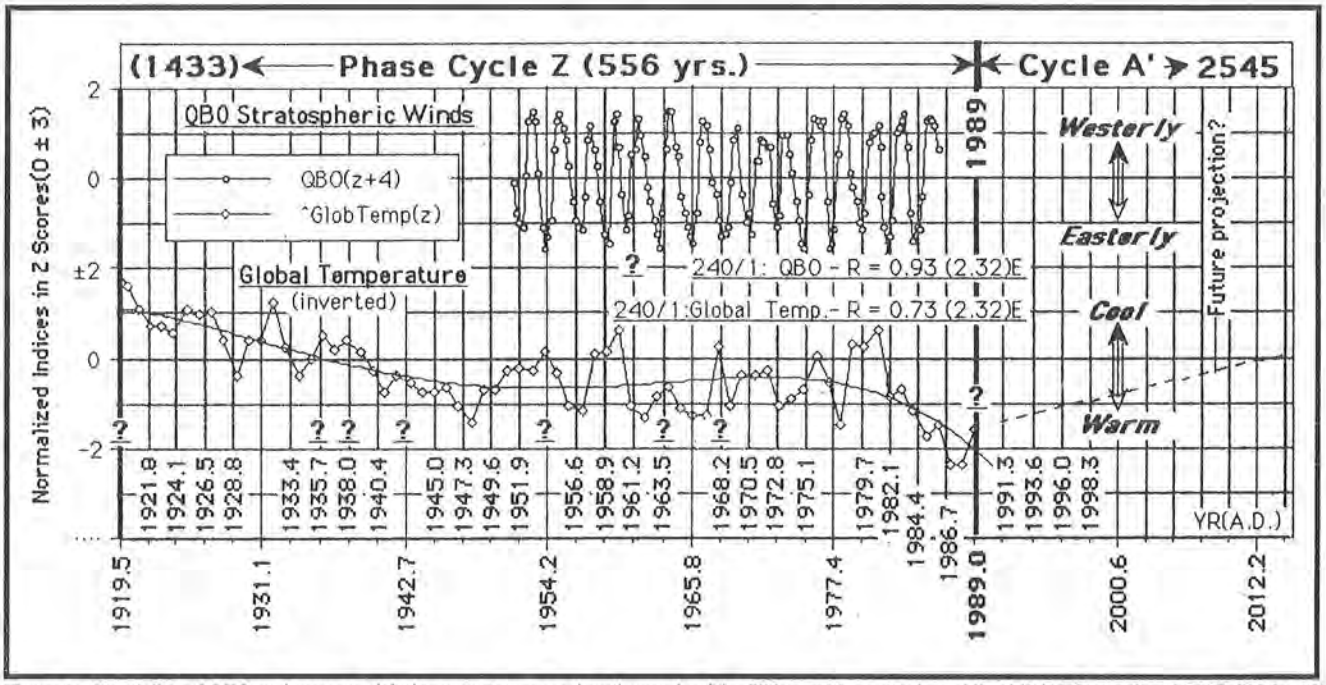

Figure 8 Correlation of QBO and average global temperature record on timescale of the 556-year Phase Cycle and its 48/1 (11.58-year) and 240/1 (2.32-year) resonances. Annual average temperature indices from Jones and Wigley (1990); monthly QBO indices from Burroughs (1992) replotted at 3-month intervals. Although the QBO easterlies seem strongly in phase with the 240/1 resonance, it is apparently only weakly reflected in the secondary trends of Jones and Wigley's version of the global temperature record. Compare with Figure 9.

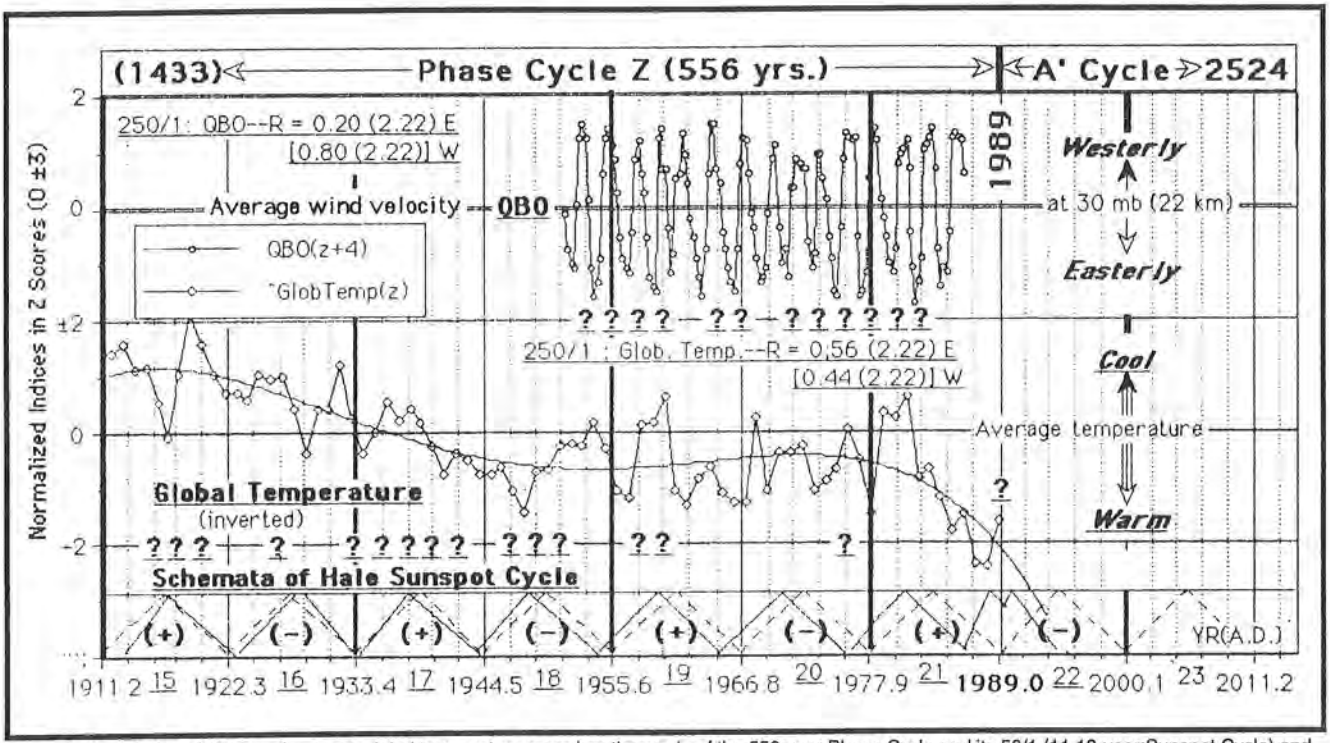

Figure 9 Correlation of QBO and average global temperature record on timescale of the 556-year Phase Cycle and its 50/1 (11.12-year:Sunspot Cycle) and 250/1 (2.22-year) resonances. Annual temperature indices from Jones and Wigley (1990); monthly QBO indices from Burroughs (1992). The 5/1 resonance of the average Sunspot Cycle (though showing a tantalizingly strong tendency for association with the westerly wind epicycle) is evidently too short for consistent phasing with the QBO and apparently is not reflected in Jones and Wigley's version of global temperature. Sunspot schemata from Figure 6. Solid lines = observed turning points of the numbered Sunspot Cycles. Note the progressive decrease in cycle-length toward end of Phase Cycle Z, or consistent with Friis-Christensen and Lassen's (1991) correlation of shortening cycle-length with increasing global temperature (Figure 5).

In Figure 10, a much stronger correlation is suggested between the 240/1 (QBO) resonance and the Southern Oscillation tropical air-pressure/ temperature records. This result is generally compatible with the GCMs that generate QBO-type stratospheric winds from tropospheric circulation dynamics and with energy transfer from troposphere to stratosphere. The seemingly stronger correlation of the 240/1 resonance with the QBO than with the Southern Oscillation, however, suggests that tidal- resonance modulation or amplification in the stratosphere is more linear than that in the denser lower atmosphere. If, in fact, the out-of-phase portions of both records represent nonlinear phase reversals, the larger number of such reversals in the ENSO suggest sporadic decoupling of the two systems, both of which evidently occasionally respond differentially to the same driving function.

The correlation with the El Niño series is strikingly weaker, suggesting that some critical parameter(s) has been missed in modeling the ENSO. Most El Niños coincide with Southern Oscillation temperature troughs but are missing or displaced during others. Independent analyses by Jin *et al* (1994) and Tziperman and others (1994) are consistent in suggesting that the seasonal El Niño phenomenon is a function of a low-order nonlinear transition to chaos forced by the annual cycle. After all, they note, El Niño is a winter phenomenon. But some El Niños still phase with the resonance model. Missing 1989 (no El Niño, presumably because of nonlinear phase reversals in both QBO and ENSO records), the model predicted the 1991 and 1993 El Niños and predicts El Niños for 1996 and 1998 if no nonlinearities or other distorting variables intervene. A big if, implying that unless missing variables are found, or unless timing and phasing of nonlinearities become predictable by refined theory or precursor signals, El Niño and other higher frequency weather phenomena will remain essentially unpredictable over the long run.

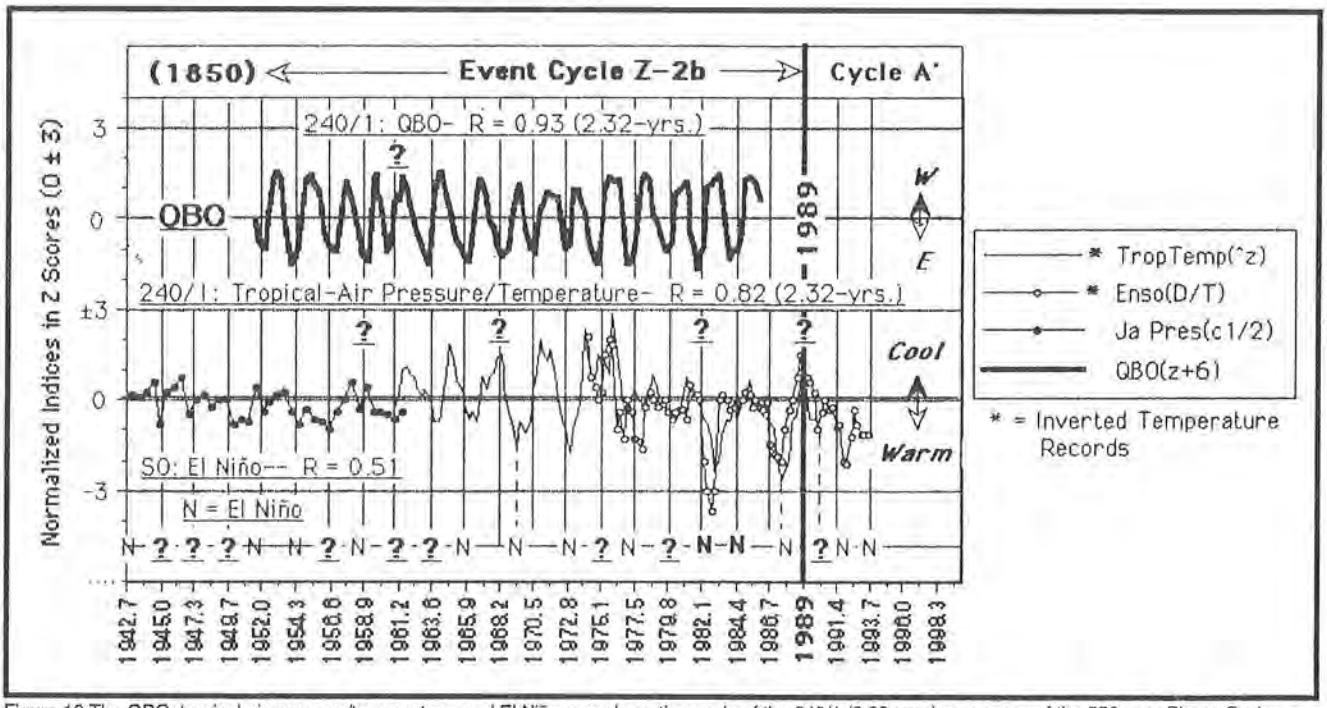

Figure 10 The QBO, tropical air pressure/temperature, and El Niño records on timescale of the 240/1 (2.32-year) resonance of the 556-year Phase Cycle. Tropical temperature indices from Burroughs (1992), ENSO indices from Kerr (1993), Jakarta air-pressure indices from deBoer (1967), and El Niño dates from Quinn and others (1987). The generally strong correlation of the QBO and SO/temperature with the 240/1 resonance strongly suggests tidal-force modulation of one or both of these stratospheric and tropospheric oscillatory systems. The El Niño-Southern Oscillation correlation is strikingly weaker, suggesting that other critical variables are involved, including possible nonlinear phase-reversals near 1961 and 1989 in the QBO, and near 1958, 1968, 1982, and 1989 in the air pressure/temperature records. Alternatively, these differences could result from nonlinear response to the annual cycle.

Summary

The recent application of Chaos Theory to atmospheric dynamics seems to provide an explanation for some of the perplexing order/disorder patterns of high-frequency weather records. However, even the longest instrumental records (about 100 years) are too short to permit statistical discrimination between random events and nonlinear responses (Tziperman *et al* 1994) or, for that matter, between linear and nonlinear responses. With this caveat, I tentatively conclude the following:

- The fifth resonance (2.22 years) of the Sunspot Cycle (= the 250/1 resonance of the 556-year tidal-force cycle) is seemingly too short to match the oscillations of the QBO which, therefore, is probably not directly driven by solar processes.

- Instead, a strong match, both in timing and average duration, with the intrinsically stronger 240/1 (2.32-year) resonance of the 556-year tidal-force cycle, strongly suggests that the QBO may be either modulated or amplified by atmospheric tidal resonances.

- The generally strong correlation between the QBO and tropical Southern Oscillation, in turn, suggests that one or probably both of these stratospheric and tropospheric oscillations are modulated or amplified by the same tidal-resonance system. The greater number of presumed nonlinear phase reversals in the ENSO record, however, suggests that the two atmospheric levels are coupled loosely enough to permit occasional differential nonlinear responses to the same driving function. Parameterization of modulating tidal resonances may improve some GCMs by increasing the amplitude of the simulated QBO-type oscillations.

- The strikingly weaker correlation between the Southern Oscillation and El Niño events strongly suggests that some critical parameters are missing in the GCMs specifically designed to predict El Niño occurrence. The missing ingredient may be low-order nonlinear phases during transition to chaos as driven by the annual cycle. Another possible explanation for El Niño irregularity is occasional nonlinear phase reversals. In any case, unless missing variables are found, or unless nonlinearities become predictable by refined theory or precursor signals, the timing of El Niño will probably remain unpredictable. Thus, in high-frequency weather analyses, we may be on a journey toward chaos but still not quite there.

Acknowledgment

To my wife, colleagues, and friends who have urged me to continue my decades-long research on high-resolution paleoclimatic records.

References

Bergthorsen, P. 1969. An estimate of drift ice and temperature in Iceland in 1000 years. *Jour. of Jökull* 19:94-101.

Berry, M.S. 1982. *Time/Space and Transition in Anasazi Prehistory.* University of Utah Press, Salt Lake City. 147 pp.

Beug, Hans-Jurgen. 1982. Vegetation history and climatic changes in central and southern Europe. Pages 85-102 in *Climatic Change in Late Prehistory.* A. Harding, editor. Edenburg University Press, Edenburg.

Burroughs, W.J. 1992. *Weather Cycles: Real or Imaginary?* Cambridge University Press, Cambridge. 201 pp.

Cariolle, M., M. Amodel, M. Deque, J.F. Mahfauf, P. Simon, H. Teyssedre. 1993. A quasi-biennial oscillation signal in General Circulation Model simulations. *Science* 261:1313-1316.

Dean, J.S., and W.J. Robinson. 1978. Expanded tree-ring chronologies for the southwest United States. *Chronology Series III, Laboratory of Tree-Ring Research,* Univ. of Arizona, Tucson. 58 pp.

deBoer, H.J. 1967. Meteorological cycles. Pages 564-572 in *The Encyclopedia of Atmospheric Sciences and Astrogeology.* R. Fairbridge, editor. Reinhold, NY.

Epstein, S., and C.I. Yapp. 1976. Climatic implications of the D/H ratio of hydrogen in C/H groups in tree cellulose. *Earth Planet. Sci. Letters* 30:252-266.

Friis-Christiansen, E., and K. Lassen. 1991. Length of solar cycle: An indicator of solar activity closely associated with climate. *Science* 254:698-700.

Fritts, H.C. 1967. Tree-ring analysis (dendroclimatology). Pages 1008-1026 in *The Encyclopedia of Atmospheric Sciences and Astrogeology.* R.W. Fairbridge, Editor. Reinhold. New York.

Graumlich, L.J. 1992. A 1000-year record of climatic variability in the Sierra Nevada, California: Handout, Am Quat Assoc, 12th Biennial Meeting. August 24-26, University of California, Davis.

Gribbin, J.R. 1976. *Forecasts, Famines and Freezes.* Walker and Company, New York.

Heusser, C.J. 1965. A Pleistocene phytogeographical sketch of the Pacific Northwest and Alaska. Pages 469-483 in *The Quaternary of the United States.* H.E. Wright Jr and D.J. Frey, editors. Princeton Univ. Press, Princeton, New Jersey.

Jin, F.F., J.D. Neelin, M. Ghil. 1994. El Niño on the Devil's staircase: Annual subharmonic steps to chaos. *Science* 264:70-72.

Jones, P.D., and T.M.L. Wigley. 1990. Global warming trends. *Scientific American.* August 1990:84-91.

Karlstrom, T.N.V. 1961. The glacial history of Alaska: Its bearing on paleoclimatic theory. *Annals New York Academy of Science* 95 Article 1:290-340.

Karlstrom, T.N.V. 1964. *Quaternary Geology of the Kenai Lowland and Glacial History of the Cook Inlet Region, Alaska.* U.S. Geological Survey Professional Paper 443. 69 pp.

Karlstrom, T.N.V. 1988. Alluvial chronology and hydrologic change of Black Mesa and nearby regions. Pages 45-91 in *The Anasazi in a Changing Environment.* G.J. Gummerman, editor. School of American Research Advance Seminar Book. Cambridge University Press, London.

Karlstrom, T.N.V. 1995. A 139-year dendroclimatic cycle, cultural/environmental history, sunspots and longer-term cycles. Pages 137-159 in *Proceedings of the Eleventh Annual Pacific Climate (PACLIM) Workshop.* C.M. Isaacs and V.L. Tharp, editors. Interagency Ecological Program Technical Report 40. California Department of Water Resources.

Kerr, R.A. 1993. El Niño metamorphosis throws forecasters. *Science* 262:656-657.

Lamarche, V.C. Jr. 1974. Paleoclimatic inferences from long tree-ring records. *Science* 183:1043-1048.

Mitchell, M., J.C.W. Stockton, D.M. Meko. 1979. Evidence of a 22-year rhythm of drought in the western United States related to the Hale Solar Cycle since the 17th century. In *Solar-Terrestrial Influences on Weather and Climate.* B.M. McCormac and T.A. Seliga, editors. D. Reidel, Hingham, Mass.

Nilsson, T. 1964a. Standardpollen diagramme und 14C datierungen aus dem Agaröds Mosse im mittieren Schonen. *Lunds Universitets Ärskrift N.F.* Avd. 2. Bd 59, Nr 7: 1-52 Häkan Ohissons Boktryckeri, Lund.

Nilsson, T. 1964b. Enwicklungsgeschichtliche studien im Ageröds Mosse, Schonen. *Lunds Universitets Arsshift N.F.* Avd. 2. Bd 59. Nr 8:1-34 Häkan Ohlssons Boktryckeri, Lund.

Oeschger, H., M. Welten, U. Eicher, M. Moll, T. Riesen, U. Siegenthaler, S. Wegmuller. 1980. 14C and other parameters during the Younger Dryas cold phase. *Radiocarbon* 22:299-310.

Pandolfi, L.J., E.K. Kalil, P.R. Doose, L.H. Levine, L.M. Libby. 1980. Climate periods in trees and a sea sediment core. *Radiocarbon* 22:740-745.

Patzelt, G. 1980. Neue Ergebnisse der Spat- und Postglaziolforschung in Tirol. *Osterr. Geogr. Ges. Jahresber.* 76/77:11-18.

Pettersson, O. 1914. Climatic variations in historic and prehistoric time. *Svenska Hydrogr Biol Komm Skriftern* 5.

Quinn, W.H., V.T. Neal, S.E. Antunex. 1987. *Jour. Geophs. Res.* 92:144-149.

Scuderi, L.A. 1987. Glacial variations in the Sierra Nevada, California, as related to a 1200-year tree-ring chronology. *Quat. Research* 27:220-231.

Tziperman, E., L. Stone, M.A. Cane, H. Jaosh. 1994. El Niño chaos: Overlapping of resonances between the seasonal cycle and the Pacific Ocean-atmosphere oscillator. *Science* 264:72-74.

Chronological Records of Climate-Related Events and Societal Consequences

Gary D. Sharp

Abstract

A chronology of documented regional and global warm and cold event records is collated along with documented ecosystem response records and health threat/sequellae records for the historical period. Patterns of societal response to cold periods punctuated by warm periods have been associated with considerable human health impacts, stimulated by blooms in disease vectors such as rodents and insects. The recent ENSO/SOI records provide insights into these sequences, and historical detectivery such as that by Quinn and associates provides unique opportunities to explore the ENSO warm event as far back into history as the mid-seventeenth century.

Great interest is awakening in trying to understand societal and ecosystem responses to climate regime shifts. Longer time scales of cool and warm climatic periods also provide tantalizing clues about pre-human evolution, as well as regional climatic precursors for local civilizations to begin and thrive around the globe. While debates over the future have captured many persons' interest, it is important to maintain as open a perspective as possible on the merits of examining the relationships between regional, local, and global consequences of climate swings and events, as well as the frequent volcanic and seismic cataclysms that punctuate these warming and cooling scenarios. I have tried to post a firm set of climate observations upon which to begin a synthesis of regional responses for well-documented areas.

In: C.M. Isaacs and V.L. Tharp, Editors. 1996. *Proceedings of the Twelfth Annual Pacific Climate (PACLIM) Workshop, May 2-5, 1995.* Interagency Ecological Program, Technical Report 46. California Department of Water Resources.

Appendix A
AGENDA

Twelfth Annual Pacific Climate (PACLIM) Workshop
Asilomar Conference Center, Pacific Grove, California
May 2-5, 1995

PACLIM is a multidisciplinary workshop broadly focused on climate phenomena occurring in the eastern Pacific and western Americas. Its purpose is to understand the climate effects in this region by bringing together specialists from diverse fields including both physical and biological sciences. Time scales range from weather to paleoclimate.

Convened at the Asilomar Conference Center, the atmosphere of the Workshop is intentionally informal, and room and board are provided for the participants. The Workshop is organized by a committee of representatives from several organizations, but historically it has been spearheaded by U.S. Geological Survey scientists. Held annually, the Workshop has benefited from funding and other forms of support from several agencies (public and private).

AGENDA

Twelfth Annual Pacific Climate (PACLIM) Workshop
Asilomar Conference Center, Pacific Grove, California
May 2 - 5, 1995

Asilomar Meal Schedule
Breakfast 7:30-9:00 am
Lunch 12:00-1:00 pm
Dinner 6:00-7:00

Tuesday Evening **May 2, 1995**

Moderator: Caroline Isaacs

7:00-7:10	Welcome and Announcements
7:10-7:30	Interannual Variability in the Tropics During 1985-1994 Gerald D. Bell and Vernon Kousky, Climate Analysis Center
7:30-7:45	Recent Trends in Tropical Pacific Climate Nathan Mantua, IRICP Research and Development Pilot Project, SIO
7:45-8:05	Recent Winters in the Western United States and Relation to ENSO Patterns Kelly T. Redmond, Western Regional Climate Center, Reno, Nevada
8:05-8:25	Influence of Climatology on Rainfall Thresholds for Initiation of Debris-Flows on the California Coast Raymond C. Wilson, U.S. Geological Survey, Menlo Park, California
8:25-8:45	California Water Outlook in 1995 Maurice Roos, California Department of Water Resources, Sacramento, California
8:50 —	Social Gathering

Wednesday Morning **Invited Talks** **May 3, 1995**

Interdecadal Climate Variability Over the Pacific and Western Americas

Moderator: Tim Baumgartner

8:30-9:10	Ocean-Atmosphere Variability from the Instrumental Record — Natural Decadal Variability and Possible Anthropogenic Change Nicholas E. Graham, Scripps Inst. of Oceanography, La Jolla, California
9:10-9:50	Mechanisms of Upper-Ocean North Pacific Ocean Thermal Variability in a 1970-88 Simulation Arthur J. Miller, Dan Cayan, Warren B. White, and Mojib Latif; Scripps Institution of Oceanography, La Jolla, California
9:50-10:10	*Break*
10:10-10:50	Climate Forcing by Changing Solar Radiation Judith Lean, Naval Research Laboratory, Washington, D.C.
10:50-11:20	Decadal Hydroclimatic Variability over Western North America Dan Cayan, Michael Dettinger, and Henry Diaz; Scripps Institution of Oceanography, La Jolla, California
11:20-12:00	The Terrestrial Ecosystem Response in Western North America Tom Swetnam and Julio Betancourt, Univ. of Arizona, Tucson, Arizona

Wednesday Afternoon — **May 3, 1995**

Interdecadal Climate Variability (continued)

Moderator: Dan Cayan

1:30-2:10 — Effects of Interdecadal Climate Variability on the Oceanic Ecosystems of the Northeast Pacific Ocean
Robert C. Francis, S.R. Hare, A.B. Hollowed and W.S. Wooster;
University of Washington, Seattle, Washington

2:10-2:50 — Terrestrial Record of Interdecadal Climate Variability in Western North America
Malcolm Hughes, University of Arizona, Tucson, Arizona

2:50-3:10 — *Break*

3:10-3:50 — The Marine Paleorecords from Varved Sediments and Tropical Corals
Tim Baumgartner, Robert Dunbar, and B. Linsley;
Scripps Institution of Oceanography, La Jolla, California

3:50-4:30 — Societal Implications of Interdecadal Climate Variability
Roger Pulwarty, NOAA, Boulder, Colorado

Wednesday Evening — **Invited Talk** — **May 3, 1995**

7:30-8:10 — The Little Ice Age: Glacier Variations and Climate Since 1250 A.D.
Stephen Porter, Director, Quaternary Research Center,
University of Washington, Seattle, Washington

Thursday Morning — **May 4, 1995**

Moderator: Paul Smith

8:30-8:50 — Offshore Coho Salmon Populations Near the Pacific Northwest and Large-Scale Atmospheric Events
David Greenland, Department of Geography, Eugene, Oregon

8:50-9:10 — Long-Term Changes in the Equatorial Pacific Trade Winds
Anna Lebedeva and Allan J. Clarke; Florida State University. Tallahassee, Florida

9:10-9:30 — Stream Salinity in Response to Discharge (climate), Western United States
David Peterson, Dan Cayan, Michael Dettinger, Jeanne DiLeo, Caroline Isaacs,
Larry Riddle, and Richard E. Smith; U.S. Geological Survey, Menlo Park, California

9:30-10:00 — One-Minute Poster Introductions

10:00-10:35 — *Break*

10:35-10:55 — Interdecadal Variability in the Spatial Structure of Wind and SST of the California Current System
Franklin B. Schwing, Roy Mendelssohn and Richard Parrish;
Pacific Fisheries Environmental Group, Monterey, California

10:55-11:15 — A Ten-Year Time Series of Zooplankton Anomalies off the British Columbia Coast
David L. Mackas, Institute of Ocean Sciences, Sidney, Canada

11:15-11:35 — Climate-Related Long-Term Faunal Changes in a California Rocky Intertidal Community
James P. Barry, Charles H. Baxter, Rafe D. Sagarin, and Sarah E. Gilman;
Monterey Bay Aquarium Research Institute, Pacific Grove, California

11:35-11:55 — Decadal Patterns in Atmospheric Carbon Dioxide as Indicators of Changing Growth and Decay of Terrestrial Vegetation
Charles D. Keeling and Timothy Whorf; Scripps Institution of Oceanography, La Jolla, California

Thursday Afternoon **May 4, 1995**

Moderator: Larry Bensen

1:50-2:10 Chronic and Catastrophic Influences of the Environment on the Population Dynamics of the Common Fishes
Paul E. Smith, NOAA, La Jolla, California

2:10-2:30 An 800-year Paleoflood Record from the Sacramento Valley, California
Roger Byrne, University of California, Berkeley, California

2:30-2:50 Decadal Variation in the Trans-Pacific Migration of Northern Bluefin Tuna *(Thunnus Thynnus)* Coherent with Climate-Induced Change in Prey Abundance
Jeffrey J. Polovina, Southwest Fisheries Science Center, Honolulu, Hawaii

2:50-4:30 Poster Presentations

Thurday Evening **Invited Talk** **May 4, 1995**

7:30-8:10 Causes and Impacts of Decadal Climate Variability Over the North Pacific and North America
Tim Barnett, Scripps Institution of Oceanograpy, La Jolla, California

Friday Morning **May 5, 1995**

Moderator: Mike Dettinger

8:30-8:50 The Terrestrial Paleorecord of Climate Change Over the Last Thousand Years in the Canadian Rockies
Brian H. Luckman, Department of Geography, University of Western Ontario, London, Canada

8:50-9:10 Synoptic Dendroclimatology: A Process-Based Approach for Linking Tree-Ring Information to Atmospheric Circulation Over the Pacific and North America
Katherine K. Hirschboeck, Fenbiao Ni, Michelle L. Wood, and Connie A. Woodhouse; Laboratory of Tree-Ring Research, University of Arizona, Tucson, Arizona

9:10-9:30 Integrating Varve and Tree-Ring Time Series for Southern California Climate Reconstruction: A Twentieth Century Outlook
Franco Biondi, Carina Lange, Kimberly Cobb, and W.H. Berger; Scripps Institution of Oceanography, La Jolla, California

9:30-10:00 *Break*

10:00-10:20 Oxygen-18 Variation in Lake Lahontan, Lake Russell and Owens Lake During the Last Glacial-Interglacial Transition
L.V. Benson, J.W. Burdett, M. Kashgarian, and S. Lund; U.S. Geological Survey, Boulder, Colorado

10:20-10:40 Oxygen Isotope Analysis of Corals from the Gulf of California and the Gulf of Panama: Application and Implications for Coral-Based Paleoclimate Reconstructions
William A. Jones, Jr. Robert B. Dunbar, and Gerard M. Wellington; U.S. Geological Survey, Boulder, Colorado

10:40-11:00 Holocene Paleoclimate from a Sierra Nevada Lake
Scott Anderson, Northern Arizona University, Flagstaff, Arizona

Appendix B

POSTER PRESENTATIONS

Twelfth Annual Pacific Climate (PACLIM) Workshop
Asilomar Conference Center, Pacific Grove, California
May 2-5, 1995

Twelfth Annual Pacific Climate (PACLIM) Workshop
Asilomar Conference Center, Pacific Grove, California
May 2-5, 1995

Multiple-Proxy Lacustrine Record of Moisture Transport Over Western North America from 24 to 12 kyrs BP, Lake Estancia, New Mexico
Bruce D. Allen, Roger Y. Anderson, and Crayton J. Yapp;
Earth and Planetary Science, University of New Mexico, Albuquerque, New Mexico

Evidence for Possible Changes in Large-Scale Upwelling in the California Current in the Last 600 Years
Tim Baumgartner and John Southon, Scripps Institution of Oceanography and CICESE

A Late Pleistocene Paleohydrological Record of Sierra Nevada Runoff from Owens Lake, California
J. Platt Bradbury, U.S. Geological Survey, Denver, Colorado

Can Lake Sediments Provide a Record of Tropical Storms? The Case of Laguna de Juanacatlán, Jalisco, Mexico
Roger Byrne, D. Allen, E. Edlund, C. Polansky, and L. Menchaco;
University of California, Berkeley, California

Decadal Variability Over the North Pacific Ocean
Dan Cayan, Warren B. White, and Arthur J. Miller;
Scripps Institution of Oceanography, La Jolla, California

Geographic Patterns in the Lag of Temperature Response to Insolation for El Niño vs. La Niña
R.G. Craig, J.L. Betancourt, and D.E. Jones; Kent State University, Kent, Ohio

Disturbance Climate in the Columbia River Basin
Sue A. Ferguson and Mirium R. Peterson, USDA Forest Service, Seattle, Washington

Atmospheric Circulation Patterns Associated with Tree Growth Anomalies in the Central and Southern Sierra Nevada Mountains
Gregg Garfin, Laboratory of Tree-Ring Research, University of Arizona, Tucson, Arizona

On the Strength of the California Current: A Record From the Southern Baja California Margin
Juan Carlos Herguera, Tim Herbert, and Vicente Ferreira Bartrina;
CICESE, Ensenada, Baja California, Mexico

Changes in Mass Balance of South Cascade Glacier, North Cascades, from 1959 to 1994
Steven Hodge, Robert Krimmel, and E.G. Josberger;
U.S. Geological Survey, Tacoma, Washington

Interdecadal Shifting of the North Pacific Jet Stream — El Niño Events
Stephen H. Holets, Pacific Gas and Electric, San Francisco, California

The QBO, El Niño and Tidal Resonance Model
Thor Karlstrom, U.S. Geological Survey, La Conner, Washington

Physical, Chemical and Biological Characterization of Water Year Types in the San Francisco Bay Estuary
Peggy W. Lehman, California Department of Water Resources, Sacramento, California

Oceanographic Variability at Clipperton Atoll Since the 1880s: Stable Isotopic Evidence from Massive Corals
Brad Linsley and Robert Dunbar, Rice University, Houston, Texas

Evidence Supporting Global Warming from a Mid-Latitude, High Elevation Site
Mark Losleben, Rice University, Houston, Texas

Reconstructing Twentieth-Century Flood Patterns in Havasu Creek, Arizona, Using Historical and Dendrochronologie Data
Theodore S. Melis and William M. Phillips, U.S. Geological Survey, Tucson, Arizona

Interdecadal Variability in the Bakun Upwelling Indices
Heather Parker, NOAA, National Fisheries Service

Rock-Magnetic and Geomagnetic Secular Variations From Late Pleistocene Lake Estancia, New Mexico
H.D. Rowe, J.W. Geissman, B.D. Allen, and R.Y. Anderson;
Earth and Planetary Sciences, University of New Mexico, Albuquerque, New Mexico

Climate-Driven Hydrologic Transients in Holocene Lake Records
Alison J. Smith, Department of Geology, Kent State, Kent, Ohio

Chronological Records of Climate-Related Events and Societal Consequences
Gary D. Sharp, Center for Climate/Ocean Resources Study, Monterey, California

Changes in the Hydrometeorological Regime in the Pacific Northwest
John Vaccaro, U.S. Geological Survey, Tacoma,Washington

Interannual to Decadal Scale Variations in Glacier Mass Balance
Roy A. Walters, U.S. Geological Survey, Denver, Colorado

Seasonal to Decadal Scale Variability in a Radiolarian Time Series and Its Relationship to Climate
Amy L. Weinheimer and Daniel R. Cayan, Scripps Institution of Oceanography, La Jolla, California

Response of PNW Vegetation to Large-Scale Changes in Climate During the Last 100 kyr
Cathy Whitlock, University of Oregon, Eugene, Oregon

A High Frequency Paleoclimatic Record for the Late Holocene from Southern Nevada Derived from Aquatic and Terrestrial Pollen
Peter E. Wigand, Desert Research Institute, University of Nevada, Reno, Nevada

Relationships Between Climate and Atmospheric Circulation in the Sonoran Desert Region
Connie A. Woodhouse, Laboratory of Tree-Ring Research,
University of Arizona, Tucson, Arizona

Apendix C

ATTENDEES

Twelfth Annual Pacific Climate (PACLIM) Workshop
Asilomar Conference Center, Pacific Grove, California
May 2-5, 1995

ATTENDEES

Twelfth Annual Pacific Climate (PACLIM) Workshop
Asilomar Conference Center, Pacific Grove, California
May 2-5, 1995

David Adam
U.S. Geological Survey
345 Middlefield Road
Menlo Park, CA 94025
(P) (415) 329-4970
(F) (415) 329-4975
dadam@mojave.wr.usggs.gov

Bruce Allen
Dept. of Earth and Planetary Sciences
University of New Mexico
Albuquerque, NM 87131
allen@triton.unm.edu

Diana Anderson
University of California, Riverside
Dept. of Earth Sciences
Riverside, CA 92521
(P) (909) 878-2194
(F) (909) 787-4324
amargosa@ucrac1.ucr.edu

Kirk Anderson
University of California, Riverside
Dept. of Earth Sciences
Riverside, CA 92521
kirk@ucrac1.ucr.edu

Roger Y. Anderson
Dept. of Planetary Sciences
University of New Mexico
Albuquerque, NM 87131
(P) (505) 277-1639
(F) (505) 277-8843
ryand@triton.unm.edu

Scott Anderson
Northern Arizona University
PO Box 5694
Flagstaff, AZ 86011
(P) (602) 523-5821
(F) (602) 523-7290
sa@nauvax.ucc.nau.edu

Edward Armstrong
Moss Landing Marine Lab.
P.O. Box 950
Moss Landing, CA 95039
(P) (408) 755-8682
(F) same
armstrong@mlml.calstate.edu

Tim Barnett
Climate Research Division, UCSD
Scripps Institution of Oceanography
La Jolla, CA 92093-0224
(P) (619) 534-3223
(F) (619) 534-8561
tbarnett@ucsd.edu

Jim Barry
MBARI
160 Central Ave.
Pacific Grove, CA 93950
(P) (408) 647-3726
(F) (408) 649-8587
barry@mbari.org

Tim Baumgartner
Scripps Institution of Oceanography
UCSD, 9500 Gilman Dr., Dept. 0227
La Jolla, CA 92093-0227
(P) (619) 534-22171
(F) (619) 534-7641
trbaumgartner@ucsd.edu

Larry Benson
U.S. Geological Survey
3215 Marine Street
Boulder, CO 80303
(P) (303) 541-3005
(F) (303) 447-2505
lbenson@dcolka.cr.usgs.gov

Wolf H. Berger
Scripps Institution of Oceanography
UCSD, Geological Research Division
La Jolla, CA 92093-0215
(P) (619) 534-2750
(F) (619) 534-0784
wberger@ucsd.edu

Julio Betancourt
U.S. Geological Survey
1675 W. Anklam Road
Tucson, AZ 87505
(P) (602) 760-6821
(F) (602) 670-806
jlbetanc@dazton.wr

Franco Biondi
UCSD, Geological Research Division
Scripps Institution of Oceanography
La Jolla, CA 92093-0215
(P) (619) 534-7174
(F) (619) 534-0784
fbiondi@ucsd.edu

George Boehlert
Pacific Fisheries Environmental Group
P.O. Box 831
Monterey, CA 93942
george_boehlert@ccgatessp.nmfxs.gov

J. Platt Bradbury
U.S. Geological Survey
Box 25046, DFC, MS-919
Denver, CO 80225
(P) (303) 236-5666
(F) (303) 236-5690
bradbury@greenwood.cr.usgs.gov

Roger Byrne
Museum of Paleontoloogy
UC Berkeley
Berkeley, CA 94720
(P) (510) 643-8108
(F) (510) 642-3370
arbyrne@cmsa.berkeley.edu

Eric M. Cathcart
University of San Diego
1103 Fresno St., Apt. H
San Diego, CA 92110
(P) (619) 299-4946
(F) (619) 299-4946
ericm@teetot.acusd.edu

Dan Cayan
Scripps Institution of Oceanography
UCSD, Climate Research Division
La Jolla, CA 92093-0224
(P) (619) 534-4507
(F) (619) 534-8561
dcayan@ucsd.edu

Bonnie Claus
U.S. Geological Survey
Box 2504, DFC, MS 934
Denver, CO 80225
(P) (303) 236-5717
(F) (303) 236-8822
claus@bpgsvr.cr.usgs.gov

Canduace Cloy
Western Michigan University
Geology Department
Kalamazoo, MI 49008-5128
(P) (517) 629-8878
(F) (517) 629-2609

Walter E. Dean
U.S. Geological Survey
Box 25046, DFC, MS 939
Denver, CO 80225
(P) (303) 236-5760
(F) (303) 236-0459
dean@sedproc.cr.usgs.gov

Michael Dettinger
U.S. Geological Survey
5735 Kearny Villa Road, Suite O
San Diego, CA 92123-1135
(P) (619) 637-6845
(F) (619) 637-9201
mddettin@s101pcasnd.wr.usgs.gov

Henry Diaz
NOAA-ERL-CDC
325 Broadway
Boulder, CO 80303
(P) (303) 497-6649
(F) (303) 497-7013
hfd@ncdc.noaa.gov

Rob Dunbar
Geology and Geophysics
Rice University
6100 S. Main
Houston, TX 77005
(P) (713) 527-4883
(F) (713) 285-5214
dunbar@rice.edu

Mark Eakin
NOAA Office of Global Programs
1100 Wayne Avenue, Suite 1225
Silver Spring, MD 20910
(P) (301) 427-2089
(F) (301) 427-2073
mark_eakin@ogp.noaa.gov

Eric Edlund
UC Berkeley
Dept. of Geography
501 Earth Sciences Bldg.
Berkeley, CA 94720
(P) (510) 643-8108
(F) (510) 642-3370
eric@pollen1.berkely.edu

Stewart Fallon
University of San Diego
3323 Oliphant St.
San Diego, CA 92106
(P) (619) 272-4085
(F) (619) 272-4085
sfallon@teetot.acusd.edu

John Field
Scripps Institution of Oceanography
UC San Diego
La Jolla, California 92093
(P) (408) 427-1543
jfield@coast.ucsd.edu

Sue Ferguson
USDA Forest Service
Pacific Northwest Research Station
4043 Roosevelt Way, NE
Seattle, WA 98105-6497
(P) (206) 553-7815
(F) (206) 553-7709
ferguson@dorothy.cfr.washington.edu

Robert C. Francis
University of Washington
School of Fisheries, WH-10
Seattle, WA 98195
(P) (206) 543-7345
(F) (206) 685-7471
rfrancis@fish.washington.edu

James V. Gardner
U.S. Geological Survey
3475 Deer Creek Road
Palo Alto, CA 94304
(P) (415) 354-3087
(F) (415) 354-3191
jim@octopus.wr.usgs.gov

Gregg Garfin
Laboratory of Tree-Ring Research
University of Arizona
Tucson, AZ 85721
(P) (602) 621-2992
(F) (602) 621-8229
cgarfin@ltrr.arizona.edu

E.R. Garnett
Canadian Wheat Board
423 Main Street, P.O. Box 816
Winnepeg, Manitoba R3C 2P5
(P) Canada 983-3563
(F) Canada 983-4031
ray_garnett@canwheatbrd.ca

Donald Gautier
U.S. Geological Survey
Box 2504, DFC, MS 934
Denver, CO 80225
(P) (303) 236-5740
(F) (303) 236-8822)
gautier@bpgsvr.cr.usgs.gov

Nick Graham
Scripps Institution of Oceanography
Climate Research Div., UCSD
La Jolla, CA 92093-0224
(P) (619) 534-0382
(F) (619) 534-8561
graham@grace.ucsd.edu

Sarah Gray
Marine Science, Univ. San Diego
5998 Alcala Park
San Diego, CA 92110
(P) (619) 260-4095
(F) (619) 260-6804
sgray@teetot.acusd.edu

David Greenland
University of Oregon
Dept. of Geography
Eugene, OR 97403-1251
(P) (503) 346-4541
(F) (503) 346-2067
greenlan@oregon.uoregon.edu

Martha L. Hemphill
Quaternary Sciences Center
Desert Research Institute
P.O. Box 60220
Reno, NV 89506
(P) (702) 673-7407
(F) (702) 673-7397
hemphill@maxey.dri.edu

Juan-Carlos Herguera
Scripps Institution of Oceanography
UCSD, Marine Research Division
La Jolla, CA 92093-0218
(P) (619) 534-6510
(F) (619) 534-6510
herguera@cicese.mx

Katie Hirschboeck
University of Arizona
Lab. of Tree Ring Research
Tucson, AZ 85721
(P) (602) 621-6670
(F) (602) 621-6670
katie@ltrr.arizona.edu

Steven Hodge
U.S. Geological Survey
University of Puget Sound
Tacoma, WA 98416
(P) (206) 593-6516
(F) (206) 383-7967
smhodge@orca_paktcm.wr.usgs.gov

Stephen Holets
PG&E
77 Beale St., Rm 1651, MCB16A
San Francisco, CA 94177
(P) (415) 973-4530
(F) (415) 957-9348
shh2@tesabsgo@gsv

Malcolm Hughes
University of Arizona
Tree Ring Lab.
West Stadium 105
(P) (602) 621-6470
(F) (602) 621-8229
mhughes@ltrr.arizona.edu

Caroline Isaacs
U.S. Geological Survey
345 Middlefield Road, MS 999
Menlo Park, CA 94025
(P) (415) 354-3014
(F) (415) 354-3224
caroline@octopus.wr.usgs.gov

Anne Jeton
U.S. Geological Survey
333 W. Nye Lane
Carson City, NV 89706
(P) (702) 887-7628
(F) (702) 887-7629

David E. Jones
Kent State University
Kent, OH 44242
(P) (216) 672-7987
djones@gilbert.kent.edu

William A. Jones, Jr.
Dept. of Geology and Geophysics
Rice University
Houston, TX 77251
(P) (713) 527-8101 (ext. 2527)
(F) (713) 285-5214
billj@rice.edu

Thor Karlstrom
U.S. Geological Survey
4811 SW Brace Pt. Drive
Seattle, WA 98136
(P) (206) 933-6933

Charles David Keeling
Scripps Institution of Oceanography
UCSD, Geological Research Division
La Jolla, CA 92093-0220
(P) (619) 534-4230
(F) (619) 534-0784
cdkeeling@ucsd.edu

Timothy R. Klett
U.S. Geological Survey
Box 25046, DFC, MS 960
Denver, CO 80225
(P) (303) 236-5740
(F) (303) 236-2288
tklett@bpgsvr.cr.usgs.gov

Carina Lange
Scripps Institute of Oceanography
UCSD, Geological Research Division
La Jolla, CA 92093-0215
(P) (619) 534-4605
(F) (619) 534-0784
clange@ucsd.edu

John Laurmann
Stanford University/Civil Eng.
c/o 3372 Martin Road
Carmel, CA 93923-8230
(P) (408) 625-6696
(F) (408) 625-6696

Judith Lean
Naval Research Institute
Code 7673L
Washington, DC 20375
(P) (202) 767-5116
(F) (202) 404-7997
lean@demeter.nrl.navy.mil

Anna Lebedev
Oceanography Dept.
Florida State University
Tallahassee, FL 32306-3048
(P) (904) 644-1854
(F) (904) 644-2581
albedev@ocean.fsu.edu

Peggy Lehman
California Department of Water Resources
3251 "S" Street, Room C-27
Sacramento, CA 95816-7017
(P) (916) 227-7551
(F) (916) 227-7554
plehman@water.ca.gov

Brad Linsley
Dept. Geology and Geophysics
Rice University
6100 S. Main St.
Houston, TX 77005-1892
(P) (713) 527-4880
(F) (713) 285-5214
blinsley@ruf.rice.edu

Mark Losleben
University of Colorado
Boulder, CO 80303
(P) (303) 492-8842
(F) (303) 492-8842
markl@culter.colorado.edu

Brian Luckman
Department of Geography
University of Western Ontario
London, Canada N6A 5C3
(P) (519) 679-2111, ext 5012
(F) (519) 661-3750
luckman@sscluwo.ca

Ronald Lynn
Southwest Fisheries Center
La Jolla, CA 92037
(P) (619) 453-2820

David Mackas
Institute of Ocean Sciences
PO Box 6000
Sidney, B.C.
V8L 4B2 Canada
(P) (604) 363-6442
(F) (604) 363-6479
mackas@ios.bc.ca

Nate Mantua
Scripps Institution of Oceanography
UCSD, Climate Research Division
La Jolla, CA 92093-0224
(P) (619) 534-1868
(F) (619) 534-8561
mantua@lagoa.ucsd.edu

Vera Markgraf
INSTAAR
University of Colorado
1560 30th Street
Boulder, CO 80309
(P) (303) 492-5117
(F) (303) 492-6388
markgraf@spot.colorado.edu

Ted Melis
University of Arizona
4500 West Speedway Rd.
Tucson, AZ 85745
(P) (602) 670-6821
(F) (602) 670-6806
tsmelis@sun1paztcn.wr.usgs.gov

Arthur J. Miller
Scripps Institution of Oceanography
UCSD, Climate Research
La Jolla, CA 92093-0224
(P) (619) 534-8033
(F) (619) 534-8561
ajmiller@ucsd.edu

Ed Mercurio
Hartnell College
647 Wilson Sstreet
Salinas, CA 93901
(P) (408) 424-3497
(F) (408) 755-6751

Tom Murphree
Dept. of Meteorology, MR-ME
Naval Postgraduate School
Monterey, CA 93943-5000
(P) (408) 656-2723
(F) (608) 656-3061
murphree@osprey.met.nps.navy.mil

Fenbiao Ni
Lab. of Tree-Ring Research
University of Arizona
105 West Stadium
(P) (520) 621-9731
(F) (520) 621-8229
ni@air.atmo.arizona.edu

Shirley A. Oscarson
U.S. Geological Survey
Box 25046, DDFC, MS 934
Denver, CO 80225
(P) (303) 236-5711
(F) (303) 236-2288
oscarson@bpgsvr.cr.usgs.gov

Heather Parker
NOAA, Nat. Mar. Fish. Service
P.O. Box 831
Monterey, CA 93942
(P) (408) 656-3311
(F) (408) 656-3319
heather_parker@ccgate.ssp.nmf.gov

David Peterson
U.S. Geological Survey
345 Middlefield Road
Menlo Park, CA 94025
(P) (415) 354-3366
(F) (415) 254-3363
dhpete@rcamnlwr.usgs.gov

Thomas Piechota
UCLA, Civil and Eng. Department
3066 Engineering 1
Los Angeles, CA 90024-1593
(P) (310) 206-8612
(F) (310) 206-7245
piechota@seas.ucla.edu

David Piper
U.S. Geological Survey
345 Middlefield Road, MS 902
Menlo Park, CA 94025
(P) (415) 329-5187
(F) (415) 329-5110
dzpiper@mojave.wr.usgs.gov

Jeffrey Polovina
NOAA, SW Fisheries Sci. Center
2570 Dole Street, Honolulu Lab.
Honolulu, HI 96822-2396
(P) (808) 943-1221
(F) (808) 943-1290
jpolovin@honlab.nmfs.hawaii.edu

Steven Porter
University of Washington
Quaternary Research Center (AK-60)
Seattle, WA 98195
(P) (206) 543-1166
(F) (206) TRE-3836
scporter@u.washington.edu

D. Roger Pulwarty
CIRES/CDC
University of Colorado, Boulder
Boulder, CO 80309
(P) (303) 492-0963
(F) (303) 492-2468
rsp@cdc.noaa.gov

Kelly Redmond
Western Regional Climate Center
Desert Research Institute
P.O. Box 60220
Reno, NV 89506-0220
(P) (702) 677-3139
krwrcc@sage.unr.edu

Larry Riddle
Scripps Institution of Oceanography
Climate Research, UCSD, 0224
La Jolla, CA 92093-0224
lriddle@ucsd.edu

Maurice Roos
California Department of Water Resources
1416 Ninth Street
P.O. Box 942836
Sacramento, CA 94236-0001

Harry Rowe
Dept. of Earth and Planetary Sciences
University of New Mexico
Albuquerque, NM 87131
(P) (505) 277-6629
(F) (505) 277-8843
hrowe@ccarina.unm.edu

Arndt Schimmelmann
Indiana University
Dept. of Geological Sciences
Geology 129, 1005 East 10th
Bloomington, IN 47405-5101
(P) (812) 855-7645
(F) (812) 855-7961
aschimme@indiana.edu

Frank Schwing
PFEG-NMFS
PO Box 831
Monterey, CA 93942
(P) (408) 656-3298
(F) (408) 656-3319
franklin_schwing@ccgate.ssp.nmfs.gov

Gary Sharp
Center for Climate/Ocean Resources Study
PO Box 2223
Monterey, CA 93940
(P) (408) 449-9212
(F) (408) 647-4225
gsharp@igc.apc.org

Saxon Sharpe
Quaternary Sciences Center
Desert Research Institute
P.O. Box 60220
Reno, NV 89506
(P) (702) 673-7307
(F) (702) 673-7397
ssharpe@maxey.dri.edu

Allison Smith
Dept. of Geology
221 McGilvrey Hall
Kent State University
Kent, Ohio 44242
(P) (216) 672-3709
(F) (216) 762-7949
asmith@kentvm.kent.edu

Paul Smith
NOAA/NMFS
Southwest Fisheries Science Center
La Jolla, CA 92038-0271
(P) (619) 546-7169
(F) (619) 546-5656
paulsmit@its.ucsd.edu

Scott Starratt
U.S. Geological Survey
345 Middlefield Road, MS 959
Menlo Park, CA 94025
sstarratt@isdnml.wr.usgs.gov

Ted Strub
Oregon State University
Ocean Admin. Bldg. 104
Corvallis, OR 97331-5503
(P) (503) 737-3015
(F) (503) 737-2064
pts@osuvax.oce.orst.edu

Robert Swanson
Climatological Consulting Corp.
1216 Babel Lane
Concord, CA 94518
(P) (510) 676-2228
(F) (510) 676-2228

Tom Swetnam
Tree Ring Lab., West Stadium 58
University of Arizona
Tucson, AZ 85721
(P) (602) 621-2112
(F) (602) 621-8229
tswetnam@ltrr.arizona.edu

Sus Tabata
Inst. of Ocean Sciences
P.O. Box 6000
9860 West Saanich Road
Sidney, BC, Canada V8L 4B2
(P) (604) 363-6573
(F) (604) 363-6746
tabata@ios.bc.ca

John Vaccaro
U.S. Geological Survey
1201 Pacific Avenue, Suite 600
Tacoma, WA 98402
(P) (206) 593-6510
(F) (206) 593-6514
jvaccaro@maildwatcm.wr.usgs.gov

Janvan Wagtendonk
National Biological Service
Yosemite Field Station
El Portal, CA 95318
(P) (209) 372-0465
(F) (209) 372-0569
jan@yose.nbs.gov

Roy A. Walters
U.S. Geological Survey
1201 Pacific Ave., Ste. 901
Tacoma, WA 98402
(P) (206) 593-6505
(F) (206) 593-6514
roy@brrermailcr.usgs.gov

John B. Weeks
U.S.Geological Survey
Box 25046, DFC, Ms 412
Lakewood, CO 80225-0046
(P) (303) 236-5021
(F) (303) 236-5034
jbweeks@usgs.gov

Amy L. Weinheimer
Scripps Institution of Oceanography
UCSD, Geological Research Div.
La Jolla, CA 92093-0220
(P) (619) 534-7549
(F) (619) 534-0784
aweinheimer@ucsd.edu

G. James West
U.S. Bureau of Reclamation
3429 Oyster Bay
Davis, CA 95616
(P) (916) 978-4542
(F) (916) 978-5284
jwest@smp700.mp.usbr.gov

Cathy Whitlock
Dept. of Geography
University of Oregon
Eugene, OR 97403-1251
(P) (503) 346-4566
(F) (503) 347-2067
whitlock@oregon.uoregon.edu

Peter Wigand
Quaternary Science Center
Desert Research Institute
Reno, NV 89506
pwigand@maxey.ddri.edu

Ray Wilson
U.S. Geologoical Survey
345 Middlefield Road, MS-998
Menlo Park, CA 94025
rwilson@mojave.wr.usgs.gov

Michelle Lee Wood
Lab. of Tree-Ring Research
University of Arizona
105 West Stadium
Tucson,AZ 85721
(P) (520) 621-9731
grad2@ccit.arizona.edu

Connie Woodhouse
Lab. of Tree-Ring Research
University of Arizona, Bldg. 58
Tucson, AZ 85721
(P) (602) 621-9731
(F) (602) 621-8229

Warren Wooster
University of Washington
School of Marine Affairs
Seattle, WA 98195
(P) (206) 685-2497
(F) (206) 543-1417

James R. Young
Southern California Edison
P.O. Box 800
2244 Walnut Grove Ave.
Rosemead, CA 91770
(P) (818) 302-9191
(F) (818) 302-9730
youngjr@sce.com